The Influence of Rheology on the Cracking of Plastic Concrete

by

John Temitope Kolawole

Dissertation presented for the degree of
Doctor of Philosophy in Engineering
in the Faculty of Engineering
at Stellenbosch University

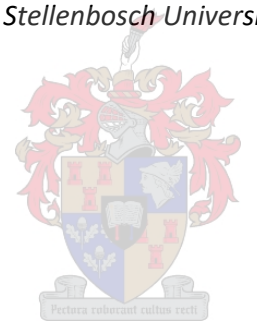

Supervisor: Dr Riaan Combrinck
Co-supervisor: Prof William Peter Boshoff

March 2020

Declaration

By submitting this dissertation electronically, I declare that the entirety of the work contained therein is my own, original work, that I am the sole author thereof (save to the extent explicitly otherwise stated), that reproduction and publication thereof by Stellenbosch University will not infringe any third party rights and that I have not previously in its entirety or in part submitted it for obtaining any qualification.

This dissertation includes one original paper published in peer-reviewed journal and three unpublished publications. The development and writing of the papers (published or unpublished) were the principal responsibility of myself and, for each of the cases where this is not the case, a declaration is included in the dissertation indicating the nature and extent of the contributions of co-authors.

March 2020

Summary

Plastic cracking occurs during concrete's early hours and impairs its serviceability and durability. The early hours refer to the time of mixing to the time around the final set. Concrete possesses rheological properties during the plastic phase while settlement and shrinkage leading to plastic cracking also occur during this phase. Therefore, there is bound to be an interaction between the concurrent concrete's rheological behaviour and cracking behaviour. During this same plastic phase, concrete possesses pronounced rheo-viscoelastic properties that influence the plastic cracking behaviour. The heterogeneous nature of concrete coupled with its time-dependent behaviour (due to hydration) at early hours makes investigations into the above-identified properties in relation to plastic cracking complicated and lacking in the literature. With this in mind, the goal of this study was to establish links between the rheo-related properties of concrete and its plastic cracking.

Experimental investigations started with concrete mixes designed for varied rheological properties but similar hardened properties. Rotational and dynamic shear rheometries were employed to characterise the plastic phase of the concrete in order to establish the shear rheo-physical and rheo-viscoelastic properties. The plastic cracking behaviour of the concrete mixes were also investigated. Analytical methods were, thereafter, used to predict the occurrence of plastic cracking of the concrete mixes.

Results show that concrete can both be thixotropic and rheopectic due to rheology modifiers and condition pre-history. Various thixotropy evaluation methods adopted for the study showed similar trends except for the hysteresis loop area that was dependent on the concrete's initial set condition and was, therefore, pegged as merely suitable for qualitative measurement. Plastic concrete's viscoelastic behaviour is majorly influenced by hydration, coarse solid volume fraction and constituent materials such as rheology modifiers. Furthermore, it was discovered that plastic concrete possesses pseudo-strain hardening ability under the application of linear (microscopic) shear strain. This was similar to the physical (macroscopic) response earlier detected as shear thickening and rheopexy.

The study further shows that self-settlement is the major dominating process during the early plastic phase of concrete's cracking behaviour and takes the form of a gravitational shearing process. This self-settlement is directly linked to the yield stress and thixotropy of the concrete. This same process influences the plastic shrinkage and rate of capillary pressure during the period of the self-settlement, thereby, linking the plastic shrinkage and rate of

capillary pressure to the yield stress and thixotropy. Plastic concrete generally possesses the inherent ability to relax early restrained cracking stress, but its ability for strain dissipation heavily depends on the material constituents such as rheology modifiers. The analytical methods for prediction revealed that the plastic concrete damage tends to be strain-oriented with a pressure-insensitive form of ductile failure. In addition, the cracking strains during the self-settlement period are mainly shear-related. Finally, it was proposed that it is possible to control the concrete mix design to avoid damage/microcracking associated with the plastic phase.

Opsomming

Plastiese kake kom gedurende die vroeë ure van beton voor en verswak die diensbaarheid en duursaamheid daarvan. Die vroeë ure verwys na die tyd van meng tot die tyd rondom die finale set. Beton besit reologiese eienskappe gedurende die plastiese fase, terwyl versakking en krimping ook gedurende hierdie fase plaasvind. Daarom sal daar interaksie tussen die reologiese gedrag van die beton en plastiese krake wees. Gedurende dieselfde plastiese fase besit beton duidelike reovisko-elastiese eienskappe wat die plastiese kraakgedrag beïnvloed. Die heterogene aard van beton, gekoppel met die tyd-afhanklike gedrag daarvan (as gevolg van hidrasie) in die vroeë ure, maak ondersoeke na die bogenoemde eienskappe met betrekking tot plastiese krake ingewikkeld, en dit ontbreek in die literatuur. Hiermee in gedagte, was die doel van hierdie studie om die skakels tussen die reo-verwante eienskappe van beton en plastiese krake te bepaal.

Eksperimentele ondersoeke het begin met betonmengsel ontwerp vir verskillende reologiese eienskappe maar soortgelyke verharde eienskappe. Rotasie en dinamiese skuif reometrie is gebruik om die plastiese fase van die beton te karakteriseer om die skuif reofisiese en reovisko-elastiese eienskappe te bepaal. Die plastiese kraakgedrag van die betonmengsels is ook ondersoek. Daarna is ontledingsmetodes gebruik om die ontstaan van plastiese krake van die beton te voorspel.

Resultate toon dat beton beide tiksotropies en reopekties kan wees as gevolg van reologie-modifiseerders en voorgeskiedkundige toestand. Die verskillende tiksotropiese evaluasiemetodes gebruik vir die studie het soortgelyke tendense getoon, behalwe vir die histerese lus-area wat van die beton se aanvanklike versakkingstoestand afgehang het en daarom slegs geskik is vir kwalitatiewe meeting. Die visko-elastiese gedrag van beton word grootliks deur hidrasie, growwe soliede volume-fraksie en samestellende materiale soos reologie-modifiseerders beïnvloed. Verder is gevind dat plastiese beton pseudo-vervormingsverhardingsvermoë onder die aanwending van liniêre (mikroskopiese) skuifspanning besit. Dit was soortgelyk aan die fisiese (makroskopiese) gedrag wat vroeër as skuifverdikking en reopeksie waargeneem is.

Die studie toon verder dat self-versakking die hoof dominerende proses gedurende die vroeë plastiese kraakgedrag van beton is en die vorm van 'n gravitasie skuifproses aanneem. Hierdie self-versakking word direk verbind met die skuifvloeispanning en tiksotropie van die beton. Dieselfde proses beïnvloed die plastiese krimping en die tempo van kapillêre druk gedurende die tydperk van die self-versakking, wat die plastise krimping en tempo van kapillêre druk met die skuifvloeispanning en tiksotropie verbind. In die algemeen besit plastiese beton die inherente vermoë om vroeë plastiese kraakvorming-spannings te ontspan, maar die vermoë is grootliks afhanklik van die materiaal-bestanddele soos reologie-modifiseerders. Die ontledingsmetodes vir voorspelling het onthul dat die plastiese beton-skade geneig is om spanningsgeoriënteerd te wees met 'n druk-onsensitiewe vorm van duktiele faling. Bykomend

is die kraakvorming-spannings gedurende die self-versakkingstydperk hoofsaaklik skuif verwant. Laastens is voorgestel dat dit moontlik is om betonmengsels te ontwerp om beskadiging/mikrokrake wat met die plastiese fase geassosieer word, te beheer.

Acknowledgements

I would like to appreciate and thank the following people for their assistance and support during my study:

- My promoters, Prof Billy Boshoff and Dr Riaan Combrinck, for their continued support and guidance.
- The World Academy of Science (TWAS), The National Research Foundation (NRF) and Pretoria Portland Cement (PPC) for their financial support during the study.
- The staff in the laboratory and workshop at the Civil Engineering and Process Engineering Departments of Stellenbosch University, for their assistance and time during the experimental work.
- The administration staff of the Civil Engineering Department of Stellenbosch University, for their assistance and time.
- My parents and siblings, for their prayers, advice, humour and unconditional support.
- Friends and family, who played significant roles throughout the study period.
- Finally, my Creator and God, for giving me the opportunity, strength and ability to conduct and finish this study.

Table of contents

List of figures

List of tables

Chapter 1: Introduction

Concrete is a versatile material that has been used for centuries. However, its constituents and properties continue to evolve, and research into its behaviour continues to advance. One such research area is concrete's behaviour in its fresh and plastic states. The properties of fresh and plastic concrete have a significant influence on the eventual properties of hardened concrete. Deficiencies in the early age concrete can impair the finished product and its serviceability. One of the deficiencies of early age concrete is cracking. When these cracks occur in the early hours after casting the concrete, it is referred to as plastic cracking. The early hours refer from the time of mixing to the time around the final set. Concrete during this stage is referred to as plastic because it has a fluid or viscous nature which can easily be shaped or moulded. Hence, plastic cracking is the cracking that occurs during the plastic state of concrete. However, the exact time when concrete changes from a plastic state to a solid state with no viscous properties is unknown but is generally assumed to be around the final setting time (Combrinck, 2016; Lura *et al.*, 2009; Sant, Dehadrai, Bentz and Weiss, 2009; Sant, Dehadrai, Bentz, Lura, *et al.*, 2009).

Cracking in concrete can cause severe durability issues. Cracks aggravate durability problems by increasing the ingress of deteriorating agents such as water and chlorides, leading to increased cracking and accelerated corrosion of steel reinforcement (Safiuddin *et al.*, 2018; Mehta and Monteiro, 2006). Cracks in concrete can occur at different stages of its life due to varying factors. However, plastic cracks refer to the cracks that occur in the fresh/plastic state of concrete before it solidifies around the final setting time (Combrinck, 2016; Lura *et al.*, 2009; Sant, Dehadrai, Bentz and Weiss, 2009; Sant, Dehadrai, Bentz, Lura, *et al.*, 2009). Plastic cracking aggravates the durability problems at an early and premature time in the concrete's life (Nguyen *et al.*, 2017). Plastic cracking should, therefore, be avoided as best as possible. Plastic cracking can occur in two forms, plastic settlement cracking and plastic shrinkage cracking. Plastic settlement cracking occurs due to differential settlement of concrete (Combrinck *et al.*, 2017; Combrinck, 2016; CCIP-048, 2010) while plastic shrinkage cracking occurs due to shrinkage caused by internal pressure build-up as pore water evaporates (Ghourchian *et al.*, 2018; Slowik *et al.*, 2008). Both often occur consecutively with overlaps in concrete (Combrinck *et al.*, 2018a).

Concrete's solid particles are responsible for its plastic settlement, and as they settle, they displace water to the surface as bleeding (Sonebi and Bartos, 2002). Differential settlement is the cause of plastic settlement cracking in concrete. Any form of restraint within a concrete specimen such as steel reinforcement or change in formwork dimension can be responsible for the non-uniform

settlement (Combrinck *et al.*, 2017). These form of cracks can be found along the longitudinal and transverse lengths of reinforcing steel bars and the longitudinal length of change in sections of concrete slabs. Major factors that have been identified in the literature to influence plastic settlement are water and aggregate content, fine content, wall effect, formwork geometry, and capillary pressure (Safiuddin *et al.*, 2018; Kim *et al.*, 2014; CCIP-048, 2010; Kwak and Ha, 2006; Powers, 1968).

Evaporation is majorly responsible for plastic shrinkage. Once all the bleed water has evaporated, the concrete pore water starts evaporating causing internal pressure build-up within the concrete specimen (Combrinck, 2016). This leads to the water surface in the pores to form concave water menisci due to adhesive forces and surface tension (Slowik *et al.*, 2009). The pore water evaporation causes plastic shrinkage while the internal stress build-up leads to plastic shrinkage cracking if the concrete is restrained. However, after the final setting time, the concrete has solidified enough to resist the plastic shrinkage stresses and cracking (Combrinck, 2016). For a better understanding of plastic cracking behaviour of concrete, processes involved are demarcated in three phases and explained further in the study. These are the plastic phase before the initial setting time, the semi-plastic phase between the initial setting time and final setting time, and the solid phase after the final setting time.

Fresh concrete flows and behaves like a fluid material until it stiffens and solidifies by hydration (Roussel, 2012). Hence, fresh concrete has rheological properties during the plastic phase. Rheology is the study of deformation and flow of matter. The matter can take a form in between a liquid and solid, as long as it can flow. Concrete rheology is the study of the flow properties of concrete in the fluid/plastic state. In engineering terms, rheometry allows the behaviour of complex materials to be predictable by characterising its flow properties. The characterisation is achieved by establishing the relationship between the shear stress to which a material is subjected and the shear rate (time variation of the deformation regarding flow) using shear rheometry. The constant of such relationship is termed viscosity for simple fluids (Newtonian's fluid) such as water and is given as:

$$\tau = \mu\dot{\gamma} \qquad \text{Equation 1.1}$$

where τ is the shear stress, μ is the viscosity, and $\dot{\gamma}$ is the shear rate.

Complex fluids such as concrete have a non-zero viscosity at zero shearing state referred to as the yield stress (τ_0) as shown below and in Figure 1.1.

$$\tau = \tau_0 + \mu\dot{\gamma} \qquad \text{Equation 1.2}$$

where τ_0 is the yield stress.

Equation 1.2 is also referred to as a Bingham model. More models representing complex behaviours of unconventional concrete such as that containing admixtures include the Herschel-Bulkley model and modified Bingham model shown below respectively.

$$\tau = \tau_o + K\dot{\gamma}^n \quad \text{Equation 1.3}$$

$$\tau = \tau_o + \mu\dot{\gamma} + c\dot{\gamma}^2 \quad \text{Equation 1.4}$$

where K is the consistency factor, n is the flow behaviour index, and c is a second order parameter.

Viscosity is the intrinsic property of the material in the form of resistance to flow and can vary with the shear rate for non-Newtonian fluids while the yield stress is the shear stress at which the material starts to flow or deform.

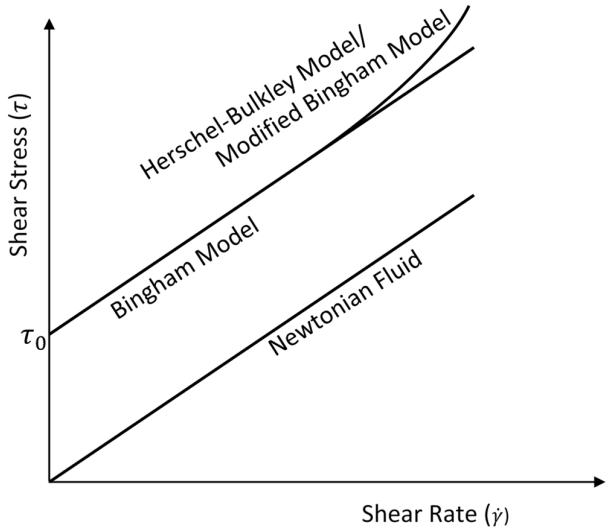

Figure 1.1: Stress-strain curve for Newtonian and Bingham fluids (Adapted from Mezger (2014), Roussel (2012), and Szecy (1997))

In general, concrete possesses rheological properties during the plastic phase while settlement and shrinkage leading to plastic cracking also occur during this phase up to the final setting time. Therefore, there is bound to be an interaction between concrete's rheological behaviour and cracking behaviour concurrently occurring during the plastic phase. With these in mind, four research steps form the research objectives (Section 1.2) of this study.

Fresh concrete is idealised as a suspension of particles (aggregates) in a fluid-like cement paste, the cement paste is also a suspension of binder particles in a fluid-like mixture of water and admixtures (Zhang *et al.*, 2019; Szecsy, 1997; Ferraris and Gaidis, 1992). This means that fresh concrete is a structured fluid of more than one phase (Franck, 2004). This heterogeneity makes the rheological characterisation of concrete complex. For the purpose of this research, rheological testing of

concrete was done in two forms: static or rotational rheometry as well as dynamic or oscillatory rheometry, with special focus on the thixotropy aspect of static rheometry. Thixotropy as a structuration process is important for this study as it indicates the increase in shear resistance of concrete, that is, the increase in structural build-up during the plastic phase. Therefore, the first step of investigation for this study was to exhaustively evaluate the thixotropy of conventional concrete. This was done by using rotational shear rheometry to evaluate the rheo-physical parameters of concrete.

As noted earlier, fresh concrete acts as a fluid, but as hydration progresses it loses its fluidity to become stiffened and solidified. The hydration reduces the fluid-like (viscous) properties while increasing the solid-like (elastic) properties. The point where concrete's plastic properties end is believed to be around the final setting time. Hence, plastic concrete is both elastic and viscous, that is, it possesses viscoelastic properties that diminish with time due to hydration. Plastic cracking and processes leading to plastic cracking happen within this period of concrete until it gains enough strength to resist the plastic cracking. Viscoelasticity refers to a combination of viscous and elastic properties of a material resulting in behaviours such as creep and stress relaxation. Stress relaxation is the reduction in stress under constant deformation while creep is the increase in deformation under constant stress. These viscoelastic properties of plastic materials can be characterised by dynamic shear rheometry (also known as small amplitude shear oscillation – SAOS). The dynamic shear rheometry can also be used to complement the static shear rheometry in evaluating shear and thixotropic properties. This was the second research step taken for the study. In essence, rheological investigation (the combination of both rotational and dynamic shear rheometry) of plastic concrete was used in establishing its shear resistance and viscoelastic behaviour.

The viscoelastic behaviour of fresh concrete is found to be nearly non-existent in literature. Scaling down to mortar, there is also a scarcity of research on fresh cement mortar's viscoelasticity. However, typical rheo-viscoelastic properties of fresh cement paste have been established in the literature. It was, therefore, decided for this study to exclusively start with the investigation of rheo-viscoelastic behaviour of fresh cement paste and progressively scale up to mortar and concrete using dynamic shear rheometry. Thereafter, the rheo-viscoelasticity of plastic concrete up to two hours of age (the initial setting time) was investigated.

This study examined the complete plastic cracking behaviour of concrete as the third research step and attempts to link this to the rheology as a first step towards conceptualising rheological approach to plastic cracking. Shear resistant properties of concrete which were of keen interest (among

others) in this study include yield stress, yield strain, shear modulus and thixotropy while the key viscoelastic properties include creep and stress relaxation. These constitute the rheo-physical and rheo-viscoelastic behaviours of the concrete, respectively. In order to diversify the rheological properties of the concrete, rheology modifiers such as viscosity modifying agent (VMA), superplasticiser (SP) and increased water content were incorporated in the concrete mixes of the study.

As the fourth and final research step, the prediction of plastic cracking was attempted while incorporating the influence of the viscoelasticity, with the focus on the possible failure or microcracking that can potentially occur during the plastic phase. In literature, currently available prediction and modelling of plastic cracking in concrete neglect the roles of the viscoelastic properties and the possible occurrence of damage/micro-cracking during the plastic phase before the semi-plastic phase.

In essence, shear rheometry was used as a tool to characterise the plastic phase of concrete and to determine concrete's resistant shear properties and viscoelastic influence on plastic cracking which is scarce in the literature. Attempts were also made to show that the early part of this phase is shear dominated. Some of the shear resistance properties (such as peak and residual yield stress and thixotropy) of the fresh/plastic concrete mixes were investigated using an ICAR rheometer (Germann Instruments A/S, 2015; Koehler and Fowler, 2004) and combined with the results obtained from the rheo-viscoelastic testings (such as yield strain, shear modulus, 1 and 2-hour yield stress, and concurrent normal stress) done by using the Anton Paar Physica MCR501 rheometer. Furthermore, the possible occurrence of damage/microcracking during the plastic phase of concrete was modelled and predicted.

1.1. Motivation and purpose of study

As noted earlier, rheology and plastic cracking of concrete are phenomena occurring concurrently during the plastic phase of concrete, therefore, there is bound to be an interaction between them. Furthermore, this phase of concrete is plastic with less elastic behaviour making shear rheometry a more appropriate method to characterise this phase compared to mechanical tensile methods often advocated and used in literature. Hence, this study sets out to establish the relationship between the rheo-related properties of concrete and its plastic cracking. This includes predicting the plastic cracking using a rheo-related approach. With this in mind, the objectives, significance and methodology for this study are set out and discussed in the subsequent sections.

1.2. Research objectives

From the motivation highlighted in the previous section, this study was undertaken in four phases that define the objectives. Each of these phases or objectives also form a separate journal article as itemised as follows.

- To experimentally investigate the rotational shear rheometry of fresh concrete
  Paper title: Estimating the thixotropy of conventional concrete: influence of viscosity modifying agent, superplasticiser and water. Construction and Building Materials 225 (2019), 853-867
- To experimentally study the viscoelastic properties of plastic concrete
  Paper title: Rheo-viscoelastic behaviour of cement-based materials: cement paste, mortar and concrete (Submitted to Construction and Building Materials).
- To evaluate the plastic cracking behaviour of concrete
  Paper title: Plastic cracking behaviour of concrete and its interdependence on rheo-physical properties (Submitted to Construction and Building Materials).
- Predicting the occurrence of damage/microcracking of concrete during the plastic phase
  Paper title: Shear rheo-viscoelasticity approach to plastic cracking of concrete: experiments and model (Submitted to Cement and Concrete Research).

1.3. Methodology

The methodologies adopted for each phase of the study in order to achieve the objectives are as follows.

- An in-depth literature review for each theme of the study. This includes the behaviour of plastic concrete in terms of cracking, rheology and viscoelasticity. The review also includes the methods and approaches to modelling the plastic cracking of concrete.
- Conduct trial tests to develop mixes with adequate workability that is suitable for all considered forms of testing such as plastic cracking, rotational and dynamic shear rheometry. The mixes should have varied rheological properties with similar hardened properties.
- Conduct several extensive rotational shear rheometry tests as part of Objective 1.
- Conduct several dynamic shear rheo-viscoelastic tests for Objective 2.

- Conduct plastic cracking tests including influencing parameters (such as settlement, shrinkage, capillary pressure, evaporation, bleeding, and setting times) and show how rheology influences them, for Objective 3.
- Analyse all experimental results and draw suitable conclusions for each phase of the study.
- Finally, model the occurrence of damage/microcracking of concrete during the plastic phase for Objective 4.

1.4. Research significance

The underlining reason for this study is to broaden the understanding of the plastic cracking behaviour of concrete, and from a rheological point of view, this study is the first of its kind internationally. This study provides information on the rheological shear properties of plastic concrete such as yield strength, shear modulus, yield strain capacity of plastic concrete which are scarce in the literature. Furthermore, there are limited resources on the viscoelasticity of plastic concrete including its creep and relaxation properties. By extension, the results of this study are important in understanding the behaviour of fresh and plastic concrete. The model from this study helps in assessing the potential for plastic cracking in concrete. Improved understanding of plastic cracking behaviour can help in ultimately avoiding plastic cracking by active material and mix design. These have economic and environmental advantages and can assist in creating a more suitable built environment.

Based on the introduction in Section 1 and the results obtained for each phase of the study, significant academic contributions of the research are itemised as follows.

- To contribute to the body of knowledge on the rheological and thixotropic behaviour of conventional concrete.
- To improve the body of knowledge on the viscoelastic behaviour of fresh cement-based materials by progressively incorporating aggregates (fine and coarse, in order to form mortar and concrete respectively) in rheologically modified cement paste. The knowledge on the early age development of shear and viscoelastic properties of the plastic concrete is also added.
- To improve the understanding of plastic cracking behaviour of concrete in order to predict the extent and duration of plastic settlement, plastic shrinkage and capillary pressure rate during the self-settlement period using simple rheological tests.
- Creating a prediction model for the occurrence of damage or micro-cracking in plastic concrete (before the initial setting time) with the incorporation of the viscoelastic influence.

1.5. Report outline

Chapter 1 introduces the study, as well as the motivation and purpose of the study. The study's objectives, methodology and significance are also described.

Chapter 2 forms the background study for this research. The chapter is a review of related literature on each theme of the study, that is, it offers explanations on the research themes.

Chapter 3 presents the first phase of the study that metamorphosise into the first journal article. It is an exhaustive characterisation of the rheological behaviour of fresh concrete with focus on the thixotropy. It is titled "Measuring the thixotropy of conventional concrete: influence of viscosity modifying agent, superplasticiser and water."

Chapter 4 is the second journal article describing the viscoelastic behaviour of cement-based material using rheological methods. It is titled "Rheo-viscoelastic behaviour of fresh cement-based materials: cement paste, mortar and concrete."

Chapter 5 is the third journal article establishing the relationship between the plastic cracking parameters of concrete and its rheo-physical parameter. It is titled "Plastic cracking behaviour of concrete and its interdependence on rheo-physical properties."

Chapter 6 is the fourth journal article on predicting the plastic cracking of concrete using the shear (rheo-physical) and rheo-viscoelastic behaviour of concrete earlier established. It is titled "Shear and rheo-viscoelasticity approach to plastic cracking of concrete: experiments and model."

Chapter 7 summarises the major conclusions from the phases of the study as well as recommendations for possible future studies.

Chapter 2: Background study

This chapter provides the background on the research objectives of the study. It provides basic explanations of the different research themes. Basic explanations are given on plastic concrete, rheology of concrete including yield stress, viscosity, shear thickening/thinning, rheopexy/thixotropy, and rheo-viscoelasticity. Other topics covered are shear rheometry and plastic cracking behaviour of concrete.

2.1. Plastic concrete

Concrete is made of four to five basic materials, namely cement, fine aggregates, coarse aggregate, water, admixtures and/or additives (Mehta and Monteiro, 2006; Petrou *et al.*, 2000). When these constituents are mixed together, fresh concrete is formed which is fluid and has flow properties. However, the fluidity of fresh concrete does not last forever but decreases with time due to the influence of the cement hydration process. The addition of water to the cement content in concrete causes hydration which is responsible for the loss of fluidity and gain of stiffness of fresh concrete. The inclusion of the bulk components of concrete, that is fine and coarse aggregates, aggravates the stiffening of the fresh concrete which is also a factor of its fluidity loss. A measure of the stiffening of fresh concrete is by setting time, which is used in this study to demarcate the stiffening phases of concrete. The setting of concrete refers to the evolution of its solidification, the exact point of transition from fluid-to-solid is quite tricky and vague but is believed to be around the final setting time (Sant, Dehadrai, Bentz, Lura, *et al.*, 2009). The setting of cement-based materials can be monitored and identified using various techniques such as the Vicat test, shrinkage method, rheological test, ultrasonic testing, and electrical conductivity methods (Subramaniam and Wang, 2010; Sant, Dehadrai, Bentz, Lura, *et al.*, 2009). The Vicat test was employed for this study.

The Vicat setting time refers to the duration from adding water to the dry constituents of concrete being mixed (cement, fine and coarse aggregates) up to a period where the concrete has stiffened enough to resist a certain level of stress. The initial setting time indicates when the material has a shear stress resistance of 20 kPa and the final setting time indicates a shear stress resistance of 32 kPa (Sant, Dehadrai, Bentz, Lura, *et al.*, 2009; Sant *et al.*, 2008). Vicat setting times are a classical and most common method of indicating setting in cement-based materials and have been shown to scale/correlate well with other methods (Lootens *et al.*, 2009; Sant, Dehadrai, Bentz, Lura, *et al.*, 2009). The initial setting period/time is regarded to be a dormant or induction period of concrete's hydration and start of solidification (Peng and Jacobsen, 2013), after this time up to the final setting time is the period when concrete's hydration amplifies and reaches its peak (Figure 2.1) . From

available literature, this peak often correlates well with the transition of concrete to solid by the various techniques including Vicat test (Yoo *et al.*, 2016; Lootens *et al.*, 2009; Sant, Dehadrai, Bentz, Lura, *et al.*, 2009; Sant *et al.*, 2008; Sun *et al.*, 2006; Nachbaur *et al.*, 2001; Jiang and Roy, 1992). Figure 2.1 shows the stiffening development of concrete as explained earlier and how it relates to other properties development in concrete.

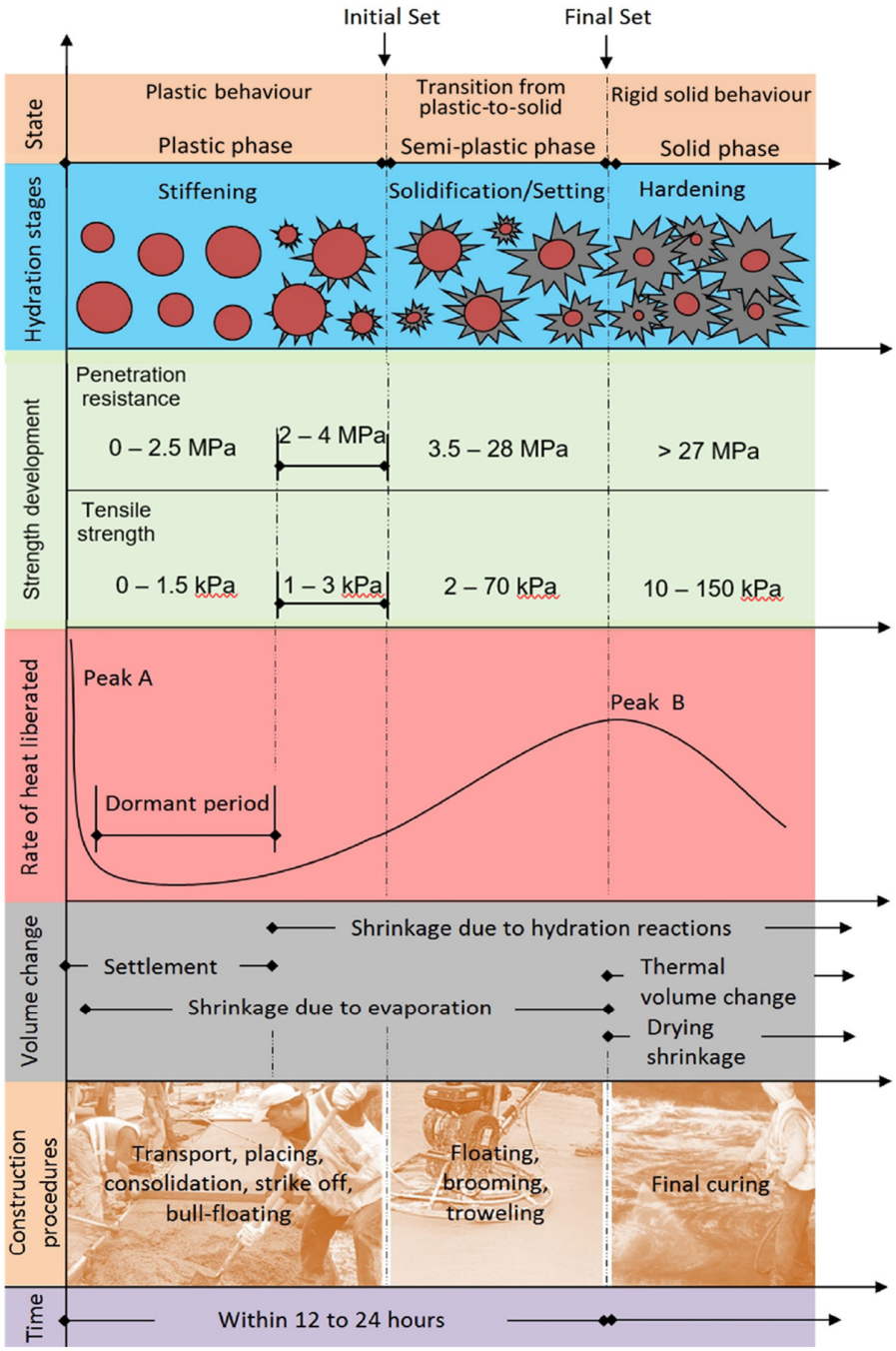

Figure 2.1: Different stages in the hydration process (Adapted from (Combrinck and Boshoff, 2019; Khan, 2018; Combrinck, 2016; Yoo *et al.*, 2016; Roziere *et al.*, 2015; Dao *et al.*, 2009).

It can, therefore, be concluded that hydration of cement is responsible for the stiffening phases of concrete and, hence, fluidity loss. Concrete, up to the initial setting time, has the ability to be mouldable to different shapes but starts to lose this ability after the initial setting time up to the final setting time where it can no longer be moulded (Combrinck, 2011). This is demonstrated in Figure 2.2 (Combrinck, 2011). The term "plastic" from the Greek word "plastikos" means mouldable, and is used for materials that are malleable and can be mouldable into solid shapes (Powers, 1993). Hence, the period up to the initial setting time can be referred to as the "plastic phase", the period between the initial to the final setting time as the "semi-plastic phase" and the period after the final setting time as the "solid phase". These are the setting/solidification phases adopted for this study as shown in Figure 2.1 and other related figures in the thesis. These mouldability and setting phases of concrete up to the final setting time brings about the term "plastic concrete". Cracking that occurs during this plastic state is referred to as plastic cracking.

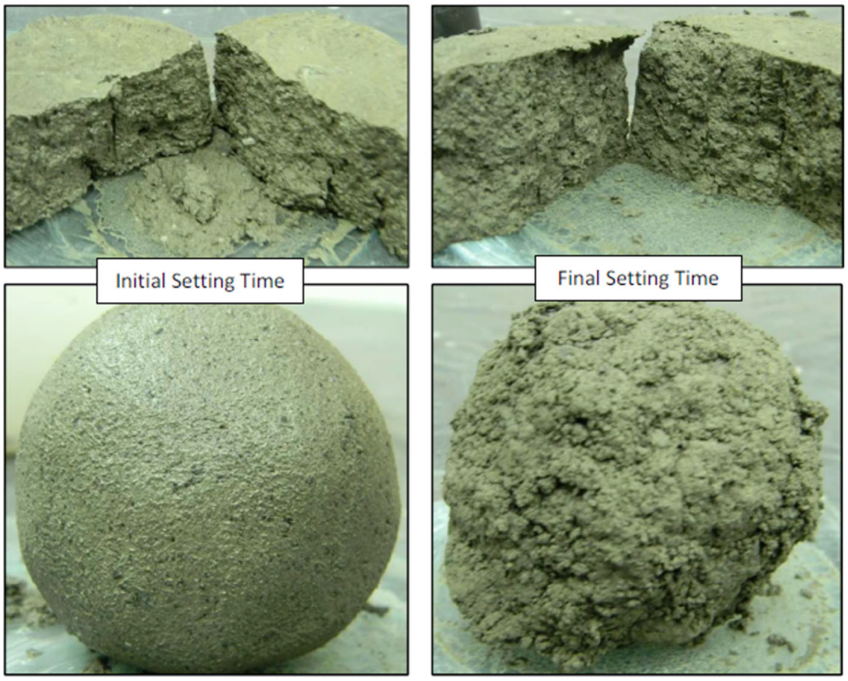

Figure 2.2: Pictures of moulded concrete at the initial and final setting times (Combrinck, 2011)

2.2. Rheology of concrete

From the earliest use of the word "rheology" in 1929, it was defined as the study of the flow of matter that takes the form between liquids and solids (Szecsy, 1997; Barnes, 1989). The most common form of interest is the simple shear flow or deformation (Roussel, 2012), hence the term shear rheology, which is the focus of this study. The initial quest for the study of concrete's rheology by early researchers was for its workability (Szecsy, 1997). Rheology was seen as the scientific approach to quantify and predict the flow behaviour of concrete, which defines its workability. ACI

116R (2000) defined workability as the property of freshly mixed concrete which determines the ease and homogeneity with which it can be mixed, placed, consolidated, and finished. That is, a workable concrete must be homogeneous, consistent, flowable, and compactible and should not segregate nor bleed excessively. The definition above is the qualitative approach to workability. As noted earlier, fresh concrete is a fluid (a state of matter that falls between liquid and solid) material with flow properties, hence, it has rheological properties. However, these rheological properties change with time, majorly due to stiffening and hydration that increases its solidification/setting. From the experience of this study, concrete's rheological properties are almost completely lost at the end of the plastic phase (initial setting time). Therefore, the rheology of concrete can be easily measured up to its initial setting time.

Quantitatively or empirically, rheological parameters and behaviours have been established that directly relate to workability, defining the rheology of concrete. They include yield stress (static and dynamic), viscosity (plastic and apparent), shear thinning, shear thickening, thixotropy, and rheopexy. These parameters and behaviours are discussed in the next sections. The quest or motivation for the study of rheology for this study is not for workability but for understanding the plastic phase of concrete. This is important because plastic cracking behaviour which is the primary intent of this study dominates the period between the end of mixing concrete up to the final setting time of concrete, that is, plastic-to-semi-plastic-to-solid phase. Hence, it theoretically and conceptually makes sense to say that there is bound to be an interaction between the rheological behaviour and plastic cracking behaviour during the plastic period. This forms the first conceptual theme for this study, other themes are highlighted during the course of this background study.

It is worth mentioning in this section that, over the years, progress in the rheology research has metamorphosized beyond the overall macroscale response of materials in terms of bulk shear flow or deformation. Microstructural (microscale) response of fluid materials to minute/micro cyclic shear stimulus or deformation referred to as dynamic mechanical analysis (to investigate a property known as viscoelasticity) has been in the forefront of cement-based materials' rheology. The classical or conventional method is referred to as rotational or static shear rheometry while the latter method is also termed oscillatory or dynamic shear rheometry. This is discussed later in this chapter as part of the background study.

2.2.1. Shear yield stress and strain

In solid mechanics, the yield stress and strain of a material refer to the maximum stress and strain the material can withstand before its breakdown (Hibbeler, 2014), they often define the design

strength and strain capacity of such material. In fluid mechanics, a material will only start to flow or deform after the applied shear stress or strain is above the yield stress or strain (Gerhart *et al.*, 2018). That is, a sample with a yield point will not flow if the external force applied to it does not exceed the internal structural forces (Mezger, 2014). Below the yield point, the material exhibits elastic behaviour with delayed recovery (Mezger, 2014). Fresh concrete behaviour inadvertently falls in line with the principles of fluid mechanics (preferably termed yield stress and strain in literature) but, as time progresses during the plastic state, it gradually deviates towards the principles of solid mechanics. The former principle being a form of ductile yield process while the latter being a form of brittle fracture process (Hibbeler, 2014), hence, plastic concrete behaviour falls between the two forms. As shown in Figure 2.1, during the dormant period of hydration, little or no pronounced mechanical (tensile and penetration) properties are developed, even up to the initial setting time. However, it has been established that a unique phenomenon called thixotropy gradually increases the shear yield stress (as a form of a reversible structuration) of cement-based materials during this period (Rahman *et al.*, 2014; Roussel, 2012; Roussel *et al.*, 2012), though not necessarily the shear yield strain (Yuan, Lu, *et al.*, 2017). The principle of thixotropy is explained later. The shear yield stress of concrete is in two forms, viz static and dynamic yield stress, these are explained below.

2.2.1.1. Static yield stress

When fresh concrete is at rest, that is, not flowing or under shear deformation, the static yield stress is its maximum resistance to shear stress before yielding or start of flow (Mezger, 2014). Based on the earlier submission in the previous section, static yield stress can be said to define the shear strength of plastic concrete, at least up to the initial setting time when plastic concrete loses its rheological properties. Plastic concrete behaves like a solid when the applied stress is smaller than the static yield stress and like a liquid when this stress is larger than the static yield stress (Roussel, 2012). The solid-like response of the plastic concrete below the static yield stress can be viscoelastic or viscoplastic depending on the magnitude of the applied stress. Viscoelastic response refers to an elastic response of the concrete to a small magnitude of applied load/stress below a critical value known as linear viscoelastic limit (this is explained in the next paragraph) while the viscoplastic response refers to an inelastic (plastic) response to a larger magnitude of applied stress (above the linear viscoelastic limit but below the static yield stress). The term “visco” originates from the fluid-like (viscous) properties of plastic materials such as that of the concrete during the plastic phase.

Like other rheological materials such as polymers (Mezger, 2014), two critical yield points have been established in the literature for cement-based materials (Roussel, 2012; Roussel *et al.*, 2012). The first critical yield point is the point below which the material has a linear elastic form of response/deformation with delayed recovery (viscoelastic), it is also referred to as the critical stress/strain or linear viscoelastic range/limit (LVR/LVL) (see Section 2.2.5.1). The second critical yield point is well above the first one and signifies the flow or failure point in which the material fails or starts to flow. In between the first and the second yield points, the material shows plastic or irreversible deformation/response (viscoplastic) in which the microstructure is overly stretched or bridged microcracks forms. These two critical yield points are illustrated in Figure 2.3 (Roussel *et al.*, 2012) and Figure 2.4 (Nehdi and Al Martini, 2009).

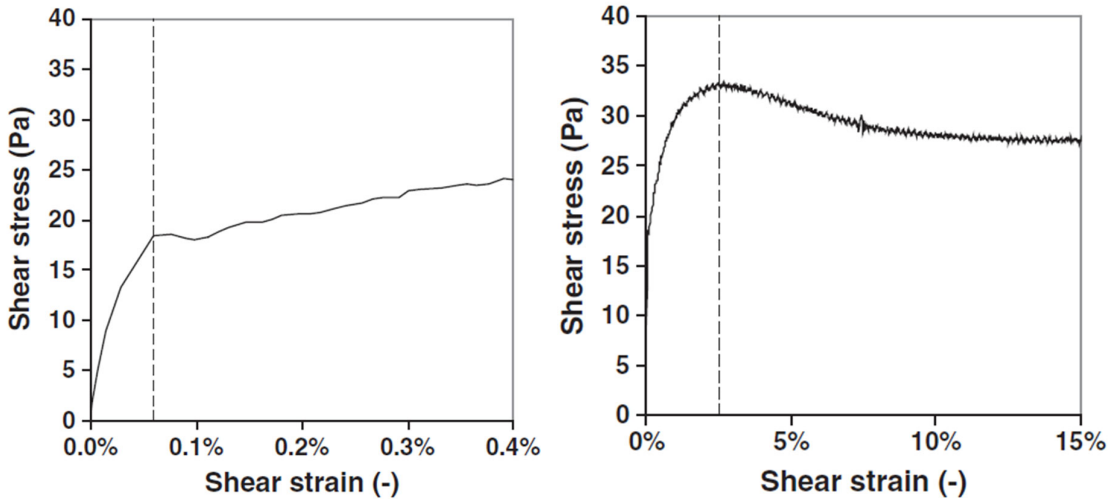

Figure 2.3: Critical yield points for a cement paste sample shown on different scales (a) first yield point or linear viscoelastic limit (LVR) (b) second yield point or flow point (Roussel *et al.*, 2012)

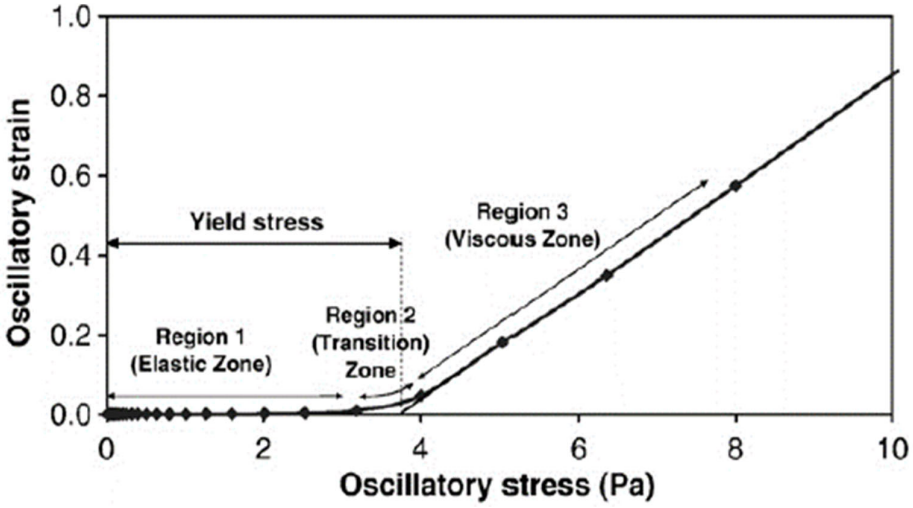

Figure 2.4: Critical yield points for a cement paste sample, first yield point or linear viscoelastic limit (end of Region 1) and second yield point or flow point (end of Region 2) (Nehdi and Al Martini, 2009)

As noted earlier, thixotropy particularly increases the static yield stress of concrete during the plastic phase as a form of reversible structuration. That is, thixotropy technically increases the shear strength of concrete during the dormant period of hydration. It can, therefore, be said that the evolution of static yield stress of concrete during the plastic phase majorly includes the effects of thixotropy (which is reversible) and not necessarily the permanent influence of hydration on the shear strength.

2.2.1.2. Dynamic yield stress

After a fluid has started flowing, dynamic yield stress refers to the stress required for the fluid to continue flowing or stop flowing (Qian and Kawashima, 2016; Koehler and Fowler, 2004). For fresh and plastic concrete under zero deformation (at rest), the application of shear load gradually breaks down the structure until it reaches the peak value that defines the static yield stress and shear strength respectively, afterwards there is a strain-softening until it reaches a residual yield stress and residual shear strength respectively. This residual yield stress may sometimes be referred to as dynamic yield stress by some authors (Kruger *et al.*, 2019; Jiao *et al.*, 2017), but it should be noted that this value is shear rate dependent (see Section 2.3.1.1) as compared to that evaluated from a flow curve result fitted with a model (Kolawole *et al.*, 2019a; Koehler and Fowler, 2004). This is depicted in Figure 2.5.

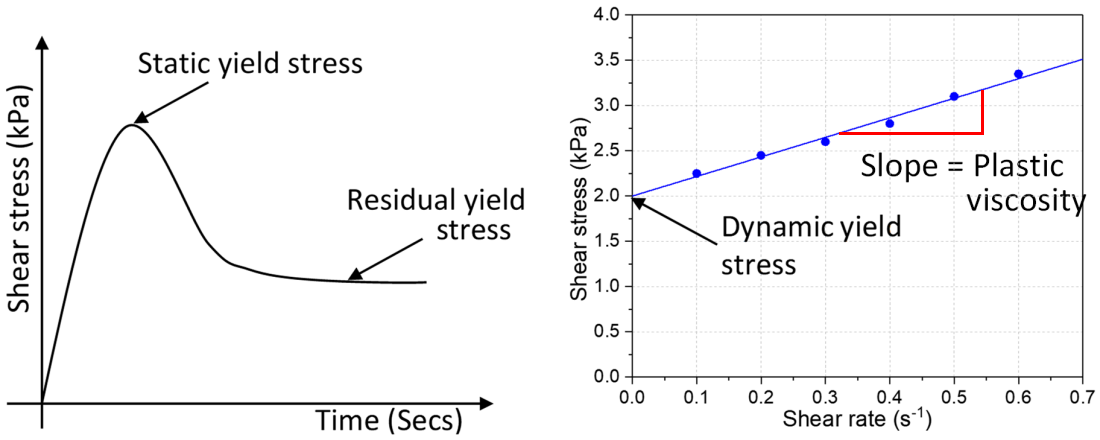

(a) Stress growth test (b) Flow curve test

Figure 2.5: Rheological test showing the static yield stress and dynamic yield stress

Practical application of concrete flow that can lead to a residual or dynamic yield stress is the vibration of concrete. The vibration of concrete causes its matrix to regain fluid behaviour with measurable shear resistance and cohesion (ACI 309.1R, 2008), that is, the vibration can be likened to a shear deformation. Furthermore, it has been reported in literature that vibration of a fresh concrete mix reduces its static yield stress to dynamic yield stress or to about half of the static yield

stress of a non-vibrated concrete (Li and Cao, 2019; Juradin, 2011; ACI 309.1R, 2008; Banfill, 2003; Tattersall and Baker, 1988). In fact, Banfill *et al.* (2011) stated that the vibration of concrete overcomes its static yield stress to cause flow under its own weight. The aftermath stress experienced under this vibration conditions is the dynamic yield stress. This vibration or shear deformation has, however, been reported not to influence the yield strain and viscosity of concrete (Yuan, Lu, *et al.*, 2017; Qian and Kawashima, 2016; ACI 309.1R, 2008). Concrete at rest after vibration, can therefore, gradually increase in yield strength due to thixotropy during the plastic phase before the drastic permanent influence of hydration. This idea is employed in this study for the fourth research theme (shear rheo-viscoelastic approach to plastic cracking).

The yield stresses and shear strengths (as part of rheo-physical properties) of the study's concrete mixes (fresh and plastic concrete) were rheologically evaluated in this study to determine their shear resistance to cracking. However, the dynamic yield stress of the fresh concrete mixes was one of the rheological emphases since the mixes were normally vibrated on a vibration table for the purpose of plastic cracking tests which formulates the third research theme.

2.2.2. Viscosity

Viscosity is defined as "the force per unit area necessary to induce motion/flow of a fluid" (Szecsy, 1997). In practical terms, it is the resistance created within the fluid structure against flow often due to internal friction (Mezger, 2014; Roussel, 2012). The less viscous a fluid is, the more easily the fluid can flow while a thickened fluid with high viscosity will flow less. Conceptually, it is similar to the stiffness of solid materials (Mezger, 2014). Complex fluids such as concrete do not have a constant viscosity but exhibit two forms of viscosity, namely plastic and apparent viscosity (Szecsy, 1997). This is explained in the next sections.

2.2.2.1. Plastic viscosity

For simple fluids, the plastic viscosity is taken as the shear stress divided by the shear rate. The shear rate refers to the rate at which shear strain is applied to the fluid. The constant plastic viscosity is possible for simple fluids (Newtonian fluid) and Bingham model fluids where the relationship between the shear stress and shear rate is constant at all shear rates. For a modified Bingham model fluid, this relationship is not constant (see

Figure 1.1). The viscosity at individual shear rates differs. Therefore, the plastic viscosity is taken as the slope of the line of best fit for the shear stress versus shear rate plot as shown in Figure 2.5b, that is, the average over a range of shear rates (Szecsy, 1997).

2.2.2.2. Apparent viscosity

Apparent viscosity is the viscosity of a fluid under fixed conditions such as certain shear rate and temperature (Mezger, 2014). Cement paste and concrete exhibit this behaviour, that is, they have varying viscosities depending on the shear load/rate (shear rate dependent). Therefore, apparent viscosity is estimated as the ratio between an applied shear rate and response shear stress of a fluid (Roussel *et al.*, 2010). Increasing or decreasing the applied shear rate will influence the value of the ratio. For some complex fluids such as concrete, the apparent viscosity can change with time under continuous shearing, this phenomenon is known as shear thickening/thinning and is explained in the next section.

2.2.3. Shear rate dependent rheological behaviour – shear thickening and thinning

Some complex fluids exhibit unique behaviours often referred to pseudoplastic power law (Tattersall and Baker, 1988), this is when the fluid changes its apparent viscosity under continuously applied shearing (Mezger, 2014). An increase in the apparent viscosity is referred to as shear thickening while a decrease in the apparent viscosity is referred to as shear thinning (Figure 2.6). That is, a shear thickening material will continuously become denser or thickened under the application of continuous shearing while a shear thinning material will continuously become softer or more viscous under constant shear rate. This can inadvertently lead to a state change in the material. In solid mechanics, it is referred to as strain hardening and softening while it is referred to pseudo-strain hardening and softening in the fracture behaviour of plastics (Kinloch and Young, 1995). These latter terms are also used for the purpose of behaviour of plastic concrete in this study. It is often idealised that shear thinning, and thickening is not permanent nor time-dependent (Chhabra, 2010), that is, reducing the fluid shearing makes the viscosity follow the same ascending path while stopping the shearing will make the fluid recover to its steady viscosity almost immediately. When a fluid exhibits shear thickening or thinning that is time-dependent, it is referred to as rheopexy and thixotropy respectively, and these are explained in the next section.

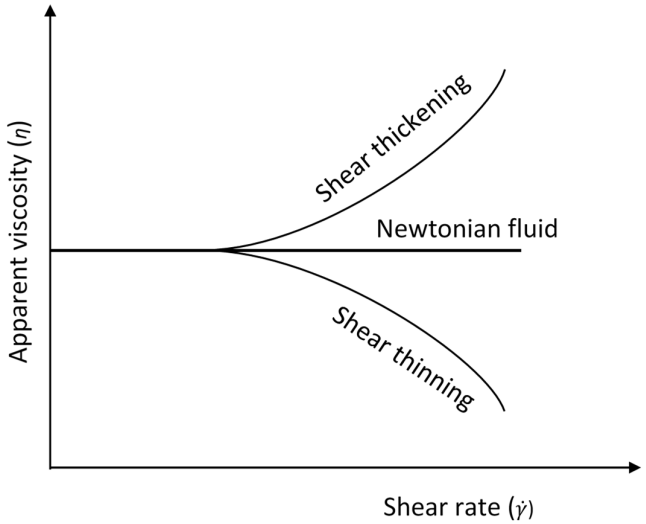

Figure 2.6: Shear thickening and thinning of complex fluids

Cement-based materials including concrete as a complex fluid are well known to be a shear thinning material (Roussel *et al.*, 2012), however, the inclusion of admixtures and influence of shear rate can make it exhibit shear thickening (Kolawole *et al.*, 2019a; Roussel *et al.*, 2010). In fact, results of this study (Kolawole *et al.*, 2019a) and that of (Chougnet *et al.*, 2007) show that concrete and cement can switch between shear thinning and thickening depending on factors such as resting time and deformation history. Factors identified in literature to be responsible for shear thickening and thinning are solid volume fraction, structural breakdown, alignment of rod-like particles during shearing, repulsion (steric or electrostatic) between suspended particles (Maybury and Ho, 2017; Bouras *et al.*, 2008; Phan *et al.*, 2006; Cyr *et al.*, 2000; Hoffman, 1998; Barnes, 1989).

2.2.4. Time dependent rheological behaviour – rheopexy and thixotropy

Rheopexy, also referred to as anti-thixotropy (Larson and Wei, 2019; Barnes, 1997), refers to the time-dependent thickening (increase in viscosity) of a material under continuous shearing (Chhabra, 2010). In other words, rheopexy is a time-dependent shear thickening. The corollary of this holds true, that is, rheopexy is the decrease in viscosity or yield stress (more fluidity) of a fluid under rest. The term anti-thixotropy was because thixotropy was defined as a macroscopic behaviour before rheopexy was discovered. The rheopexy phenomenon is usually of less research significance since they are uncommon (Chhabra, 2010). However, similar to shear thickening and thinning, cement-based material can switch between thixotropy and rheopexy due to shearing conditions as obtained in this study (Chapter 3) or due to the effects of pressurisation (Kim *et al.*, 2017). Thixotropic behaviour was discovered in 1923 but the term “thixotropy” was only coined in 1927 in the first paper that properly described the phenomenon (Barnes, 1997). Thixotropy is the increase in the thickening (yield stress and viscosity) of a material under rest and the time-dependent decrease of

the yield stress and viscosity under shearing (Larson and Wei, 2019). For example, the apparent viscosity of concrete that has undergone a rigorous oscillatory flow for ten minutes will be different from the concrete that underwent the same flow for thirty minutes or a gentle linear flow for ten minutes. Likewise, the yield stresses of such concretes will differ. The effects of thixotropy and rheopexy are idealised to be reversible and never permanent (Yuan, Zhou, *et al.*, 2017). For example, thixotropy of concrete has been established to be the gradual reduction of its viscosity under shear followed by a gradual recovery of the structure after stress removal (Ahari *et al.*, 2015; Barnes *et al.*, 2001).

Under rest, the thickening of cement-based materials is termed structuration or structural build-up or sometimes referred to as flocculation/coagulation/agglomeration. Over the years, the origin of thixotropy of cement-based materials has been well researched but remains controversial. A school of thought believes that it is dominantly due to colloidal flocculation at rest and particle-particle network from colloidal interaction and direct contact breakdown under shear (Qian and Kawashima, 2018; Yuan, Zhou, *et al.*, 2017). Another school of thought is that thixotropy is due to formulation of pseudo-contact hydration products during the dormant period of cement-based material hydration (Roussel, 2012; Roussel *et al.*, 2012). These early hydration products form on surfaces of cement particles to form CSH bridges or links between particles and form rigid networks (Roussel *et al.*, 2012; Roussel, 2006). These CSH bridges are easily broken under shear and simply form back under rest once there is an adequate reservoir of chemical species (mineral phases) responsible for the CSH bridges (Roussel *et al.*, 2012). A decisive judgement from this study (Chapter 4) and literature will be that both are responsible for thixotropy at a different magnitude of varying material-scales and timescales (see next paragraph).

For concrete, beyond the dormant and plastic phase where reversible thixotropy no longer exists, hydration becomes rapid and leads to a permanent form of structuration (Roussel *et al.*, 2010). Therefore, the term structuration refers to both the effects of thixotropy (that is, flocculation and pseudo-contact hydration products) and (permanent forms of) hydration at different timescales. In essence, both occur concurrently but the effects of thixotropy are reversible and on a shorter timescale while the effects of hydration mainly become permanent on a longer timescale (Roussel *et al.*, 2010) (towards the end of the plastic phase). It must be expressed in this section that, from the technical hands-on experience and obtained results of this study (Chapters 3 and 4), flocculation/coagulation/agglomeration is more pronounced for cement paste for a few minutes and occurs very rapidly before the influence of hydration kicks-in. The flocculation/coagulation/agglomeration is less noticeable for mortar and concrete with large unreactive aggregates and the main driving force for its thixotropy is hydration.

Thixotropy can be evaluated in terms of its macroscopic or microscopic response. The macroscopic response involves the development of the rheo-physical properties of concrete such as yield stress and viscosity. This form of evaluation usually destroys the material's structure. Microscopic response entails the use of non-destructive small amplitude oscillatory shearing to monitor the structural build-up with time. This is explained further in Section 2.3.2.5. Thixotropy, as a physical phenomenon (macroscopic response), becomes important for this study for its role in the evolution/increase of yield stress with time for fresh concrete and shear strength for plastic concrete up to the initial setting time earmarked to indicate the end of intrinsic rheological manifestation of concrete. Therefore, thixotropy was exhaustively (experimentally) evaluated for this study for the purpose of investigating plastic concrete's macroscopic structuration.

2.2.5. Rheo-viscoelastic behaviour of concrete

Viscoelasticity is the property of materials that exhibit both viscous and elastic tendencies when subjected to deformation (Marques and Creus, 2012) such as shearing. Though, it is arguable that certain percentages of viscous tendencies are found in most solid materials such as hardened concrete (Bazant and Gettu, 1992; Rossi and Acker, 1988; Bazant, 1975), fluid and plastic materials such as fresh and plastic concrete has pronounced viscous properties. As noted earlier, these viscous (fluid-like) properties reduce with time while the elastic (solid-like) properties increases with time due to the effects of stiffening and hydration (Sun *et al.*, 2006). Ideally, materials with pronounced viscous and elastic properties naturally occur in a state between liquid and solid, that is, they are often plastic. It is, therefore, convenient to characterise their viscoelasticity using rheological methods (Mezger, 2014; Ali and Kesler, 1965), hence the name rheo-viscoelasticity. On the other hand, test for viscoelasticity of solid materials such as hardened concrete (which are usually in the forms of creep and relaxation) involves the application of sustained mechanical loads for long period of time with no link to plastic rheological measurements (Shen, Jiang, Jiao, *et al.*, 2017; Shen, Jiang, Wang, *et al.*, 2017; Briffaut *et al.*, 2012; Tao and Weizu, 2006; Bissonnette and Pigeon, 1995). Therefore, the plastic phases of concrete which are the focus of this study qualifies to be characterisable by rheological methods to establish its viscoelastic behaviour since these phases have measurable rheological properties.

As noted earlier, advancement in rheology led to the possibility of viscoelastic characterisation of plastic materials via rheological methods (Mernard, 1999). It involves the application of cyclic/oscillatory form of small shear deformation stimuli, a process known as dynamic mechanical analysis. This process/method is discussed further in Section 2.3.2. The basic and important

viscoelastic properties which are of significance to engineers include creep and relaxation, because they influence materials response to strain and stress application as shown in Figure 2.7. However, rheo-viscoelastic approach goes beyond these. It allows engineers and material scientists to be able to determine some earlier identified rheological properties (that is, rheo-physical properties) such as static yield stress, apparent viscosity, shear thickening and thinning, and thixotropy. How these physical properties differ (in values) from the earlier discussed classical method is another subject matter among rheology scientists/society. Furthermore, the rheo-viscoelastic methods allow basic material properties such as linear viscoelastic range, shear modulus (stiffness), storage (elastic component of) modulus, loss (viscous component of) modulus, and phase angle to be determinable. The physical meanings of these latter properties are addressed in the subsequent sections while the methodology to determine them are discussed later in the chapter.

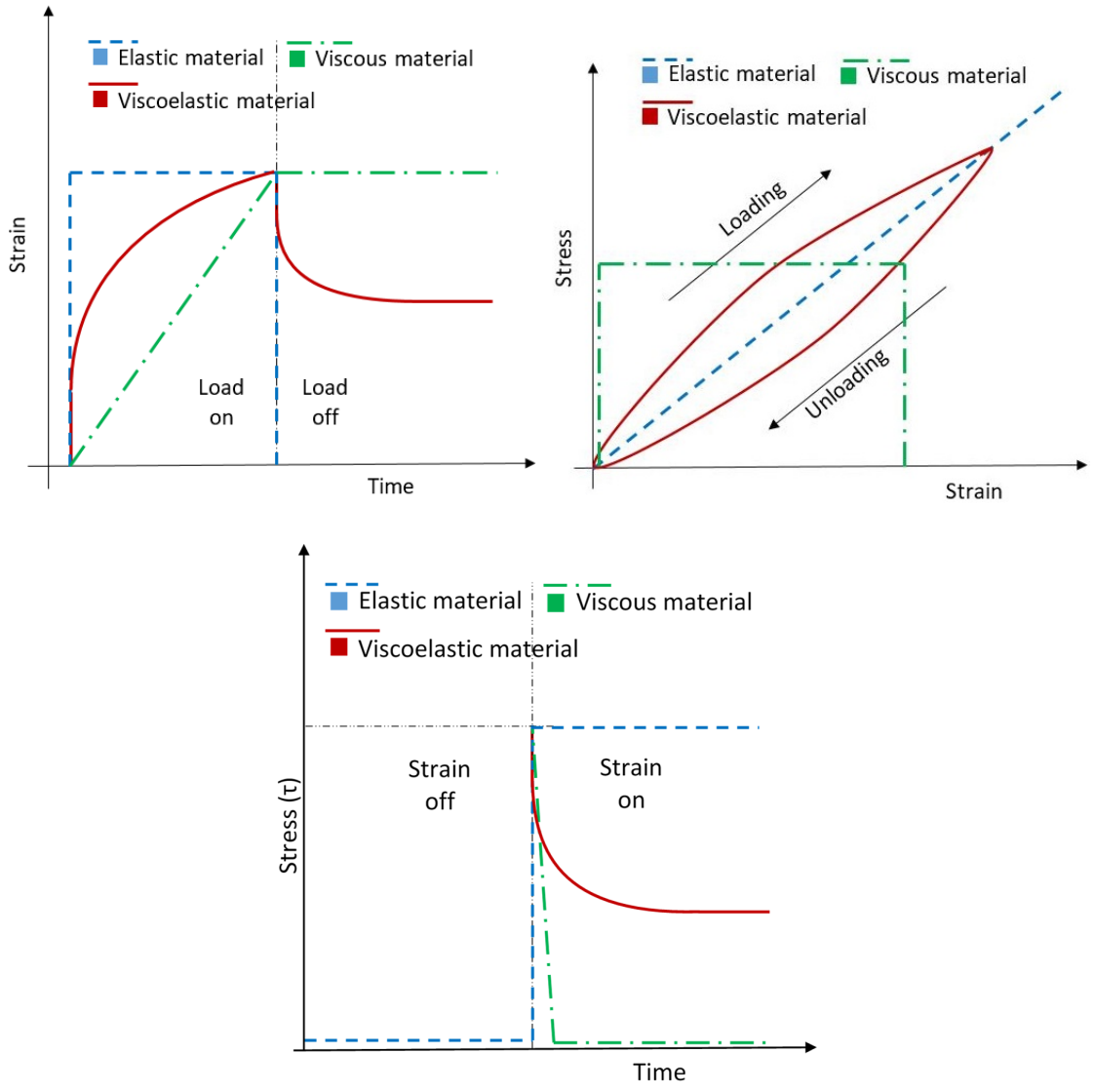

Figure 2.7: Responses of elastic, viscous and viscoelastic material to stress and strain

2.2.5.1. Linear viscoelastic range (LVR)

Linear viscoelastic range (LVR) refers to the largest magnitude of stimulus (strain or stress application) in which a material sample can be subjected without destroying its microstructure (Ma *et al.*, 2018; Mezger, 2014; Nachbaur *et al.*, 2001). It is also referred to as the linear viscoelastic region/limit (LVL) or critical strain. That is, the sample behaves like an elastic (solid-like) material or responds linearly within this range of stimulus with a delayed recoverable form of deformation. It is believed that within the LVR, the sample particles are in close contact with one another or cross-linked which yields a linear response to the stimulus (Qian and Kawashima, 2016; Nehdi and Al Martini, 2007; Schultz and Struble, 1993). Above the LVR, the sample's structure starts to disintegrate resulting in some irreversible form of deformation. It is believed that the applied stimulus above the LVR causes (the samples' particles to become separated or) an overstretching of the samples' microstructure (Qian and Kawashima, 2016; Nehdi and Al Martini, 2007; Schultz and Struble, 1993) resulting in possible micro-cracking/fracturing that are still bridged until complete failure. This range, above the LVE response but, before the material failure results into what is referred to as non-linear viscoelastic behaviour or viscoplastic behaviour. This is explained further in Section 2.3.2.

With respect to an elastic material's response to loading, an elastic material will linearly or elastically respond to a stimulus (such as normal strain) over a larger magnitude of range while the linear response range of VE material is rather smaller as shown in Figure 2.8. The figure reveals the difference in the magnitudes of the linear ranges of typical elastic and viscoelastic materials and the behaviour after the linear range. Moreover, the LVR of a VE material has a viscous part to its recovery. That is, though the response during LVR loading is elastic-like, there is a viscous component of the recovery (i.e., LVE response = elastic component + viscous component) due to energy dissipation as shown in Figure 2.8. This elastic and viscous component is expressible in terms of the stiffness (complex shear modulus) as storage and loss modulus, respectively. Furthermore, during a typical stimulus application, the viscous part of the response will be experienced as a phase lag between the applied stimulus (such as sinusoidal strain) and measured response (sinusoidal stress) of the VE material expressed as the phase angle (Mezger, 2014; Mernard, 1999). This is not the case for a purely elastic material. These terms are explained subsequently.

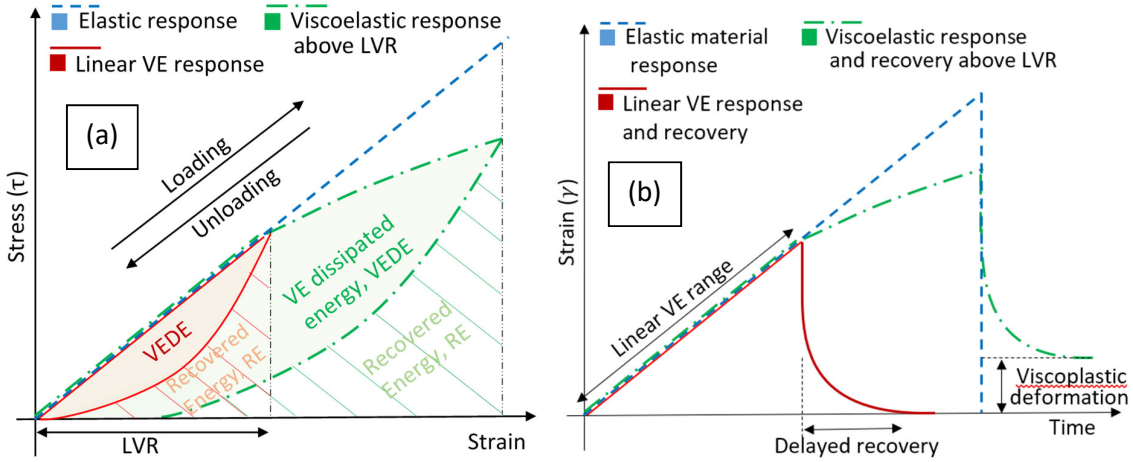

Figure 2.8: Typical responses of viscoelastic material to loading and unloading process

2.2.5.2. Shear modulus (G)

The shear modulus (G) is obtainable from rheo-viscoelastic tests and is often referred to as the complex shear modulus (G*) because of its sinusoidal oscillatory form of determination (Mezger, 2014). It is expressed as the relationship between the response shear stress and stimulus sinusoidal shear strain within the LVR. G is the shear stiffness of a material, that is, the measure of the resistance to shear deformation (Kim *et al.*, 2018). It is important that the G value is obtained within the linear viscoelastic range (LVR) because there is a reduction in the value of G above the LVR due to the viscoplastic response from overstretching the microstructure or micro-cracking.

2.2.5.3. Storage modulus (G'), loss modulus (G'') and phase angle (δ)

Storage modulus (G') is the measure of the deformation energy stored by a viscoelastic material during the application of a shear deformation (Mezger, 2014). That is, G' represents the elastic behaviour of the specimen material. It is an indication of the elastic component of the deformation energy that is responsible for shape recovery of the sample after the load is removed. A material that completely stores the deformation energy will show a linear reversible deformation behaviour after a load cycle (Figure 2.8a). Furthermore, G' indicates the intensity of cross-linking and interaction between the particles of VE materials, since this translates into the amount of deformation that can be stored (He *et al.*, 2018a). The loss modulus (G'') indicates the deformation energy that is used up or dissipated by the sample during the application of shear deformation (Figure 2.8a). That is, the component of the deformation energy that is dissipated or lost due to shape change (called viscous or frictional heating) and leads to some delayed recovery. A part of this frictional heat may heat up the sample or some part lost to the external environment (Mezger, 2014). It represents the viscous component of the deformation energy that is applied. A complex

sum of the storage and loss modulus yields the complex shear modulus as shown in Equation 2.1 while the relationship between the storage and loss modulus yields the phase angle (Equation 4.5).

$$G^* = G' + iG'' = |G^*|\cos\delta + i|G^*|\sin\delta = \sqrt{|G'|^2 + |G''|^2} \quad \text{Equation 2.1}$$

$$\tan\delta = \frac{G''}{G'} \quad \text{Equation 2.2}$$

G^*, G' and G'' are the complex, storage and loss modulus respectively, δ is the phase lag between the shear strain and stress, $i^2 = -1$.

The phase angle (δ) is the phase lag between an applied sinusoidal stimulus (strain or stress) and the measured sinusoidal VE material response (stress or strain respectively). The dynamic or sinusoidal form of application helps to measure this phase lag. The phase angle takes a value between 0° and 90°, the higher the phase lag, the more viscous the sample material and vice versa.

Table 2.1: Viscoelastic parameters of various material states Adapted from (Mezger, 2014; Nachbaur *et al.*, 2001)

Ideally viscous material	Viscoelastic liquid	Viscoelastic suspension or solid	Ideally elastic material
Viscous	Less viscous	Less solid	Solid
δ = 90°	90° > δ > 45°	45° > δ > 0°	δ = 0°
tan δ → ∞	tan δ > 1	tan δ < 1	tan δ » 0
G' → 0	G'' > G'	G' > G''	G" → 0
$G^* = iG''$	$G^* = G' + iG''$	$G^* = G' + iG''$	$G^* = G'$

2.2.5.4. Creep and creep recovery

This refers to the peculiar behaviour of viscoelastic material under sustained load or stress. A viscoelastic material subjected to a continuous application of constant stress undergoes increasing strain or deformation with time. The removal of such stress or load causes a viscoelastic recovery which, like the creep phase, has an elastic component, viscoelastic component and viscous components of the recovery. This is illustrated in Figure 2.9. This behaviour, which is in contrast to purely elastic behaviour (Figure 2.7), is mainly due to the viscous component of the viscoelasticity. Typical results of this behaviour of plastic materials can give information on the ability of the concrete to dissipate induced strains under sustained loading. It is, therefore, necessary to establish the creep and creep recovery behaviour of plastic concrete in order to evaluate how it can potentially influence the plastic cracking behaviour. For example, the dissipation of restrained settlement and shrinkage strains can potentially reduce the effective strains causing plastic cracking,

thereby reducing the plastic cracking potential. In another dimension, it has been shown in literature that creep of concrete at early age can help in reducing the effective strains experienced due to drying shrinkage by creeping in the opposite direction to the shrinkage strains (Khan, Castel, *et al.*, 2017; Hossain and Weiss, 2004).

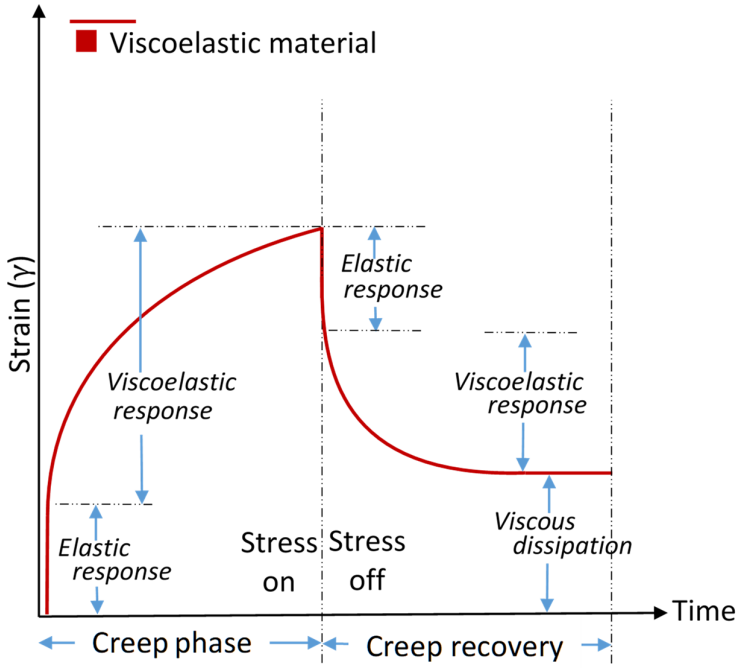

Figure 2.9: Creep and creep recovery pattern of a viscoelastic material

Creep of hardened concrete is well established in the literature, however, that of plastic concrete is scarce. The available study where creep (tensile) was examined at an early age was at 16 hours after casting (Østergaard *et al.*, 2001). Others were at later ages when the concrete is hardened (Shen, Jiang, Jiao, *et al.*, 2017; Shen, Jiang, Wang, *et al.*, 2017; Briffaut *et al.*, 2012; Tao and Weizu, 2006; Bissonnette and Pigeon, 1995). From available literature, creep behaviour of hardened concrete is usually evaluated from tensile or compressive stress using standard mechanical or new micro-indentation methods. For this study, rheological methods using dynamic shear rheometry was used for evaluating the creep and creep recovery of the plastic concrete. The presence of free water in concrete is believed to be responsible for creep (Rossi and Acker, 1988; Bazant, 1975). Water within the pores of concrete is not held permanently in position and can diffuse through the pores, the diffusion process (including that of some adsorbent solids) under continuously applied load is responsible for the change in dimension experienced as creep (Bazant, 1975). By implication, it is expected that as the viscous property of plastic concrete reduces due to stiffening and hydration, the creep ability and the attendant rheological capability of evaluation should reduce.

2.2.5.5. Stress relaxation

Stress relaxation is the ability of viscoelastic (VE) materials to relieve or reduce the induced stress in its microstructure over time. That is, when stress is developed in a VE material such as plastic concrete due to sustained strain application such as restrained settlement and shrinkage, the viscous component of the viscoelasticity makes the developed stress to be reduced over time. In practical terms of plastic cracking behaviour of concrete, stress relaxation can supposedly reduce the stress that develops from the restrained strains to a residual stress, thereby, reducing the cracking potential of plastic concrete. This residual stress can be said to be, hypothetically, responsible for plastic cracking initiation. This is illustrated in Figure 2.10 for a typical viscoelastic material showing the viscous and viscoelastic response, and the residual stress. Comparing this figure with Figure 2.7c reveals how plastic concrete (more viscoelastic material) will behave differently from that of hardened concrete (more elastic material). Similar to the creep, the stress relaxation ability of plastic concrete is expected to decrease as the concrete age increases due to the phase change from plastic nature to a stiff solid caused by stiffening and hydration. This was already shown in the study of Combrinck and Boshoff (2019) and Khan (2018) and was confirmed in this study.

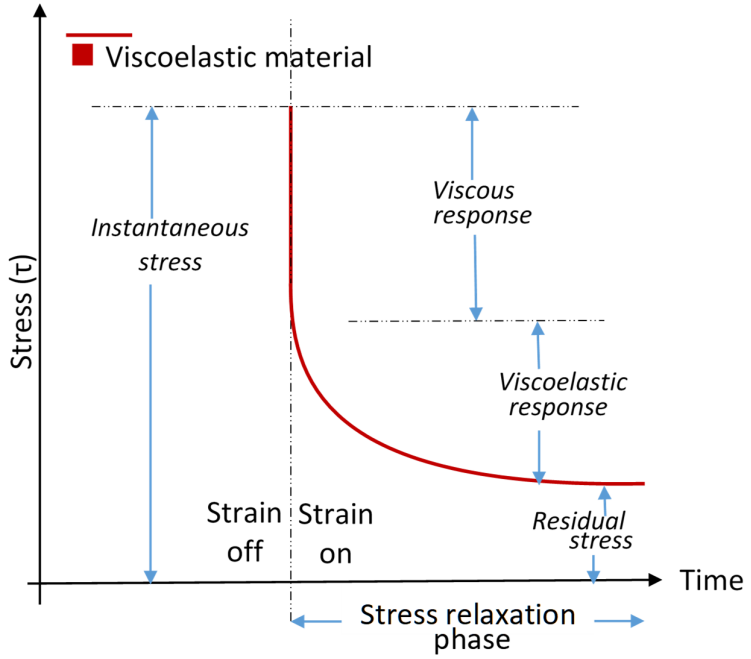

Figure 2.10: Typical stress relaxation pattern of a viscoelastic material

Arguably, the first article on relaxation dates to 1966 on polycrystalline magnesium (Gibbs, 1966). While the relaxation of hardened concrete has been established in previous researches, there is a scarcity of literature on stress relaxation of concrete in its fresh/plastic state. Apart from predicted

relaxation studies on hardened concrete, few experimental researches on relaxation are available in the literature (Bazant and Gettu, 1992; Taylor and Maurer, 1973) and they all made use of compressive strains. The available experimental research on stress relaxation used compressive strains applied to hardened concrete at ages 40 and 270 days (Taylor and Maurer, 1973) and 28 days (Bazant and Gettu, 1992), while others predicted compressive stress relaxation from compressive creep results. However, Combrinck and Boshoff (2019) and Nguyen *et al.* (2017) recently carried out a tensile stress relaxation test of concrete at a minimum of 1 and 5 hours respectively after mixing. The equipment set up required for early age concrete tensile tests is complicated, hence, many authors regard this as unattractive (Nguyen *et al.*, 2017; Combrinck, 2016; Pane and Hansen, 2002). There is, therefore, a scarcity of literature on shear (rheological-based) stress relaxation of concrete in its plastic state.

Similar to concrete creep, the presence of free water in concrete is believed to be responsible for stress relaxation since there is practically no relaxation in a completely dry concrete (Rossi and Acker, 1988). The application of instantaneous force for stress relaxation tests creates distributed microcracks in the concrete specimen. These microcracks allow for movement of water molecules from the micropores to the microcracks causing post cracking shrinkage. The stress from this post cracking shrinkage is believed to be responsible for the relaxation, by counteracting over time the stress induced by the constant strain of the test (Rossi and Acker, 1988). However, according to Kolver *et al.* (1999) and Altoubat and Lange (2001), creep is responsible for stress relaxation of concrete. For example, in the case of autogenous shrinkage of restrained concrete, the shrinkage causes internal stresses while the relaxation test load counteracts these internal stresses as a stress relaxation mechanism. The two above mechanisms were postulated for hardened concrete.

2.3. Measurement of rheological properties – shear rheometry

Shear rheometry refers to the process of applying shear deformation to fluid materials in order to examine and quantify its rheo-related properties. The process encompasses measuring systems, instruments, tests and analysis methods (Mezger, 2014). As noted earlier, shear rheometry, in engineering terms, allows the flow or shear deformation behaviour of complex materials such as fresh and plastic concrete to be characterised and predicted. It involves the basic principle of establishing the relationship between simple shear stimulus and the response of a sample, the stimulus and response can be shear stress and strain/rate or vice-versa (Roussel, 2012). Shear rheometry can be carried out using two basic test modes (Mezger, 2014). By applying a controlled shear strain or rate to the sample while measuring the response stress developed in samples

(shortened as CSR tests), instruments capable of this are referred to as strain-controlled rheometers. The second mode is to apply a controlled shear stress to the sample while monitoring the response strain or deformation of the sample (shortened as CSS test), sometimes the raw data can be in terms of torque and deflection respectively. Rheology instruments capable of the latter method are referred to as stress-controlled rheometers, however, it is common nowadays to have instruments capable of both methods (Mezger, 2014).

Over the years, the geometries that have been standardised for cement-based material's shear rheometers include cone and plate, parallel plates, coaxial, and vane geometries (Flatt and Schober, 2012). The conversion of instruments' raw data in relative units to rheological parameters in absolute units is based on various equations derived for each of the geometries (Mezger, 2014; Roussel, 2012). Testing methods of rheo-related properties of cement-based materials can be categorised majorly into two forms based on the kinds of motion, that is, rotational shear rheometry and dynamic shear rheometry. These are explained further in Sections 2.3.1 and 2.3.2.

2.3.1. Rotational shear rheometry

Rotational shear rheometry, also known as static shear rheometry, involves the application of one-directional rotational shearing to a sample to characterise its rheological properties. It is one of the widely and conventional used test method of rheometry (Ferraris and Martys, 2012). Most available rotational shear rheometers are often strain-controlled in which one surface rotates at a controlled rate while the response of the material is measured on the same rotating face (Ferraris and Martys, 2012). The vane geometry such as the ICAR rheometer (Germann Instruments A/S, 2015; Koehler and Fowler, 2004) used for this study comprises of a cylindrical container for the concrete and a rotating vane immersible into the container. Conversion equations for the measured raw data such as torque (Nm) and shear speed (rev/min) to rheological parameters such as shear stress (Pa) and shear rate (s^{-1}) for the ICAR rheometer (vane geometry) are given in Chapter 3.

Two basic tests are often performed or associated with rotational shear tests, they are the stress growth and flow curve tests (Koehler and Fowler, 2004). These are explained in the next sections.

2.3.1.1. Stress growth test

This is the test performed mainly to establish the yield parameters of concrete such as static and residual yield stress as shown in Figure 2.5a (Saak *et al.*, 2001). It is usually performed at a constant shear rate, however, the choice of shear rate is very important and should be preferably small but not excessively small (Koehler and Fowler, 2004). The optimum shear rate is material and rheometer geometry dependent (Koehler and Fowler, 2004). At a too small shear rate, the concrete structure

may reform (due to thixotropy) before reaching the yield stress resulting in a relatively high static yield stress (Koehler and Fowler, 2004). Also, at a high shear rate, several detrimental effects such as shear thickening, shear banding, particle migration (Qian and Kawashima, 2018; Koehler and Fowler, 2004; Geiker *et al.*, 2002) can influence the results. Hence, this method for evaluating the static and residual yield stress has been considered by some authors to be shear rate dependent (Qian and Kawashima, 2016, 2018; Yuan, Zhou, *et al.*, 2017). The selected speed of 0.025 rev/s, as used in this study and recommended for ICAR rheometer by the manufacturer, is from numerous trial tests to evaluate the influence of its vane speed on the static yield stress of concrete (see (Koehler and Fowler, 2004)).

It is believed that rotational shear rheometry yields the macroscopic or physical response of a material. That is, the application of irreversible continuously increasing shearing destroys the microstructure of the concrete sample and makes it difficult to depict the transition phases such as the concrete's shift from elastic response to viscoplastic response (He *et al.*, 2018a; Yuan, Zhou, *et al.*, 2017). Therefore, rotational shear rheometry is more appropriate to give information on the flow point or transition (viscoplastic) zone of concrete than the linear viscoelastic region (see Figure 2.4).

2.3.1.2. Flow curve test

This form of rotational shear rheometry test is often done to determine the flow parameters of concrete such as dynamic yield stress and viscosity (both plastic and apparent) as shown in Figure 2.5b. It is carried out on a steady state concrete (Nehdi and Al Martini, 2007), with sufficient thixotropic structure broken down. It is often carried out in the form of shear rate steps or ramps of increasing or decreasing shear rate after adequate pre-shearing which is plotted against the shear stress (Germann Instruments A/S, 2015; Mezger, 2014). Relevant flow parameters are thereafter determined by fitting rheological models that are relevant to concrete (see Chapter 1) to the flow curve data. It is believed that that the flow curve test depicts the rheological behaviour of concrete for various construction process such as pumping, placing and transportation (Nehdi and Al Martini, 2007). However, selected shear rates must be relevant to the intended process.

2.3.2. Dynamic shear rheometry (DSR)

As earlier stated, the advancement of research in the field of rheology has evolved beyond the macroscopic/physical flow or deformation of cement-based materials and now involves microscopic response. Though, the initial motivation for applying DSR to cement-based material was to understand the vibrational compaction of fresh concrete (Banfill, 1991), investigations into the

microscopic or microstructural response/deformation of cement-based materials have been made possible with the dynamic shear rheometry (DSR). DSR is also known as oscillatory shear rheometry (OSR) or dynamic mechanical analysis (DMA). It involves the application of oscillatory shearing (F_d) to a sample such as cement-based material and analysing the sample's response to the shearing, which is illustrated in Figure 2.11 and Figure 2.12.

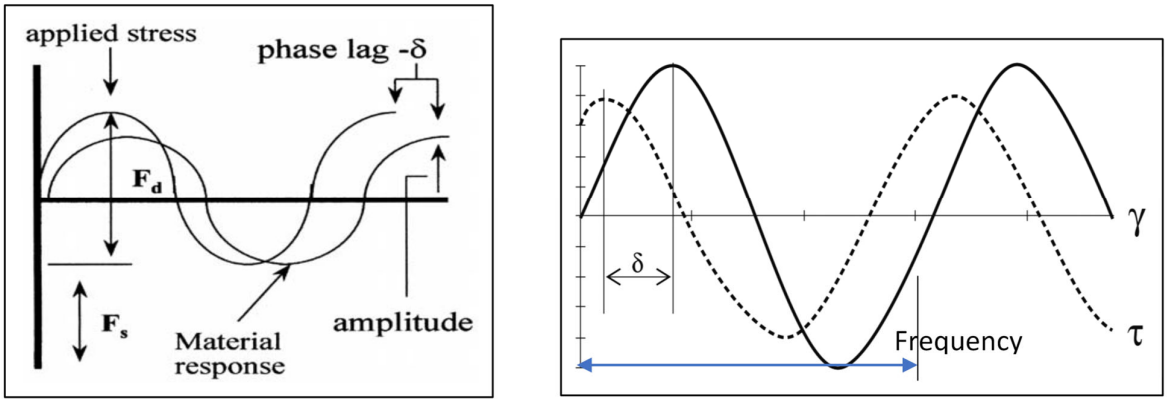

(a) (b)

Figure 2.11: Schematic diagram of dynamic shear analysis showing the phase lag (δ) (a) applied oscillatory shear stress (F_d) and materials' response (strain), F_s is the static or clamping force (Mernard, 1999) (b) applied oscillatory shear strain (γ) and material shear stress response (τ) (Mezger, 2014)

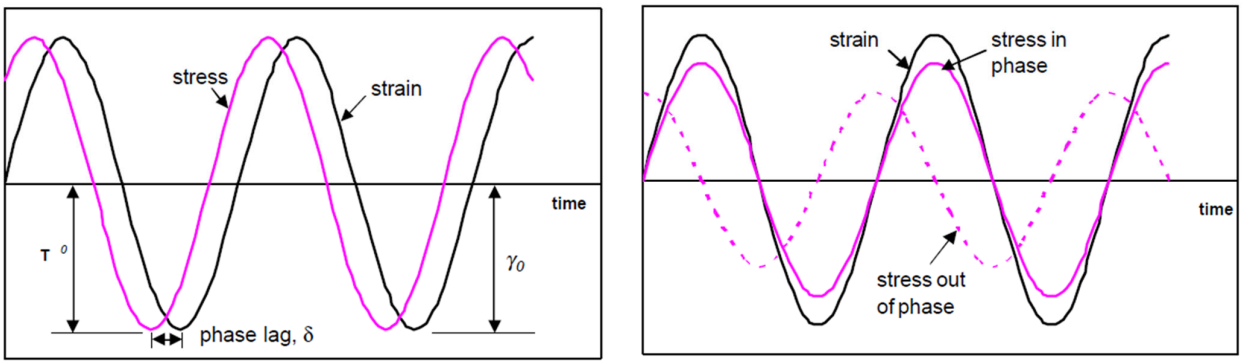

(a) (b)

Figure 2.12: Typical stress and strain relation of a viscoelastic material subjected to sinusoidal strain (Sun *et al.*, 2006) (a) Stimulus strain and response stress, showing the phase lag (δ) between them and (b) showing the response stress separated into components in and out phase with the stimuli strain

DSR can be categorised into two regimes or forms, small amplitude oscillatory shear (SAOS) and large amplitude oscillatory shear (LAOS) (He *et al.*, 2018a; Mezger, 2014; Hyun *et al.*, 2011) as shown in Figure 2.13. Both are named differently based on the amplitude (i.e. maximum value of stimuli strain/stress) of the applied shear. SAOS is commonly used for the purpose of linear viscoelasticity characterisation while LAOS can be used to examine the viscoplastic and viscous behaviour of materials (region above the linear viscoelastic range LVR – see Section 2.2.5.1) but is rarely used (He

et al., 2018a; Hyun *et al.*, 2011). Therefore, it is common to interchangeably use the terms SAOS and DSR. In the case of this study, the focus was on SAOS for characterising the rheo-viscoelasticity of concrete. Unlike rotational shear rheometry, SAOS is believed to be non-destructive, therefore, distinctively more tuned at detecting and giving good information on the transition process from the linear viscoelastic response to viscoplastic response (He *et al.*, 2018a; Yuan, Zhou, *et al.*, 2017).

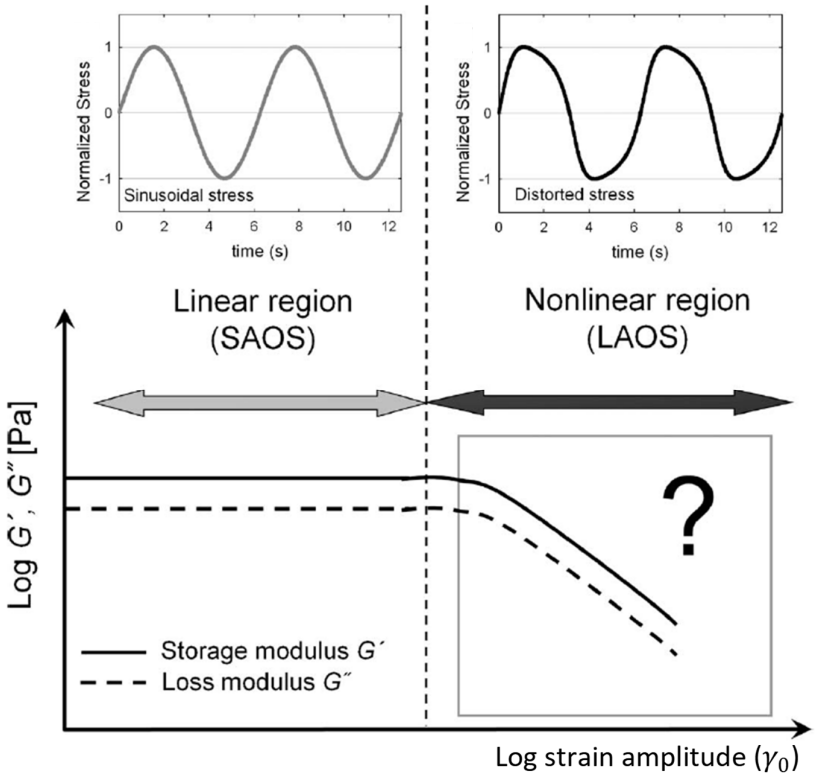

Figure 2.13: Dynamic shear rheometry showing the difference between SAOS and LAOS (Hyun *et al.*, 2011)

Like the rotational shear rheometer geometry used for this study, a smaller version of a vane-in-cup geometry (Roussel, 2012) was used with a Physica MCR 501 rheometer (Anton-Paar, 2009). Derived conversion constants/coefficients from raw data to rheological parameter for the rheometer (vane-in-cup) are given in Chapter 4 (as supplied by the manufacturer). Basic DSR tests carried out to fully characterise rheo-viscoelasticity of the cement-based materials include amplitude sweep, frequency sweep, creep and creep recovery, stress relaxation and thixotropy. Some description of these tests is in the sections that follow, more details of the tests and that of the dynamic rheometer are given in Chapter 4.

2.3.2.1. Amplitude sweep

This is a major test necessary to determine the shear-related properties of viscoelastic (VE) materials and characterise the VE behaviour. For this study, the amplitude sweep was strain-controlled by pre-setting the shearing rate (constant angular frequency) and testing at a variable strain amplitude

(stimuli) increasing with time. It can, therefore, be referred to as a strain sweep (Mezger, 2014). The applied strain and measured stress at a given time (t) of a cycle is given below while the typical raw data (relative units) and rheological parameters (absolute units) are given in Table 2.2 (Mezger, 2014).

$$\gamma(t) = \gamma_A . \sin \omega t \qquad \text{Equation 2.3}$$

$$\tau(t) = \tau_A . \sin(\omega t + \delta) \qquad \text{Equation 2.4}$$

where γ_A is the strain amplitude, τ_A is the stress amplitude, and δ is the phase angle in degrees, ω is the angular frequency.

The rheometer only measures two independent data results or responses as shown in Table 2.2 and these are converted to other parameters as shown below (He *et al.*, 2018a; Yuan, Lu, *et al.*, 2017; Qian and Kawashima, 2016; Mezger, 2014; Nehdi and Al Martini, 2007; Nachbaur *et al.*, 2001; Schultz and Struble, 1993).

$$G^* = \frac{\tau(t)}{\gamma(t)} \qquad \text{Equation 2.5}$$

$$G' = \frac{\tau_A}{\gamma_A} \cos \delta \qquad \text{Equation 2.6}$$

$$G'' = \frac{\tau_A}{\gamma_A} \sin \delta \qquad \text{Equation 2.7}$$

Table 2.2: Controlled shear strain raw data and rheological parameters of typical oscillatory tests (Mezger, 2014)

Oscillation CSR	Pre-set (stimulus)	Results (response)
Raw data	Deflection angle $\varphi(t)$ (mrad)	Torque $T(t)$ (mNm) and phase angle δ (°)
Rheological parameters	Strain (deformation) $\gamma(t)$ (%)	Shear stress $\tau(t)$ (Pa) and δ (°)

2.3.2.2. Frequency sweep

These are oscillatory tests carried out at variable frequencies that increase or decrease with time but at a constant amplitude of strain (for the case of this study). That is the maximum value of the deflection angle or strain (amplitude) is kept constant, only the time period for each oscillation cycle (shearing rate) is continuously increasing or decreasing (Mezger, 2014). Frequency sweeps are used to establish the range of frequency where the sample has stable and linear response that can be selected for other rheo-viscoelastic tests. At adequately low frequency, the viscoelastic (VE) material is oscillated slowly with ample time to relax the response stress before the start of another cycle of strain leading to no residual stress (Schultz and Struble, 1993). At relatively high frequency,

the VE material is oscillated faster than its relaxation time leading to residual stress build-up in each cycle of the test (Schultz and Struble, 1993). Frequency sweeps can also be used to examine the time-dependent linear deformation behaviour of VE materials since frequency is the inverse value of time (Mezger, 2014). Short-term behaviour under deformation is simulated by high frequencies while long-term behaviour is simulated by low frequencies (Mezger, 2014). Additionally, a frequency sweep gives an indication of shear thickening or thinning in cement-based material by monitoring the G' and G'' response to increasing/decreasing frequency (shearing rate) (Mezger, 2014; Saasen *et al.*, 1991).

2.3.2.3. Creep and creep recovery test

This test is used to analyse the viscoelastic (VE) behaviour of cement-based materials described in Section 2.2.5.4. It involves two shear stress steps, an immediate application of a step shear stress from zero to a pre-set value that is kept constant for a period of time. The second step follows by immediately removing the shear stress, that is, an immediate step from the initial pre-set value to zero while the response of the sample is monitored (Mezger, 2014). Care must be taken to ensure that the pre-set shear stress is within the previously linear viscoelastic range of the material.

2.3.2.4. Stress relaxation test

The stress relaxation test is used to investigate the viscoelastic (VE) behaviour of cement-based material described in Section 2.2.5.5. The test is performed by applying a pre-set step shear strain to a sample for a period of time while monitoring the response of the VE material, the pre-set strain is held constant for a period of time (Mezger, 2014). Likewise, the linear viscoelastic range of the material should not be exceeded.

2.3.2.5. Thixotropy test

The thixotropy of concrete described in Section 2.2.4 can be investigated by small amplitude oscillatory shear (SAOS). This form of investigation is a non-destructive microscopic probing into cement-based material microstructure in which very small and constant amplitude stimuli (shear strain in the case of this study) and frequency (shear rate) below the linear viscoelastic range (LVR) are used to monitor the structuration. The rheo-viscoelastic parameter monitored for this test, in this study, is the storage modulus since it is believed to indicate the intensities of physical cross-linking/interactions of particles and solid-like (elastic) tendencies of the cement-based particles, hence, a good indication for structuration (He *et al.*, 2018a; Yuan, Lu, *et al.*, 2017; Yuan, Zhou, *et al.*, 2017). A typical thixotropy test (as used in this study) is the three interval thixotropy test – 3ITT (Mezger, 2014). It is performed in three stages, the first stage involves the SAOS test of the sample

to establish a reference state of the material, this is followed by a second stage where the microstructure is subjected to heavy shearing to destroy the structure. The third stage of test is exactly the same as the first stage to monitor the restructuration up to and beyond the reference state of the first stage. It is believed that the employed SAOS test does not interfere with the restructuration since the selected shear amplitude and frequency are well below the LVR which does not disturb the structure (Anton-Paar, 2009).

2.4. Plastic cracking behaviour of concrete

Cracks in concrete can occur at different stages of its life due to various factors. However, plastic cracking refers to the cracking that occurs in the plastic state of concrete before it solidifies, that is from the time of mixing to the final setting time. As stated earlier, the exact point in time where the plastic state of concrete ends is ambiguous but is believed to be around the final setting time (Combrinck, 2016; Lura *et al.*, 2009; Sant, Dehadrai, Bentz and Weiss, 2009; Sant, Dehadrai, Bentz, Lura, *et al.*, 2009). All the processes that lead to plastic cracking, occurring between the time of mixing up to the final setting time, constitute the plastic cracking behaviour of concrete (Combrinck and Boshoff, 2013). These processes include but are not limited to bleeding, evaporation, setting times, mix constituents and proportions, restraint conditions, environmental conditions, capillary pressure build-up, plastic settlement, and plastic shrinkage (Sayahi, 2016; Leemann *et al.*, 2014; Combrinck and Boshoff, 2013; CCIP-048, 2010; Slowik *et al.*, 2008; Holt and Leivo, 2004; Dias, 2003; Uno, 1998). Major processes which are the focus of this study include setting time, evaporation, bleeding, capillary pressure, plastic settlement and plastic shrinkage. These are the measurable processes that drive the cracking behaviour of plastic concrete. It should, however, be noted that the two key pre-conditions for plastic cracking are bleeding/particle settling and evaporation, without them, plastic cracking may not occur.

How the major processes lead to the plastic cracking behaviour is explained in this paragraph. When fresh concrete is cast, it starts to bleed, this bleeding is due to the gravitational downwards sinking of the solid particles that allows the liquid phase to collect at the surface as bleed water. The presence of conditions for evaporation causes the bleed water to evaporate from the concrete surface as bleeding starts and continues. The downward sinking of the solid particles manifests in the whole concrete body as plastic settlement. Some authors refer to it as vertical plastic shrinkage (Ghourchian *et al.*, 2019). The complete evaporation of the surface bleed water causes the evaporation to access and dry up the pore water of the concrete which leads to negative capillary pressure build-up in the pores. The capillary pressure build-up later leads to horizontal plastic

shrinkage. The stiffening and setting of the concrete allow its skeletal structure to resist the plastic settlement and shrinkage with time. Summarily, the two sources of deformation during the plastic phase which when restrained causes plastic cracking are the plastic settlement and shrinkage strains. Hence, plastic cracking can take two forms which are plastic settlement cracking and plastic shrinkage cracking.

Plastic cracking can compromise the serviceability, durability and aesthetics of concrete (Ghourchian *et al.*, 2018; Leemann *et al.*, 2014) and should, therefore, be completely avoided. An example is accelerated corrosion of reinforcing steel bars at an early age (Combrinck, 2016).

2.4.1. Plastic settlement cracking

Plastic settlement cracking is due to differential settlement in concrete (Combrinck *et al.*, 2017; Combrinck, 2016; CCIP-048, 2010), that is, the vertical movement of concrete under gravity. The major component responsible for the settlement is the concrete's solid particles, ranging from cement particles to stone particles. As the particles settle in the fresh concrete, they displace water to the surface causing bleeding (Powers, 1968). There are three major forces acting on a settling particle, downward gravitational force, upward viscous drag and upward buoyancy force (Combrinck, 2016; Saak *et al.*, 2001; Powers, 1968). Their interaction and magnitude determine the settlement rate. The concrete settlement ends around the end of the plastic phase (Figure 2.4) of the plastic concrete when hydration accelerates (Combrinck, 2016). Settlement can also end when the particles settle to a saturated point and touch one another to prevent further settlement.

Uniform settlement across a fresh concrete specimen causes no cracks but if the settlement is not the same across the specimen, plastic settlement cracking can occur. That is, plastic settlement cracking is due to differential settlement within different sections of the concrete. Any form of restraint within a concrete specimen can be responsible for the non-uniform settlement. One of the most common is obstruction across the section of the concrete specimen such as steel reinforcement or the reduced vertical dimension of a specimen (Combrinck *et al.*, 2017). A typical manifestation is fine line cracks on a concrete slab along the length of reinforcing steel bars with the cracks having the same spacing as the reinforcement. Another major cause of differential settlement and cracking is a change in the formwork section (Combrinck *et al.*, 2017) such as L-beam and T-beam joint, causing cracks along the length of the joint. The extent of the potential for cracking is dependent on the difference between opposite settlement zones (Combrinck, 2016).

The extent of plastic settlement cracking depends on the amount/rate of settlement and degree of differential settlement. Factors influencing the former include setting times, concrete depth, water

content, aggregate dispersion, fine content, wall effect and capillary pressure (Safiuddin *et al.*, 2018; Yim *et al.*, 2013; CCIP-048, 2010; Kwak and Ha, 2006; Powers, 1968). Factors affecting the latter include formwork geometry, steel bars, concrete cover and factors influencing the amount/rate of settlement. Plastic settlement cracking can be prevented by utilising means of reducing the amount/rate of settlement as well as the degree of differential settlement or re-vibrating the concrete (Combrinck, 2016). Ways of reducing the settlement include the use of ultra-fine sand, micro fibres, air entrainers or increasing the cover to reinforcing steel and avoiding a sudden change in sectional depth (Combrinck *et al.*, 2017; CCIP-048, 2010; Powers, 1968).

2.4.2. Plastic shrinkage cracking

Concrete freshly cast settles under its weight due to gravity. The settling particles displace bleed water which evaporates if exposed to the external environment. Once the bleed water has completely evaporated, the pore water starts evaporating causing internal pressure build-up within the concrete specimen (Combrinck, 2016; Slowik *et al.*, 2008). There is potential for plastic shrinkage cracking only if the pore water is evaporated out of the plastic concrete. The pore water evaporation causes plastic shrinkage while the internal stress build-up leads to plastic shrinkage cracking if the concrete is restrained. However, at the end of final setting time, the concrete has solidified enough to resist the plastic shrinkage stresses and cracking.

Evaporation is therefore primarily responsible for plastic shrinkage cracking while the process behind the cracking is the capillary pressure build-up in the concrete's pores. According to Combrinck (2016), there are three stages of plastic shrinkage cracking. The first stage is when the bleeding rate is more than the evaporation rate, thereby there is always bleed water at the top of the concrete and capillary pressure cannot develop. As the bleeding closes to an end and evaporation continues, stage two begins. This is the drying time when the cumulative evaporation exceeds that of bleeding and pore water starts evaporating. As soon as pore water in concrete starts evaporating, a negative capillary pressure starts building up and the water surface in the pores curves downward (as concave water menisci) due to adhesive forces and surface tension (Slowik *et al.*, 2009), leading to downward and horizontal contraction.

According to Combrinck (2016), this can also result in downward forces responsible for an additional settlement that can aggravate plastic settlement cracking. As evaporation continues, the third stage comes next. At this stage, the concave water meniscus becomes smaller and eventually collapses leading to air entry into the concrete pores as weak spots, nevertheless, negative capillary pressure build-up continues at adjacent pores. This capillary pressure build-up is ideally relieved by the

downward and horizontal contraction, however, any form of restraint to this pressure widens the weak spots at the air-entry pores to form plastic shrinkage cracks.

Major factors affecting plastic shrinkage cracking are evaporation, bleeding, material constituents, mix proportion, setting and restraint (Sayahi, 2016; Boshoff and Combrinck, 2013; Combrinck and Boshoff, 2013; CCIP-048, 2010; Uno, 1998). However, the extent of cracking is complex due to a combination of these factors in unpredictable ways, making the influence of one or several factors in increasing the risk of cracking even more complex (Combrinck, 2016; Sayahi, 2016; CCIP-048, 2010). Measures of preventing plastic shrinkage cracking include protecting the concrete surface from evaporation and airstream, and using curing methods that prevent further evaporation when the bleed water has evaporated (CCIP-048, 2010; ACI 308R, 2001; Uno, 1998).

2.4.3. Combined plastic settlement and shrinkage cracking

Practically in the field, plastic settlement cracking can hardly be separated from plastic shrinkage cracking, that is, plastic cracks found in concrete specimens are often the combined effect of settlement and shrinkage cracking. For example, if a crack occurs on a concrete slab, it will be difficult to distinguish if it is due to plastic settlement or plastic shrinkage. Therefore, it is necessary to consider cracking caused by combined plastic settlement and plastic shrinkage. Figure 2.14 shows typical plastic settlement and shrinkage cracking, and reveals that if any of the two forms of cracking is to occur individually without interference from each other, they occur in a quick succession of each other. Therefore, distinguishing the individual cracks and the interaction between them remains complex (Combrinck *et al.*, 2017; Combrinck, 2016). Generally, plastic settlement cracking occurs first before plastic shrinkage cracking (Combrinck, 2016).

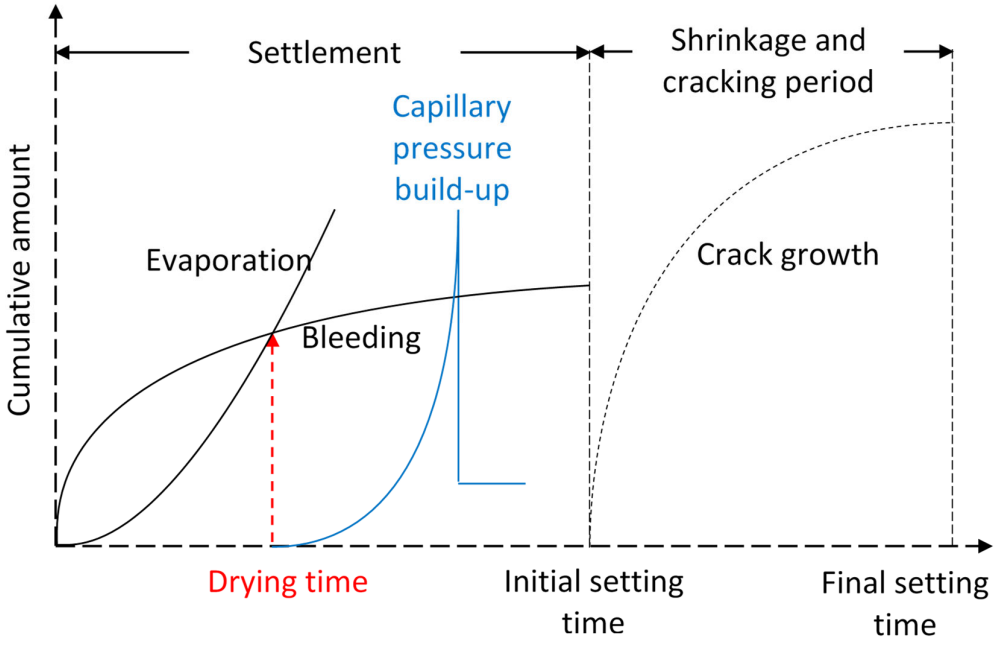

Figure 2.14: Typical plastic settlement and plastic shrinkage cracking (Combrinck, 2011, 2016; Boshoff and Combrinck, 2013; Maritz, 2012)

For example, a study by Combrinck *et al.* (2018a) showed that, though no reference was made in the ASTM C1579 (2006) proposed mould on the influence of plastic settlement cracking, multiple fine cracks were observed (identical to pure plastic settlement cracking) before significant capillary pressure build-up in environmental conditions simulated to delay capillary pressure build-up and plastic shrinkage. These cracks were very fine and hard to distinguish at the surface at such an early age due to the influence of bleeding; likewise, internal cracks were observed at the restraints. The study later concluded that the ASTM C1579 (2006) mould results in plastic settlement cracking amplified by plastic shrinkage cracking; leading to significant crack widening earlier than normally expected.

2.5. Summary

This chapter provides the needed background on the themes/objectives of this study. These include the description of plastic concrete, discussions on the rheological behaviour and structuration of concrete, the viscoelasticity of fresh and plastic concrete. Furthermore, methods of evaluating rheology of concrete were discussed, followed by the behaviour of plastic concrete in terms of cracking. This background study is not only useful for understanding the research themes of the study but also to give insights into the conceptual frameworks for the study.

During the review of the literature necessary for this background study, some gaps relevant to the objectives of the study were identified. They include the scarcity of modelling studies focused on

the initiation of shear microcracking of plastic concrete especially during the self-settlement phase. Also, studies on fresh/plastic concrete's viscoelasticity are also nearly non-existent in literature, including measurement of creep and stress relaxation by rheological methods.

Chapter 3: Measuring the thixotropy of conventional concrete: influence of viscosity modifying agent, superplasticiser and water

This chapter has been published as a journal paper in the Construction and Building Materials, Elsevier BV, with impact factor 4.046. Details of the paper are below:

Kolawole, J.T., Combrinck, R. & Boshoff, W.P. (2019). Measuring the thixotropy of conventional concrete: The influence of viscosity modifying agent, superplasticiser and water. Construction and Building Materials. 225:853–867.

Declaration by the candidate:

With regard to Chapter 3, the nature and scope of my contribution were as follows:

Nature of contribution	Extent of contribution (%)
This paper/chapter is part of the candidate's PhD research. All experimental work, the analysis, interpretation and presentation of data, as well as the writing of the manuscript were conducted by the candidate.	90%

The following co-authors have contributed to Chapter 3:

Nature of contribution	E-mail address	Nature of contribution	Extent of contribution (%)
Dr Riaan Combrinck	rcom@sun.ac.za	PhD research supervision, proofreading manuscript and insightful amendments	5%
Prof William Peter Boshoff	billy.boshoff@up.ac.za	PhD research supervision, proofreading manuscript and insightful amendments	5%

Signature of candidate: .....

Date: 8 October 2019

Declaration by co-authors:

The undersigned hereby confirm that

The declaration above accurately reflects the nature and extent of the contributions of:

1. The candidate and the co-authors to Chapter 3,
2. No other authors contributed to Chapter 3 besides those specified above, and
3. Potential conflicts of interest have been revealed to all interested parties and that the necessary arrangements have been made to use the material in Chapter 3 of this dissertation.

Signature of co-authors	Institutional affiliation	Date
	Department of Civil Engineering, Stellenbosch University	8 October 2019
	Department of Civil Engineering, University of Pretoria	8 October 2019

3.1. Abstract

This study sets out to evaluate the thixotropy of conventional concrete containing rheology modifiers using various methods of rotational rheometry. Five mixes were examined: the control, two mixes with viscosity modifying agent (VMA) and superplasticiser (SP) respectively, a mix with combined viscosity modifying agent and superplasticiser (VMA+SP) and the last mix with an increase in water content. These mixes were formulated to achieve concrete with varying rheological properties. Tests were carried out to examine the evolution of rheology parameters (static yield stress, dynamic yield stress and plastic viscosity), thixotropy index, shear thinning and thickening, structuration properties, torque decay pattern (with a subsequent drop in apparent viscosity), and hysteresis loop. Results show that conventional concrete known to be a shear thinning and thixotropic material, can possess anti-thixotropic (rheopexy) and shear thickening properties depending on the condition pre-history, resting time, shearing rate and inclusion of rheology modifiers. These factors also influence the magnitude of the thixotropy but not necessarily the evolution of thixotropy. Inclusion of VMA in conventional concrete showed only slight influence (both increasing and decreasing depending on the method of measurement) on its thixotropic behaviour while the inclusion of SP, VMA+SP and increased water considerably influenced concrete's thixotropic behaviour in a similar pattern. However, each rheology modifier resulted in a unique influence. VMA significantly improves the evolution of concrete's viscosity; inclusion of SP tends to result in a rheopectic concrete; addition of VMA+SP and pre-shearing of concrete may result in an unstable thixotropy, while SP can initially dominate the thixotropic behaviour of concrete containing both VMA and SP, VMA's influence may later surpass that of SP; more water in concrete tends to result in a lesser rate of thixotropic structure breakdown.

3.2. Introduction

Rheology is the study of the flow of fluids and thixotropy is a rheological phenomenon arising from the time-dependent microstructural response of a fluid due to shearing or resting. Fresh concrete is known to exhibit thixotropy (Roussel, 2006, 2012). For a concrete at rest, thixotropy is the increase in yield stress and viscosity with time (Roussel, 2006), resulting in a concrete that has rested to require more stress to initiate flow than concrete prepared fresh. This phenomenon is transient as the thixotropy breaks down when concrete is subjected to shear (Roussel, 2006). Anti-thixotropy is the opposite of thixotropy which causes some fluid to increase in viscosity due to the action of shear (Barnes, 1997); this phenomenon is also referred to as rheopexy (Chhabra, 2010). Time-independent thixotropy and rheopexy are referred to as shear thinning and shear thickening respectively (Chhabra, 2010); which can lead to a change in a fluid's state (Barnes, 1997). Shear thinning reduces concrete's viscosity (becoming more fluid) under continuous shearing while shear thickening increases the concrete's viscosity under the influence of shearing. Thixotropy in concrete is complex due to the time-dependent reversibility and microstructural rebuild which has no definite pattern of spatial molecule rearrangement (Barnes, 1997) and the concurrent influence of hydration (Roussel *et al.*, 2012; Flatt, 2004).

Thixotropy of concrete originates from the flocculation/coagulation, dispersion and hydration of cement particles (Ahari *et al.*, 2015) in the liquid phase (Quanji, 2010). When concrete is at rest, cement particles flocculate and hydrate to form gel structures and links between particles causing changes in the microstructure (Assaad *et al.*, 2003a). The flocculation and dispersion is an interplay of Van der Waals forces, electrostatic forces, and steric hinderance (Roussel, 2012; Quanji, 2010; Khayat *et al.*, 2002; Tattersall and Banfill, 1983). However, Roussel (2012) proved that the major source of cement's thixotropy is hydration which originates from CSH nucleation bridges between particles which is more powerful than colloidal flocculation forces between these particles. These hydration bonding forces are responsible for concrete's structuration; it can be broken and reformed quickly as long as there is enough water and cement particles responsible for the CSH nucleation bridges (Roussel *et al.*, 2012; Nonat *et al.*, 1997; Jiang *et al.*, 1995). Flocculation and structuration of concrete should not ideally influence its liquid phase and should not be mistaken for stiffening which is as a result of continuous hydration or drying that reduces the liquid phase in concrete. While both can occur concurrently in concrete, increased stiffening tends to make concrete lose its rheological properties.

Thixotropy in concrete has two phenomenal explanations depending on the application of interest: the build-up of its internal structure, i.e. flocculation/coagulation/structuration; and how it breaks down, i.e. deflocculation/decoagulation/destructuration. High viscosity reduces workability of concrete while at low levels it increases risks of segregation (Khayat *et al.*, 2008). High levels of thixotropy can help in reducing segregation and formwork pressure distribution with time (Roussel, 2006; Assaad *et al.*, 2003a). Thixotropy of concrete at rest during the dormant stage of hydration can increase the yield stress to a level where it can resist loads of additional layers of casting without increasing the lateral stress on formwork (Assaad *et al.*, 2003b).

There are various ways of determining thixotropy based on the degree of structuration at rest or destructuration at various shear rates (Khayat *et al.*, 2012), one is by finding the evolution of yield stress and viscosity of concrete with time by employing very low shear rates (Ahari *et al.*, 2015; Dzuy and Boger, 1985). Another method is to apply a constant shear rate to concrete and examining the decrease in shear stress over time (Rahman *et al.*, 2014; Roussel, 2006; Assaad *et al.*, 2003a). A traditional method is the use of a hysteresis loop (Abebe and Lohaus, 2017; Ahari *et al.*, 2015; Ferron *et al.*, 2007; Barnes, 1997; Tattersall and Banfill, 1983). It was defined by Assaad *et al.* (2003a) as the work done per unit time per unit concrete volume to break down all linkages and internal friction before reaching an equilibrium state. Roussel (2006) warned that this method does not give a quantitative value that is intrinsic to the concrete rheological property but is a good way to qualitatively compare mixes. Roussel, therefore, proposed a method that measures thixotropic properties of concrete as a means of quantifying concrete's structuration.

Some of the measurable parameters often used to characterise rheology of concrete are slump, static yield stress, dynamic yield stress, plastic viscosity and these parameters can be easily varied by rheology modifiers such as viscosity modifying agents (VMA), superplasticiser (SP) and water content. VMA is known to increase the yield stress and viscosity of concrete (Jiao *et al.*, 2017; Ahari *et al.*, 2015; Bouras *et al.*, 2012) by thickening the liquid phase of concrete with their polymer entanglement (Bouras *et al.*, 2012; Khayat, 1998). Superplasticisers (SP) improve the flow of concrete by dispersing cement particles through electrostatic and/or steric hinderance, thereby, reducing yield stress (Jiao *et al.*, 2017; Shen, Jiang, Jiao, *et al.*, 2017; Flatt and Schober, 2012; Artelt and Garcia, 2008; Gołaszewski and Szwabowski, 2004; Ur'ev *et al.*, 1997) but not necessarily the plastic viscosity. The combination of VMA and SP can potentially increase the rheological performance of concrete (Jiao *et al.*, 2017; Schmidt *et al.*, 2010; Prakash and Santhanam, 2006).

Increased water content in concrete reduces yield stress and plastic viscosity of concrete (Ahari *et al.*, 2015).

Some studies on thixotropy of cementitious materials have been on cement pastes/mortar (Yuan, Zhou, *et al.*, 2017; Bouras *et al.*, 2012; Roussel *et al.*, 2012; Quanji, 2010; Wallevik, 2009; Ferron *et al.*, 2007) because of the ease of measurement and equipment limitations. Other available studies on thixotropy of concrete has mainly been on self-compacting concrete (Ahari *et al.*, 2015; Rahman *et al.*, 2014; Khayat *et al.*, 2012; Roussel, 2006; Assaad *et al.*, 2003a) because of its peculiarity of being susceptible to segregation, instability and high formwork pressure. How the rheology modifiers influence the thixotropy of conventional concrete is lacking in the literature.

This study, therefore, aims at contributing to the body of knowledge on the thixotropy of concrete. Rheology of conventional concrete was altered using readily available rheology modifiers such as viscosity modifying agent, superplasticiser and water while the thixotropy of the ensuing mixes was evaluated exhaustively.

3.3. Experimental framework

3.3.1. Rheometer

Over the years, various rheometers have been invented to measure the rheology of concrete (Brower and Ferraris, 2006; Koehler and Fowler, 2004; Lapasin *et al.*, 1983), however few of them are practically usable in the field, majorly due to bulkiness and method of measurement (Hocevar *et al.*, 2013; Roussel, 2012; Koehler and Fowler, 2004). The ICAR rheometer was employed for use in this study. It is rugged, portable and easy to use, it was developed at the International Centre for Aggregate Research (ICAR) at the University of Texas in Austin (Koehler and Fowler, 2004). The ICAR rheometer is composed of a cylindrical container, driver head containing the electric motor and torque meter, four blade vane and computer (Figure 3.1 and Table 3.1). The container has a series of strips along its inside to prevent concrete slippage during testing. It is a rotational strain-controlled rheometer for measuring the static rheometry of concrete. It can be used for stress growth tests that give the static yield stress and torque decay or used for flow curve tests that give the dynamic yield stress and plastic viscosity as shown in Figure 3.2. Raw data of the torque and speed of the vane during testing can be used to calculate the Bingham model's rheological parameters (Equation 3.1).

$$\tau = \tau_o + \mu\dot{\gamma} \qquad \text{Equation 3.1}$$

Where τ is the shear stress, μ is the viscosity, τ_0 is the yield stress and $\dot{\gamma}$ is the shear rate.

Figure 3.1: ICAR rheometer

Table 3.1: Details of the ICAR rheometer

Minimum Torque (Nm)	0.01 Nm
Maximum Torque (Nm)	20 Nm
Maximum rotation speed	0.60 rev/s
Minimum rotation speed	0.01 rev/s
Vane size	63.5 mm radius, 127 mm height
Bucket size	305 mm diameter, 312 mm height
Concrete volume	22 litres

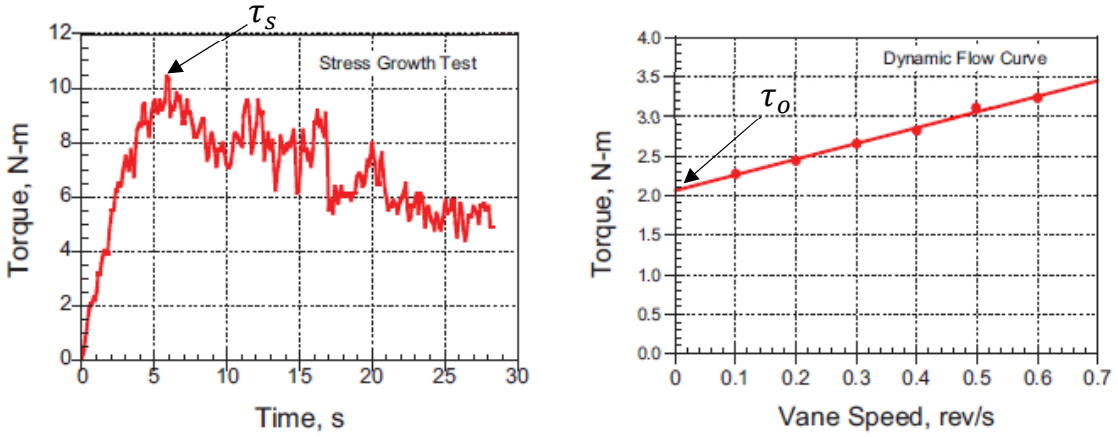

Figure 3.2: A typical stress growth and flow curve test from ICAR rheometer's computer

3.3.2. Material properties and mix design

The chemical properties of cement used for this study are shown in Table 3.2, the mix proportions and the constitutive materials used are given in Table 3.3 while the particle size distribution for the sand and stone are shown in Figure 3.3. Five concrete mixes were used for this study and they were formulated with the premonition of achieving varying rheology properties. The VMA and superplasticiser were measured by weight as a percentage of the cement. A modified polysaccharide liquid VMA and polycarboxylate ether (PCE) liquid superplasticiser were used. The

VMA has a specific gravity of 1.0, pH of 9.5, chloride content of less than 0.1% and sodium oxide content of less than 1% while the superplasticiser has a specific gravity of 1.05, pH of 7, chloride content of less than 0.1% and sodium oxide content of less than 1%. They were both added to the mixing water before adding the water to the dry constituents in the concrete mixer.

Table 3.2: Chemical properties of the cement

Oxides	CaO	Al_2O_3	Fe_2O_3	K_2O	MgO	MnO	Na_2O	P_2O_5	SiO_2	TiO_2	LOI
%	62.7	3.45	2.86	0.51	1.13	0.05	0.26	0.15	19.28	0.18	6.39

Table 3.3: Mix proportions and properties of the concrete mixes

Mixes	Material constituent (kg/m^3)				
	C	CV	CS	CVS	CW
Water	217	217	217	217	223
Cement - CEM II 52.5N	395	395	395	395	374
Specific surface area	1.336 m^2/g				
Malmesbury fine sand	774	774	774	774	796
Water absorption	8.57%				
Specific gravity	2.60				
6mm Greywacke stone	1029	1029	1029	1029	1018
Water absorption	1.65%				
Specific gravity	2.75				
VMA	-	0.6%	-	0.4%	-
Superplasticiser	-	-	0.6%	0.4%	-
w/c ratio	0.55	0.55	0.55	0.55	0.6
Slump (mm)	100	100	175	170	185
Initial setting time (mins)	360	360	420	320	420
Final setting time (mins)	420	420	510	420	480
C – control; CV – control + VMA; CS – control + SP; CVS – control + VMA + SP; CW – control + water					

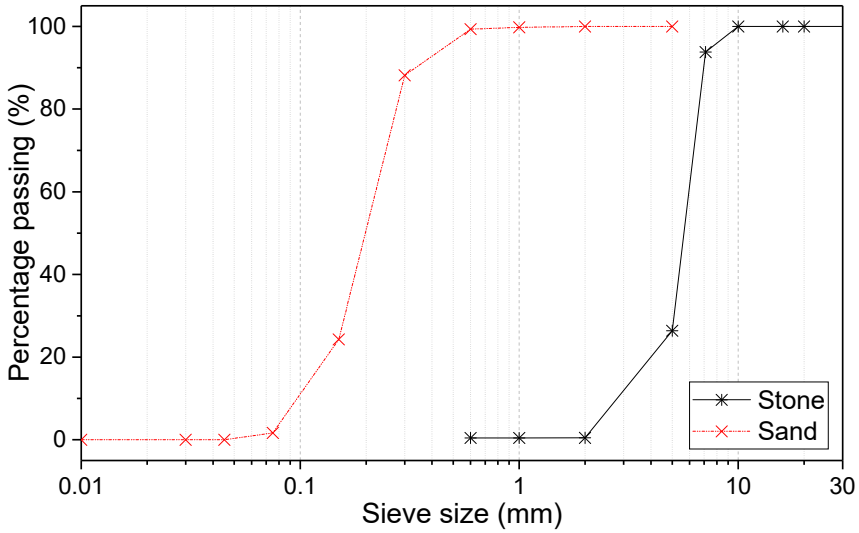

Figure 3.3: Particle size distribution of the aggregates

After adding stone, cement and sand to the concrete mixer, the materials were dry mixed for one minute before adding the mixing water. “Malmesbury” name of the used fine sand originates from its source, that is, Malmesbury town in Western Cape province, South Africa. Thereafter, the concrete was mixed for three minutes, that is, a total of four minutes mixing. The slump of the concrete was measured immediately for all sets. Concrete was then scooped into the ICAR bucket without vibration (as recommended by the manufacturer) and transferred to a climate-controlled room for testing, the climate room is maintained at a temperature of 23±2^{o}C and relative humidity of 65±3%. The time from the end of mixing to the start of test in the rheometer took approximately 10 minutes for all concrete sets, and the age of concrete is regarded as zero at the end of mixing. The setting time test was carried out in accordance to BS EN 196-3 (2005) after sieving out the mortar from the concrete while the gradation curve, water absorption and specific gravity of the aggregates were carried out in accordance to BS EN 933-1 (2012) and BS EN 1097-6 (2013) respectively.

3.3.3. Rheology tests

Rheology parameters were initially measured for all the concrete mixes. Stress growth tests were carried out on the concrete mixes at rest to determine the static yield stress of the concrete at a vane speed of 0.025 rev/s, followed by a flow curve test on the concrete at steady state to determine the dynamic yield stress and plastic viscosity. The steady state was achieved by a pre-shear of 0.5 rev/s for 60 seconds; this also helped to achieve comparable results and breakdown any thixotropic structure in the concrete (Koehler and Fowler, 2004; Geiker *et al.*, 2002). Three different samples were tested for each mix and the average reported in Table 3.4.

Table 3.4: Rheology properties of the concrete mixes

	Concrete mixes				
Parameters	C	CV	CS	CVS	CW
Static yield stress (τ_s, Pa)	3652.4	3803.8	1240.7	1329.9	1131.9
Dynamic yield stress (τ_o, Pa)	1155.9	1105.3	633.6	776.5	553.4
Plastic viscosity (μ Pa.s)	15.3	16.6	6.8	2.9	4.7

3.3.3.1. Static yield stress (τ_s)

From Figure 3.2a, the peak torque of the stress growth test at a vane speed of 0.025 rev/s is used in the calculation of the static yield stress using Equation 3.2.

$$\tau_s = \frac{2T}{\pi D^3 \left(\frac{H}{D} + \frac{1}{3}\right)} \qquad \text{Equation 3.2}$$

Where τ_s – static yield stress (Pa), T – peak torque (Nm), D – diameter of the vane, H – height of the vane.

3.3.3.2. Dynamic yield stress (τ_o) and plastic viscosity (μ)

From Figure 3.2b, the y-intercept of the flow curve is used in calculating the dynamic yield stress while the gradient is used in calculating the plastic viscosity. The flow curve test was carried out from a speed of 0.5 rev/s to 0.05 rev/s, measuring 10 points at 5 seconds per point. The recorded torque is plotted against the vane speed, which is used to calculate the Bingham model parameters using a modified Reiner-Riwlin equation (Equation 3.3 and Equation 3.4) (Germann Instruments A/S, 2015; Koehler and Fowler, 2004). Equation 3.3 applies to the case when all the concrete in the cylinder flows while Equation 3.4 is used when the shear stress in a portion of the concrete is below the yield stress, resulting in a dead zone of zero shear forming an annulus (Germann Instruments A/S, 2015; Koehler and Fowler, 2004).

$$\Omega = \frac{T}{4\pi h\mu}\left(\frac{1}{R_1^2} - \frac{1}{R_2^2}\right) - \frac{\tau_o}{\mu} ln \frac{R_2}{R_1} \qquad \text{Equation 3.3}$$

$$\Omega = \frac{T}{4\pi h\mu}\left(\frac{1}{R_1^2} - \frac{2\pi h\tau_o}{T}\right) - \frac{\tau_o}{2\mu} \ln \frac{T}{2\pi h\tau_o R_1^2} \qquad \text{Equation 3.4}$$

Where Ω – rotation speed (rad/sec), T – torque (Nm), μ – plastic viscosity (Pa.s), τ_o – dynamic yield stress (Pa), R_1 – cylinder radius, R_2 – vane radius.

3.3.4. Thixotropy evaluation and tests

The deformation pre-history of the concrete influences the measurement of thixotropy (Barnes, 1997) and include the mixing and casting method used to fill the rheometer. Methods that can be used to establish a consistent initial condition for test samples are: fixed resting time after placing samples, and pre-shearing at a selected rate and time followed by a resting time. Other aspects include mechanical inertia of the rheometer instrument, local damage around tips of the rheometer's vane, and wall slippage (Rahman *et al.*, 2014; Barnes, 1997). For this study, the ICAR rheometer is strain-controlled and therefore has torque transducers (Koehler and Fowler, 2004), minimising the influence of its mechanical inertia (Franck, 2005). In addition, the ICAR rheometer container has a series of strips along its inside to prevent concrete slippage during testing. The initial conditions of the test samples were achieved based on the following test program.

3.3.4.1. Test procedures

Two procedures, depicted as Sets A and B, were used to establish a consistent initial condition for all the test samples depending on the thixotropy test of interest, viz:

- Allowing the concrete to rest for a specified time after mixing, that is, 10 minutes and 30 minutes. Note that this time includes filling the rheometer's container and transporting it to a climate-controlled room which takes about 10 minutes. This procedure is depicted as Set A. A fresh concrete sample was used for each of the rest periods (10 and 30 minutes) to avoid the influence of the test(s) that was carried out after each rest period.
- Applying a pre-shear of 0.5 rev/s for 60 seconds to the concrete sample to reach a steady state followed by specified resting times of 5 minutes, 15 minutes and 30 minutes. This procedure is depicted as Set B. Note that the same concrete sample was used between each of these rest periods for this second procedure.

3.3.4.2. Thixotropy evaluation using rheology tests

Conducting rheology tests as in Section 3.3.3 combined with the two test procedures mentioned in the previous section, the following were evaluated to characterise the thixotropy of the concrete mixes.

- **Rheological evolution**

Static yield stress (τ_s), dynamic yield stress (τ_o), and viscosity (μ) of all the mixes were determined to examine their evolution with time and an index calculated subsequently. The thixotropy index is simply the difference between the τ_s and τ_o (Yuan, Zhou, *et al.*, 2017; Koehler, 2013) as a percentage of the τ_o (Equation 3.5). This idea comes from the fact that τ_o represents the yield stress after thixotropy has been broken down by the pre-shear (i.e. equilibrium state) while the τ_s represents that of a material at rest with substantial thixotropy development. The thixotropy index, therefore, indicates how much of the concrete structure was built (as thixotropy) within the specified period.

$$\text{Thixotropy index} = \frac{\tau_s - \tau_o}{\tau_o} \times 100\% \qquad \text{Equation 3.5}$$

- **Shear thinning and thickening**

For the flow curves of the concrete mixes, the Herschel-Bulkley model (Equation 5) was fitted to determine the mixes' shear thinning or thickening properties. Shear thinning or thickening in concrete can be evaluated by fitting either the Herschel-Bulkley model or modified Bingham model

(Li *et al.*, 2017; Khayat *et al.*, 2008; Cyr *et al.*, 2000) to the flow curve of the concrete mixes. For this study, the Herschel-Bulkley model was used because it was found to give a better fit (higher coefficient of determination, R^2) with a minimum R^2 of 0.92 while modified Bingham model had a minimum R^2 of 0.89.

Herschel-Bulkley's model: $\tau = \tau_o + K\dot{\gamma}^n, \tau \geq \tau_o$ Equation 3.6

τ is the shear stress, K is the consistency factor, τ_0 is the yield stress, $\dot{\gamma}$ is the shear rate, and n is the flow behaviour index which indicates the degree of shear thickening or thinning. When $n > 1$, the concrete possesses a potential for shear thickening while it has shear thinning property when $n < 1$. As noted in the Section 3.3.5, due to the geometry of the rheometer, relative parameters of rheology (Torque and shear speed) were used in fitting the model (Li *et al.*, 2017; Cyr *et al.*, 2000).

- **Structuration at rest and de-structuration under shear**

Using a thixotropy model proposed and validated by Roussel (2006) (Equations 3.7 – 3.13), the structuration properties of the concrete were evaluated from the rheology test results. The model quantitatively measures the structuration rate (A_{thix}), structuration state (λ) and structuration characteristic time (T) of a fluid concrete. In simplified form, it is a Bingham's model but with a parameter called structuration state (λ) introduced to incorporate the thixotropy property, it can be summarised as follows:

$$\tau = (1 + \lambda)\tau_o + \mu\dot{\gamma} \quad \text{Equation 3.7}$$

$$\frac{\partial\lambda}{\partial t} = \frac{1}{T} - \alpha\lambda\dot{\gamma} \quad \text{Equation 3.8}$$

λ is the structuration state of the material, T is the characteristic time of structuration, and t is time and α is a thixotropic parameter. It is assumed that the time for concrete to reach a fully structured state is relatively high compared to the time required to de-structurate (characteristic time of de-structuration). That is, $1/T = 0$ leading to Equation 3.9 and Equation 3.10.

$$\frac{\partial\lambda}{\partial t} = -\alpha\lambda\dot{\gamma} \quad \text{Equation 3.9}$$

$$\lambda = \lambda_o e^{-\alpha\dot{\gamma}t} \quad \text{Equation 3.10}$$

The evolution of the shear stress with time becomes

$$\tau(t) = \left(1 + \lambda_o e^{-\alpha\dot{\gamma}t}\right)\tau_o + \mu\dot{\gamma} \quad \text{Equation 3.11}$$

For concrete at rest, shear rate ($\dot{\gamma}$) is zero, therefore, the apparent yield stress evolves as shown in Equation 3.12.

$$\tau_o(t) = (1 + \lambda)\tau_o = \tau_o + \tau_o \frac{t}{T} = \tau_o + A_{thix}t \qquad \text{Equation 3.12}$$

With

$$A_{thix} = \frac{\tau_o}{T} \qquad \text{Equation 3.13}$$

A_{thix} is referred to as structuration rate. These structuration parameters (A_{thix}, λ, T) were evaluated for the concrete mixes.

3.3.5. Thixotropy tests – Torque decay and reduction in apparent viscosity

To examine how the thixotropy in concrete is broken down over time and the effect of shear rate, stress growth tests (as torque decay) at 0.02, 0.05 and 0.275 rev/s were carried out for a considerable time after the peak torque was reached and the steady state surpassed. Furthermore, the torque recorded is a measure of the resistance of the concrete to shearing and the decay over time show how this resistance reduces, thereby giving an evaluation of the rate of thixotropic dissipation of the concrete mixes. The 10 minutes resting time was only tested for Set A concrete while 5, 15, and 30 minutes resting times were tested for Set B. However, only 10 minutes resting time of Set A and 30 minutes resting time of Set B were reported for the torque decay because other resting times yielded little or no decay. The duration of this torque decay majorly depended on when a steady torque (i.e. steady state) was reached and is taken to be when the difference between consecutive torque measurements is less than 2% within a period of two minutes.

Due to shearing of the concrete samples, the apparent viscosity is expected to reduce with time until it reaches a steady value at the steady state; therefore, the drop in apparent viscosity also indicates the breakdown of thixotropy. Due to the ICAR rheometer geometry, absolute rheology parameters (shear rate and apparent viscosity) may not be calculable and are prone to error from the equipment's raw data/relative values (shear speed and torque), however it is known that the torque is proportional to the shear stress and shear speed proportional to the shear rate (Roussel, 2012; Brower and Ferraris, 2006; Mezger, 2006; Koehler and Fowler, 2004). Therefore, the reduction in apparent viscosity ($\Delta\mu_{app}$) due to the torque decay as a measure of thixotropy breakdown was calculated from the relative values of torque and shear speed (Ahari *et al.*, 2015) as shown in Equation 3.14.

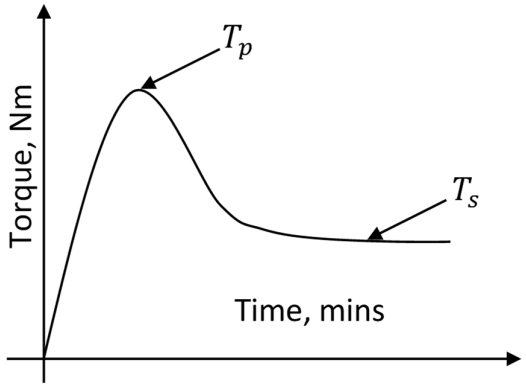

Figure 3.4: Typical torque decay graph for concrete at low shearing speed

$$\Delta\mu_{app} = \frac{T_p - T_s}{shear\ speed} \qquad \text{Equation 3.14}$$

where T_p – peak torque (Nm), T_s – steady torque (Nm).

3.3.6. Thixotropy tests – Hysteresis loop

Hysteresis loop, referred to as breakdown area by some authors (Ahari *et al.*, 2015; Assaad *et al.*, 2003a), is the area between measured series of torques/shear stresses at increasing shear speeds/rates when concrete is at rest and after its structural breakdown at decreasing shear speeds/rates (Figure 3.5). This test involved carrying out two flow curve tests consecutively. The first was carried out on the concrete at rest from a low shear rate (0.05 rev/s) to high shear rate (0.5 rev/s), followed by shearing the concrete at 0.5 rev/s for 60 seconds to breakdown thixotropic structure and the second flow curve test was done at a decreasing speed of 0.5 rev/s to 0.05 rev/s. The area between the two curves is referred to as the hysteresis loop area; if there is no thixotropic structure in the test sample, the curves are expected to follow the same path.

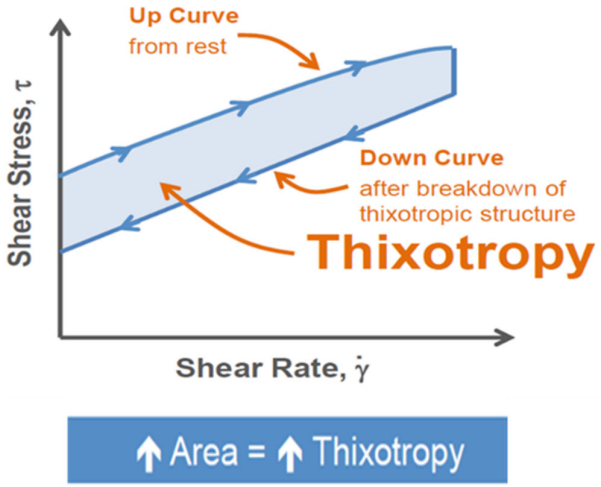

Figure 3.5: Typical hysteresis loop (Koehler, 2013)

3.4. Results and discussion

3.4.1. Rheological evolution

3.4.1.1. Static yield stress

Static yield stress (τ_s) gives an indication of the extent of structuration of concrete (Ahari *et al.*, 2015; Assaad *et al.*, 2003b) and its evolution with time shows how thixotropy builds up (Figure 3.6). For this test, low shear speed of 0.025 rev/s breaks the interparticle and attractive forces in the concrete to measure its shear strength at the peak shear stress (static yield stress). From Figure 3.6, the results of Set A were generally higher than that of Set B because of its initial conditions; Set A was not sheared to have a steady equilibrium state before the resting time while Set B was pre-sheared to achieve equilibrium before its resting time. Set A has some inherent deformation pre-history due to placement into the ICAR rheometer and movement on a trolley to the climate-controlled room for testing leading to a degree of transient consolidation. The mixes can be classified into two groups of similar τ_s values: the control mix (Mix C) and the mix containing VMA (Mix CV) have similar results while mixes containing SP (Mix CS), VMA+SP (Mix CVS) and more water (Mix CW) have similar results (that is, Mixes C/CV and Mixes CS/CVS/CW groups). This grouping is similar to the slump values of the mixes (Table 3.3), that is, less workable concrete has higher τ_s at the 10 minutes resting time.

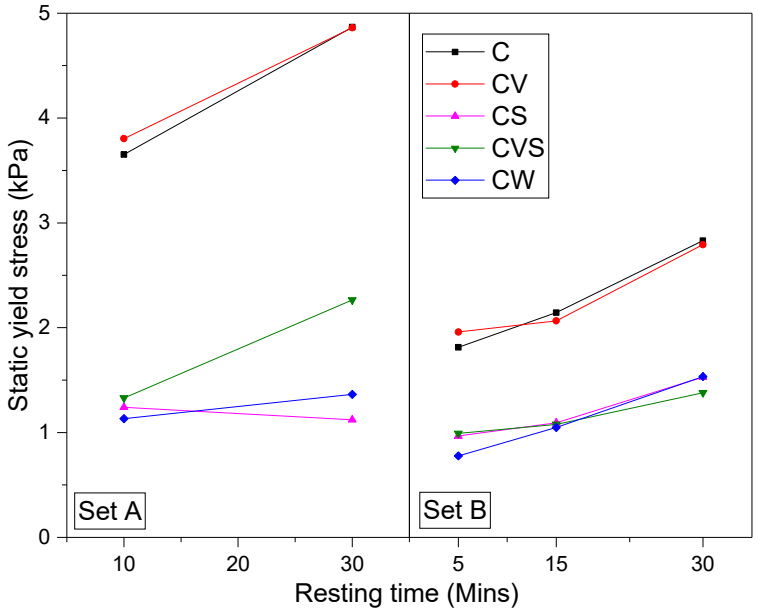

Figure 3.6: Evaluation of static yield stress of the concrete mixes with time

For Sets A and B, the inclusion of VMA in concrete did not significantly influence the values and evolution of τ_s. This is probably because the specific VMA was engineered to enhance the robustness of concrete, that is viscosity (Chryso, 2012), rather than the τ_s. Moreover, VMA mainly

acts on the liquid phase of concrete by absorbing water as cover around its chains (Isik and Ozkul, 2014; Khayat and Mikanovic, 2012) and therefore has an influence on the interparticle and attractive forces in the concrete. It is also evident that Mixes C and CV have similar setting times, hence, their CSH bridges leading to structuration may build-up in a similar manner to yield similar τ_s (Roussel *et al.*, 2012). Inclusion of SP, VMA+SP and water reduced the values of τ_s for both sets but not necessarily the evolution as resting time increased. The results of Mix CVS imply that SP is dominant compared to the VMA in the mix. Superplasticiser is known to repel water molecules in concrete by adsorbing to cement particle surfaces (Mardani-Aghabaglou *et al.*, 2013; Flatt and Schober, 2012) which implies that it acts on the solid phase of concrete to improve its flow (Jiao *et al.*, 2017; Artelt and Garcia, 2008; Gołaszewski and Szwabowski, 2004) while water increases the liquid phase of concrete (Ahari *et al.*, 2015). However, after 30 minutes resting time for Set A, the VMA in Mix CVS significantly increase the τ_s compared to Mixes CS and CW. This may mean that adequate resting triggered the dominance of VMA as compared to SP in Mix CVS. Additionally, Mix CVS has a lower initial setting time (at 23°C) out of the trio (Mixes CS/CVS/CW) which may mean that its CSH nucleation bridges builds faster to yield a better structuration at 30 minutes resting time (Roussel *et al.*, 2012). The observed evolution of τ_s in Mix CVS of Set A may also be due to the advantage of VMA polymer entanglement and viscous thickening (Bouras *et al.*, 2012; Khayat, 1998) that with time surpassed the influence of the SP in Mix CVS. The same apparent difference in the evolution of τ_s between Mix CVS and Mixes CS/CW for Set B is not evident. This difference between Sets A and B in the evolution of τ_s in Mixes CS/CVS/CW may be due to the initial conditions, the pre-shear of Set B allowed for the true measurement of τ_s after equilibrium for the three mixes without the influence of deformation pre-history while for Set A, the deformation pre-history may have suppressed the influence of both SP and water.

It can be deduced that the amount of energy required to initiate the flow of concrete depends upon its initial conditions and resting time; the more the resting time, the more energy required.

3.4.1.2. Dynamic yield stress

The dynamic flow curves for all the mixes are shown in Figure 3.7 for Set A at 10 minutes resting time. The insert shows a typical flow curve (Mix CVS) having a negative slope at low shearing speeds of 0.05 rev/s to 0.15 rev/s. This implies that at very low speeds, the Bingham model may not fully describe the flow of concrete; this negative slope at low speeds may be due to shear localisation or re-coagulation in the concrete due to decreasing shear rates. Shear localisation could occur at low speeds because the effective shearing of the vane reduces as the radial distance from the vane

increases which leads to concrete near the perimeter of the container not being sheared (Qian and Kawashima, 2018; Koehler and Fowler, 2004; Geiker *et al.*, 2002). Furthermore, as the shear rates decreases from 0.5 rev/s at steady state to slower 0.05 rev/s, the concrete may re-coagulate and rebuild leftover links due to shift in equilibrium from the steady state at a certain low speed (e.g. 0.15 rev/s for Mix CVS) (Qian and Kawashima, 2018; Geiker *et al.*, 2002); this equilibrium shift may be due to viscosity bifurcation as noted by Qian and Kawashima (2016) and Coussot *et al.* (2002). To eliminate these errors and improve the fit to the Bingham's model, deviating points at low speeds were eliminated from the flow curve, e.g. 0.05 rev/s and 0.1 rev/s for Mix CVS. It should be noted that the flow curves containing these deviating points at low speed often resulted in unrealistic values of dynamic yield stress and plastic viscosity; moreover, results obtained after eliminating the deviating points were similar to those obtained during preliminary test when the flow curve test was done from 0.2 rev/s to 0.6 rev/s. Besides, the ICAR rheometer manual specifies a minimum of five points of measurements for the flow curve.

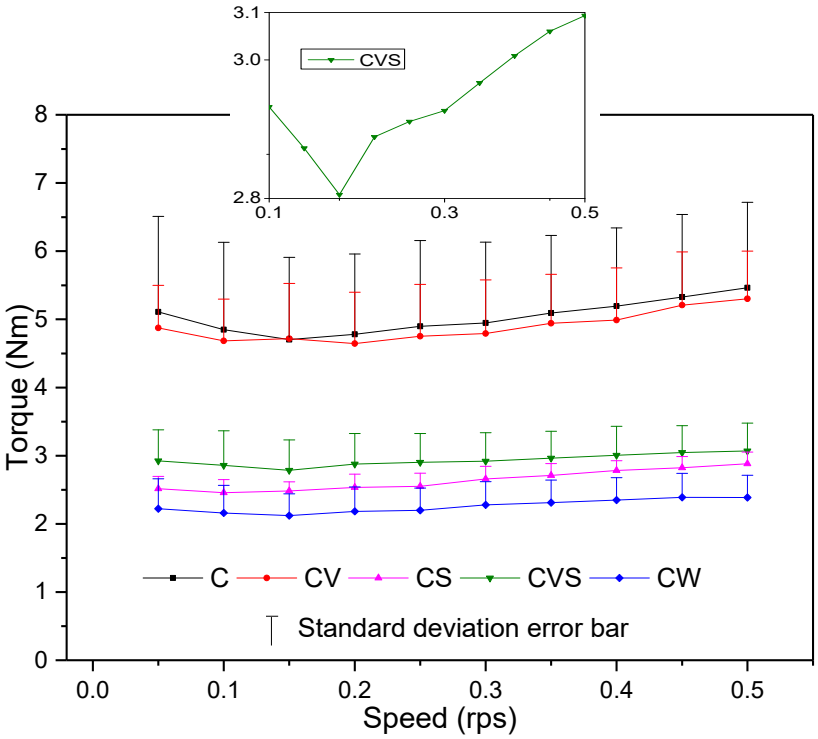

Figure 3.7: Flow curves for all the concrete mixes

Figure 3.8 depicts the results of the dynamic yield stress (τ_o) tests. Theoretically, τ_o should not be influenced by thixotropy since the pre-shear breaks down built structure in the concrete, however, the extent of the breakdown depends on the pre-shear rate and duration. It can be assumed that the pre-shear specification for this study was adequate since the τ_o values were similar between Sets A and B for each mix; likewise, there was little or no evolution of τ_o with time for both sets.

That is, the thixotropy was completely broken down for each test no matter the amount of resting time. The results of τ_o fall into the same group classification of the static yield stress (Mixes C/CV and Mixes CS/CVS/CW); however, the Mix CVS has slightly higher values than those of Mixes CS and CW probably because of the viscous thickening ability of the VMA over SP in Mix CVS. That is, the inclusion of both VMA and SP in concrete reduced its structure vulnerability to breakdown since Mixes CS, CVS and CW have similar τ_s before thixotropy break down.

This may imply that the amount of energy required to maintain the flow of concrete is relatively the same up to 30 minutes resting time irrespective of the concrete's initial condition. Unlike τ_s, the influence of VMA in Mix CVS is independent of the initial condition and resting time of the concrete samples, likewise, SP was dominant in Mix CVS for the τ_o.

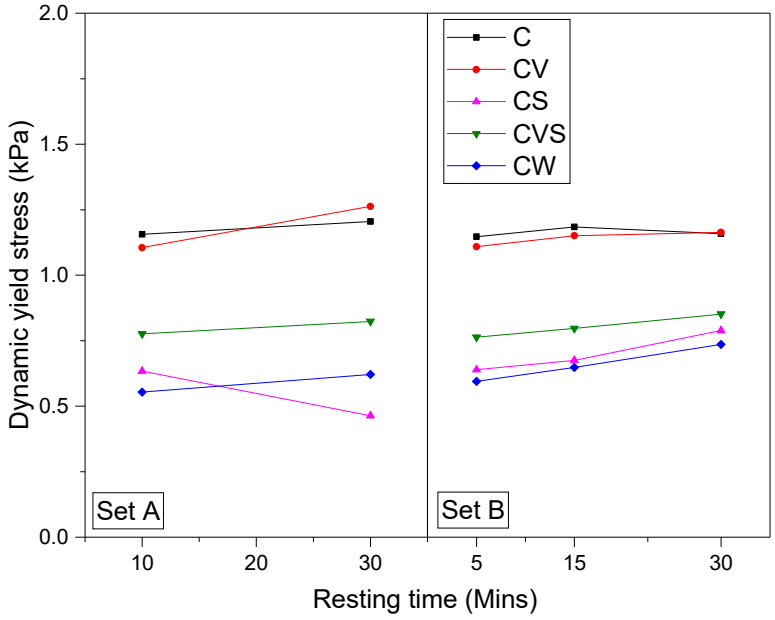

Figure 3.8: Evolution of dynamic yield stress of the concrete mixes with time

3.4.1.3. Plastic viscosity

The plastic viscosities (μ) of the mixes were also obtained from the flow curve tests and are shown in Figure 3.9. The figure reveals that all the mixes have a general increase in μ as resting time increases except for the Mix C. For both sets, Mix C had a significant initial decrease in μ probably because it becomes stiffer as resting time increases unlike Mixes CS and CW with delayed setting time, Mixes CV and CVS with VMA engineered to improve viscosity (Chryso, 2012). For Set B, the μ of the control increased later (30 minutes resting time) probably because the same concrete sample was used for all resting times; that is, the flow curve test at 15 minutes resting time may have broken down any initially developed stiffness which may take more time to redevelop. It is known that increased water content in concrete reduces its yield stress and viscosity; however, Mix CVS had

slightly lesser μ than Mix CW but similar or higher τ_s and τ_o (Figure 3.6 and Figure 3.8). This may imply that inclusion of both VMA and SP in concrete provides lesser resistance to flow than increasing the water content, though similar or larger force may be required to initiate/maintain the flow. Meanwhile, the inclusion of VMA in concrete improves its viscosity, and it becomes more pronounced as resting time increases.

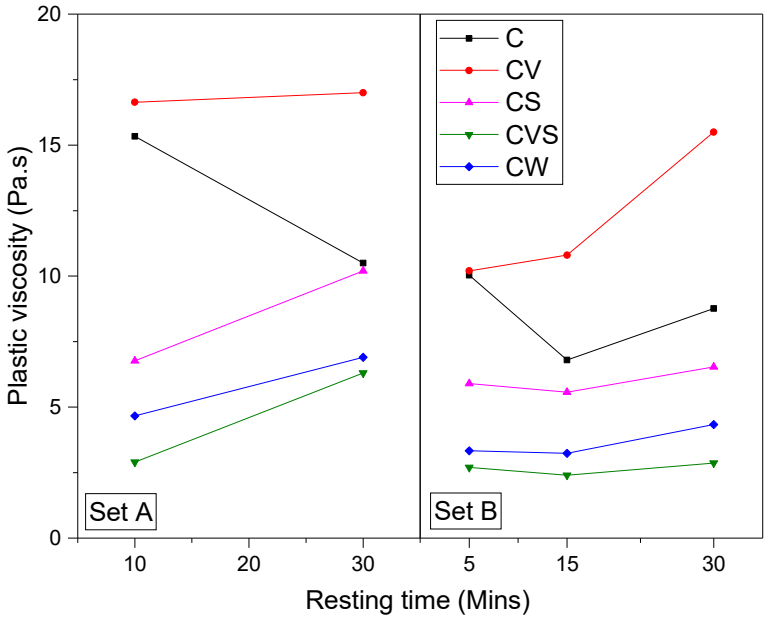

Figure 3.9: Plastic viscosity of the concrete mixes

3.4.1.4. Thixotropy index

Figure 3.10 represents the indices of thixotropy calculated from the values of τ_s and τ_o. The indices indicate that there is a general increase in the amount of structuration in the concrete mixes as resting time increases. Set A mixes shows a similar grouping of results (Mixes C/CV and Mixes CS/CVS/CW) as for the τ_s while there is only a subtle difference in results for Set B mixes. The results observed for Set B reveal that pre-shearing dampens the influence of rheology modifiers on the thixotropy evolution. That is, rheology modifiers influence the structuration in concrete but concrete subjected to shearing to reach a steady state before testing have a reduced influence.

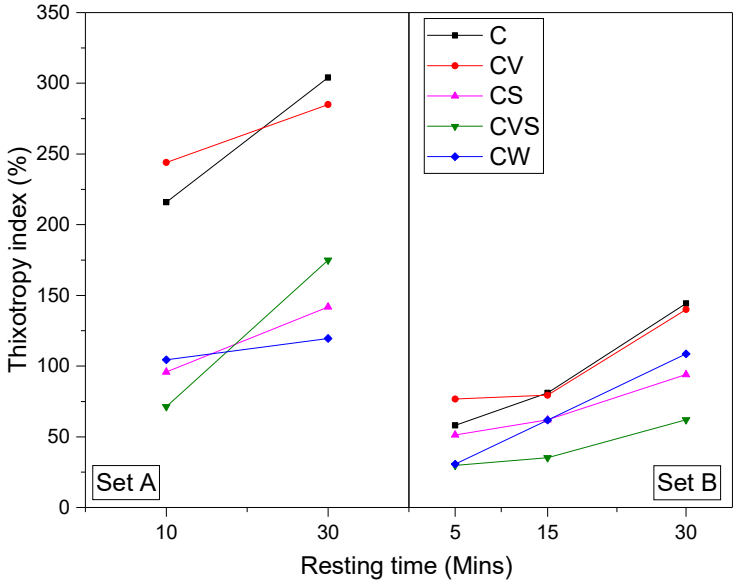

Figure 3.10: Thixotropy indices of the concrete mixes

3.4.2. Shear thinning and thickening

Thixotropy is a time-dependent shear thinning, and rheopexy is time-dependent shear thickening (Chhabra, 2010). It is, therefore, necessary to examine the potential of the mixes to exhibit shear thinning or thickening. While it is well known that concrete displays shear thinning (Roussel, 2012), there is a scarcity of literature on its shear thickening behaviour. Literature on shear thickening of cementitious materials are mostly on cement paste or mortars (Maybury and Ho, 2017; Bouras *et al.*, 2008, 2012; Yahia, 2011; Saric-Coric *et al.*, 2003; Cyr *et al.*, 2000) and also few on self-compacting concrete (Li *et al.*, 2017; Feys *et al.*, 2008). Moreover, the literature on how the rheology modifiers influence the shear thinning and thickening of conventional concrete is scarce.

Figure 3.11 shows the shear thinning/thickening indices of the concrete mixes, as obtained by fitting the Herschel-Bulkley model to their flow curves. All the equations have a good fit ranging from 0.92 to 0.99. As noted earlier, deviating points at low speeds were eliminated from the flow curve since the ICAR rheometer manual specifies a minimum of five points for the flow curve. Values plotted in Figure 3.11f have been normalised for easy depiction of the degree of shear thinning and thickening.

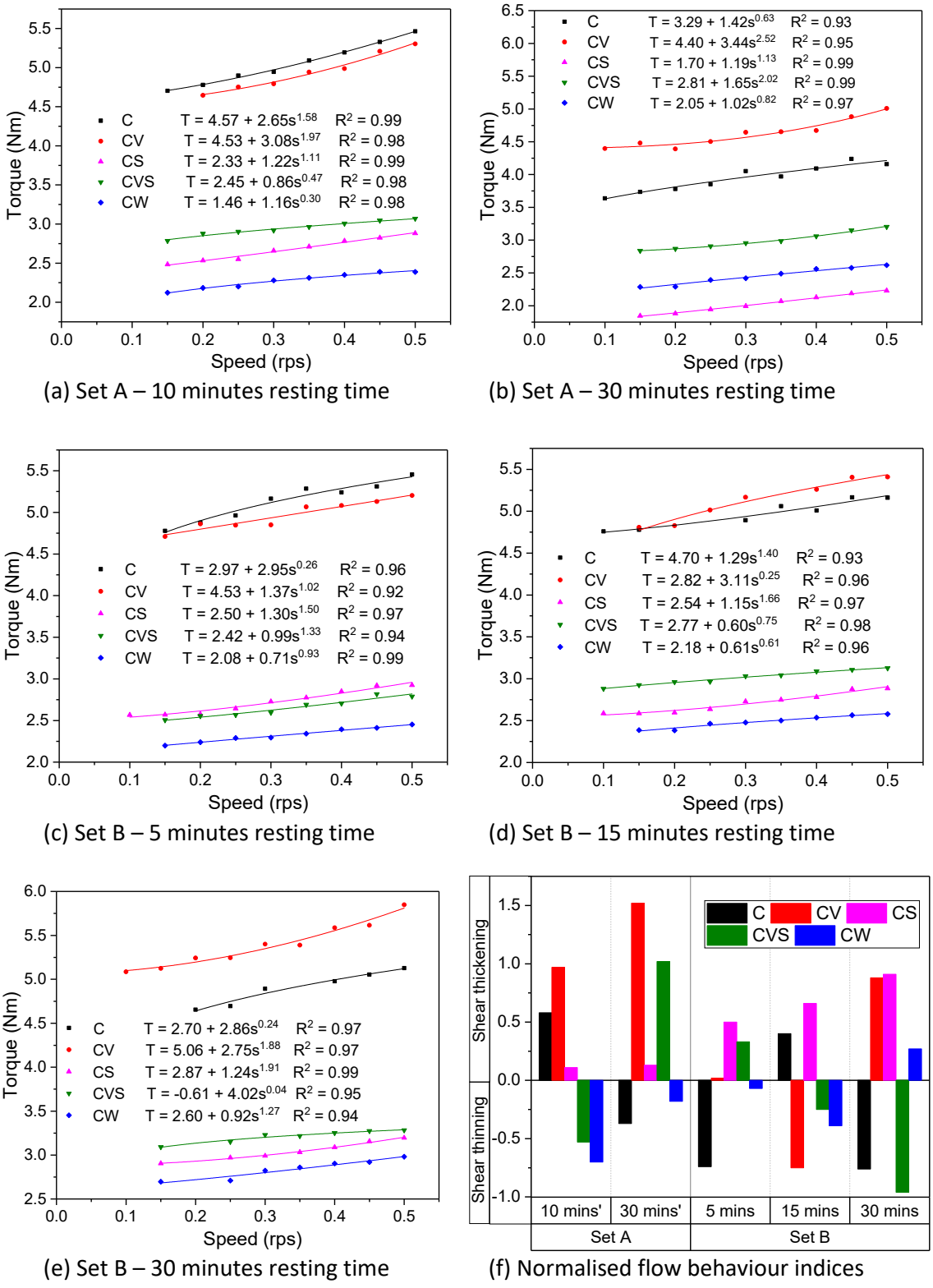

(a) Set A – 10 minutes resting time

(b) Set A – 30 minutes resting time

(c) Set B – 5 minutes resting time

(d) Set B – 15 minutes resting time

(e) Set B – 30 minutes resting time

(f) Normalised flow behaviour indices

Figure 3.11: Indices for shear thinning and thickening using Herschel-Bulkley model

Figure 3.11 shows that the rheology modifiers influenced the shear thickening or thinning potentials of concrete. This is further influenced by the initial conditions of the mixes and resting time with no definite pattern except for CS. That is, the same concrete sample (Set B) can switch between shear

thinning and thickening; Chougnet *et al.* (2007) also reported this observation for cement suspensions. Inclusion of superplasticiser in concrete made it exhibit shear thickening flow behaviour at all resting times and initial conditions; that is, the presence of PCE superplasticiser can cause concrete to have transiently increased viscosity under shearing. The more the resting time and shearing for CS (Set B of Figure 3.11f), the more the shear thickening potential. For shear thickening to occur in a suspension, it should have a high solid volume fraction, and some sort of repulsion between the suspended particles should occur (Bouras *et al.*, 2008; Phan *et al.*, 2006; Cyr *et al.*, 2000; Hoffman, 1998; Barnes, 1989). Therefore, the shear thickening of CS may be due to the repulsive electrostatic and/or steric hinderance of SP which may be accentuated by the shearing to increase concrete's liquid phase thickening. Viscosity modifying agent caused shear thickening in Set A concrete (even at a higher magnitude than superplasticiser), but with no definite pattern in Set B. However, the inclusion of more water in concrete tends to make concrete a shear thinning material; this may be due to lesser solid volume fraction.

In conclusion, it can be deduced that the inclusion of VMA or SP in concrete can make concrete a shear thickening material. However, the steady state history of VMA concrete can influence its shear thickening behaviour. Inclusion of both VMA and SP in concrete can result in shear thickening or thinning depending on the resting time and deformation history. Increasing the water content in concrete can potentially increase its shear thinning behaviour. Therefore, concrete that is generally known to be a shear thinning and thixotropic material can also become shear thickened with rheopexy potentials due to rheology modifiers, resting time and shear pre-history.

3.4.3. Structuration at rest and de-structuration under shear

Figure 3.12 (a-c) shows the rate of structuration (A_{thix}), structuration state (λ) and characteristic time to structuration (T) respectively. The A_{thix} indicates the rate at which the structure/thixotropy of each mix builds up, the λ indicates the level of thixotropy/structure the concrete has built, while the T is the intrinsic time required for the concrete mixes to reach a truly structured state (i.e. level of maximum thixotropy/structuration). It can be observed that the results in Figure 3.12b are very similar to those obtained for the thixotropy index (Figure 3.10), that is, the λ indicates the degree of thixotropy within a specified period of time and pre-condition.

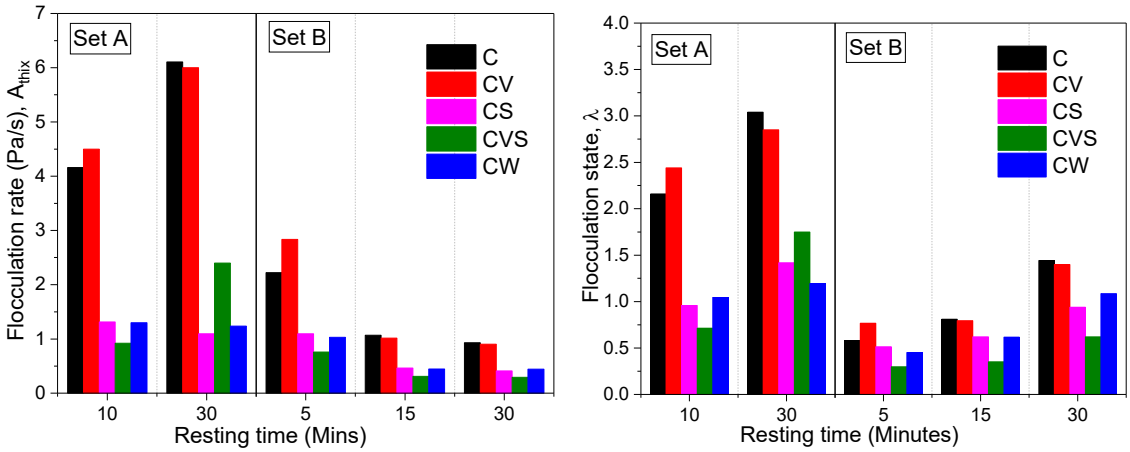

(a) Structuration rate (A_{thix})

(b) Structuration state (λ)

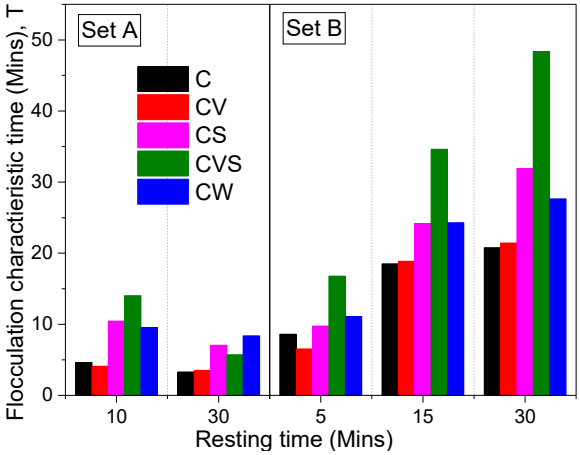

(c) Structuration characteristic time (T)

Figure 3.12: Structuration properties of the concrete mixes

From the three plots in Figure 3.12 (a-c), Set A mixes show different structuration properties to Set B mixes mainly because of the varying initial conditions. For the A_{thix} of Set A, the more the resting time, the more the rate of structuration while it is the contrary for Set B. That is, the steady state pre-history makes the Set B mixes to reach similar rate of flocculation in time (15 vs 30 minutes resting time) and requiring more time (T) to reach its maximum thixotropy as resting time increases (Set B of Figure 3.12c). The increasing T with time may be due to using the same concrete sample for the different resting times (Set B Figure 3.12c) as against what was obtained in Set A. The results can also be grouped (Mixes C/CV and Mixes CS/CVS/CW) as for τ_s; however, Mix CVS required a relatively high time to reach its maximum thixotropy especially for Set B corroborating Mix CVS instability to the pre-shearing as also concluded for the shear thinning and thickening indices.

3.4.4. Torque decay

Figure 3.13a shows a typical torque decay recorded by the ICAR rheometer in seconds for Set A mixes at 10 minutes resting time and 0.02 rev/s shearing rate. The plots were thereafter normalised

using the peak torques of the mixes as shown in Figure 3.12b to allow for easy visualisation of the rate of structure/thixotropy breakdown at the varying shear speeds. The pre-peak (0 to 50 seconds) and post-peak are also presented on different time scales to show the evolution of the torque before and after reaching its peak values respectively. It should be noted that 10 minutes resting time was only tested for Set A mixes while 5, 15, and 30 minutes resting times were tested for Set B mixes. However, only 10 minutes resting time of Set A and 30 minutes resting time of Set B were reported for the torque decay because other resting times yielded little or no decay.

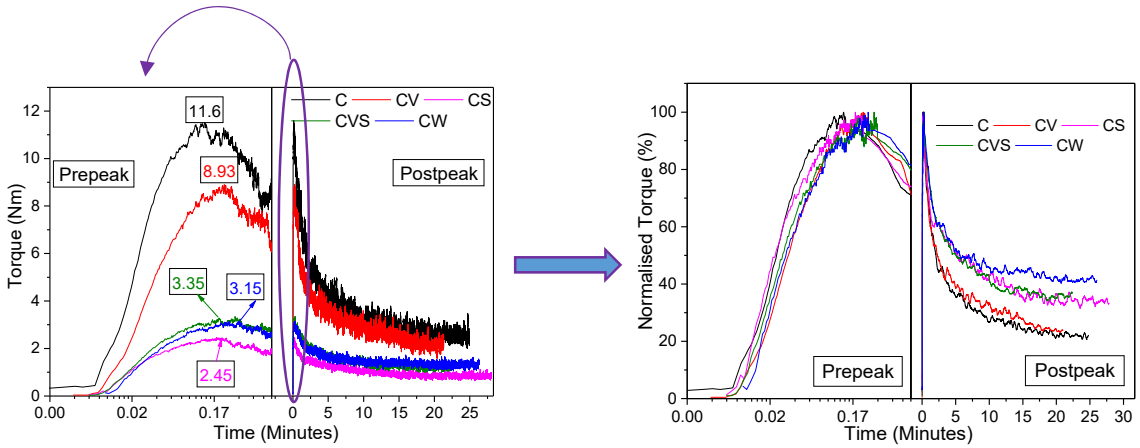

(a) Typical raw torque decay (b) Typical refined torque decay

Figure 3.13: Processing of the raw data for torque decay

Figure 3.14 to Figure 3.16 show the torque decay at specified shearing speeds of the rheometer's vane. It was observed that high shearing speeds caused the torque to reach its peak quicker and decay faster. The mixes behaved differently at the varying shear speeds and resting times. At low shearing speed, the inclusion of water resulted in the least decay; however, with higher speed of shearing, the inclusion of SP in concrete tends to reduce the decay. Moreover, at higher speed, the inclusion of water and SP resulted in concrete with seemingly rheopectic/shear thickening behaviour (increasing torque with continuous shearing – Figure 3.16a). A similar observation was made from Mix CS's flow curve in Figure 3.11f but contrary to that of Mix CW which was mostly shear-thinning. Another interesting observation was that the pre-shearing condition, increasing resting time and increasing shearing speeds make Mixes CS and CW attain peak torques (> 100%) higher than that obtained for Set A mixes. This reinstates the fact that they may both become rheopectic depending on the set condition.

Mixes C and CV show the highest decay while Mixes CS, CVS and CW always show the least decay irrespective of the resting time. This implies that the thixotropic structure of Mixes C and CV are

susceptible to higher rates of breakdown while the inclusion of SP, VMA+SP and more water in concrete can reduce the rate of its thixotropic structure breakdown.

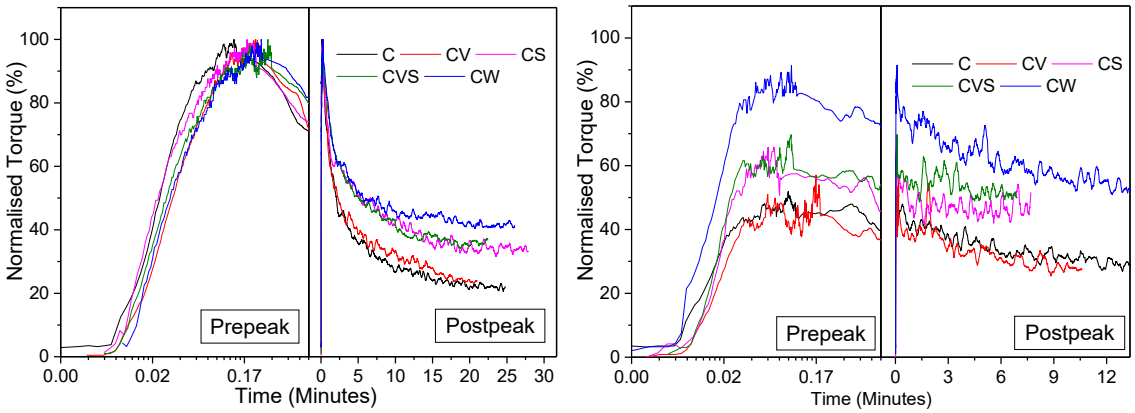

(a) 10 minutes resting time – Set A (b) 30 minutes resting time – Set B

Figure 3.14: Torque decay at 0.02 rev/s

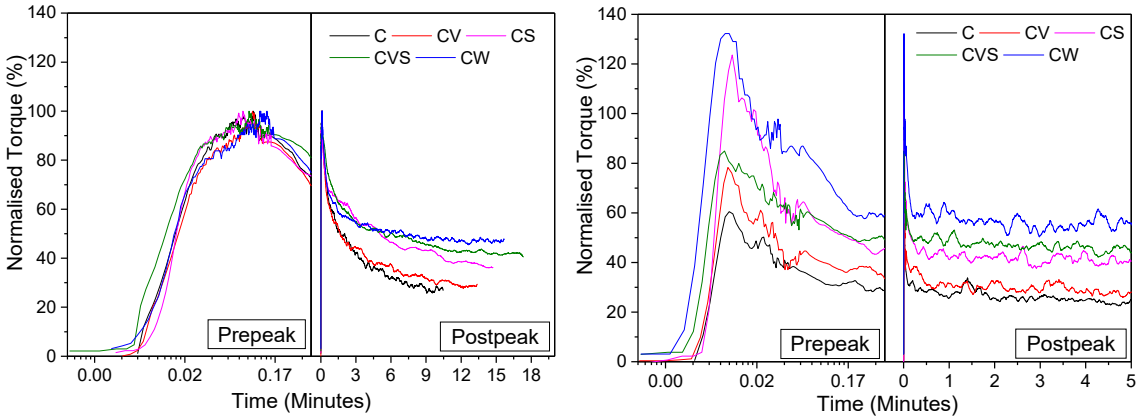

(a) 10 minutes resting time – Set A (b) 30 minutes resting time – Set B

Figure 3.15: Torque decay at 0.05 rev/s

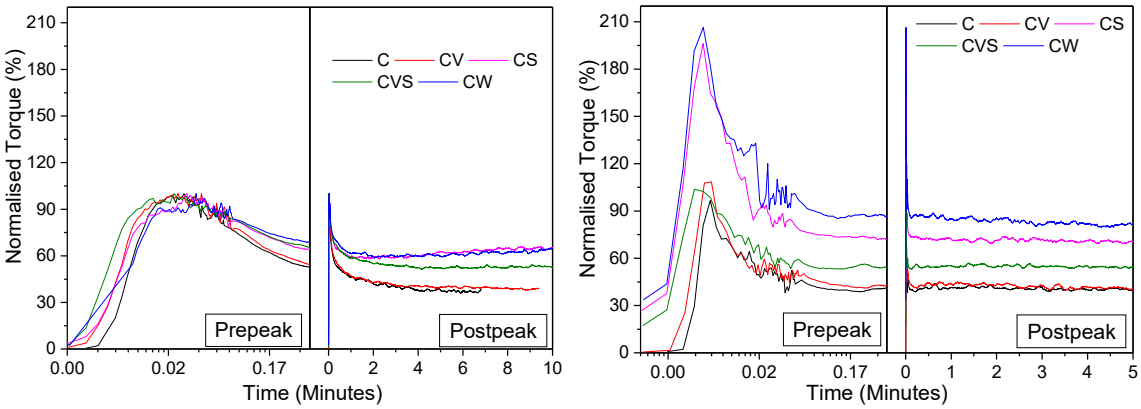

(a) 10 minutes resting time – Set A (b) 30 minutes resting time – Set B

Figure 3.16: Torque decay at 0.275 rev/s

3.4.5. Reduction in apparent viscosity

Reduction in apparent viscosity due to continuous shearing indicates the amplitude of thixotropic structure breakdown in the concrete mixes (Ahari *et al.*, 2015) due to varying shear rates. From Figure 3.17, increasing shear speed tends to significantly decrease the change in apparent viscosity and the difference between the mixes. Also, allowing the concrete to rest more makes it lose more viscosity during shearing; this could be due to increased stiffening as the resting time increases. This may imply that the stiffer the concrete, the more its susceptibility to losing its thixotropy due to shearing. The same grouping (Mixes C/CV and Mixes CS/CVS/CW) of result as that indicated for τ_s was obtained here with both Mixes C and CV showing the highest viscosity drop. However, prior pre-shearing results in Mix CV losing its viscosity more than the Mix C.

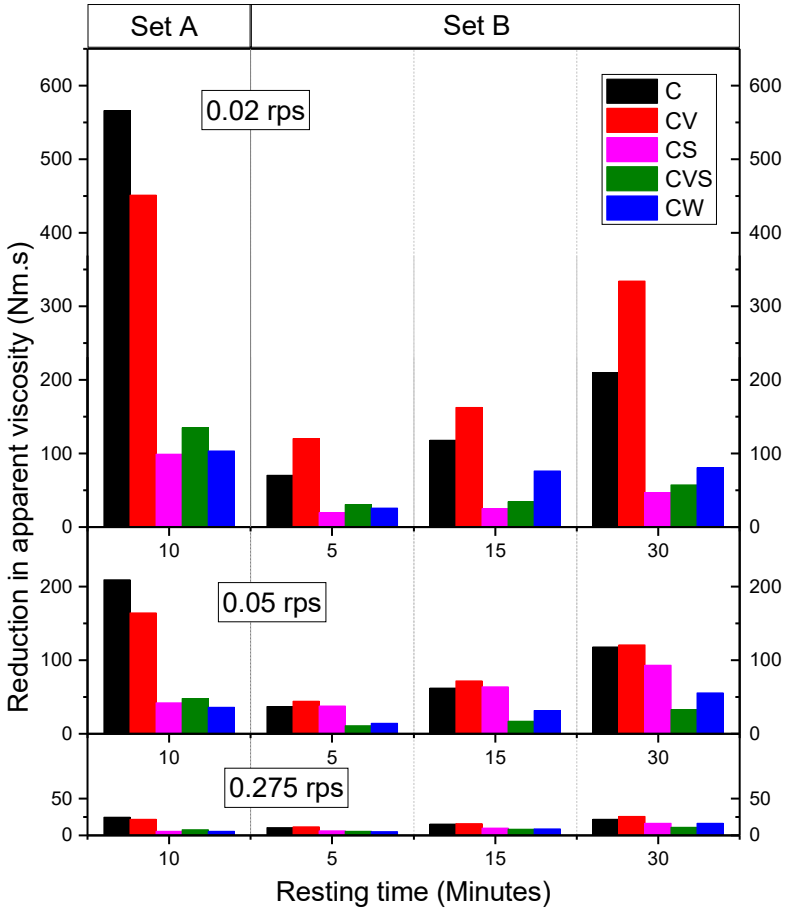

Figure 3.17: Reduction in apparent viscosity due to continuous shearing

3.4.6. Hysteresis loop

Figure 3.18 is the results of the hysteresis loop test, 10 minutes resting time was only tested for Set A mixes. Results of Figure 3.18 were taken from Figure 3.19. In Figure 3.19, the rows represent resting times and sets while the columns are the mixes. Each row is plotted on the same scale to allow for easy comparison. The shaded portion of the loop represents thixotropic values which are

plotted in Figure 3.18. From Figure 3.18, all Set A mixes had thixotropic values while Set B mixes included rheopectic values (negative values); this is because, after the rigorous shearing, the decreasing speed plot had higher torque values than the increasing speed plot. Chhabra (2010) noted that it is possible for the same material to exhibit both thixotropy and rheopexy, such established materials include thick suspensions of Kaolin, dune sand, and corn flour in water. In such cases, the equilibrium between the rate of structural rebuild and breakdown can tilt to either side (Chhabra, 2010) depending on the set condition of the samples. Geiker *et al.*, (2002) warned against reporting negative slope of flow curve as shear thickening when the concrete is not pre-sheared for steady state. This is not the case for this study because immediately after the increasing speed test, the concrete was pre-sheared for 60 seconds at 0.5 rev/s before decreasing the shear speed to measure the torque. Tests in which the decreasing speed test was immediately performed after the increasing speed (without pre-shear) are susceptible to this error. From Set B mixes in Figure 3.18, only Mix CS consistently showed rheopectic values which reinforces previous results from its shear thickening (Figure 3.11f) and torque decay (Figure 3.16a).

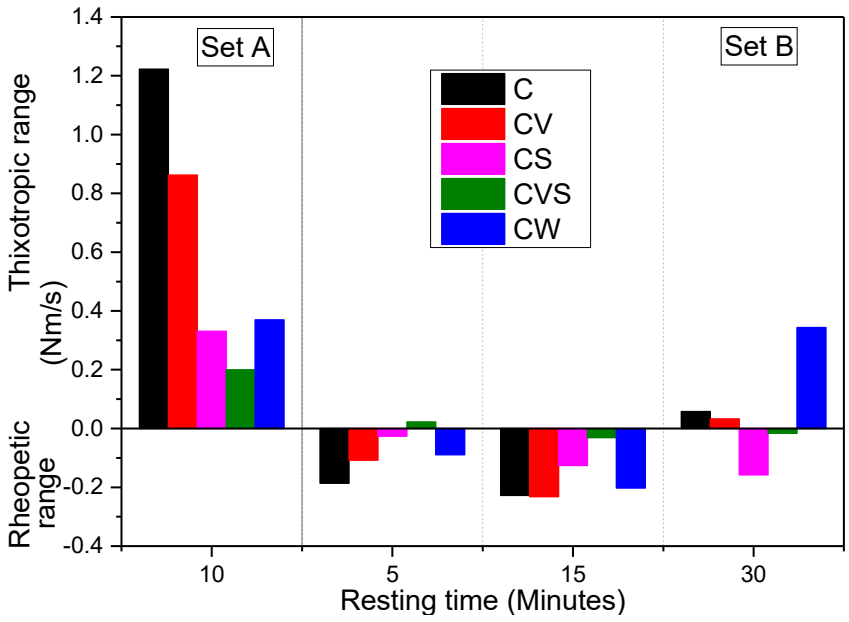

Figure 3.18: Hysteresis loop area of the concrete mixes

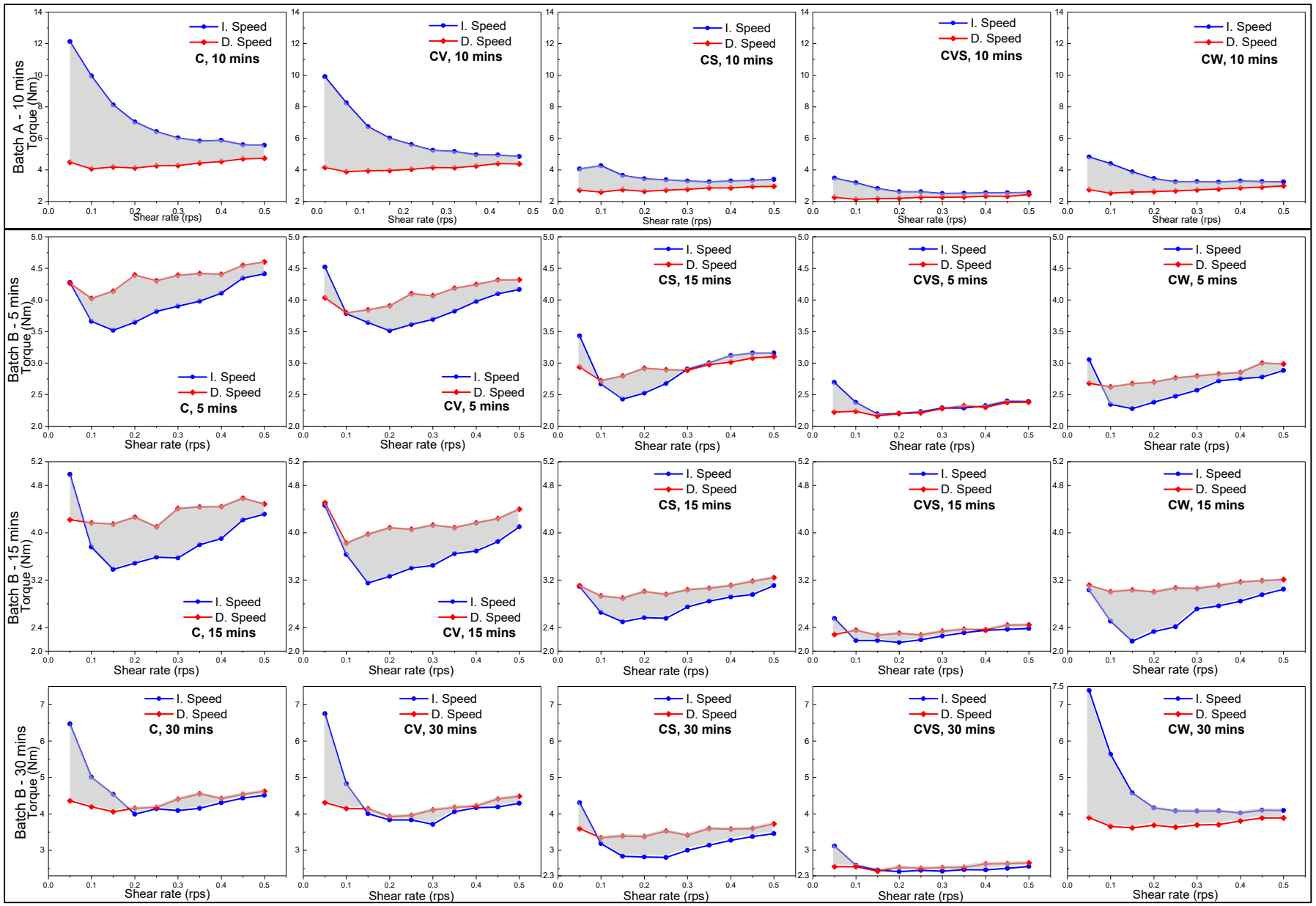

Figure 3.19: Hysteresis loop of the concrete mixes (I. Speed – Increasing shear speed; D. Speed – Decreasing shear speed)

3.4.7. Relationship between thixotropy evaluation methods

As noted earlier, thixotropy of concrete can be evaluated from either its internal structure build-up (structuration) or how it breaks down (destructuration). Evaluation of rheology evolution (static yield stress, dynamic yield stress, plastic viscosity, thixotropy index) and flocculation properties are from structuration while torque decay, reduction in apparent viscosity and hysteresis loop are from destructuration. Figure 3.20 shows the relation between these methods. Thixotropy index (T.I.), reduction in apparent viscosity ($\Delta\mu_{app}$), and flocculation rate (A_{thix}) consistently showed similar evaluation results between the mixes. Hysteresis loop area (H.L.A.) evaluation results pattern depended on the concrete mixes' shearing pre-history; it has the former pattern if the concrete wasn't pre-sheared (Figure 3.20a – Set A (10 minutes resting time)) or has rested enough after shearing (Figure 3.20d – Set B (30 minutes resting time)). H.L.A. had a similar pattern with the flocculation characteristic time (T) when there's less resting time after pre-shearing (Figure 3.20b and c – 5 minutes resting time and 15 minutes resting time of Set B respectively). These implies that H.L.A. is influenced by concrete initial set condition and, therefore, majorly qualitative (Roussel, 2006).

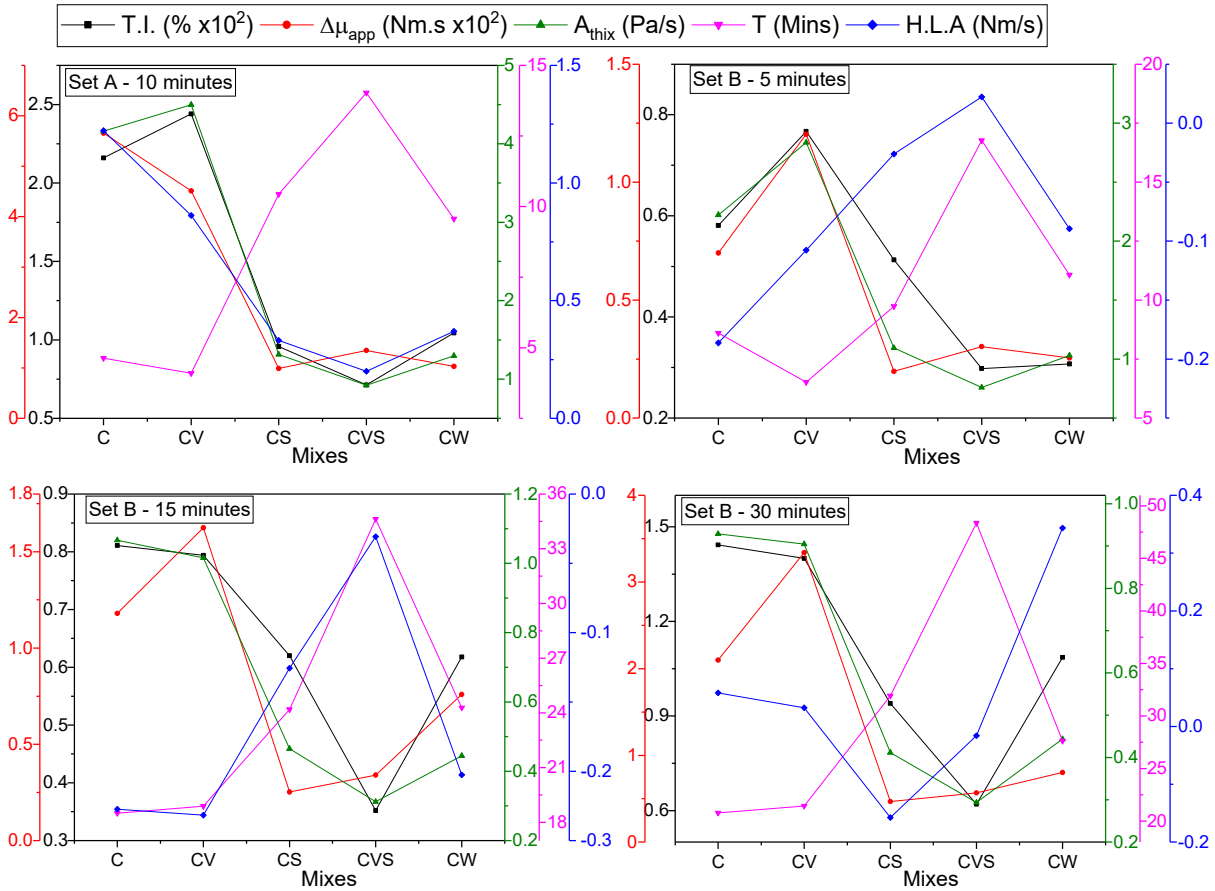

Figure 3.20: Relation between thixotropy measurement methods (T.I. – thixotropy index, $\Delta\mu_{app}$ – reduction in apparent viscosity, A_{thix} – structuration rate, T – flocculation characteristic time, H.L.A. – hysteresis loop area)

3.5. Conclusion and recommendation

This study examined the thixotropy of rheologically modified conventional concrete using various methods. Readily available rheology modifiers such as viscosity modifying agent (VMA), superplasticiser (SP) and water were utilised to vary the rheology of conventional concrete. From the results, the following conclusions can be made.

- As the resting time of concrete increases, concrete mixes allowed to reach steady state before resting generally showed opposite trends to those without shearing pre-history.
- The inclusion of VMA in concrete does not significantly change its rheological and thixotropic properties except for the plastic viscosity. VMA significantly increased the plastic viscosity of concrete as resting time increased.
- The inclusion of SP, both VMA and SP, and more water in concrete significantly influenced its thixotropic and rheology properties, mainly reducing these properties in a similar pattern.
- The initial set condition of the concrete affected the influence of the rheology modifiers on the thixotropy index. Shearing pre-history dampened the influence of the rheology modifiers on the thixotropy index evolution.
- Thixotropic properties of concrete containing both VMA and SP (Mix CVS) can become unstable due to pre-shearing. While the SP in Mix CVS initially dominated its thixotropic behaviour, VMA's influence later surpassed the influence of SP.
- The inclusion of VMA or SP in concrete can cause shear thickening. However, the shear thickening behaviour of VMA concrete can be changed by the shear history while that of SP concrete was found to be independent of resting time and shear history.
- Pre-shearing concrete before resting can make it rheopectic, though its rheopexy may diminish into thixotropy as resting time increases. However, concrete containing SP may retain its rheopexy for longer rest periods. Furthermore, concrete containing SP and more water may turn rheopectic when being sheared continuously at high speeds (e.g. ≥ 0.275 rev/s).
- The rheology modifiers (especially increased water) reduced the rate and degree of concrete's structure breakdown except for VMA which had relatively no influence.
- Thixotropy evaluation results showed fairly similar relation between the mixes, independent of concrete's initial set condition except for thixotropic loop area. This implies that the

hysteresis loop is limited as a qualitative evaluation method while other methods are better for quantitative evaluation.

This study contributes to the body of knowledge on thixotropy of conventional concrete, revealing how rheology modifiers influence the shear thinning/thickening, structuration and thixotropic structure breakdown of concrete. These results can help concrete batchers to make informed decisions on related thixotropic applications such as potential pumping difficulty due to shear thickening and mix instability due to continuous shearing in a ready-mix truck. As a recommendation, the thixotropy of the concrete can be further evaluated using dynamic rheometry and comparatively gauged with the results of this paper.

Chapter 4: Rheo-viscoelastic behaviour of fresh cement-based materials: cement paste, mortar and concrete

This chapter has been submitted as a journal paper to the Construction and Building Materials, Elsevier BV, with impact factor 4.046. Details of the paper are below:

Kolawole, J.T., Combrinck, R. & Boshoff, W.P. (2019). Rheo-viscoelastic behaviour of fresh cement-based materials: cement paste, mortar and concrete. Submitted to Construction and Building Materials.

Declaration by the candidate:

With regard to Chapter 4, the nature and scope of my contribution were as follows:

Nature of contribution	Extent of contribution (%)
This paper/chapter is part of the candidate's PhD research. All experimental work, the analysis, interpretation and presentation of data, as well as the writing of the manuscript were conducted by the candidate.	90%

The following co-authors have contributed to Chapter 4:

Nature of contribution	E-mail address	Nature of contribution	Extent of contribution (%)
Dr Riaan Combrinck	rcom@sun.ac.za	PhD research supervision, proofreading manuscript and insightful amendments	5%
Prof William Peter Boshoff	billy.boshoff@up.ac.za	PhD research supervision, proofreading manuscript and insightful amendments	5%

Signature of candidate: 

Date: 8 October 2019

Declaration by co-authors:

The undersigned hereby confirm that

The declaration above accurately reflects the nature and extent of the contributions of:

1. The candidate and the co-authors to Chapter 4,
2. No other authors contributed to Chapter 4 besides those specified above, and
3. Potential conflicts of interest have been revealed to all interested parties and that the necessary arrangements have been made to use the material in Chapter 4 of this dissertation.

Signature of co-authors	Institutional affiliation	Date
	Department of Civil Engineering, Stellenbosch University	8 October 2019
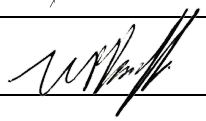	Department of Civil Engineering, University of Pretoria	8 October 2019

4.1. Abstract

The viscoelasticity of fresh fine cement-based material can be investigated by rheological means using dynamic shear rheometers, hence, the term rheo-viscoelasticity. However, due to the coarse constituents of mortar and concrete, classical rheometers do not qualify for the measurement of their viscoelastic behaviour. This study, therefore, sets out to experimentally investigate the rheo-viscoelastic behaviour of cement-based materials containing rheology modifiers, by progressively evaluating the viscoelasticity of cement paste-mortar-concrete by dynamic shear rheometry. The rheology modifiers include viscosity modifying agent (VMA), superplasticiser (SP), and water while the tests carried out are strain sweep, shear rate sweep, creep and creep recovery, stress relaxation and three interval thixotropy test (3ITT). The results show a trend of improved linear viscoelastic behaviour of the control fresh cement-based materials due to increased aggregate volume fraction and size. However, the rheology modifiers widely varied this trend, tending to make it difficult to approximate the rheo-viscoelastic behaviour of mortar and concrete from that of the cement paste as generally suggested in the literature. Some of the unique properties observed and distinctively influenced by the aggregates and modifiers include ductility, microstructure thickening and flocculation/hydration-driven structuration.

4.2. Introduction

Dynamic shear rheometry (DSR), sometimes referred to as small amplitude oscillatory shearing (SAOS), is a test method that can be used to characterise viscoelastic (VE) materials by linking rheology to viscoelasticity (Kim *et al.*, 2018; Hyun *et al.*, 2011; Sun *et al.*, 2006), hence, the term "rheo-viscoelasticity". It involves applying a sinusoidal oscillatory shear strain/stress (stimulus) to a VE sample while monitoring the response of the sample. Viscoelastic materials possess both viscous and elastic properties, hence, the response of the VE sample has a phase lag (δ) to the stimulus (Mezger, 2014). In terms of rheology of fresh cement-based materials, dynamic/oscillatory shear rheometry is considered advantageous over static/rotational shear rheometry because the latter causes the de-structuration of the microstructure (Ma *et al.*, 2018; Yuan, Lu, *et al.*, 2017; Nehdi and Al Martini, 2009; Mahaut, Mokéddem, *et al.*, 2008) due to irreversible continuously increasing shearing. Therefore, the rotational shear rheometry does not give insights into the microstructure but rather the overall structure's macroscopic response while SAOS allows the understanding of the microstructural behaviour of VE materials.

Characterisation of VE materials via shear rheometry often starts from an amplitude sweep (strain amplitude, in the case of this study) in order to determine the microstructural response and linear viscoelastic range (LVR). The LVR is the range of strain where the VE material behaves like an elastic material (viscoelastic solid), above this limit, the material's microstructure is disturbed and it behaves like a viscoelastic liquid (Ma *et al.*, 2018; Mezger, 2014; Nachbaur *et al.*, 2001). The viscoelastic liquid regime before flow occurs defines the viscoplastic behaviour of VE materials (He *et al.*, 2018a; Conte and Chaouche, 2016; Hyun *et al.*, 2011). It is believed that within the LVR, the particles are in close contact with one another and their interactions yield a linear elastic behaviour (Qian and Kawashima, 2016; Nehdi and Al Martini, 2007; Schultz and Struble, 1993). The amplitude sweep is often followed by the frequency sweep to investigate the influence of shear rate on the linear VE behaviour (Nachbaur *et al.*, 2001). Below a certain frequency/rate, the VE material has adequate time to relax and release residual energy within its microstructure and elastically return to equilibrium (Sun *et al.*, 2006; Banfill, 1991). At certain high frequency/rate, the VE material's microstructure suffers degradation from residual energy. In other words, frequency sweep can be used to investigate the time-dependent linear deformation behaviour of VE materials using a range of frequencies (Mezger, 2014; Saasen *et al.*, 1991), since frequency is the inverse of time. High frequencies of the sweep simulate the short-term deformation response while the low frequencies simulate the long-term response. This can be likened to the response of a VE material to a quick but heavy (impact) loading and to an extended but light loading, respectively. Other DSR tests used to

characterise viscoelastic materials include creep and creep recovery, stress relaxation and thixotropy tests.

When a force is applied to a VE material, it experiences an initial instantaneous deformation, followed by a gradually increasing deformation (delayed response) (Figure 4.1a). If the stress is removed, the VE material recovers some strain due to its elastic property while some portion of the strain becomes permanent. This phenomenon is simulated and quantified by the creep and creep recovery test. The stress relaxation test simulates and quantifies the behaviour of a VE material subjected to a sustained strain. A typical VE material relaxes/relieves the associated stress (Figure 4.1b). The test can be extended to a repeated sequence to examine the viscoelastic behaviour response to repeated loading. VE behaviours are also time-dependent for most materials (Mezger, 2014; Mewis and Wagner, 2009). Fresh cement-based materials, for example, exhibit a reversible time-dependent VE behaviour mainly due to structuration (Qian and Kawashima, 2016, 2018; Roussel *et al.*, 2012; Sun *et al.*, 2006). This is sometimes referred to as thixotropy/rigidification. Two main forces drive this time-dependency of cement-based materials – flocculation of the particles and hydration. A thixotropy test helps in quantifying the time-dependency of the viscoelasticity. Shear thickening and thinning have been reported in concrete's rheology (Li *et al.*, 2017; Feys *et al.*, 2008) as the time-independent increase and decrease (respectively) in the microstructure's resistance under shearing. In polymer engineering and as later obtained in this study, increase and decrease in the structuration under SAOS is referred to as microstructure thickening and softening respectively. These are sometimes referred to as pseudo-strain hardening and yielding, respectively (Kinloch and Young, 1995).

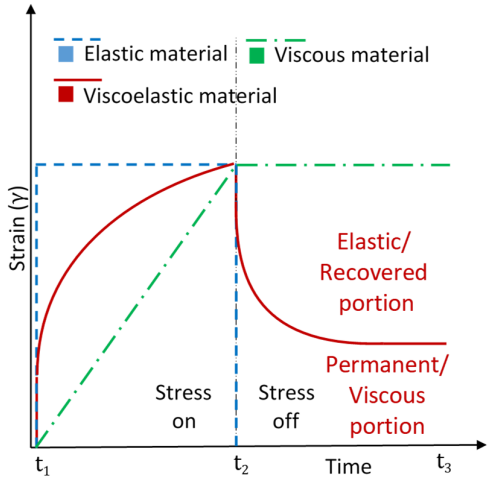

(a) Creep and creep recovery of a VE material

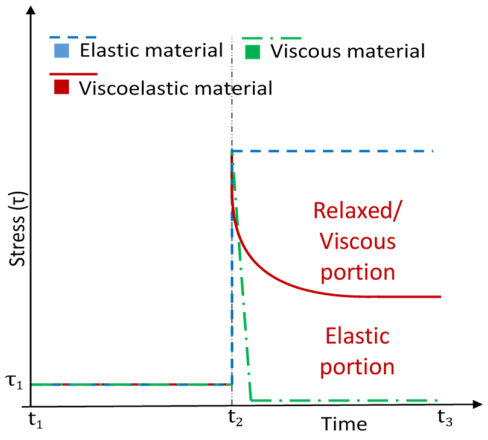

(b) Stress relaxation of a viscoelastic material

Figure 4.1: Viscoelastic behaviour/response to a sustained (a) shear stress and (b) strain

The initial goal of this study was to investigate the rheo-viscoelasticity of concrete, but it was nearly non-existent in literature. Scaling down to mortar, limited studies are available on cement mortar (He *et al.*, 2018a,b; Wang *et al.*, 2015). Scaling down further to cement paste, studies abound on SAOS tests of cement paste (Hu *et al.*, 2019; Qian and Kawashima, 2018; Yuan, Zhou, *et al.*, 2017; Choi *et al.*, 2016; Nehdi and Al Martini, 2007; Sun *et al.*, 2006; Nachbaur *et al.*, 2001; Struble and Schultz, 1993; Banfill, 1991; Papo and Caufin, 1991). However, recent studies on SAOS of cement paste are directed towards the structural build-up (thixotropy and early hydration) rather than fully characterising the VE behaviour. Admixtures such as rheology modifiers can influence the rheo-viscoelastic properties of the cement paste. While the influence of superplasticiser (SP) and water content on the viscoelastic properties of cement paste has been established by various authors (Yuan, Lu, *et al.*, 2017; Yuan, Zhou, *et al.*, 2017; Jayasree *et al.*, 2011; Nehdi and Al Martini, 2007; Sun *et al.*, 2006; Papo and Piani, 2004; Schultz and Struble, 1993), the influence of viscosity modifying agent (VMA) and combined VMA+SP remains scarce in literature.

It is believed that aggregates, which makes up about 60 – 75% of mortar and concrete, are unreactive/inert components/fillers added to cement paste (Mehdipour and Khayat, 2018; Jiao *et al.*, 2017; Zhang, 2011; Mehta and Monteiro, 2006; Newman and Choo, 2003). Aggregates, therefore, can potentially accentuate the VE behaviour of cement paste, how this occurs remains largely unknown. Moreover, most practical applications of fresh cement-based materials are in the form of mortar and concrete whose rheo-related behaviours are different and more complicated than cement paste (He *et al.*, 2018a; Sun *et al.*, 2006; Ferraris and Gaidis, 1992). A typical source of this complexity is the porous nature of cement paste structure and its interfacial transition zone with aggregate (Sun *et al.*, 2006). It is, therefore, necessary to exclusively investigate the viscoelastic behaviour of fresh cement mortar and concrete using SAOS. Most available studies on rheo-related properties of cement-based materials (such as paste, mortar and concrete) are independent studies leading to vastly varying material constituents, instruments' artefacts, and methodology inconsistencies (Lapasin *et al.*, 1983). This does not give room to experimentally observe the behavioural progression and links of cement paste-mortar-concrete, for example, how the inclusion of fine and coarse aggregates influences the established VE behaviour of fresh cement paste.

This study, therefore, aims at improving the body of knowledge on the viscoelastic behaviour of fresh cement-based materials by progressively incorporating aggregates (fine and coarse, in order to form mortar and concrete respectively) in rheologically modified cement paste. The resulting 15 mixes were rheologically investigated to establish their viscoelastic behaviour.

4.3. Experimental framework

4.3.1. Dynamic shear rheometer

One of the reasons for the scarcity of literature on the rheo-viscoelastic behaviour of cement mortar and concrete is due to the limited availability of sophisticated instruments capable of handling the coarse and heterogeneous nature of the cement mortar and concrete. Small amplitude oscillatory shear (SAOS) application require highly accurate and sophisticated kind of measurements (Yuan, Zhou, *et al.*, 2017; Mezger, 2014) which is difficult for materials containing large particles (Hu and Wang, 2011). A special building material cell (BMC 90) capable of testing materials of about 5mm particles with a modular vane in cup geometry (Figure 4.2) (Anton-Paar, 2016) was attempted for use. The BMC 90 consists of a cup with a modular insert cage with serrations to prevent wall slippage during testing and a two hollow blades vane (modular stirrer model ST59-2V-44.3/120) with flow breakers to enhance mix-up effects (Figure 4.2). The BMC 90 was attached to a Physica MCR 501 rheometer from Anton Paar (Anton-Paar, 2009).

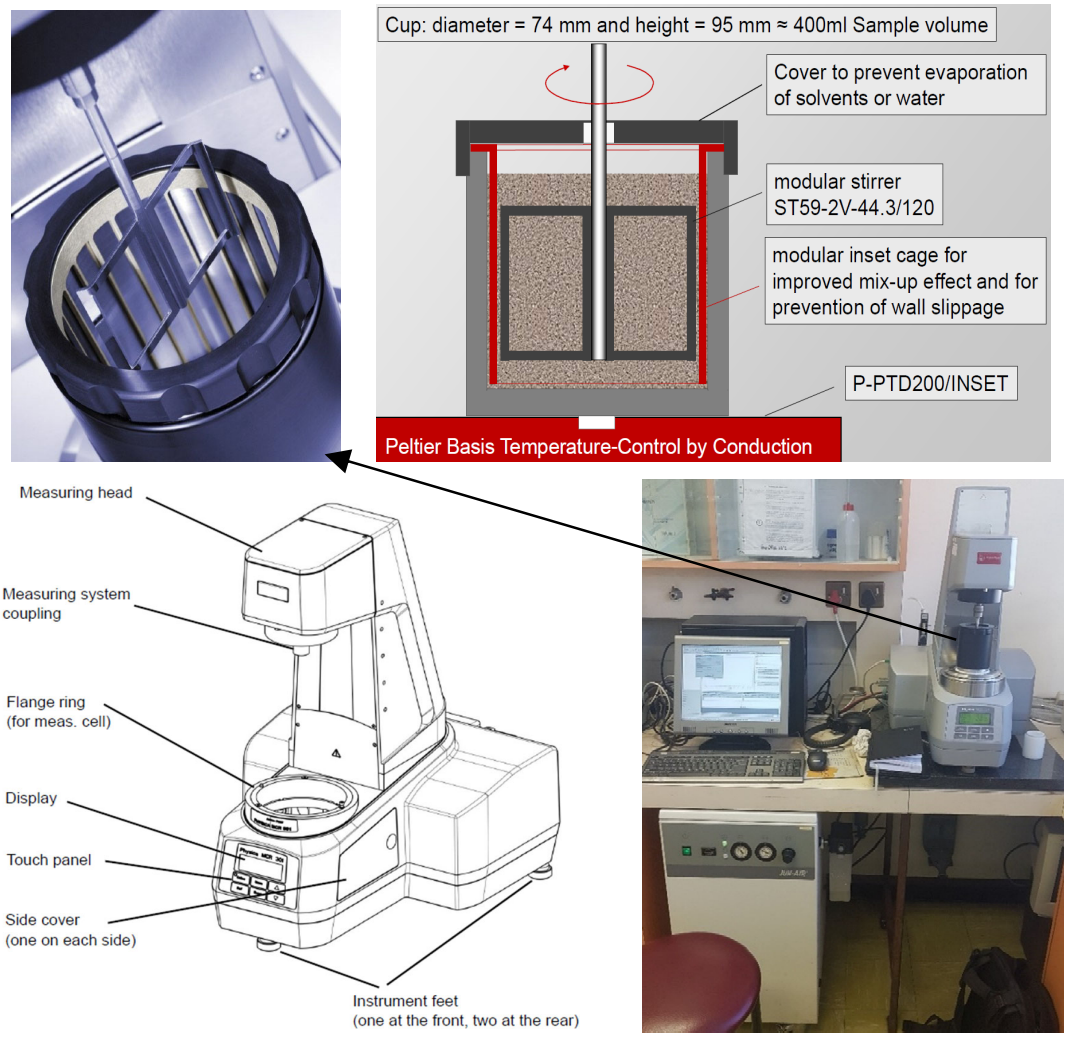

Figure 4.2: Special building material cell (BMC 90) (Anton-Paar, 2016) and MCR 501 rheometer

Table 4.1: Details of the Physica MCR 501 rheometer (Anton-Paar, 2009)

Minimum Torque (Nm)	0.02 µNm
Maximum Torque (Nm)	230 mNm
Minimum strain rate	10^{-7}/min
Maximum strain rate	3000/min
100% strain	1 rad
Normal force range	0.01N to 50 N at 0.002 resolution
Temperature range	-150 to +1000 ^{o}C
Vane size	65 mm diameter, 60 mm height With two 22.5 mm and 53 mm hollows
Cup size	74 mm diameter, 95 mm height
Sample volume	400 mL
Conversion constant C_{SR}	1 min/s
C_{SS}	14.07 Pa/mNm

C_{SR}/C_{SS} - shear rate/shear stress conversion constants

The Physical MCR 501 rheometer is capable of both shear stress and strain controlled oscillation while it allows for samples' temperature control via a Peltier temperature device (Anton-Paar, 2012). Although the BMC is advised as a means for relative measurement by the manufacturer, using it is argued to be an important step towards closing the gap in knowledge on fresh mortar and concrete's rheo-viscoelastic behaviour. Moreover, conventional geometries (such as parallel plates, concentric cylinders, and cone-plate) associated with polymer-related researches have been shown to yield imprecise data and cause errors in dispersed/suspension systems (Kim *et al.*, 2018; Choplin and Marchal, 2010) such as cement-related researches (Nachbaur *et al.*, 2001; Lapasin *et al.*, 1983; Bhatty and Banfill, 1982). These conventional geometries have high sensitivity to sample segregation, sedimentation and friction between particles which are associated with cement-based materials. Furthermore, (Nachbaur *et al.*, 2001; Gill and Banfill, 1988; Bhatty and Banfill, 1982) using impellers in cylindrical bowls obtained similar rheological information/signature to those of conventional geometries and with lesser variance between replicate samples of the same cement paste materials/mixes. Therefore, it may be concluded that the BMC 90 geometry is a good or even the best option for coarse suspension samples, compared to other geometries of rheometers.

4.3.2. Material properties and mix design

The mix proportions and constituent materials of the mixes are shown in Table 4.2 while the chemical properties of the cement are shown in Table 4.3. Since particle size and distribution are known to influence the rheological properties of suspensions (Bentz *et al.*, 2012; Mangesana *et al.*, 2008; Olhero and Ferreira, 2004), the particle size distributions of the dry constituent materials are shown in Figure 4.3. A fine natural aggregate/sand (average particle diameter of 0.3 mm) and coarse

aggregate/stone (nominal size of 6 mm) were used for the cement-based materials to obtain cement mortar and concrete respectively. The 6 mm nominal size (Table 5.1 and Figure 4.3) used for the concrete is 1 mm above the size recommended for the BMC 90 (5 mm – Section 4.3.1). It is, however, believed that this would not negatively influence the results. Moreover, less quantity of stone (cement, sand and stone ratio of approximately 1:2:1) was used in the concrete mixes to mitigate the possible effects of the larger stone size. That is, the rheometer's torque capacity (maximum normal force and torque of the BMC 90's vane) was found to adequately handle the ensuing concrete's stiffness for at least 2 hours.

Table 4.2: Material constituents and properties

Cement-based materials			Mixes	Material constituent (kg/m^3)				
				C	CV	CS	CVS	CW
Cement concrete	**Cement mortar**	**Cement paste**	Water	217	217	217	217	223
			Cement - CEM II 52.5N	395	395	395	395	374
			Specific surface area	1.336 m^2/g				
			VMA	-	0.6%	-	0.4%	-
			Superplasticiser	-	-	0.6%	0.4%	-
			w/c ratio	0.55	0.55	0.55	0.55	0.6
			Static yield stress (Pa)	27.08	25.69	10.66	8.93	17.30
			Malmesbury fine sand	774	774	774	774	796
			Water absorption	8.57%				
			Specific gravity	2.60				
			Static yield stress (Pa)	111.72	78.34	54.18	44.44	85.37
			6mm Greywacke stone	412	412	412	412	407
			Water absorption	1.65%				
			Specific gravity	2.75				
			Static yield stress (Pa)	315.17	304.50	108.55	162.71	161.31
C – control; CV – control + VMA; CS – control + SP; CVS – control + VMA + SP; CW – control + water								

Table 4.3: Chemical properties of the cement

Oxides	CaO	Al_2O_3	Fe_2O_3	K_2O	MgO	MnO	Na_2O	P_2O_5	SiO_2	TiO_2	LOI
%	62.7	3.45	2.86	0.51	1.13	0.05	0.26	0.15	19.28	0.18	6.39

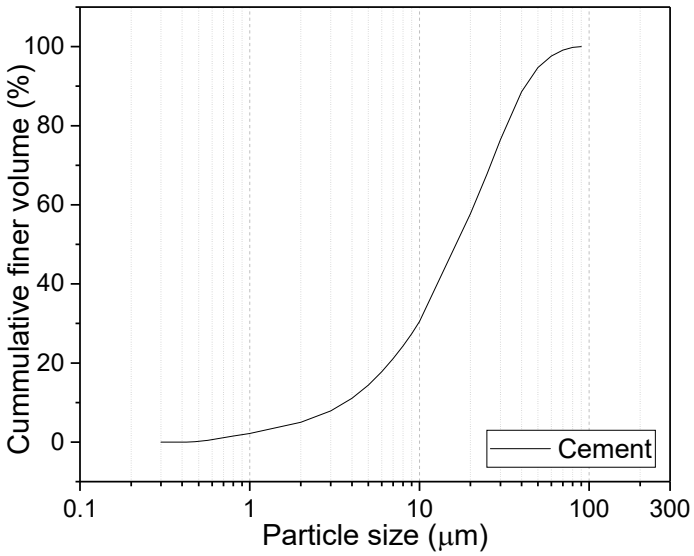

(a) Cement

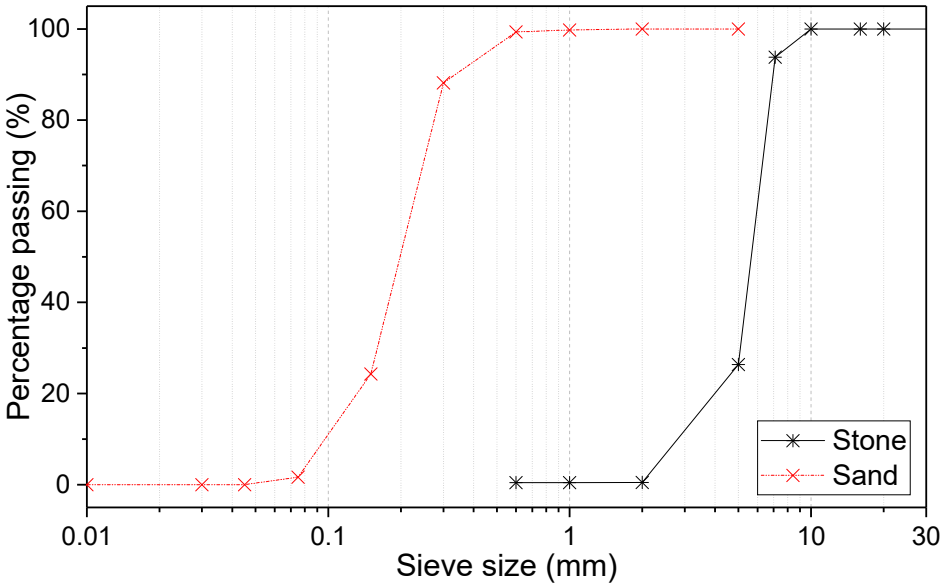

(b) Sand and stone

Figure 4.3: Particle size distribution of the dry constituents

The control mix was rheologically modified using polysaccharide-based liquid viscosity modifying agent (VMA), polycarboxylate ester liquid superplasticiser (SP) and water to yield five mixes labelled as C, CV, CS, CVS and CW (see Table 4.2). The VMA has a specific gravity of 1.0, pH of 9.5, chloride content of less than 0.1% and sodium oxide content of less than 1% while the SP has a specific gravity of 1.05, pH of 7, chloride content of less than 0.1% and sodium oxide content of less than 1%. The admixtures were added by weight of the cement to the mixing water before adding the mixing water to the dried-mixed cement-based constituents in a pan mixer. The dry materials were initially mixed for one minute before adding the mixing water and thereafter mixed for two minutes. The mixes were placed in the BMC 90 without vibration. The end of mixing was taken as time zero for all the

tests and it took about 5 minutes from the end of mixing to the start of each test. This time was maintained for all tests to minimise exogenous error from varying preparation times (Nehdi and Al Martini, 2007). After inserting the vane, the samples were allowed to rest for three minutes to reach substantial equilibration from the sampling and inlet of the modular vane disturbance (Mahaut, Chateau, *et al.*, 2008). This improves the reproducibility of results (Mazzeo, 2008). Fresh samples were prepared for each test (including duplicates) since the viscoelastic and rheological behaviours of cement-based materials are known to be time and shear pre-history dependent (Qian and Kawashima, 2018; Nehdi and Al Martini, 2007). At least two fresh samples were tested for each reported result and all the tests were carried out at a temperature of 23±2°C.

4.3.3. Rheo-viscoelastic tests

As noted earlier, when a viscoelastic (VE) material is subjected to an oscillating strain, the response stress has a phase lag/angle (δ) which is one of the parameters that define the viscoelasticity. Some of the rheo-viscoelastic parameters used to define viscoelasticity include complex shear modulus (G*), storage/elastic modulus (G'), loss/viscous modulus (G"), critical stress/strain (τ_c/γ_c), creep compliance (J), relaxation modulus (G), and thixotropic restructuration (Nachbaur *et al.*, 2001). The processing equations (He *et al.*, 2018a; Yuan, Lu, *et al.*, 2017; Qian and Kawashima, 2016; Mezger, 2014; Nehdi and Al Martini, 2007; Nachbaur *et al.*, 2001; Schultz and Struble, 1993) are:

$$\gamma_t = \gamma_A . \sin(\omega t) \quad \text{Equation 4.1}$$

$$\tau_t = \tau_A . \sin(\omega t + \delta) \quad \text{Equation 4.2}$$

$$G^* = \frac{\tau}{\gamma} \quad \text{Equation 4.3}$$

$$G^* = G' + iG'' = |G^*|\cos\delta + i|G^*|\sin\delta = \sqrt{|G'|^2 + |G''|^2} \quad \text{Equation 4.4}$$

$$\tan\delta = \frac{G''}{G'} \quad \text{Equation 4.5}$$

where γ_t and τ_t are the oscillating strain and stress respectively, γ_A and τ_A are the strain and stress amplitude, ω is the angular frequency, t is the time, G^*, G' and G'' are the complex, storage and loss modulus respectively, δ is the phase lag between the shear strain and stress, $i^2 = -1$.

These parameters are obtained from the tests highlighted in the subsequent sections and indicate the nature, state and microstructure of the test material as shown in Table 4.4.

Table 4.4: Viscoelastic parameters of various material states as adapted from (Mezger, 2014; Nachbaur *et al.*, 2001)

Ideally viscous material	Viscoelastic liquid	Viscoelastic suspension or solid	Ideally elastic material
Viscous	Less viscous	Less solid	Solid
$\delta = 90°$	$90° > \delta > 45°$	$45° > \delta > 0°$	$\delta = 0°$
$\tan\delta \rightarrow \infty$	$\tan\delta > 1$	$\tan\delta < 1$	$\tan\delta \gg 0$
$G' \rightarrow 0$	$G'' > G'$	$G' > G''$	$G'' \rightarrow 0$
$G^* = iG''$	$G^* = G' + iG''$	$G^* = G' + iG''$	$G^* = G'$

4.3.3.1. Amplitude sweep

This test yields some of the viscoelastic parameters of the cement-based materials, such as G*, G', G", γ_c (LVR limit), and δ. It involved the application of an increasing strain/stress (amplitude) at a constant shearing rate (frequency). For the purpose of this study, a controlled strain sweep was done from 10^{-4}% to 10^{2}% at a logarithm ramp of 10 points/decade and a frequency of 10 rad/s. The choice frequency value was preliminarily determined to be adequate for linear VE response. The LVR is taken as the range of strain where G' remains constant (on a logarithm scale), that is, the sample behaves as an elastic material. The limit of this range defines the γ_c and is taken as the strain associated with a 10% reduction in G' (Mezger, 2014; Subramaniam and Wang, 2010). This method is preferable because not all tests (e.g. Figure 4.4a) show an easily identifiable deflection/reduction in G' (Yuan, Lu, *et al.*, 2017). The G* defines the stiffness of the VE material (Equation 4.3) to shearing, which has elastic (G') and viscous components (G') (Kim *et al.*, 2018). G' is the storage modulus which accounts for the elastic energy stored by the VE material and reflects the crosslinking and interactions between the particles while G" is the loss modulus that accounts for the dissipated/consumed energy due to the viscous component of the viscoelasticity (He *et al.*, 2018a; Saasen *et al.*, 1991).

4.3.3.2. Frequency sweep

This involved the application of an increasing shearing rate at a constant amplitude (shear strain) within the LVR to monitor the VE response. A sweep from 100 rad/s to 0.1 rad/s at a logarithm ramp of 15 points/decade at an amplitude strain of 10^{-2}% was carried out on all the cement-based materials. The selected amplitude strain for the frequency sweep was based on the earlier determined LVR from the amplitude sweep.

4.3.3.3. Creep and creep recovery test

This test involved the application of an instant and constant shear stress (τ_0) from time t_1 to t_2 (Figure 4.1) while measuring the deformation of the sample between the time interval (Mezger, 2014). The shear stress is then removed at time t_2 while the deformation recovery with time is measured up to time t_3. Both sequences of tests are, hence, termed creep and creep recovery. For this study, 10 minutes and 30 minutes intervals ($t_1 - t_2$ and $t_2 - t_3$) were used. The time intervals were found to be sufficient for all the mixes to reach steady strain values. τ_0 values used for each mix are shown in Table 4.5 and were taken as approximately 50% of the yield value (Khan, Castel, *et al.*, 2017; Khan *et al.*, 2016). The measured deformation and recovery can be expressed as creep compliance and creep recovery compliance (J) by dividing the deformation by the applied shear stress (Mezger, 2014; Struble and Schultz, 1993),

$$J(t) = \frac{\gamma(t)}{\tau_0} \qquad \text{Equation 4.6}$$

where $J(t)$ is the creep compliance, $\gamma(t)$ is the measured strain, t is the time, τ_0 is the constant applied stress.

This makes the result material-dependent and independent of the applied shear stress (Mezger, 2014). The percentage creep recovery of the mixes was also evaluated according to:

$$\text{Percentage recovery} = \frac{J_m}{J_e}\, x\, 100\% \qquad \text{Equation 4.7}$$

where J_m is the maximum creep compliance, and J_e is the equilibrium creep compliance after recovery.

Table 4.5: Shear stress values for the creep and creep recovery test

	C (Pa)	CV (Pa)	CS (Pa)	CVS (Pa)	CW (Pa)
Paste	12	10	4	4	8
Mortar	55	40	26	21	40
Concrete	148	148	194	80	80

4.3.3.4. Stress relaxation test

For this study, a pre-strain (γ_1) of 2% of the relaxation strain was applied from time t_1 to t_2 (Figure 4.1) to level-out the possible effects of pre-stresses due to sampling (Mezger, 2014). Thereafter, an instant strain (γ_0) was applied at time t_2 and kept constant up to time t_3 while monitoring the viscoelastic behaviour of the sample in the form of stress relaxation (reduction with time). The value

of γ_0 was taken as approximately 50% of the yield strain (Table 4.6) (Khan, Castel, *et al.*, 2017; Khan, Kolawole, *et al.*, 2017). The results can be expressed as relaxation modulus to yield a material-dependent property that is independent of the applied strain (Mezger, 2014),

$$G(t) = \frac{\tau(t)}{\gamma_0} \qquad \text{Equation 4.8}$$

where $G(t)$ is the relaxation modulus, $\tau(t)$ is the measured stress, t is the time, γ_0 is the constant applied strain.

The percentage of stress relaxation was also evaluated using,

$$\text{Percentage relaxation} = \frac{G_0}{G_e}\ x\ 100\% \qquad \text{Equation 4.9}$$

where G_0 is the instantaneous relaxation modulus, and G_e is the equilibrium relaxation modulus.

The test was taken a step further to examine the influence of five repeated loadings on the VE response of the cement-based materials. The samples were allowed to rest for 5 minutes between each repetition of loading.

Table 4.6: Shear strain values for the stress relaxation test

	C (%)	CV (%)	CS (%)	CVS (%)	CW (%)
Paste	0.1	0.1	0.05	0.08	0.12
Mortar	0.3	0.2	0.2	0.2	0.2
Concrete	0.8	0.8	0.8	0.8	0.5

4.3.3.5. 3ITT thixotropy test/time-dependency of the VE behaviour

The three interval thixotropy test (3ITT) consists of three intervals of tests, the first is a test of constant amplitude and frequency within the LVR to measure the reference state of the sample without interrupting the microstructure. This is followed by the second interval, where a high amplitude and frequency is applied to destroy the sample's microstructure. The third interval is the same test as the first, which measures the reversible restructuration (degree and speed of recovery) of the sample. An amplitude strain of 0.01% at 10 rad/s was used for the first and third intervals. The parameter of interest examined during the intervals to give insights into the microstructure is G' since it is accepted to measure the structure's rigidification (Roussel *et al.*, 2019). The time-dependent nature of the cement-based materials is examined by the thixotropy test.

4.4. Results and discussion

Generally, for the rheo-viscoelastic measurements, the cement paste and mortar mixes have a smooth response (torque measurements) to the instrument's induced strains (from the vane) while the concrete mixes results have more noise due to increased stiffness from the coarse aggregate.

4.4.1. Viscoelastic behaviour of the cement-based materials

Figure 4.4 shows the response of the cement-based materials to the strain sweeps. Figure 4.4a reveals that the cement paste Mixes C and CV have similar VE behaviour with more elastic tendencies than the other mixes. That is, the inclusion of viscosity modifying agent (VMA) in cement paste did not significantly influence the VE behaviour while the inclusion of superplasticizer (SP), VMA and SP (VMA+SP), and increased water did reduce the elastic component of the VE properties while increasing the viscous component. This can be deduced from the trends of the storage/loss modulus and phase angle of the paste mixes vis-à-vis Table 4.4. However, the addition of aggregates in the mixes remarkably reduced the effects of the rheology modifiers on the VE response of the cement paste by increasing the elastic response while reducing the viscous response. Explicitly, the addition of sand to the cement paste caused an average increase of 9% in G' for Mixes C/CV and 49% for Mixes CS/CVS/CW while the addition of stones to the mortar caused an average increase of 26% in Mixes C/CV and 24% in Mixes CS/CVS/CW. The rheology modifiers also influenced the G'' values of the concrete mixes with no significant influence on the G' (Figure 4.4c). That is, the rheology modifiers caused the concrete to exhibit more flowability and energy consumption/dissipation with good stability/stiffness (He *et al.*, 2018a). These results suggest that satisfiable conclusions about concrete's VE behaviour may not be approximate-able from that of cement paste as generally suggested in literature, since the rheology modifiers diversified the trend of behaviour. This is because authors (Mehdipour and Khayat, 2018; Jiao *et al.*, 2017; Mahaut, Mokéddem, *et al.*, 2008) often specify that sand and stone are unreactive solid components in mortar and concrete and therefore, may only magnify the rheo-related properties and not diversely influence it as obtained in this study. However, as observed, the behavioural trend of the mortar is closer to that of concrete than that of the paste. Also, the increase of coarse solid volume fraction can potentially reduce the effects of rheology admixtures in cement-based materials.

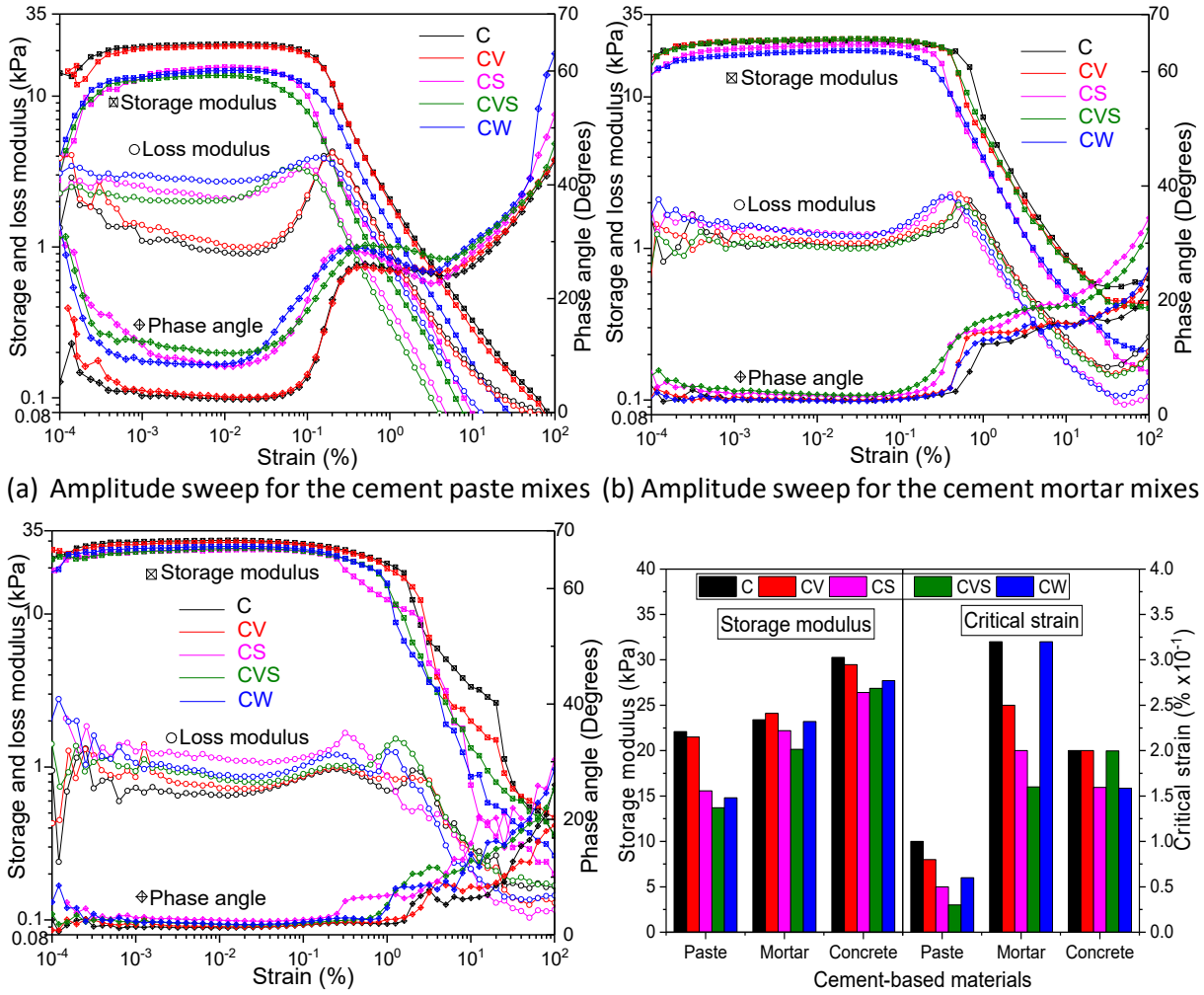

(a) Amplitude sweep for the cement paste mixes (b) Amplitude sweep for the cement mortar mixes

(c) Amplitude sweep for the cement concrete mixes (d) Storage modulus and critical strain (LVE limit) for the cement-based materials

Figure 4.4: Results of the amplitude sweep for all mixes

Figure 4.4d shows the G' and critical strain (γ_c) obtained from the amplitude sweep of the cement-based materials. Some of the factors that influence G' include particle interaction/adhesion/bridges/linking, particle packing density and level of particle dispersion (He *et al.*, 2018a; Qian and Kawashima, 2016, 2018; Nehdi and Al Martini, 2007; Sun *et al.*, 2006). The rheology modifiers are known to influence these factors (Kolawole *et al.*, 2019a). VMA is known to cause microstructure thickening by polymer entanglement (Bouras *et al.*, 2012; Khayat, 1998), thereby, improving the particles' bridging that can nullify its negative impact on G' due to dilution. The possible reason for the reduction of G' of the cement paste by SP, VMA+SP, and increased water is their increased contribution to particle dispersion (evident in the lower static yield stress in Table 4.2). In the same vein, the increased particle packing of mortar and concrete caused the increased progression in G' with reduced effects of the rheology admixtures. The LVR of cement paste in this study is in the order of 10^4 Pa and 10^{-2}% for the G' and γ_c respectively, which is also the general

consensus in the literature (He *et al.*, 2018a; Yuan, Lu, *et al.*, 2017; Nehdi and Al Martini, 2007; Nachbaur *et al.*, 2001; Schultz and Struble, 1993; Banfill, 1991). The sand/stone in mortar/concrete increased the γ_c to the order of 10^{-1}% but the stone generally reduced the absolute value compared to that of mortar. That is, the inclusion of sand in cement paste yielded a more ductile cement-based material while the addition of both sand and stone yielded a more brittle cement-based material. Ideally, wet cement paste has higher bond area and better lubricating effects around fine sand than larger sized stones (Newman and Choo, 2003) which could lead to the more ductile cement mortar. Furthermore, the bigger the size of aggregates, the weaker the interfacial transition zone between the aggregates and the bulk paste (Elsharief *et al.*, 2003) leading to a more brittle cement-based material. The rheology modifiers generally reduced the γ_c (that is, the linear viscoelastic range – LVR) of cement-based materials.

As noted earlier, the VE response of the cement-based materials beyond the LVR is synonymous to that of large amplitude oscillatory shear (LAOS) tests that gives insight into the viscoplastic response (He *et al.*, 2018a; Qian and Kawashima, 2016) and is visible on Figure 4.4a-c as the reduction of the G'/G'' and increase in δ. For the cement paste (Figure 4.4a), Mixes C/CV have similar response and Mixes CS/CVS/CW behaved similarly while for the mortar (Figure 4.4b), the observable pattern was C/CV/CVS and CS/CW. This response pattern for the mortar was also obtained for the concrete in the δ plot while the G'/G'' plots of the concrete mixes have too many fluctuations to deduce patterns. These patterns of the cement paste, mortar and concrete can be associated to the envisaged viscoplastic behaviour of the mixes, confirming the earlier conclusion regarding the differing influence of aggregates on rheo-related properties of cement-based materials.

4.4.2. Influence of rate on the viscoelastic response

Figure 4.5a shows the response of the cement paste to the shear rate sweep, it should be noted that the shearing rate sweep was done decreasingly from 100 rad/s to 0.1 rad/s within the LVR. The pastes' microstructures were generally stable for the simulated short term deformation, that is, a linear response was observed from 100 rad/s down to about 4 rad/s where there was an increase in the storage modulus (G') of the mixes. The increase in the storage modulus at lower frequencies can be due to shear thickening (that is, pseudo-strain hardening (Kinloch and Young, 1995)) which emanates from the continuous strain oscillations. That is, the paste microstructure can be said to have reached a response peak where the reducing rate of shearing allows for particle flocculate (Saasen *et al.*, 1991). Starting the sweep test for the fresh sample at a high shear rate of 100 rad/s, the cement paste could not relax the stress at each repetition of strain leading to residual stress

(Sun *et al.*, 2006). Hence, there's an increase in δ/G'' down to 4 rad/s where the stress becomes adequately relaxed which can then allow for flocculation. Expectedly, there ought to be a microstructure destruction (decrease in G') during this period (He *et al.*, 2018a) (slightly shown by Mix CV). Therefore, the relatively stable G' signifies that an inherent simultaneously occurring thickening due to the straining was occurring. This form of thickening for similar concrete mixes due to long term shearing (deformation) was qualitatively reported in a companion paper (Kolawole *et al.*, 2019a) as rheopexy. Furthermore, He *et al.* (2018) and Nachbaur *et al.* (2001) stated that if the frequency sweep shows no influence on G', then, no structural changes are occurring while Sun *et al.* (2006) reported that hydration has no substantial influence on G' of cement paste with similar w/c ratio until about 1 hour (dormant period). In essence, the long-term linear deformation behaviour of the cement paste, without the substantial influence of hydration, may be in the form of a shear thickening (pseudo-strain hardening).

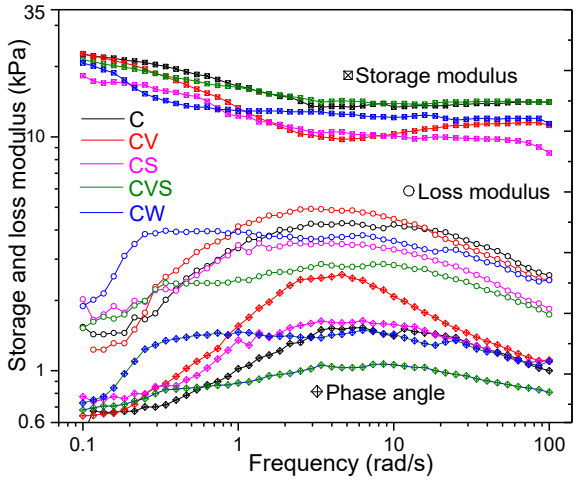

(a) Frequency sweep for cement paste mixes

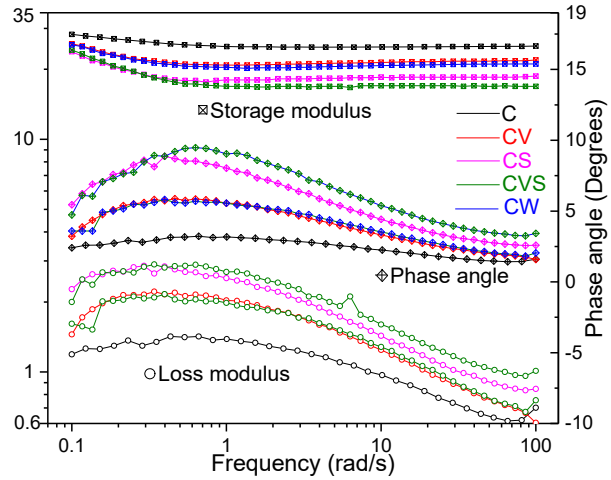

(b) Frequency sweep for the cement mortar mixes

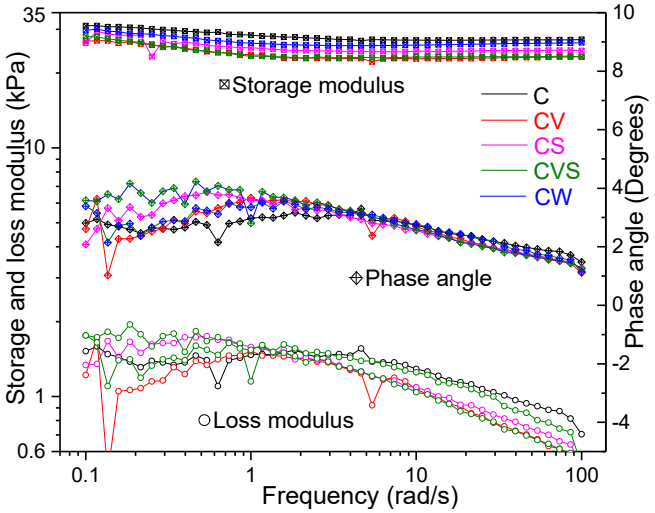

(c) Frequency sweep for the cement concrete mixes

Figure 4.5: Frequency sweep results of the cement-based materials

The rheology modifiers did not significantly change the paste response except for SP that has low G' at very high frequency, this was also reported by Papo and Piani (2004) for cement paste containing SP. However, increased water content (Mix CW) caused the thickening to start occurring only at a shear rate of approximately 0.3 rad/s while the viscosity modifying agent (VMA in Mix CV) magnifies the thickening. This could be due to the liquid phase thickening by VMA's polymer entanglement (Bouras *et al.*, 2012; Khayat, 1998). Saasen *et al.* (1991) also reported similar influence of a propanesulfonate-based copolymer on oilfield cement slurries. The response of the cement mortar mixes shown in Figure 4.5b is similar to that of the cement paste but at a lesser magnitude and the thickening starts at a lower shearing rate of about 0.6 rad/s down to about 0.1 rad/s. This implies that the inclusion of sand in cement paste reduces the variation/instability of the microstructure to extended (but low) linear deformation. The addition of stones to the mortar to make concrete (Figure 4.5c) further reduces the variation/instability. The comparative reduction due to the increasing volume fraction of the aggregates is also evident from the decreasing plot scale of the phase angle (cement-mortar-concrete) of Figure 4.5a-c. It can, therefore, be concluded that increase in the coarse solid volume fraction of cement-based materials tend to improve the microstructure stability to varying shearing rate and extended linear deformation.

4.4.3. Creep and creep recovery

The creep and creep recovery compliance of the cement-based materials shown in Figure 4.6 reveals the viscoelastic response of the microstructure to stress application and removal. Compliance is the corresponding strain due to the application of unit stress. Note that 50% of the yield stresses were adopted for each of the mixes (Table 4.5) which allows for equitable comparison. Furthermore, the viscosity and angular velocity were monitored to ensure there was no bifurcation that signifies the start of transient flow (Qian and Kawashima, 2016, 2018; Coussot *et al.*, 2002; Struble and Schultz, 1993). The rheology modifiers influenced the creep of the cement-based materials with the greatest influence on the cement paste (Figure 4.6a) while increase in the coarse aggregate volume and size reduced the creep ability. Viscosity modifying agent (VMA) reduced the creep of the cement paste by 81% while superplasticiser (SP), VMA and SP (VMA+SP), and water increased the creep compliance by 976%, 1728%, and 219% respectively. Although the paste Mix CVS showed significant creep, it still recovered substantially more than the control mix (see Figure 4.7a). Figure 4.6a shows further that the paste mixes experienced a reduction in strain after the peak value which is before the recovery phase, and pastes with higher creep also showed more strain reduction. This implies that a sudden application of stress could cause a corresponding thickening in the microstructure of cement paste. Figure 4.6b shows that only the inclusion of SP in the mortar mixes caused the

pseudo-strain hardening/thickening while only concrete Mixes C/CW in Figure 4.6c slightly exhibited the thickening. It should be noted that unlike the paste mixes, the mortar and concrete mixes showed more instantaneous recovery before the viscous delayed recovery showing that the increased coarse solid volume fraction caused more elastic behaviour. Likewise, the increased elastic behaviour can be seen from the reduced values of creep compliance due to the increased coarse solid volume fraction. The observed differing influence of the rheology modifiers in the paste-mortar-concrete mixes creep and recovery behaviour reiterates that accurate conclusions should not be made about the VE behaviour of concrete/mortar from that of the paste.

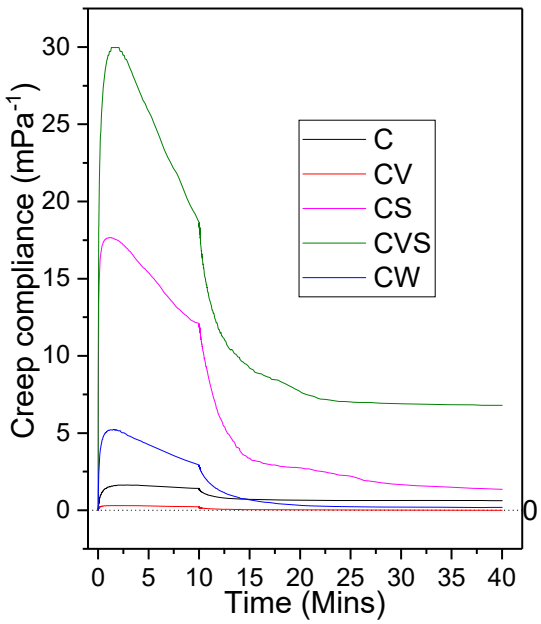

(a) Results of cement paste mixes

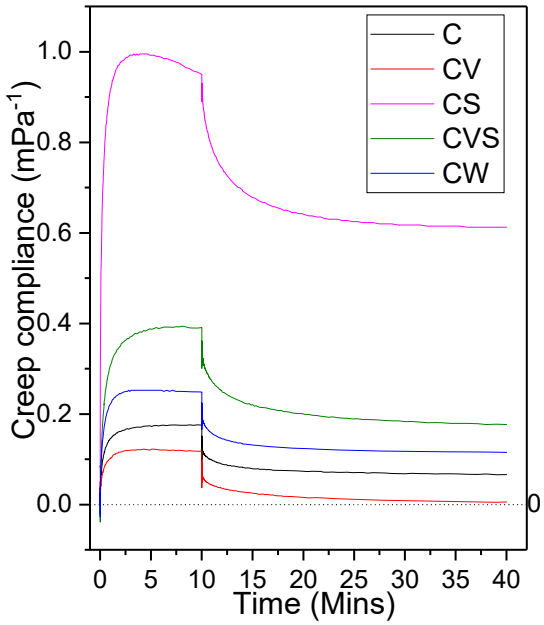

(b) Results of cement mortar mixes

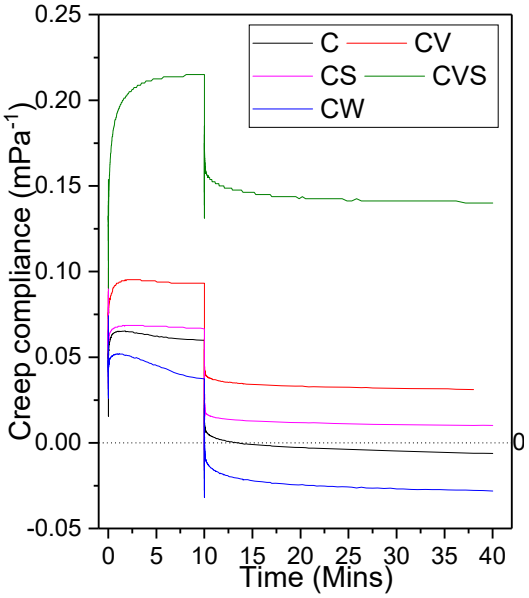

(c) Results of cement concrete mixes

Figure 4.6: Creep and creep recovery test results for the cement-based materials

From Figure 4.6c, Mixes C/CW showed a creep recovery slightly below zero, that is, the rheometer's vane (after stress removal) returned beyond the initial position at the application of the stress. The reason for this observation is unknown and not found in the literature. However, it is suggested that the sudden relieve of the liquid-filled micropores due to the stress removal may have caused some microscopic softening/yielding of the liquid in the micropores, thereby, diffusing through the micropores to assist recovery. Evidently, Mix CW with more water and liquid phase showed more of the negative creep recovery. Moreover, for hardened concrete, the presence of free water (including some adsorbent solids) is believed to be responsible for creep (Rossi and Acker, 1988; Bazant, 1975; Ward and Cook, 1969) by diffusing through the pores under a continuously applied load. Some studies (Mallick *et al.*, 2019; Brooks, 2005; Wittmann, 1973) have also shown that more capillary water and pore humidity caused a higher rate of creep in cement-based materials. It should be noted that this suggested phenomenon for the negative creep compliance values is dissimilar from the reduction in the creep/strain of the cement paste mixes after the peak values (Figure 4.6a).

Figure 4.7a shows the percentage recovery of the cement-based materials, the more the recovery, the more elastic the mix (viscoelastic solid). The viscoelastic solid kind of recovery in Figure 4.7a (that is, above 35%) shows the fact that the creep phase did not cause transient damage to the samples' microstructure (Qian and Kawashima, 2018; Struble and Schultz, 1993) which can potentially cause a viscoelastic liquid recovery (<5%). Though Jayasree *et al.* (2011) reported that SP reduced creep recovery of cement paste, the rheology modifiers (including SP) in this study generally improved the recovery of the cement paste. The earlier suggested phenomenon on micropore liquid yielding could also be responsible here, especially for Mixes CS, CVS and CW with higher dispersed structure (evident in their lower static yield stress) while the VMA polymer entanglement could help Mix CV's elastic recovery. The figure also reveals that Mixes CV/CVS consistently showed less recovery from the deformation as the aggregate volume increased. That is, increased aggregate reduced the ability of the VMA's polymer entanglement to contribute to elastic deformation behaviour. While the rheology modifiers improved the cement paste recovery (elastic behaviour), they tend to reduce the recovery of the mortar and concrete.

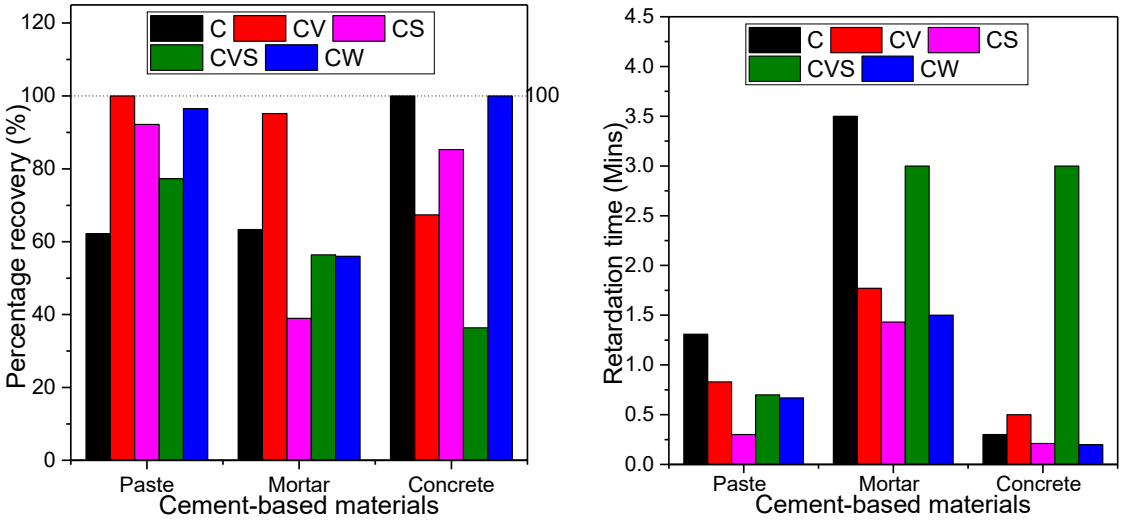

(a) Percentage recovery (b) Retardation time

Figure 4.7: Percentage recovery and retardation time of the cement-based materials

Figure 4.7b shows the retardation time of the cement-based materials. It quantifies the delayed response of the cement-based material (in terms of time) to the applied stress and can be referred to as delayed deformation or elasticity (Mezger, 2014). It is the time taken for a VE material to reach the maximum creep/strain (which is taken as 95% of the peak compliance value for this study (Mezger, 2014)), an ideally elastic material will have an instantaneous creep (response) with zero-time delay as shown in Figure 4.1. It can be observed from the results that the sand in the mortar mixes tends to cause an increased delay while the stones in the concrete mixes reduced the delay. This reiterates the ductile tendency of the cement-based materials due to the inclusion of sand and the ductility reduction due to the additional inclusion of stones, as observed for the critical strain in Section 4.4.1.

4.4.4. Stress relaxation

Figure 4.8 shows the stress relaxation modulus of the cement-based materials. Stress relaxation modulus is the stress due to the application of unit strain. Note that 50% of the yield strains were adopted for each of the mixes (Table 4.6) which allows for equitable comparison. The instantaneous stress relaxation modulus (G_0) values of the mixes are also shown in the legends of Figure 4.8 and the points marked on the plots. The figure reveals that the cement paste (Figure 4.8a) exhibited higher instantaneous stress than that of the mortar (Figure 4.8b) while that of the mortar is similar to that of the concrete (Figure 4.8c). This is because the G_0 is a function of the solid-like properties of a sample (Gregory and O'Keefe, 1990). That is, for both the mortar and concrete, a unit strain causes similar instantaneous stresses though the equilibrium relaxed stresses of the concrete mixes are higher than that of the mortar due to concrete's increased elastic properties due to increased

aggregate volume fraction. Moreover, the influence of the rheology modifiers on the instantaneous modulus became dampened due to sand and stones (cement-mortar-concrete) as similarly obtained for the storage modulus in Section 4.4.1.

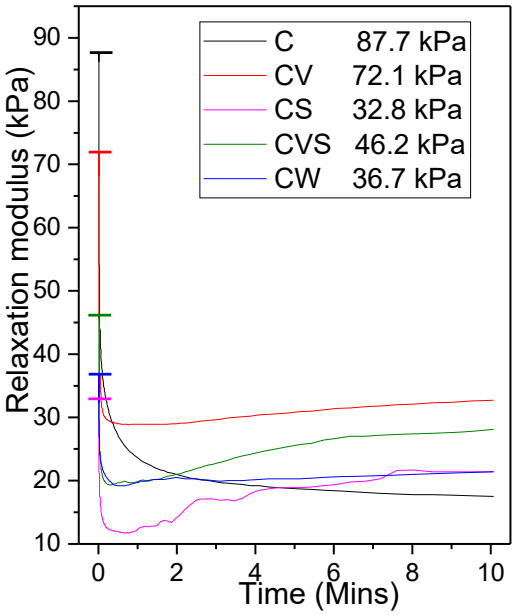

(a) Results of cement paste mixes

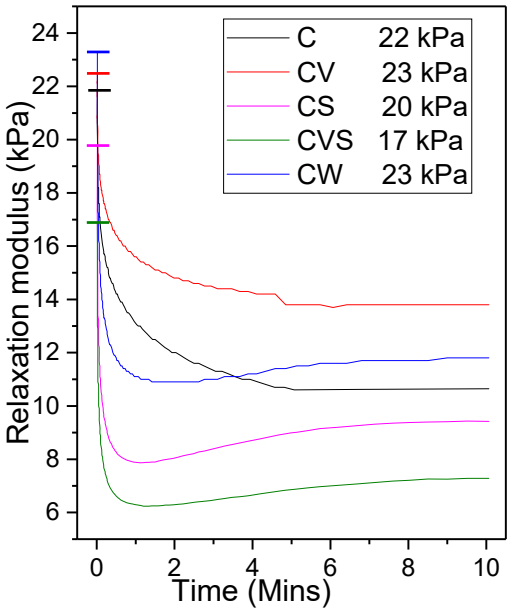

(b) Results of cement mortar mixes

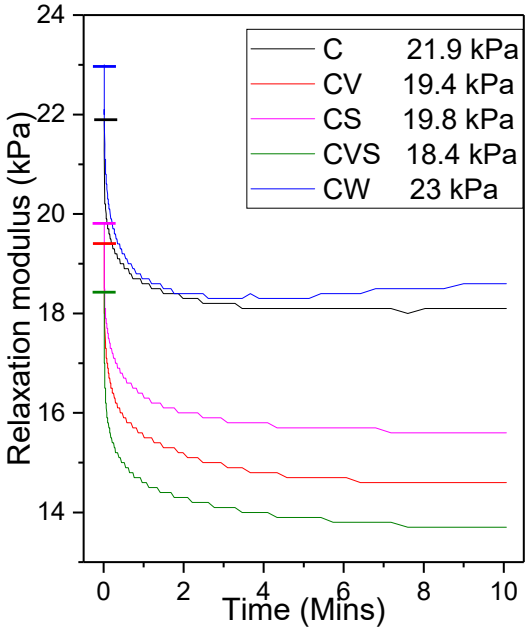

(c) Results of cement concrete mixes

Figure 4.8: Stress relaxation test results for the cement-based materials

Similar observations as that of the creep compliance are also visible in Figure 4.8a. That is, there is an increase in stress after the maximum relaxation (plot trough) for mixes containing the rheology modifiers while there was a decrease in strain after the maximum creep (plot peak) for the creep test. Some authors have argued that relaxation and creep are inverse of each other for hardened concrete (Pane and Hansen, 2002; Bazant and Gettu, 1992; Rossi and Acker, 1988; Taylor and

Maurer, 1973) and that creep is responsible for stress relaxation of hardened concrete (Altoubat and Lange, 2001; Kolver *et al.*, 1999). The noted similar observations between the creep and relaxation results of fresh cement-based materials, therefore, tend to support this argument. That is, the application of the step strain by the rheometer's vane can inherently cause creep in the opposite direction of the vane's movement, leading to stress relieve. The increase in stress after the maximum relaxation can be due to the microstructure thickening as explained for the creep behaviour. The progression of cement paste-mortar-concrete (that is, increasing aggregate volume) generally reduced this microstructure thickening. Only Mix CW (containing more water content) slightly exhibited this phenomenon for the concrete mixes which reiterates the underlining cause of stress relaxation (movement of the liquid phase of concrete through its pores (Rossi and Acker, 1988)). In fact, a completely dry hardened concrete practically exhibits no relaxation (Rossi and Acker, 1988).

Figure 4.9a shows the percentage relaxation of the cement-based materials and reveals that Mixes C/CV consistently showed a reduction in their ability to relax stress due to aggregate inclusion (paste-mortar-concrete) while the other mixes only showed significant reduction due to the inclusion of stones. The lesser the relaxation ability, the more the elastic component of the response (Mezger, 2014). Figure 4.9b shows the time needed for the cement-based materials to relax the applied stress which is taken as 95% of the equilibrium modulus and referred to as relaxation time (Mezger, 2014). Paste Mix C and mortar Mixes C/CV have very high relaxation times (compared to the other paste/mortar mixes) because they did not exhibit the increase in modulus after relaxation. However, a general increase in relaxation time was obtained in the sequence of cement paste-mortar-concrete showing the influence of increased aggregate volume fraction and size.

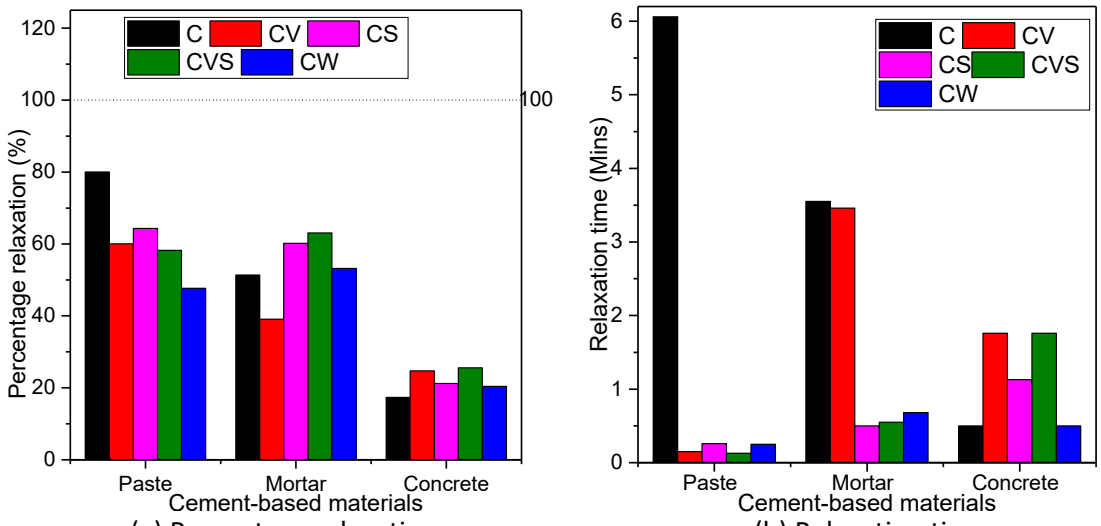

(a) Percentage relaxation (b) Relaxation time

Figure 4.9: Percentage relaxation and relaxation time of the cement-based materials

- **Influence of repeated loading**

Figure 4.10 – Figure 4.12 show the results of the stress relaxation of the cement paste, mortar and concrete, respectively, subjected to repeated strain loads after the initial/earlier loading. Note that 5 minutes of rest was allowed between each repetition of test. As observed from the result and figures, each mix (cement-mortar-concrete) becomes weaker after each repetition with the unit strain generally causing higher equilibrium stress (G_e) (stress after relaxation) but not necessarily higher instantaneous stress (G_0). Figure 4.10 reveals that for each repetition of loading, the magnitude of G_0 and degree of relaxation reduces which is mainly due to structuration that improves the elastic component. Mix CS continuously showed more relaxation than other mixes while Mix C consistently showed the least relaxation.

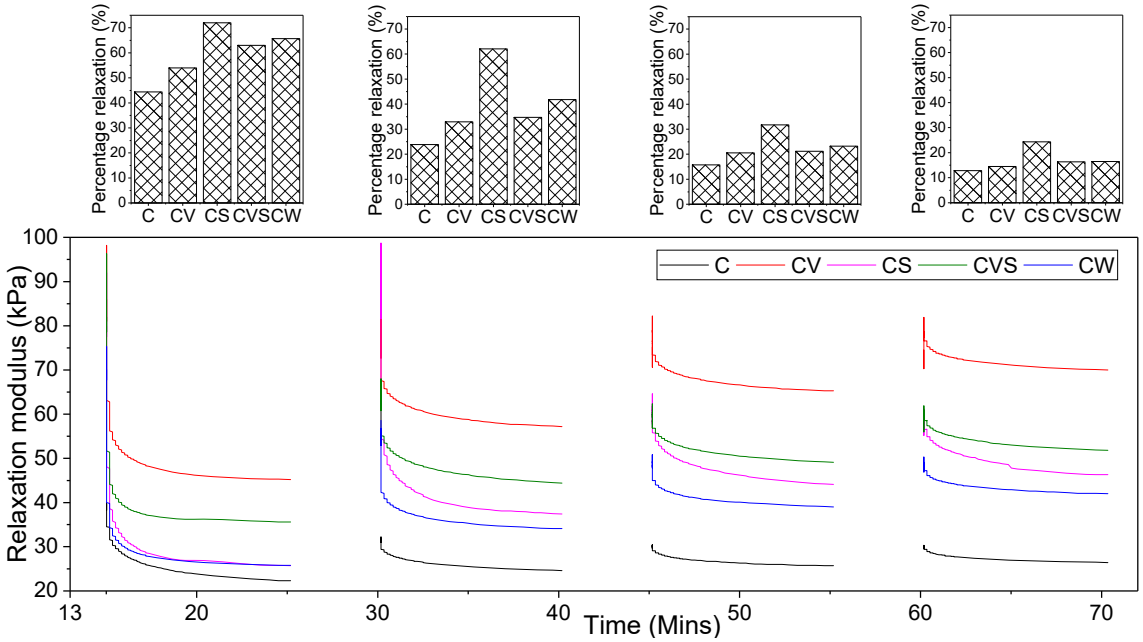

Figure 4.10: Repeated stress relaxation of the cement paste

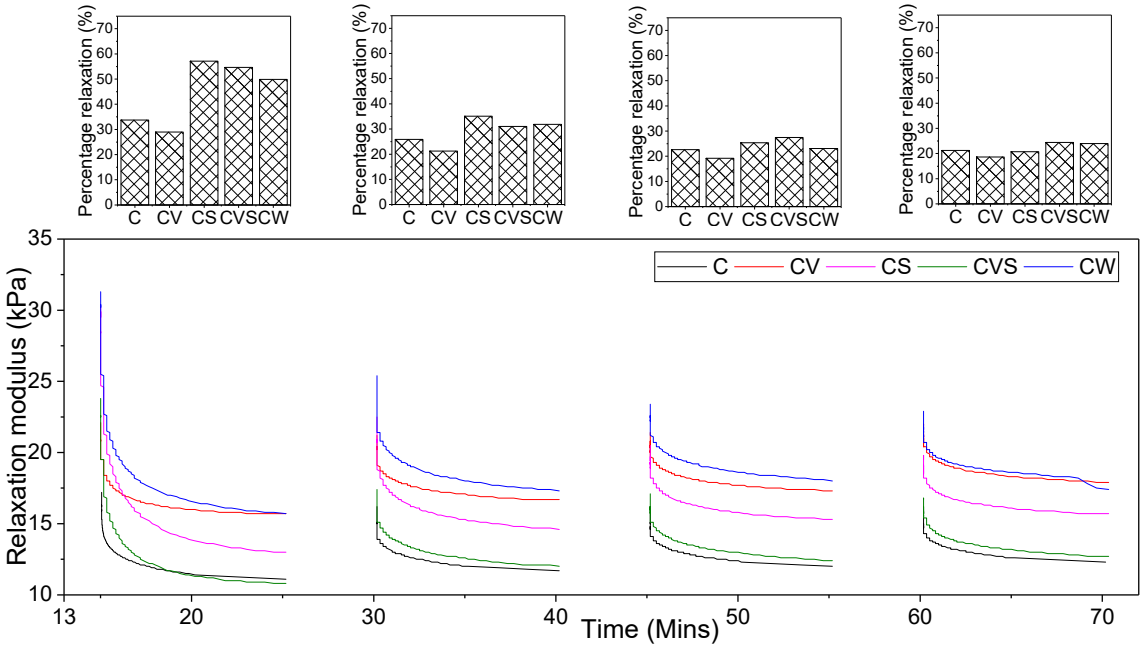

Figure 4.11: Repeated stress relaxation of the cement mortar

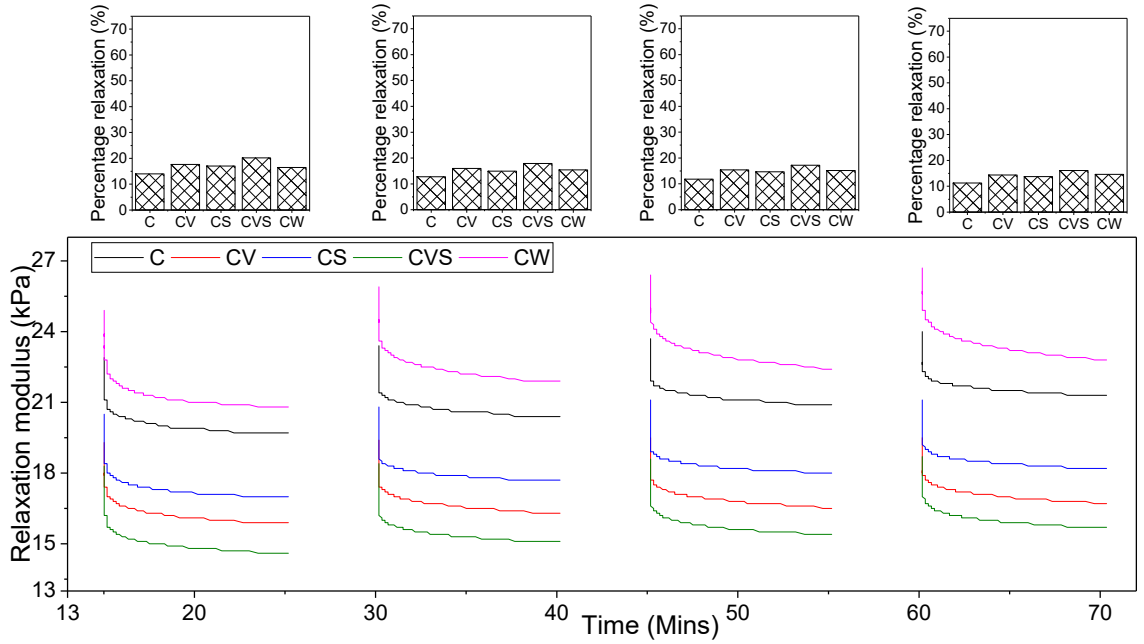

Figure 4.12: Repeated stress relaxation of the cement concrete

As expected, examining the percentage relaxation in Figure 4.10 – Figure 4.12 reveals that increased aggregate volume fraction reduced the repeated relaxation ability of the cement-based materials. Also, the increasing aggregate volume fraction and size reduced the influence of the rheology admixtures. And consistently for each repetition, Mix CS tend to have more relaxation time than other mixes for the cement-based materials, that is, Mix CS VE relaxation ability may be retainable for longer periods than those of other mixes.

4.4.5. Time-dependency of viscoelastic behaviour

Figure 4.13 shows the results of the three interval thixotropy test (3ITT), note that measurements were not recorded in the second interval where the samples' microstructure were destroyed. The low and rapidly increasing values of the storage modulus (G') for the cement paste Mix CS may be due to sampling disturbance. This rapidly increasing values are similar to that obtained at the lowest strains of the amplitude sweep (Figure 4.4a) and reported by some authors as an initial fast flocculation of cement paste after mixing (Nachbaur *et al.*, 2001; Jiang *et al.*, 1995, 1996; Schultz and Struble, 1993). It should be noted that leaving the paste sample to rest more than three minutes (as stated in Section 4.3.2) causes the cement particles to settle over time and gather water on top due to the relatively high water-cement ratio (0.55). It is, however, believed that comparable results to other mixes are obtainable since the first interval serves as a reference for the same sample (this is evident with CS having the lowest G' at the start of the third interval). The third interval of the cement-based materials, which shows the recovery/restructuration of the cement-based materials, has two stages, an initial rapid restructuration and a later steady structuration (Kruger *et al.*, 2019; Ma *et al.*, 2018; Mostafa and Yahia, 2016; Nachbaur *et al.*, 2001). The initial rapid restructuration is linkable to the flocculation of the cement-based particles (Yuan, Lu, *et al.*, 2017; Roussel *et al.*, 2012; Nachbaur *et al.*, 2001; Jiang *et al.*, 1996) and the later structuration is mainly due to hydration (Yuan, Zhou, *et al.*, 2017; Roussel *et al.*, 2012; Jarny *et al.*, 2005). This phenomenon has also been recently supported by (Mostafa and Yahia, 2017).

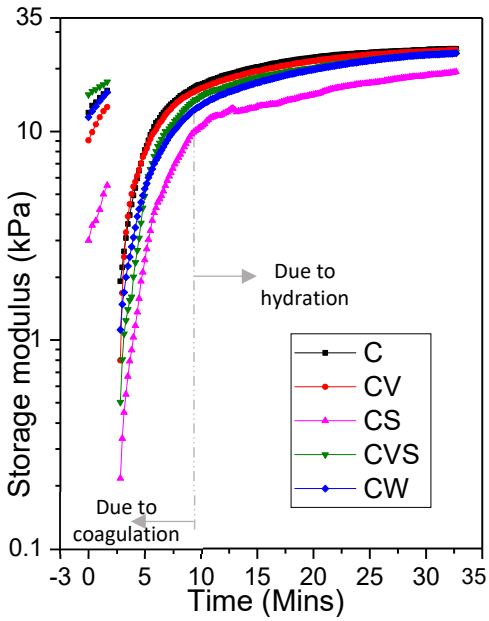

(a) Results of cement paste mixes

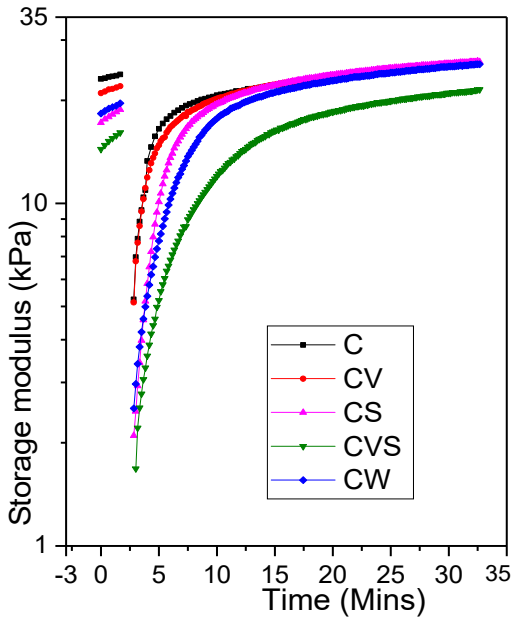

(b) Results of cement mortar mixes

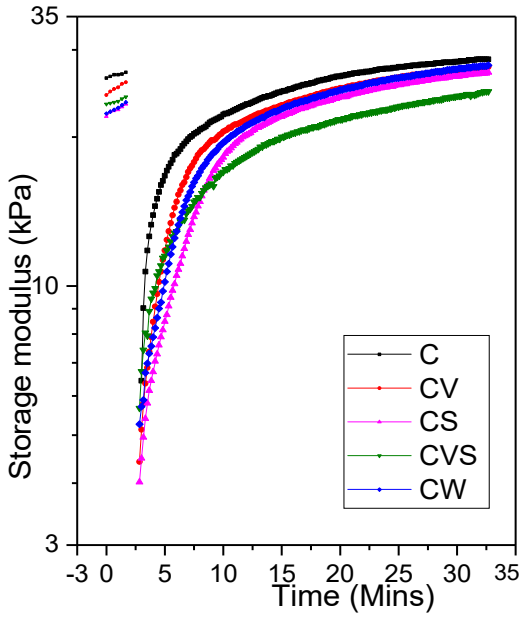

(c) Results of cement concrete mixes

Figure 4.13: Three interval thixotropy test results for the cement-based materials

Figure 4.14 shows the rate of restructuration at the third interval of 3ITT test with emphasis on the initial stage of rapid recovery (using log scale). As expected, the cement paste mixes (Figure 4.14a) have an initial increasing rate of recovery (except for Mix CV) due to the ability of cement particle to quickly coagulate as noted earlier. The initially high but decreasing rate of Mix CV can be due to the liquid thickening of the viscosity modifying agent (VMA) while the lowest flocculation rate of Mix CS can be due to the repulsive dispersion of the superplasticiser (SP). The inclusion of sand and stones in the mortar and concrete mixes limited the initial increasing rate of restructuration. By implication, the inclusion of aggregate (increase in coarse solid volume fraction and size) in cement-based materials inhibits flocculation that translates to an initial fast structure recovery, thereby, reduces the ability for flocculation-driven structuration/thixotropy. The bar chart insets in Figure 4.14a-c show the recovery time for the mixes to reach their reference structure at the first interval of the 3ITT test. The increase in aggregate volume fraction generally delayed the recovery since the cement content is the main source of the restructuration. In fact, the recovery of all the cement paste mixes were within the flocculation-driven period highlighted in Figure 4.13a.

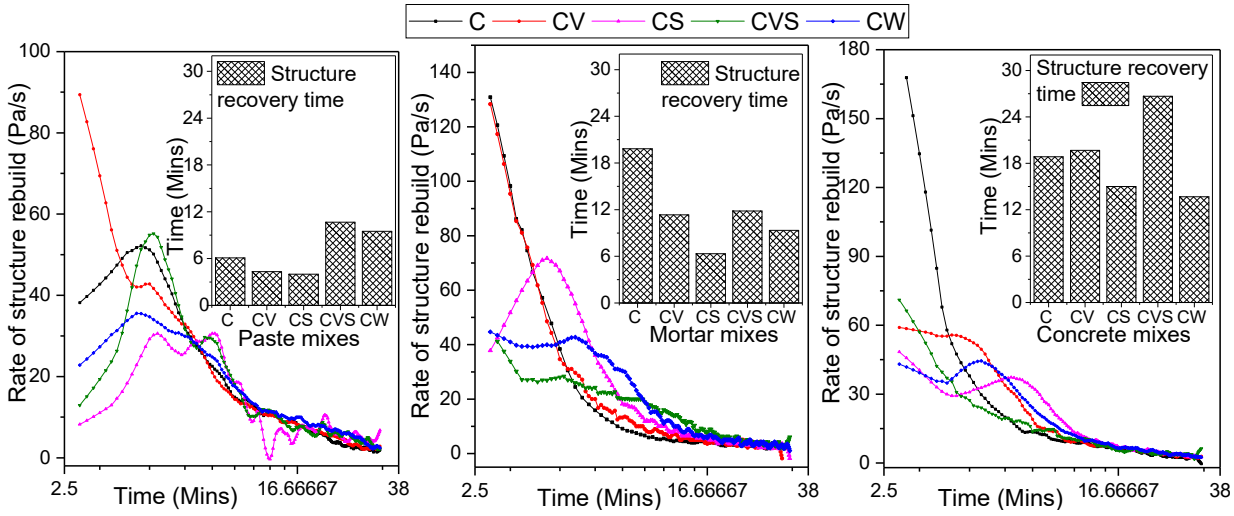

(a) Cement paste mixes (b) Cement mortar mixes (c) Cement concrete mixes

Figure 4.14: Rate of restructuration and structure recovery time

All the cement paste mixes (Figure 4.13a) showed similar structures (G') (at about 27 minutes) at the later stage of restructuration except for Mix CS which is due to its initial low G' at the first interval. The mortar mixes (Figure 4.13b) achieved similar structures (at about 17 minutes) quicker than the cement paste while the concrete mixes could not achieve similar structures by the end of the test. This implies that aggregate in cement-based materials tends to diversify how the rheology modifiers influence hydration-driven structuration. From the previous paragraph and earlier statement, it can be said that early structuration/thixotropy after mixing associated with flocculation/coagulation/agglomeration (Yuan, Lu, *et al.*, 2017; Roussel *et al.*, 2012; Nachbaur *et al.*, 2001) of cement paste particles becomes reduced and less-pronounced for concrete (due to aggregates) in which hydration (CSH bridges) becomes the major source of structuration/thixotropy (Roussel *et al.*, 2012). Oftentime, studies (Yuan, Lu, *et al.*, 2017; Yuan, Zhou, *et al.*, 2017; Wallevik, 2005) suggesting flocculation as source of structuration/thixotropy made use of cement paste.

4.5. Conclusions

This study evaluates the rheo-viscoelastic behaviour of rheologically modified fresh cement-based materials. The cement-based materials are paste, mortar, and concrete which progressively allow for examining the trend in the viscoelastic (VE) behaviour and how the rheology modifiers influenced the trend. The following inferences and conclusions can be made:

- The general trend of behaviour of the control cement paste, mortar and concrete is that, the more the coarse solid volume fraction and size, the more the linear elastic behaviour and vice-versa. However, the rheology modifiers diversified this trend of VE behaviour.

- Increase in the aggregate volume fraction and size dampens the effects of the rheology modifiers on the VE behaviour of the cement-based materials.
- Satisfactory conclusions on the VE behaviour of concrete may not be approximate-able from that of cement paste as generally suggested by in literature, especially, those containing admixtures such as rheology modifiers. That is, the aggregates diversify the rheo-viscoelastic behaviour rather than just accentuating the behaviour. The rheo-viscoelastic properties of the cement mortar are, as shown in this study, closer to that of the concrete than that of the paste.
- The inclusion of sand in the cement paste tends to yield a more ductile cement-based material (mortar) in the fresh state while including both the sand and stone tend to make the ensuing concrete more brittle. All the rheology modifiers generally decreased the critical strain of the cement-based material in the fresh state.
- The inclusion of the viscosity modifying agent (VMA) mostly did not change the linear elastic response of the cement-based material due to its polymer entanglement engineered to cause liquid phase thickening. However, the progressive inclusion of the aggregates reduced this ability. The other rheology modifiers (superplasticiser (SP), VMA+SP, and water) generally reduced the linear elastic response of the cement-based materials while they diversified the response due to the inclusion of the aggregate.
- Without the substantial influence of hydration, fresh cement-based materials tend to have a stable VE response to quick/impact linear deformation while the microstructure tends to thicken (pseudo-strain hardening) due to low and extended linear deformation because of the particles' flocculation. Increase in aggregate volume fraction tend to reduce the flocculation, and hence, the thickening property.
- Similarly, sudden application of step stress/force can cause the microstructure of fresh cement-based material to thicken. The aggregates reduce this thickening effect. Furthermore, the sudden relieve of the stress/force can cause the yielding/softening of the micropore liquid which can further assist in the creep recovery.
- Quick stress relaxation from a step strain application can also be followed by microstructure thickening. Increased aggregate volume fraction reduced this effect and also, the observable variation in the relaxation abilities between the repetitions of repeated loading.
- Increasing aggregate solid volume fraction and size reduce the flocculation-driven time-dependent VE behaviour (structuration) of the fresh cement-based material, making hydration as the main driving source of structuration/thixotropy for fresh cement concrete.

Chapter 5: Plastic cracking behaviour of concrete and its interdependence on rheo-physical properties

This chapter has been submitted as a journal paper to the Construction and Building Materials, Elsevier BV, with impact factor 4.046. Details of the paper are below:

Kolawole, J.T., Combrinck, R. & Boshoff, W.P. (2019). Plastic cracking behaviour of concrete and its interdependence on rheo-physical properties. Submitted to Construction and Building Materials.

Declaration by the candidate:

With regard to Chapter 5, the nature and scope of my contribution were as follows:

Nature of contribution	Extent of contribution (%)
This paper/chapter is part of the candidate's PhD research. All experimental work, the analysis, interpretation and presentation of data, as well as the writing of the manuscript were conducted by the candidate.	90%

The following co-authors have contributed to Chapter 5:

Nature of contribution	E-mail address	Nature of contribution	Extent of contribution (%)
Dr Riaan Combrinck	rcom@sun.ac.za	PhD research supervision, proofreading manuscript and insightful amendments	5%
Prof William Peter Boshoff	billy.boshoff@up.ac.za	PhD research supervision, proofreading manuscript and insightful amendments	5%

Signature of candidate: .....

Date: 8 October 2019

Declaration by co-authors:

The undersigned hereby confirm that

The declaration above accurately reflects the nature and extent of the contributions of:

1. The candidate and the co-authors to Chapter 5,
2. No other authors contributed to Chapter 5 besides those specified above, and
3. Potential conflicts of interest have been revealed to all interested parties and that the necessary arrangements have been made to use the material in Chapter 5 of this dissertation.

Signature of co-authors	Institutional affiliation	Date
	Department of Civil Engineering, Stellenbosch University	8 October 2019
	Department of Civil Engineering, University of Pretoria	8 October 2019

5.1. Abstract

The major processes that influence and constitute the plastic cracking behaviour of concrete include bleeding, evaporation, settlement, shrinkage and capillary pressure. These processes mainly occur during the plastic phase of concrete, during which time the concrete has significant rheological properties. It is suggested in this study that the interactions between these rheological properties and plastic cracking behaviour can be deduced by shear rheometry. Additionally, this plastic phase is dominated by self-settlement as a form of gravitational shearing that is also related to the rheo-physical properties. Therefore, the goal of this study is to show that shear rheometry can be used to understand and describe the behaviour of plastic concrete during these initial stages. To achieve this goal, the plastic cracking processes of rheologically modified concrete mixes were investigated under climate conditions independently established to cause plastic cracking with the purpose of linking the processes to the results of shear rheometry of the same concrete mixes. Results show that the plastic cracking behaviour has three unique stages identifiable from the measurements of the influencing processes and that the rheology modifiers influenced several of these stages. Due to the vibration of concrete, the initial plastic settlement period where nearly constant bleeding occurred is influenced by the permeability properties while the later plastic settlement is influenced by the dynamic yield stress and thixotropic index. During the self-settlement period, the plastic shrinkage and capillary pressure build-up rate are linked to the same dynamic yield stress and thixotropic index. It is thereafter suggested that by carrying out a relatively simple rotational shear rheology test during concrete's plastic phase, the extent of the plastic cracking processes can be determined. The structuration of concrete and its suspending fluid, only in the form of static yield stress and not the rigidification, that occurs afterwards also relates to the plastic cracking process.

5.2. Introduction

Plastic cracking refers to cracks that occur in the fresh or plastic state of concrete before it solidifies and although the exact point in time where the plastic state of concrete ends is uncertain, it is believed to be around the final setting time (Combrinck *et al.*, 2018a; Sant, Dehadrai, Bentz, Lura, *et al.*, 2009). Plastic cracking which occurs during one of the shortest phases of concrete life (Combrinck *et al.*, 2018a) can compromise the serviceability, durability and aesthetics of concrete (Ghourchian *et al.*, 2018; Leemann *et al.*, 2014).

When fresh concrete is placed, there is a movement of its solid particles under their weight (Safiuddin *et al.*, 2018), ranging from cement particles to aggregate particles (Kim *et al.*, 2014). This vertical downward movement is referred to as self-settlement in this study. Any form of constraint such as steel reinforcement or change in formwork section (Combrinck *et al.*, 2017; Al-Qassag *et al.*, 2016) within a concrete specimen can be responsible for a non-uniform settlement which leads to plastic settlement cracking (Combrinck *et al.*, 2018a,b; Safiuddin *et al.*, 2018; CCIP-048, 2010). As the particles in the fresh concrete settle, they displace water to the surface, causing bleeding (Lura *et al.*, 2007; Powers, 1968). The displaced bleed water evaporates if exposed to the external environment. Once the bleed water has completely evaporated, the pore water starts evaporating causing negative internal pore pressure build-up within the concrete specimen (Olivier *et al.*, 2018; Leemann *et al.*, 2014; Slowik *et al.*, 2008; Wittmann, 1976). The water surface in the pores starts curving downward (as concave water menisci) due to difference in pressure, adhesive forces to the pore wall and surface tension (Slowik *et al.*, 2008; Wittmann, 1976), leading to plastic shrinkage and further settlement as a form of three dimensional contraction of the concrete. This additional settlement is further termed capillary-induced settlement in the study. Any form of restraint to this contraction leads to plastic shrinkage cracking. As the evaporation continues, the radius of the concave water meniscus becomes smaller, more water rises to the surface due to capillary action and eventually collapse leading to air entry into the concrete pores as weak spots.

The processes leading to plastic cracking with other related phenomena are succinctly shown in Figure 5.1. As shown, it is believed that plastic settlement precedes plastic shrinkage, though, the settlement of plastic concrete may be further increased beyond the initial setting time due to negative capillary pressure (Combrinck *et al.*, 2018a). Weak spots and microcracks developed from differential settlement (Lin and Huang, 2010) before the initial setting time (i.e. stiffening phase) may be enlarged and propagated due to plastic shrinkage (Combrinck *et al.*, 2018a) largely occurring between the initial setting time and final setting time. However, distinguishing between these crack

types in practice is very difficult (Combrinck *et al.*, 2018a). Measurable concrete responses/factors influencing plastic cracking include bleeding, evaporation, setting times, capillary pressure build-up, plastic settlement, and plastic shrinkage while others include the setting times, mix proportions, restraint conditions and environmental conditions (Sayahi, 2016; Leemann *et al.*, 2014; Combrinck and Boshoff, 2013; CCIP-048, 2010; Slowik *et al.*, 2008; Holt and Leivo, 2004; Dias, 2003; Uno, 1998). These concrete responses/factors are onwards referred to as plastic cracking processes.

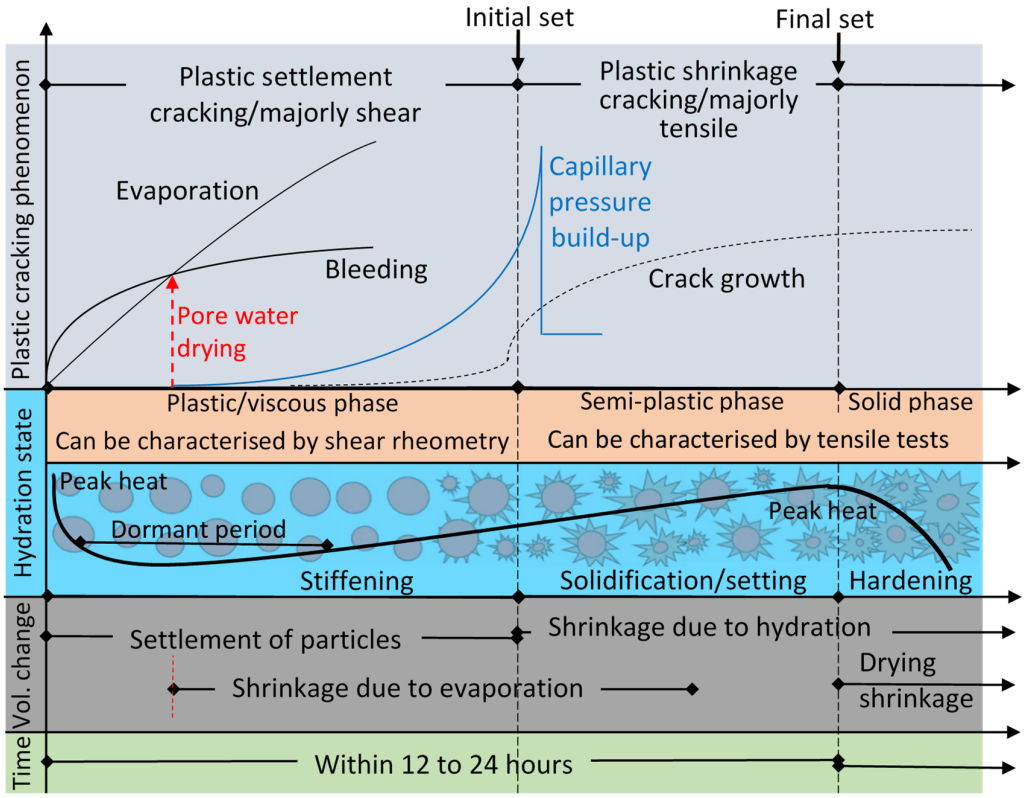

Figure 5.1: Processes leading to plastic cracking of concrete and related phenomena (Adapted from (Combrinck and Boshoff, 2013; Sant, Dehadrai, Bentz, Lura, *et al.*, 2009))

Plastic concrete during the stiffening phase (including the dormant period – Figure 5.1) has macroscopic shear rheological properties. That is, the rheological properties of cementitious materials majorly exist during its plastic phase (Kim *et al.*, 2018; Yuan, Zhou, *et al.*, 2017; Bellotto, 2013; Banfill, 1991) and progressively fades as the concrete changes from plastic to solid state due to hydration. Researches in fresh/plastic concrete (Qian and Kawashima, 2018; Rahman *et al.*, 2014; Assaad *et al.*, 2003a) are therefore inclined to characterise concrete with its shear rheo-physical properties such as yield stress and thixotropy. These shear rheological (rheo-physical) properties have been seriously overlooked in the literature and this study suggests that it needs to be considered for a better understanding of plastic cracking behaviour. The occurrence of plastic settlement in a concrete suggests that gravitational shear force predominates due to varying shapes

and sizes of coarse particles (sand and stones) in the suspension fluid (cement mortar), and can be linked to the rheo-physical properties of the concrete (Mehdipour and Khayat, 2018). Other processes leading to plastic cracking predominantly occur before the final setting time (Combrinck *et al.*, 2018a; Olivier *et al.*, 2018). By implication, a degree of interaction/interdependence between the rheological properties of concrete and the plastic cracking processes which occur concurrently during the plastic phase is anticipated, and shear rheometry has the potential to characterise and investigate such a relationship. Substantial tensile property development occurs as the concrete surpasses the final setting time into the hardening phase (solid-state). Hence, these later phases may be better suited for extensional (tensile) tests/measurements. For example, Combrinck and Boshoff (2019), Nguyen *et al.* (2017), Roziere *et al.* (2015), and Dao *et al.* (2009) reported significant increase in tensile properties of concrete (such as tensile strength, Young's modulus and fracture energy) with a significant reduction in strain capacity as the transition to solid-phase progressed.

There is a scarcity of literature revealing the interdependence of shear rheo-physical properties of concrete to its plastic cracking behaviour, as stated in the preceding paragraphs and Figure 5.1. Therefore, shear rheometry was extensively used as a method of evaluating the rheo-physical parameters of concrete for the purpose of characterising the plastic phase of conventional concrete. Some of these tests and results are already reported in (Kolawole *et al.*, 2019a) and relevant portions are used for this study. The plastic cracking behaviour of the same concrete mixes used in (Kolawole *et al.*, 2019a) were investigated in this study with the aim of linking the rheo-physical properties to the plastic cracking processes. This approach is believed to be important (at least as a first step) in order to show that the settlement phase (with some influence from plastic shrinkage) of the plastic cracking process is shear related and influenced by rheology and can be characterised by shear rheometry.

5.3. Background to the role of rheology

As noted earlier, the settling of solid particles due to density difference in concrete is responsible for plastic settlement (Zhang *et al.*, 2019). Theoretically, aggregate settlement in cement-based materials is undesirable and should be avoided because it is a source of segregation, especially for self-compacting concrete (SCC) where such settlement can easily lead to instability (Saak *et al.*, 2001). Practically, colloidal interaction in a stable cement paste dominates over the gravitational shearing tendencies of the cement particles to prevent segregation and bleeding (Mehdipour and Khayat, 2018; Perrot *et al.*, 2012). For concrete, which is more poly-dispersed and heterogeneous, settlement of the big coarse aggregates does occur at an acceptable microscopic range, during the

plastic phase, that can be neglected for static stability purposes (Assaad *et al.*, 2004). This accrues with time as the measured cumulative plastic settlement of the concrete's body, typically within thousandths (10^{-3}) of micro-strains. Concrete can be idealised as a two-phase suspension, the suspending fluid (cement paste or mortar) and the coarse solids (aggregates) (Chia *et al.*, 2005; Saak *et al.*, 2001). The settlement of a single aggregate at the top of a suspending fluid depends on the rheological properties of the suspending fluid (Saak *et al.*, 2001), specifically the yield stress and thixotropy (Peng and Jacobsen, 2013; Spangenberg *et al.*, 2012). The viscosity of the suspending fluid mainly influences the aggregate's settlement velocity after settlement has started (Roussel, 2007). Considering the numerous aggregates in concrete, the converging solid fraction due to continuing settlement and interaction (direct frictional contacts) of the aggregates cause increasing/improving solid volume interlocking and diminishing propensity for further settlement (Esmaeilkhanian *et al.*, 2014). The physics and mechanisms behind these have been studied and reported by (Spangenberg *et al.*, 2012; Roussel, 2007; Saak *et al.*, 2001). The structural rigidification (early elasticity) of fresh/plastic concrete given by the storage modulus (G') (Roussel *et al.*, 2019) has direct links to the suspending fluid structuration due to CSH formation (Mahaut, Mokéddem, *et al.*, 2008) and coarse aggregate packing. The G' is can be probed by dynamic shear rheological methods (dynamic oscillatory rheometry) known as small amplitude oscillatory shear (SAOS).

Mehdipour and Khayat (2018) and Mahaut, Mokeddem *et al.* (2008) have shown that the yield stress and thixotropy of concrete is dictated by the yield stress and thixotropy of the suspending fluid (mortar in the case of this study) and coarse aggregate packing fraction. Also, the physicochemical interactions of the interstitial fluid, which are majorly responsible for thixotropy, is not influenced by the presence of the coarse aggregates. Therefore, there is a direct link between the rheological parameters of the suspending fluid and that of the concrete by a factor related to the aggregate packing fraction (Mahaut, Chateau, *et al.*, 2008). The yield stress and thixotropic parameters of only the concrete mixes were measured for this study, which inevitably represents that of the suspending fluid.

Normal vibrated concrete (NVC) is used for this study in which normal fresh concrete is compacted on a vibration table to consolidate the concrete and let out trapped air. This is dissimilar to self-compacting concrete (SCC) which is designed to consolidate and flow under its own weight. The vibration of concrete has been shown by various studies to reduce the yield stress of the concrete and that of the suspending fluid (Li and Cao, 2019; Banfill *et al.*, 2011; Juradin, 2011; Banfill, 2003; Tattersall and Baker, 1988). According to (ACI 309.1R, 2008), vibration causes concrete's matrix to

regain fluid/flow behaviour with measurable shear resistance and cohesion. This shear resistance is synonymous to the required stress to stop the concrete from flowing (steady/dynamic yield stress, as shown in Figure 5.2). This steady/dynamic yield stress and reduced rigidification become the resistant yield stress and stiffness against aggregates' settlement, hence, plastic settlement of concrete (Petrou *et al.*, 2000). At the end of such vibration, structuration due to thixotropy builds on the dynamic yield stress and reduced rigidification (storage modulus) with time (which becomes the newly increasing static yield stress and storage modulus) to improve the stability of the suspending fluid (and the concrete correspondingly) against settling. In fact, Petrou *et al.* (2000) showed that for a stable bigger solid particle (with density difference) on a suspending fluid (cement paste), the vibration of the fluid caused the particle to settle undesirably until the vibration was stopped. Of course, the solid volume interaction/interlocking of the numerous aggregates in a typical concrete will reduce such accelerated settling exhibited by the model solid particle (Yim *et al.*, 2013).

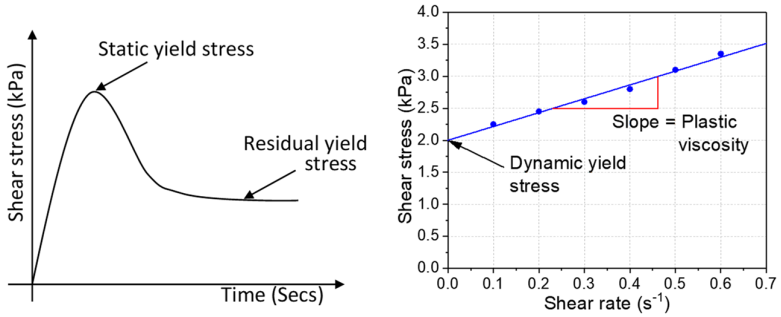

Figure 5.2: Rheological test showing the static yield stress and dynamic yield stress

Summarily, the vibration of a mould-confined fresh concrete, such as the case of this study, reduces the static yield stress to the steady/dynamic yield stress and reduces the rigidification by destroying the structure and inducing higher gravitational shearing of the coarse aggregates (Spangenberg *et al.*, 2012) that jump-starts the self-settlement. This jump-start can simultaneously cause initial rapid bleeding (evident in the initial steady bleeding rate of Figure 5.11a), making the permeability of the concrete to be linkable to the initial settlement. Suggestively, the newly increasing yield stress and rigidification (storage modulus) due to thixotropy build-up and CSH formation of the concrete and suspending fluid should dictate the self-settlement. However, as shown in Section 5.5.4.2, only the yield stress does. It will be shown later in the plastic cracking behaviour results of concrete mixes that the start of the shrinkage is noticeable on the settlement plot and serves as an indicator of a change in the plastic cracking behaviour. It may, hypothetically, imply that their interaction and factors directly/indirectly influencing them (such as yield stress and thixotropy) are interwoven. The supposed relationship between the plastic shrinkage and the rheology parameters are unknown and

therefore explored further in this study. Concrete's pore water evaporation causes the build-up of negative capillary pressure which leads to concave pore menisci that result in plastic shrinkage. The rate of negative pressure build-up can be influenced by the rise of bleed water and capillary action, which emanates from plastic settlement that is influenced by the yield stress and thixotropy. Therefore, the possible relationship between the rate of pressure build-up and the rheo-physical properties is also examined.

Rheological properties of the concrete were examined up to the initial setting time since above this period, cement-based materials tend to lose a substantial amount of its rheological behaviour (Subramaniam and Wang, 2010). It is acknowledged that this study does not provide the possible physics behind the interactions between plastic cracking process and rheological parameters, it is, however, aimed at showing the correlations and links between the two which is a step towards understanding and conceptualising a rheological approach to plastic cracking.

5.4. Materials and methods

For this study, three readily available rheology modifiers were added to the concrete to vary the rheological parameters, viz viscosity modifying agent (VMA), superplasticiser (SP) and increased water content. Polysaccharide-based liquid viscosity modifying agent and polycarboxylate ester (PCE) liquid superplasticiser were added by weight as a percentage of the cement. The VMA has a specific gravity of 1.0, pH of 9.5, chloride content of less than 0.1%, and sodium oxide of less than 1% while the superplasticiser has a specific gravity of 1.05, pH of 7, chloride content of less than 0.1%, and sodium oxide of less than 1%. They were both added to the mixing water before adding the water to the mixed dry constituents in the concrete mixer. Five concrete mixes were made from the rheology modifiers, they are the control mix (C), control mix containing VMA (CV), control mix containing SP (CS), control mix containing both VMA and SP (CVS), and the control mix with increased water content (CW). Incorporation of these modifiers changed the rheology parameters of the concrete mixes without drastically affecting the setting time and compressive strength development (Table 5.1). The materials constituents and properties of the concrete mixes are shown in Table 5.1. The setting time test was based on BS EN 196-3 (2005) using a Vicat penetration apparatus on a sieved mortar using a 4.75 mm sieve.

Table 5.1: Mix proportions and properties of the concrete mixes

Notations	Material constituent (kg/m^3)				
	C	CV	CS	CVS	CW
Water	217	217	217	217	223
Cement - CEM II 52.5N	395	395	395	395	374
Malsmebury sand	774	774	774	774	796
6mm Greywacke stone	1029	1029	1029	1029	1018
VMA	-	0.6%	-	0.4%	-
Superplasticiser	-	-	0.6%	0.4%	-
Other properties					
w/c ratio	0.55	0.55	0.55	0.55	0.6
Slump (mm)	100	100	175	170	185
Initial setting time (mins)	120	120	120	150	130
Final setting time (mins)	165	165	165	195	165
Compressive strength (7 days, MPa)	36	39	35	42	32
(28 days, MPa)	47	51	47	50	42
C – control mix; CV – control mix + VMA; CS – control mix + SP; CVS – control mix + VMA + SP; CW – control mix + water					

5.4.1. Rheological measurements

Rheology measurements of the mixes were measured using the ICAR rheometer (Koehler and Fowler, 2004) for rotational shear rheological tests and the Physica MCR501 rheometer with a building material cell (BMC 90) was used for the dynamic shear rheometry (DSR). Full details of the rotational shear rheometry tests and results can be found elsewhere (Kolawole *et al.*, 2019a). More details of the Physica MCR501 rheometer and BMC 90 can be found in (Anton-Paar, 2009, 2016). The DSR was carried out on the suspending mortar of the concrete and concrete of reduced stone content. The suspending mortar was obtained by sifting the concrete with a 4.76 mm sieve on a vibrating table. The stone content of the concrete mixes had to be reduced by 60% to facilitate the SAOS tests, more details of this can be found in companion studies (Kolawole *et al.*, 2019c,b). Using small amplitude oscillatory shear (SAOS) test, amplitude strain sweeps from $1x10^{-4}$% to 100% at a logarithm ramp of 10 points/decade and a constant rate of 10 rad/s was used to characterise the suspending mortar and concrete for its linear viscoelastic range (LVR). A three interval thixotropy (3ITT) was used to measure the rigidification (storage modulus – G') evolution with time. It involves a first interval of low shear strain at 0.01% within the LVR at a constant rate of 10 rad/s, a second interval of high shear strain and rate than the LVR, and a third interval as the first interval (Mezger, 2014). The first interval serves as the reference state of the suspending mortar while the structure is destroyed at the second interval which simulates the vibration of the concrete and the progress of restructuration (rigidification) is measured in the third interval. At least two samples were tested

for the DSR and the average reported. More details of these tests can be found in the companion study (Kolawole *et al.*, 2019b).

The model proposed by (Ma *et al.*, 2018) for structuration can be expressed as below. It was used to estimate the static yield stress and extrapolate the measured storage modulus up to the initial setting time (120 minutes),

$$\tau(t) = \tau_0 + c\lambda_{flocs} + A_{thix}t \qquad \text{Equation 5.1}$$

$$G'(t) = G'_0 + c\lambda_{rigid} + G_{rigid}t \qquad \text{Equation 5.2}$$

$$\text{Where} \quad \lambda_{flocs} \text{ and } \lambda_{rigid} = 1 + (\lambda_0 - 1)e^{-\frac{t}{\theta}} \qquad \text{Equation 5.3}$$

For the purpose of this study, $\tau(t)/G'(t)$ is the newly increasing static yield stress and storage modulus, t is the considered time after the end of vibration, τ_0/G'_0 is the initial dynamic yield stress and storage modulus at end of vibration, c is the yield stress and storage modulus at a fully flocculated state of the mortar, A_{thix}/G_{rigid} is the rate of linear evolution of the static yield stress and storage modulus, $\lambda_{flocs}/\lambda_{rigid}$ describes the flocculation and rigidification state of the mortar (values between 0 and 1) at the considered time, λ_0 is the initial flocculation and rigidification state at end of vibration (typically zero at such steady state), θ is the relaxation time required to reach fully flocculated and rigidification state.

It should be noted that all the rheological tests were done in a climate room of 23±2°C at a maximum duration of 30 minutes as oppose 40±2°C of the plastic cracking behaviour for over two hours. The study by Nehdi and Al Martini (2007), however, showed that such increased temperature can potentially increase the values of the yield stress and storage modulus.

5.4.2. Materials preparation and test procedure for plastic cracking behaviour

All materials prior to mixing were stored in a climate room at 23±2°C ambient temperature and 65±3% relative humidity at least 24 hours before testing. This ensured constant and consistent temperature for all mix materials and the freshly mixed concrete. After adding stone, cement and sand respectively to the 50L concrete pan mixer, the materials were dry mixed for one minute before adding the mixing water. The mixing water was pre-mixed with the admixtures as prescribed by the manufacturer (Chryso, 2012, 2014). Thereafter, the concrete was mixed for four minutes, that is, a total of five minutes mixing. All respective moulds were then filled halfway with concrete and vibrated for 30 seconds after which the moulds were completely filled with concrete and vibrated further for between 1 to 1.5 minutes. Bleeding and evaporation moulds were vibrated for 1 minute while plastic shrinkage moulds were vibrated for 1.5 minutes. The choice of vibration time

was due to different sizes of the moulds and time adjudged to allow all entrapped air bubbles to surface without causing segregation. All plastic cracking process tests for this study were carried out in an electronically controlled closed loop climate chamber (Boshoff and Combrinck, 2013) with 40±2°C ambient temperature, 10±3% relative humidity and 4±2 km/h wind speed. Details of the climate chamber can be found in (Combrinck, 2016; Combrinck and Boshoff, 2013). These conditions were necessary to simulate environments capable of causing plastic cracking. At least four samples of measurements were carried out for each test and the average reported, except for the capillary pressure in which two samples were used for each test.

With these environmental conditions, the Uno (1998) equation (shown below) which is based on the earlier versions of ACI 305.1 (2006) monograph yielded an evaporation rate of 0.4 kg/m^2/h, though an initial evaporation rate of about 1.3 kg/m^2/h was recorded for the control.

$$ER = 5 \times 10^6 (V + 4)[(T_c + 18)^{2.5} - r(T_a + 18)^{2.5}] \quad \text{Equation 5.4}$$

where ER – evaporation rate, V – wind velocity, T_c – concrete temperature, r – relative humidity, T_a – air temperature.

This difference was expected as the Uno (1998) equation estimates mean evaporation rate which Dao *et al.* (2010) and Morris and Dux (2005) warned are subjected to errors and should be used with caution. This is because the equation is based on the constant evaporation of the free water surface, which is dissimilar to a typical concrete surface influenced by various factors (Morris and Dux, 2005). Moreover, the climate chamber conditions simulate an environment similar to a typical arid to semi-arid region. All the tests were carried out for 6 hours except for bleeding, which stopped earlier. Time zero was taken as the time mixing ended.

5.4.3. Bleeding and evaporation tests

Bleeding tests were carried out in accordance with ASTM C232 (2004) using 120 mm diameter and 120 mm deep cylindrical bleeding moulds. A pipette was used for collecting the bleeding water every twenty minutes. The bleeding moulds were filled up to 100 mm depth and covered to minimise evaporation of the bleed water within the climate chamber. Evaporated water during measurements was accounted for by recording the weight of the samples immediately before and after each interval of bleeding measurement. Evaporation tests were done by measuring the mass loss every 20 minutes using a 200 x 200 x 100 mm mould with a 0.1 g resolution scale. The permeability coefficients of the concrete mixes were calculated using Equation 5.5 based on Darcy's law modified by Ghourchian *et al.* (2016) using the bleeding rate of the concrete mixes. The

permeability coefficient (k) describes the ease of transfer of fluids through the pore network of concrete and is independent of the pore fluid but influenced by porosity, pore size distribution and their connectivity:

$$k = \frac{b}{\frac{\rho_c}{\rho_f} - 1}$$ Equation 5.5

where k is the permeability coefficient, b is the initial constant bleeding rate which is independent of drying and shrinkage, ρ_c is the concrete density, ρ_f is the pore fluid density.

5.4.4. Plastic settlement, shrinkage and capillary pressure tests

Figure 5.3 shows the mould of 300 x 300 x 100 mm used for the plastic settlement, shrinkage and capillary pressure tests simultaneously. The free vertical settlement was captured by the top-mounted LVDT with an attached 50 x 50 mm piece of lattice wire mesh resting on the centre of the concrete surface. The mesh allows bleed water to pass through while staying in contact with the concrete surface. An LVDT is connected to each side of the mould via mounting brackets to capture the free horizontal shrinkage. These side LVDTs follow the movement of concrete markers embedded in the concrete.

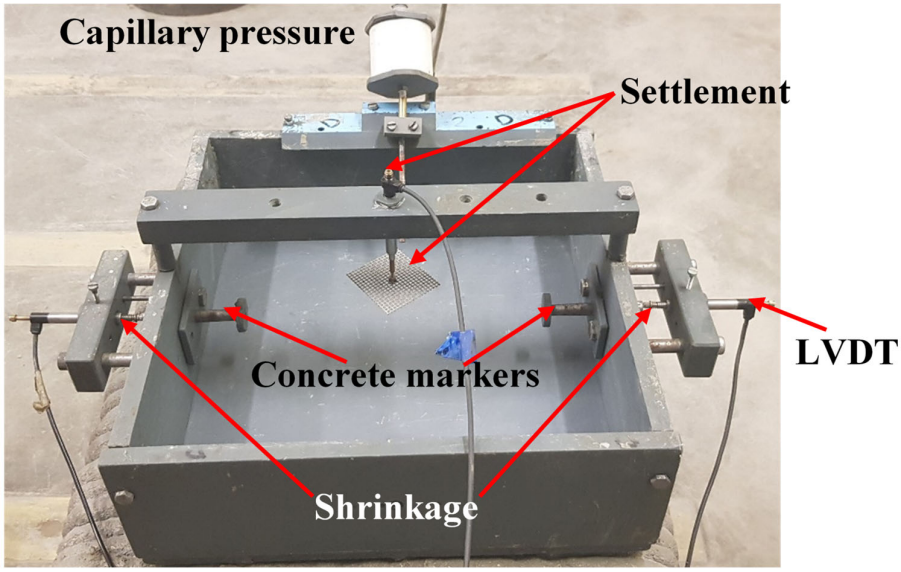

Figure 5.3: Typical mould for plastic shrinkage, settlement and capillary pressure tests

An electronic capillary pressure sensor was connected to a metal tube filled with distilled water and mounted to brackets at the top of the mould at an angle of 45°. A secondary bracket that holds the sensor to the primary bracket is fixed during concrete vibration and transportation and loosened at the start of the test to allow the sensor to settle as the concrete settles. The tip of the tube is at 50 mm below the concrete surface. The pressure sensors were zeroed after being placed in concrete

(rather than in the atmosphere) which does not allow it to record the initial pore pressure of concrete since it is not of interest for this study. Data were recorded every second for all LVDT and pressure sensor measurements.

5.4.5. Plastic cracking test

Figure 5.4 shows the mould used to investigate the plastic cracking tests. The mould is based on the one proposed in ASTM C1579 (2006) but with additional steel bars near the top ends of the moulds, which give additional restraint. More details about the mould and justification for additional steel bars can be found elsewhere (Combrinck *et al.*, 2018a; Combrinck, 2016). The onset of cracking was determined by examining the concrete surface every 10 minutes; after crack initiation, high-resolution photographs of the cracks (with a scale of reference length) were taken every 20 minutes from the start of cracking. The cracks were measured using CAD software, as shown in Figure 5.4b. The last photograph taken was used to measure a well-defined crack within 25 mm offset from the mould boundaries as described by ASTM C1579 (2006). The crack is then divided into 10 mm segments along its length and the crack width measured perpendicularly to these segments. This crack measurement layout is then copied and fitted to previous images in a corresponding layout. This is to allow for measuring cracks at approximately the same position for all crack images. The average crack area is calculated using:

$$\text{Average crack area } (\text{mm}^2) = \text{average crack width (mm)} \times \text{number of line segments} \times 10 \text{ mm} \qquad \text{Equation 5.6}$$

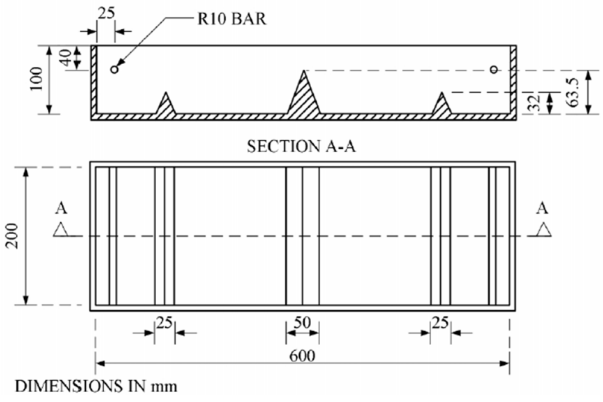

Figure 5.4a: Plastic cracking mould based on ASTM C1579 (2006)

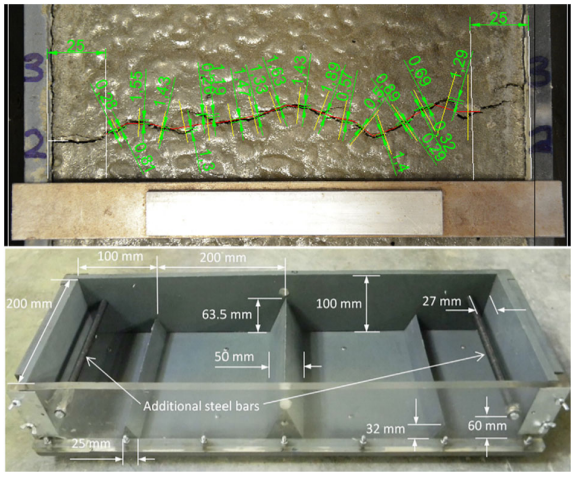

Figure 5.4b: Plastic cracking mould and specimen analysed based on CAD software

5.4.6. Statistical analysis

In order to establish the interdependence of the concrete mixes' rheo-physical properties and plastic cracking behaviour, the envisaged relationships/links between them were examined by

standard statistical analysis. The linear correlations between the experimentally-determined parameters were determined by Pearson correlation coefficients r (Ghourchian *et al.*, 2018). Based on these envisaged relationships and obtained correlation coefficients that are statistically significant (P-value ≤ 0.05), the right parameters were combined to examine the relationship. Test of collinearity was also done for the selected rheo-physical parameters (Walpole *et al.*, 2012; Hocking, 2003). Scatter plots of the coupled parameters suggest curvilinear relationships. Therefore, the coefficients of determination (R^2 and adjusted R^2) of the possible equations fitting the obtained relationship were comparatively examined in order to select the optimum equation (and avoid over-fitting) that explains the relationship (Walpole *et al.*, 2012). See the highlighted example in Table 5.2 for selecting the optimum equation as that of a quadratic equation with comparatively higher R^2 and adjusted R^2. Combining the R^2 and adjusted R^2 with the residual sum of squares (RSS) was used to quantify how the observed relationship varied with time (Walpole *et al.*, 2012; Hocking, 2003). The RSS were normalised where necessary, by dividing the RSS by the standard deviation (Pasternack and Lruzzi, 1965).

Table 5.2: Selection of optimum fitting equation based on R^2 and adjusted R^2

Regressors	Exponential	Linear	Quadratic	Multiple	Cubic
Equations	e^{x^2+3x-8}	$2x + 8$	$6x^2 + 8x - 5$	$8x_1 + 2x_2 + 1$	$x^3 + 6x^2 + 2$
R^2	0.721	0.859	0.874	0.891	0.899
Adjusted R^2	0.71	0.848	0.859	0.823	0.807

Adapted from (Ogee *et al.*, 2013; Walpole *et al.*, 2012)

5.5. Results and discussion

For the purpose of this study, the results of the shear rheometry of the concrete mixes are initially presented and discussed, followed by the plastic cracking behaviour results, and then combining both to show the relationship. Key factors influencing observable outcomes (such as plastic cracking) are often addressed independently for research purposes, in practice, they act simultaneously (Lura *et al.*, 2007). However, independently measuring the rheology and plastic cracking process to explain how they interact, for the purpose of this study, is believed to be an approach that will prove that such interactions truly exist and are interdependent.

5.5.1. Rotational shear rheological properties

The test result in Figure 5.5 is termed torque decay and it simulates the possible response of the concrete mixes to vibration or continuous shearing, further details of the test can be found in (Kolawole *et al.*, 2019a). The last part of Figure 5.5 shows the reduction in apparent viscosity calculated from the peak and steady torques due to the continuous shearing. Figure 5.6 represents

the concrete's rheological parameters without any form of shearing before resting which is termed Set A while Figure 5.7 represents the concrete with pre-shearing to achieve steady-state before allowing the concrete to rest which is termed Set B. For this study, rheo-physical properties summarised in Figure 5.6 were selected over that of Figure 5.5 because the results are in absolute rheological units while 5.6 is in relative units due to the limitations of the ICAR rheometer geometry (Kolawole *et al.*, 2019a). The selection also avoids the rate-dependent intricacies of the steady torque (Kolawole *et al.*, 2019a). The resting time shown on the figures refers to the concrete age at the time of testing. Detailed results can be found elsewhere (Kolawole *et al.*, 2019a).

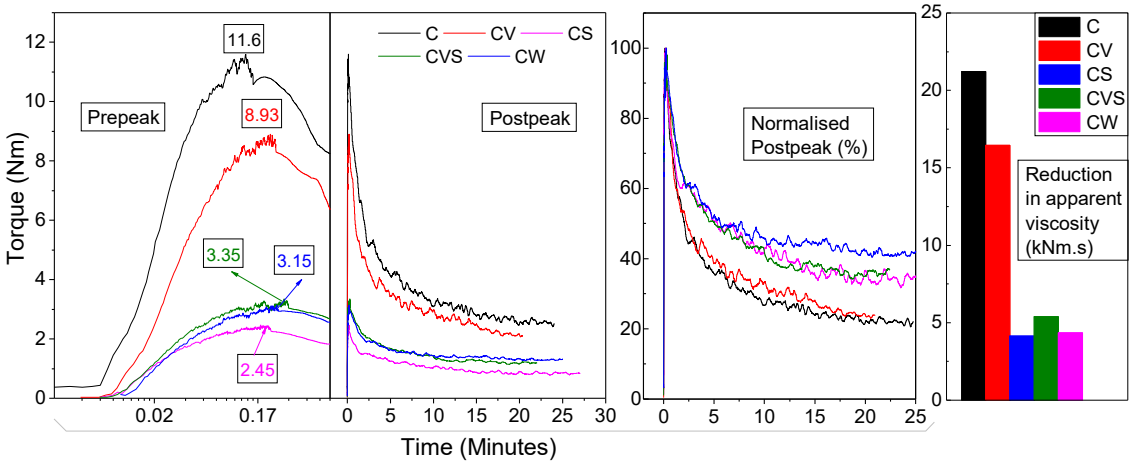

Figure 5.5: Torque decay at 0.02 rev/s shearing rate without shearing pre-condition

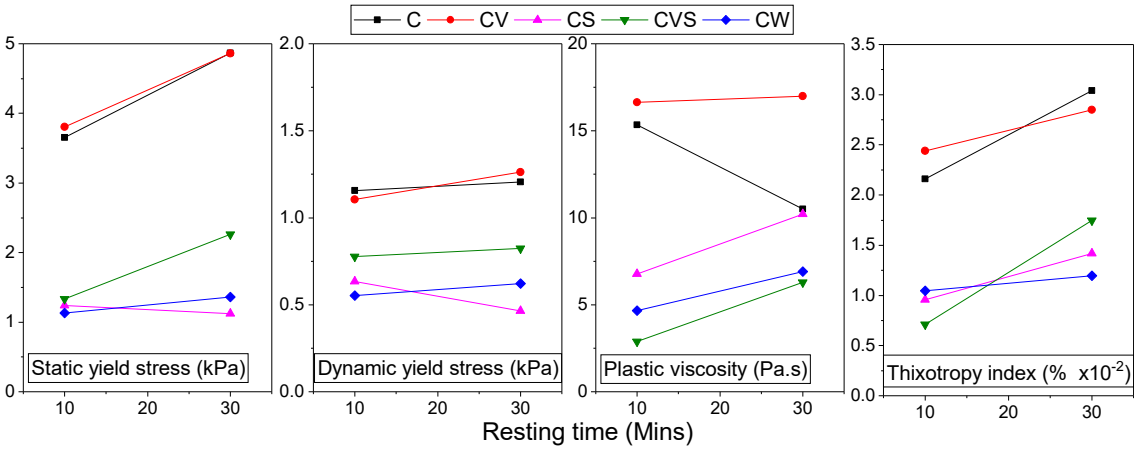

Figure 5.6: Rheological properties of the concrete mixes without shearing pre-history (Set A)

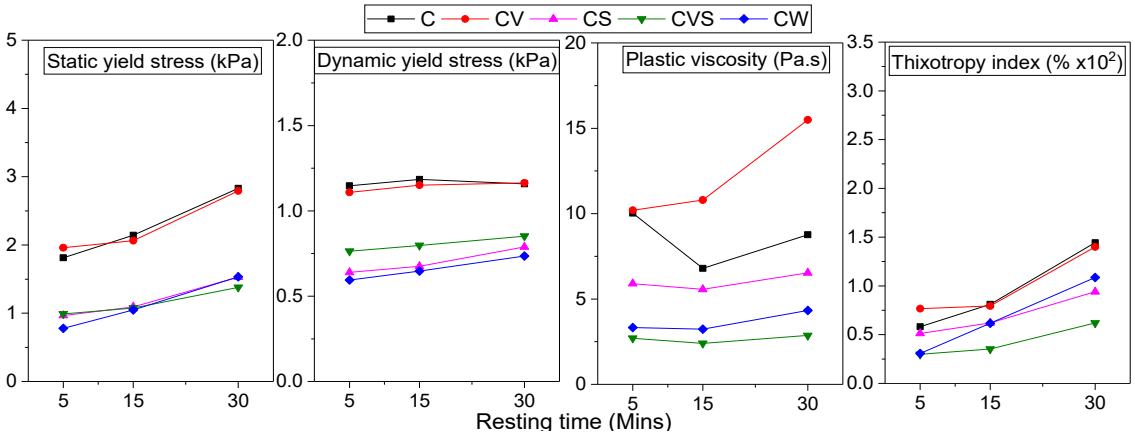

Figure 5.7: Rheological properties of the concrete mixes with shearing pre-history (Set B)

The dynamic yield stress remains fairly the same for all the concrete ages (Figure 5.6 and Figure 5.7) and condition pre-history (Set A and B) emphasising that vibration will have similar effects on the concrete's yield stress, irrespective of the concrete's prior condition. Figure 5.6 and Figure 5.7 show that mixes C and CV had similar rheology parameters while mixes CS, CVS and CW were similar (that is a grouping of C/CV and CS/CVS/CW), with only slight differences. The thixotropy index is time-dependent and quantifies the potential of the concrete mixes for early structuration (that is, increasing static yield stress). As noted earlier, the study by (Kolawole *et al.*, 2019a) on the same concrete mixes show that the rates of the thixotropy build-up are also time-dependent at least for the 30 minutes resting time, that is, a non-linear increase as also observed by (Ma *et al.*, 2018). Figure 5.8 shows the evolution of the static yield stress estimated from the Ma *et al.* (2018) model given in Equation 5.1. Material parameters for the model can be found in (Kolawole *et al.*, 2019a). Values from this were used for the correlation with the plastic cracking processes.

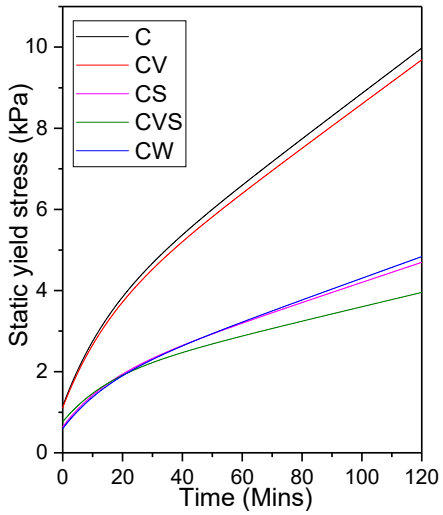

Figure 5.8: Estimated evolution of static yield stress using the model from Equation 5.1

The results of the small amplitude oscillatory test (SAOS) are shown in Figure 5.9 and Figure 5.10. Further details and other related results can be found in the companion study (Kolawole *et al.*, 2019b). The storage modulus was linearly extrapolated beyond 30 minutes up to the initial setting time (120 minutes). The linear extrapolation was based on the (Ma *et al.*, 2018) model using the linear rate (G_{rigid}) of rigidification evolution since the measured evolution up to 30 minutes fits the model.

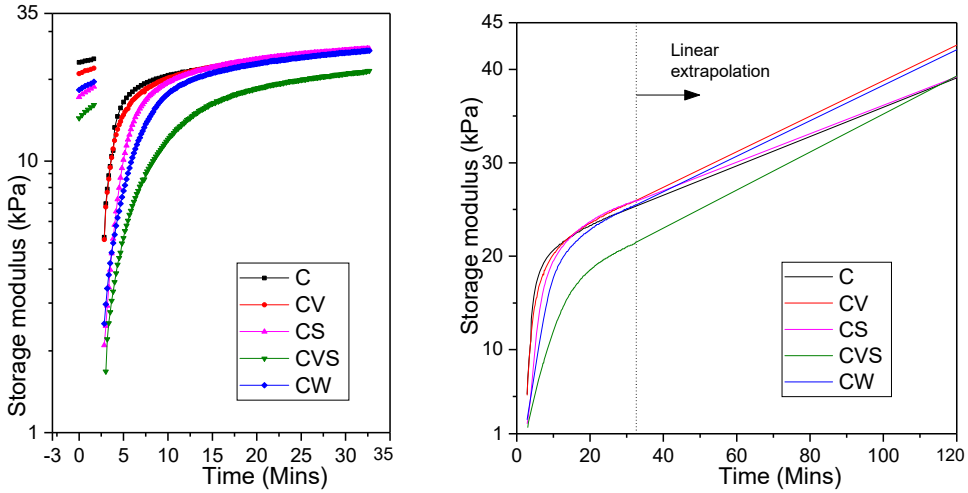

Figure 5.9: (a) 3ITT thixotropy results of the suspending mortar from SAOS (b) Extrapolated evolution of the storage modulus using G_{rigid} from Equation 5.2

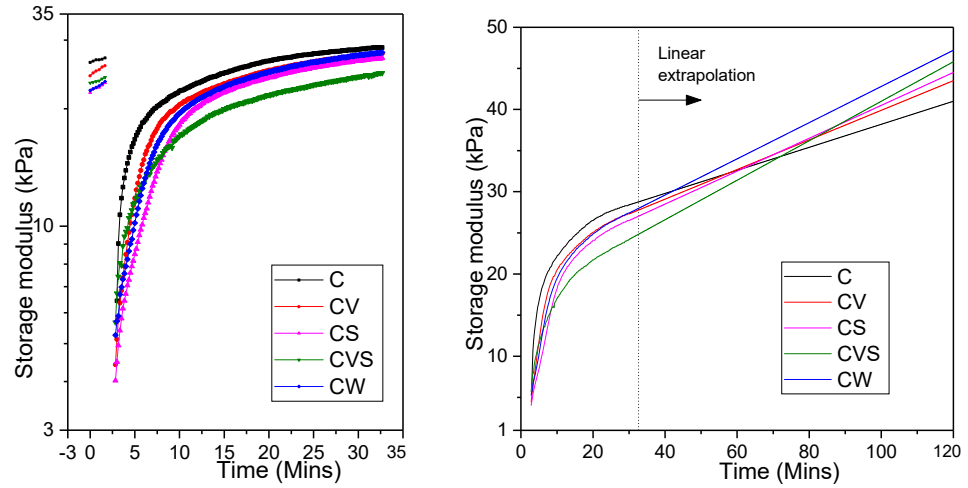

Figure 5.10: (a) 3ITT thixotropy results of the concrete from SAOS (b) Extrapolated evolution of the storage modulus using G_{rigid} from Equation 5.2

5.5.2. Plastic cracking influencing processes

5.5.2.1. Bleeding and evaporation

Figure 5.11a shows the cumulative bleeding and evaporation of the concrete mixes and Figure 5.11b shows their rates. The rates were calculated by differentiating the respective plots using Origin

software and smoothing the curves with Savitzky-Golay filter of polynomial order 1 and 4 points of window. The differentiation at a typical point is found by using a tangent to the plot at the considered point. From Figure 5.11, the synthetic modifiers used in this study were able to hold the capillary water in their pores (more than mixes C and CW) by evaporating and bleeding less. In agreement with these results, Lin and Huang (2010) also observed that cellulose-based stabilisers slightly reduced bleeding and evaporation of concrete by increasing the viscosity of the pore fluid while Leemann *et al.* (2014) found that VMA+SP increased bleeding of self-compacting concrete (SCC) (that is, VMA+SP increased bleeding more than just SP in SCC).

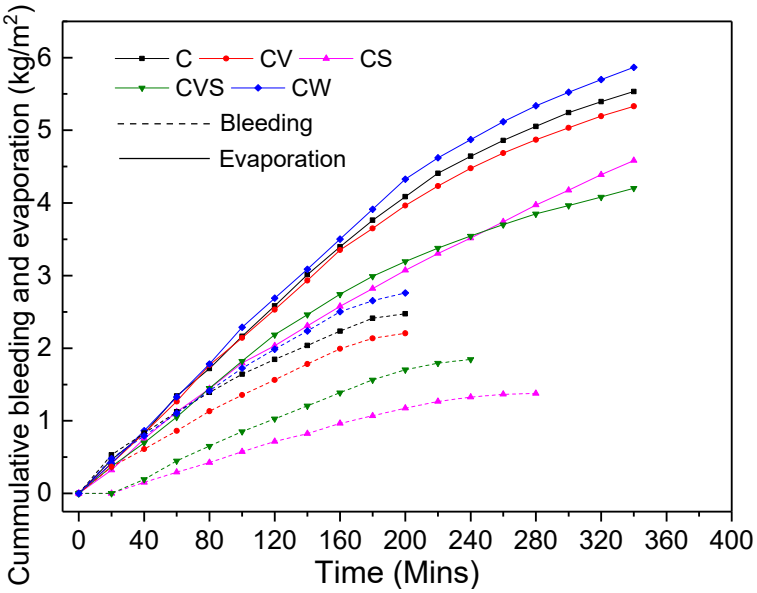

(a) Cumulative bleeding and evaporation

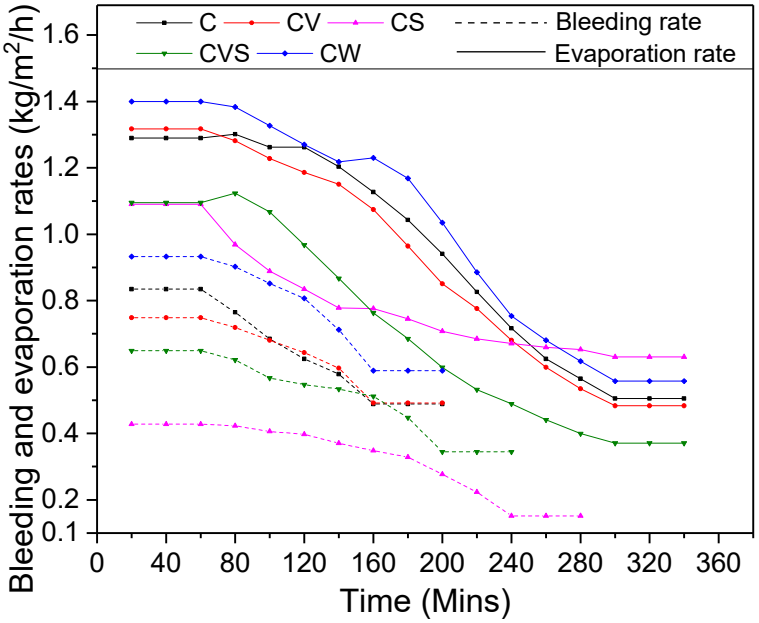

(b) Bleeding and evaporation rates

Figure 5.11: Bleeding and evaporation results for the concrete mixes

SP is known to repel concrete water molecules by adsorption (Mardani-Aghabaglou *et al.*, 2013; Flatt and Schober, 2012), thereby, water can be held within the concrete pore structure which may have led to its delayed start and longer bleeding time observed in the result. Organic VMA is known to absorb water as an envelope around its chains for thickening and travels with concrete during flow (Isik and Ozkul, 2014) and unlike SP, only act on the liquid phase of concrete (Bouras *et al.*, 2012). Therefore, mix CV may have bled and evaporated more and quicker than mixes CS and CVS because its water molecules were more readily available from the liquid phase of concrete. In essence, it can be concluded that the SP is more effective in retaining concrete pore water for longer compared to VMA.

5.5.2.2. Capillary pressure

Figure 5.12a shows the capillary pressure build-up within the pores of the concrete mixes. The pressure build-up for all the mixes has three distinct rates/stages before their sudden drop, such typical stages for mix CV are shown in Figure 5.12b (marked as 1, 2, and 3). The slopes of the lines (lines of best fit) depicting the stages were used to calculate the rate of capillary pressure shown in Figure 5.12c. Stage 1 represents the period where the pore structure readily supplies water to the surface, preventing severe rise in the capillary pressure build-up. Stage 2 presents the period where pore water is removed from within the concrete resulting in the build-up in capillary pressure. This is caused by the formation of concave menisci which also results in a 3D volume change. During Stage 2, the concrete particles can still settle vertically and hence, the 3D volume change has a significant vertical component. Stage 3 shows a much larger rate of pressure build-up compared to Stage 2. This is reasoned to be due to significantly reduced potential for particle settlement (self-settlement) in Stage 3 compared to Stage 2 where particles settle more leading to upward water transport to the surface and a slower pressure build-up. These three stages, as can be identified in Figure 5.12b, can be used as indicators of significant changes in the plastic cracking behaviour of the concrete mixes as explained further in Section 5.5.3. The cumulative bleeding observed in Figure 5.11 explains the capillary pressure results. The more the concrete mixes can retain water within its pores, that is, less evaporation and bleeding, the more the delayed rise of the capillary pressure build-up which was observed for mixes CV, CS and CVS as shown in Figure 5.12c. The delay and reduced capillary pressure build-up rate of CW is due to the presence of more water in its pores due to its increased water content (Slowik *et al.*, 2008; Wittmann, 1976).

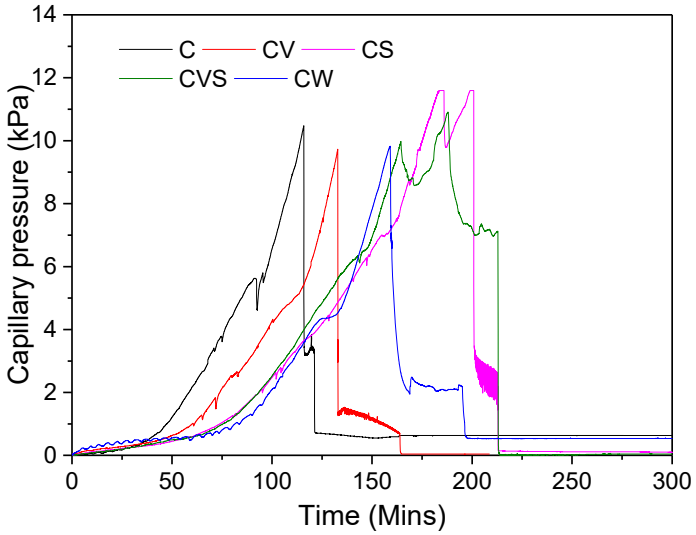

(a) Capillary pressure build-up

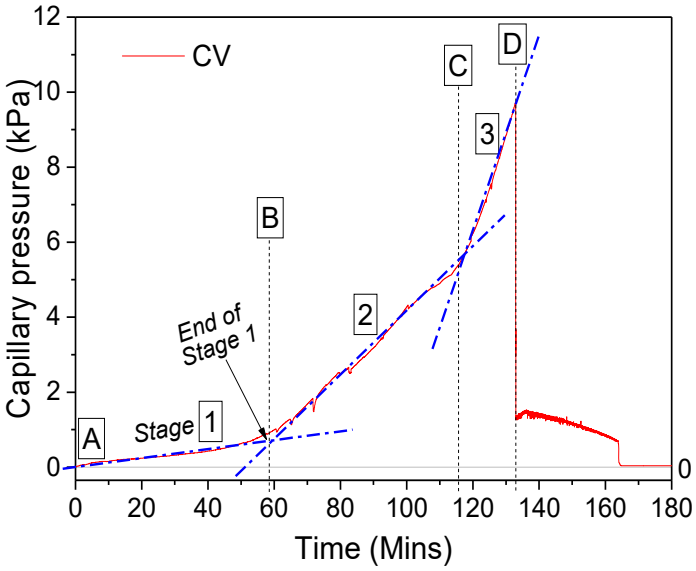

(b) Typical stages of capillary pressure build-up

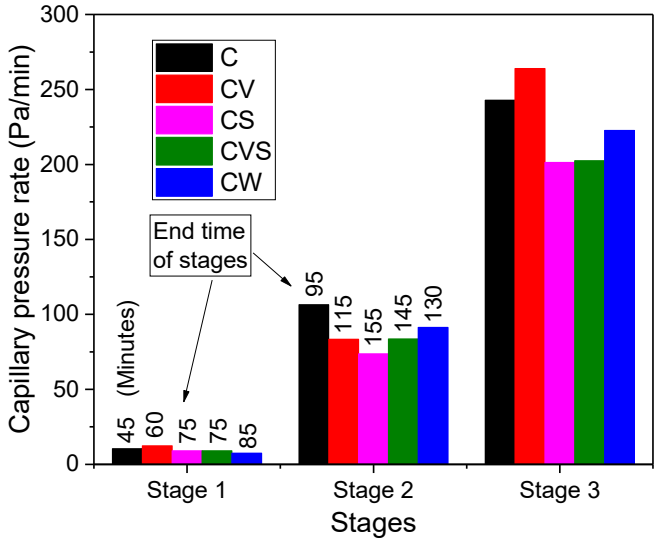

(c) Rate of capillary pressure build-up and stage end time

Figure 5.12: Negative capillary pressure results for the concrete mixes

Comparing Figure 5.12a and Figure 5.12c, the observed differences in the capillary pressure build-up (among the mixes) were due to varying delays before the rapid rise (Point B of Figure 5.12b or end time of Stage 1 in Figure 5.12c), although the rates among the mixes were slightly different especially during Stage 3.

5.5.2.3. Plastic settlement

As noted in the introduction, plastic settlement in concrete consists of two forms, mainly self-settlement due to gravitation and partly capillary-induced settlement. A direct consequence of plastic concrete's settlement is bleeding. The bleeding shows how easily water can move within the concrete to the surface (Leemann *et al.*, 2014), that is, permeability. The initial stiffness of concrete is related to the dynamic yield stress (due to vibration that causes the jump-start of settlement/flow) while the evolution of this stiffness with time can be linked to its thixotropy. Based on Equation 5.5 (Ghourchian *et al.*, 2016, 2018), the permeability properties of the concrete mixes were calculated and are shown in Table 5.3. The concrete and pore fluid densities were calculated from that of the constituent materials, while the constant bleeding rate was the initial bleeding rate from Figure 5.11b.

Table 5.3: Permeability coefficients of the mixes

Mixes	Constant bleeding rate	Concrete density	Pore fluid density	Permeability coefficients
	m/s	kg/m^3	kg/m^3	m/s
C	2.305×10^{-7}	2414	1000	1.6296×10^{-7}
CV	2.083×10^{-7}	2411	1000	1.4758×10^{-7}
CS	1.194×10^{-7}	2411	1000.52	8.4688×10^{-8}
CVS	1.777×10^{-7}	2409	1000.34	1.2618×10^{-7}
CW	2.583×10^{-7}	2402	1000	1.8425×10^{-7}

Figure 5.13 shows the plastic settlement strain of the concrete mixes with time. It represents the total vertical translation of the concrete surface. The insert in the figure shows an enlargement of the beginning part (less than 10 minutes) of self-settlement of the mixes. The influence of the mixes' permeability, hence bleeding, is evident during this period. That is, the smaller the permeability coefficient, the less the settlement observed in the mixes. However, after 30 minutes of exposure in the climate chamber, the stiffness and stiffness evolution of the mixes can be said to influence the plastic settlement (see Section 5.5.4). The extent of settlement of the mixes (order of C, CV, CVS, CS, and CW) can be linked to the liquid phase of the concrete, the less stiff it is (less dynamic yield stress), the more the settlement (see see Section 5.5.4).

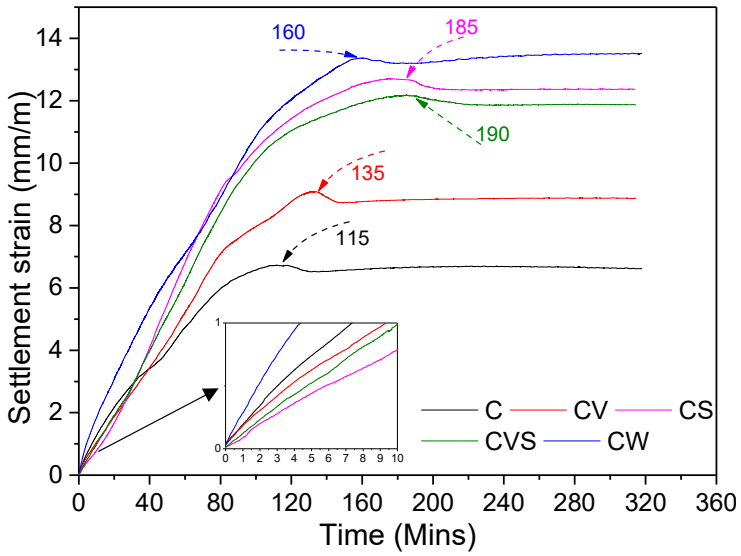

Figure 5.13: Settlement strain for the concrete mixes

The peak times indicated on the plots in Figure 5.13 are the points where the plastic settlement ceased. As noted earlier, settlement occurs during the dormant period of hydration and is assumed to end when concrete stiffens enough to resist further settlement. From the plots, it can be implied that Mixes C and CV dormant periods may be shorter than that of Mixes CVS, CS and CW. That is, their stiffening and start of solidification are quicker, though all the mixes have similar final setting time except for Mix CVS which has a 30 minutes delay (see further discussion in Section 5.5.4).

5.5.2.4. Plastic shrinkage

Results of the measured horizontal plastic shrinkage are shown in Figure 5.14. It represents the total horizontal translation of the specimen opposite edges. Two of the main factors influencing shrinkage are the capillary pressure and continuous evaporation, mix CW has similar capillary pressure build-up to mixes CS and CVS (see Section 5.5.2.2) but a higher amount of evaporation that is similar to mixes C and CV. The similar delay in the rise of capillary pressure of mixes CS, CVS and CW explains their similar delayed rise in plastic shrinkage. Furthermore, the similar evaporation of mix CW to mixes C and CV but delayed capillary pressure build-up explains why mix CW has similar shrinkage rate but a lower shrinkage amount than mixes C and CV until 180 minutes when mix CW amount of shrinkage supersedes due to its higher water content. Unlike the plastic settlement, the artificial modifiers reduced the shrinkage of the concrete mixes.

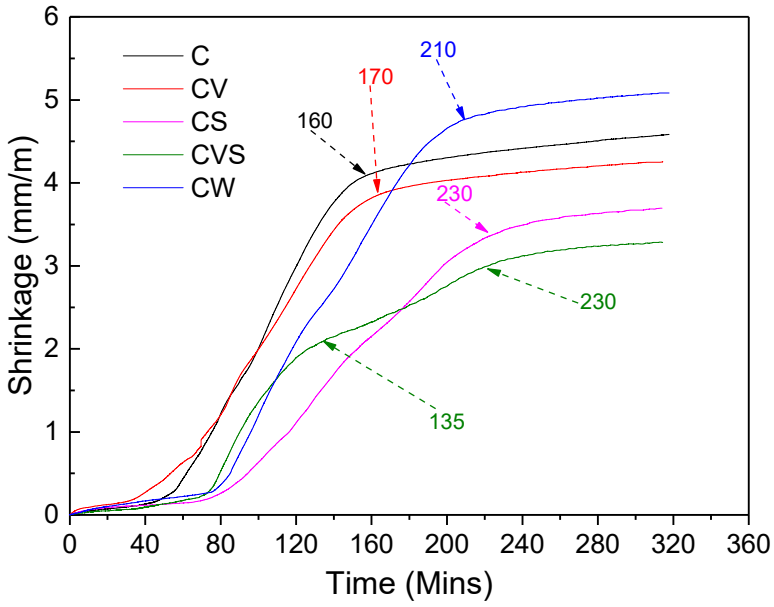

Figure 5.14: Shrinkage strain for the concrete mixes

The rapid rise in the shrinkage of the mixes are the times when capillary pressure starts to develop in the mixes (see Section 5.5.4) to cause pore contraction which in combination to plastic settlement (self-settlement and capillary-induced settlement) causes volumetric shrinkage. These delays reveal that plastic shrinkage only becomes pronounced after some settlement has occurred, in this case, mix C had undergone 65.7% of its total settlement while mixes CV, CS, CVS and CW had 57.2%, 70.9%, 69.7% and 67.2% respectively. Mix CVS shows a pronounced reduction in shrinkage rate at about 135 minutes, which is believed to be due to the ending influence of its particle settlement (self-settlement – end time of Stage 2 in Figure 5.12c), that is, the shrinkage reduced significantly when the particles stop settling. Unlike other mixes, this may imply that its particles settling in the concrete matrix has a role in making the plastic shrinkage stabilise earlier than other mixes. Points shown on the plots in Figure 5.14 indicate when the plastic shrinkage significantly stabilises. Plastic shrinkage is believed to end when the concrete has solidified enough to resist contractions due to negative capillary pressure and pore collapse. Therefore, mixes C and CV changed from plastic to solid faster than mixes CS, CVS, and CW which reiterates the stiffness evolution pattern observed with the plastic settlement (see further discussion in Section 5.5.4).

5.5.3. Plastic cracking behaviour of the concrete mixes

Figure 5.15 shows the development and details of the plastic cracking of the concrete mixes (showing the influence of the rheology modifiers). The setting times are embossed on the graphs to show their crack development in relation to their hydration evolution, generally, the less the evolution of hydration in concrete, the more the potential for plastic cracking (Ghourchian *et al.*, 2018; Alhozaimy and Al-Negheimish, 2009). Addition of viscosity modifying agent (VMA) in the

concrete increased the cracking of concrete substantially (25% higher than the control) while the superplasticiser (SP) and increased water content barely increased the final crack area (4% and 3% respectively). Inclusion of both VMA and SP greatly reduced the final cracking of the concrete by 53%. Mix CV had the highest magnitude, which may imply that it has the weakest structure against plastic settlement cracking and propagation by plastic shrinkage. The delay in the crack initiation at the surface by mix CW may be because of its increased liquid phase assisting in the filling of microcracks induced by plastic settlement. It has been reported that the time of start of cracking increases with increased water content in concrete while too little or too much water may not crack (Safiuddin *et al.*, 2018; Dias, 2003; Samman *et al.*, 1996). Likewise, the more the paste content in concrete, the more the risk of cracking. However, for CW of this study, the magnitude at the first crack is high, showing that the crack may not have readily shown on the surface but cracks may have occurred within the concrete before it appeared on the surface (Combrinck *et al.*, 2018a). Other influencing factors of the plastic cracking of the concrete mixes are their viscoelastic properties which influence their behaviour under restrained conditions. For example, mix CVS has strong strain dissipation ability which is reported in a companion papers (Kolawole *et al.*, 2019c,b) and could have caused the reduced cracking.

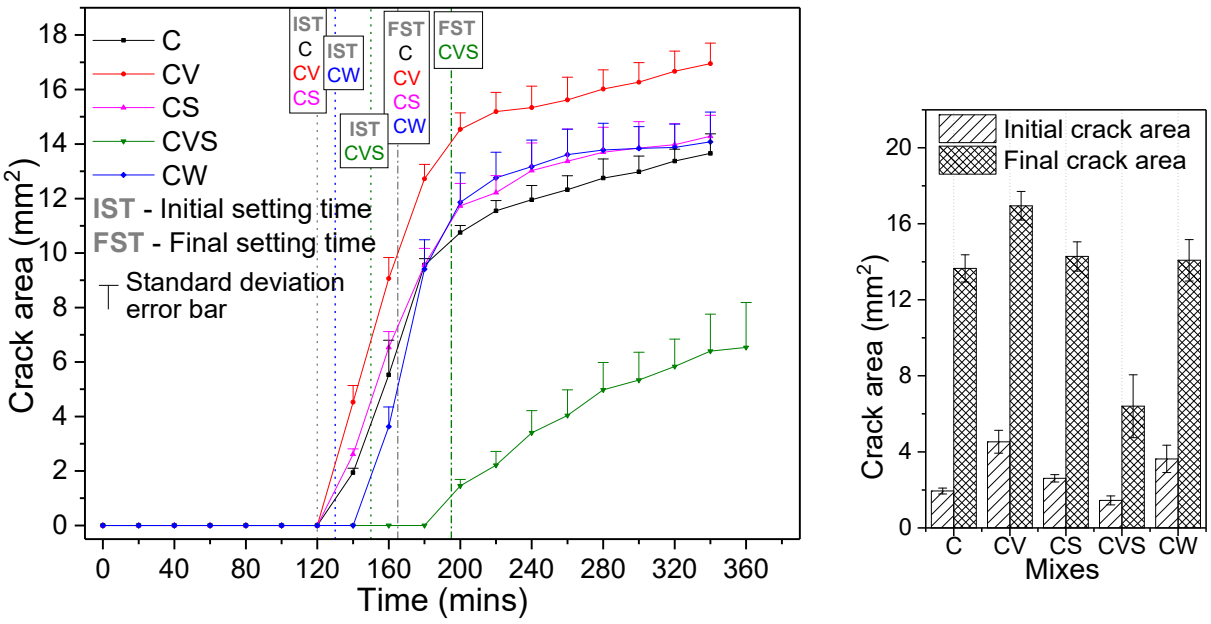

Figure 5.15: (a) Plastic cracking development of the concrete mixes, and (b) Details of the crack areas

The plastic cracking behaviour (analogous to Figure 5.1) of the concrete mixes are shown in Figure 5.16 and summarised in this section. The plastic cracking behaviour of the control (mix C – Figure

5.16a) which serves as the standard for the other mixes (CV, CS, CVS and CW) is used in explaining the plastic cracking behaviour while slight changes in the other mixes are highlighted.

Mix C bleeding, which is due to plastic settlement, was similar to the evaporation until around 45 minutes when it starts to reduce. That is, from that point onwards, the quantity of bleed water is inadequate to keep the pore water from evaporating. Hence, the increased rise in capillary pressure (start of Stage 2 of Figure 5.12b) and plastic shrinkage from that point onwards which also serves as an indicator of significant changes in plastic cracking behaviour. This indicator at the 45 minutes is also evident on the plastic settlement strain plot where there's an initial decrease in settlement rate because the concrete starts to settle less and displaces less water towards the concrete surface (less bleeding rate of Figure 5.11). That is, water menisci start forming in the concrete pores and the reduction in the settlement at this time comes from the particles starting to touch one another (caused by drying and cumulative settlement simultaneously) (Combrinck, 2016; Powers, 1968). Further settlement after this point is jointly contributed by the capillary-induced settlement and self-settlement (Leemann *et al.*, 2014). Another indicator for change in plastic cracking behaviour of mix C was around 95 minutes (start of Stage 3 of Figure 5.12b) and can be tied to the slight kink in the capillary pressure plot and change in the rate of the settlement in Figure 5.16a. This second indicator may signify the end of self-settlement contributed by the settling concrete particles. The reduced rate of settlement at this second indicator reiterates earlier submissions by Leemann *et al.* (2014) and Slowik *et al.* (2008) that capillary-induced settlement is less predominant and may have less magnitude than self-settlement. The third indicator (end of Stage 3 of Figure 5.12b) is around 115 minutes, this is when the settlement ends which marks the point when the pores' menisci could not cause further consolidation but horizontal shrinkage continues because the concrete is yet to develop enough stiffness to resist the evaporation that continues (Leemann *et al.*, 2014). Restraining the plastic settlement (where a larger part of its magnitude occurs before initial setting time as shown in Figure 5.16) causes internal shear-induced cracks which can easily propagate due to later occurring plastic shrinkage (Combrinck *et al.*, 2018a). Localised air entry into the concrete due to local pore collapse (drop in capillary pressure in Figure 5.16) serves as weak spots for the propagation of cracking due to continuous shrinkage (Slowik *et al.*, 2008). That is, internal plastic cracking could have initiated due to differential settlement before the end of Stage 3 and becomes propagated by the restrained plastic shrinkage to the surface where it becomes measurable at 140 minutes (control mix).

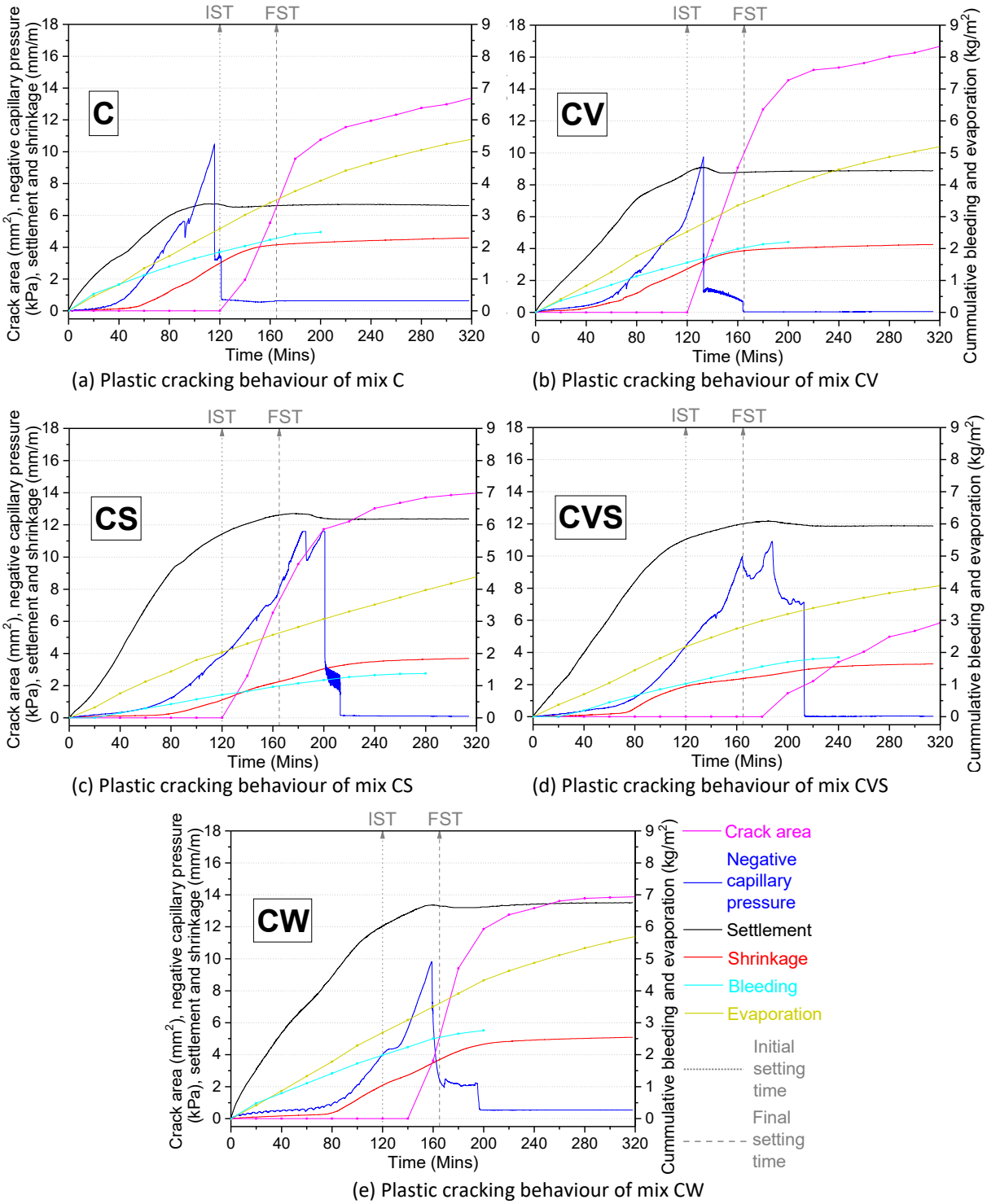

(a) Plastic cracking behaviour of mix C

(b) Plastic cracking behaviour of mix CV

(c) Plastic cracking behaviour of mix CS

(d) Plastic cracking behaviour of mix CVS

(e) Plastic cracking behaviour of mix CW

Figure 5.16: Plastic cracking behaviour of the concrete mixes

Unlike the control mix C, mix CV and CVS had no obvious change in settlement rate due to the sharp rise in capillary pressure and horizontal shrinkage, which signified the development of the pore menisci. This may mean that the new combined effect of self-settlement and capillary-induced settlement was equal to the previous single self-settlement. The observed delayed kink in the plot

of the capillary pressure in both mixes (as the second indicator of change in plastic cracking behaviour) may be because of VMA thickening of the liquid phase (Kolawole *et al.*, 2019a) causing a delayed response. For Mix CS, the end of self-settlement was rather gradual for mix CS (probably due to its fluidity – less yield stress as shown in Table 5.1) and not overly obvious on the settlement plot, but may be traced to the simultaneous kink in the capillary pressure and shrinkage plots at around 155 minutes (second indicator – Figure 5.12c). For the mixes C/CV, CS, CVS and CW, the indicative end of the self-settlement can, therefore, be assumed to be around 95, 155, 145 and 115 minutes respectively.

5.5.4. Interdependence of the rheo-physical properties and plastic cracking behaviour

Using the early rheological results within 30 minutes (dynamic yield stress and thixotropy index – after vibration) from Section 5.5.1, the results of its correlation with the plastic cracking processes (plastic settlement, plastic shrinkage and rate of negative capillary pressure build-up) are shown in Table 5.4. The correlation coefficients with statistical significance ($p \leq 0.05$) are highlighted in the tables and only these were considered for the envisaged relationship. These correlations serve as a prefix to determining the relationship between the rheo-physical properties and plastic cracking behaviour, it helps to decisively choose the right parameters for the relationship.

Table 5.4: Pearson correlation coefficients between the rheo-physical properties and plastic settlement

Rheo-physical properties		Plastic settlement								
	Concrete age	10 mins	20 mins	30 mins	40 mins	50 mins	75 mins	100 mins	125 mins	150 mins
Permeability coefficient		**0.892**	**0.823**	**0.739**	0.311	0.005	-0.379	-0.313	-0.242	-0.242
Dynamic yield stress	10 mins	-0.227	-0.363	-0.480	-0.859	**-0.971**	**-0.965**	**-0.965**	**-0.970**	**-0.970**
	30 mins	-0.024	-0.164	-0.294	-0.712	**-0.873**	**-0.931**	**-0.904**	**-0.892**	**-0.892**
Thixotropic index	10 mins	0.009	-0.131	-0.231	-0.626	-0.778	-0.854	-0.873	-0.861	-0.861
	30 mins	-0.195	-0.333	-0.449	-0.840	**-0.962**	**-0.971**	**-0.975**	**-0.978**	**-0.978**
		Plastic shrinkage								
Dynamic yield stress	10 mins	0.253	0.098	0.149	0.41	0.625	**0.852**	**0.958**	**0.895**	0.820
	30 mins	0.301	0.173	0.260	0.540	0.730	**0.905**	**0.960**	**0.980**	**0.910**
Thixotropic index	10 mins	0.621	0.535	0.576	0.719	0.834	**0.965**	**0.973**	0.833	0.834
	30 mins	0.281	0.136	0.185	0.429	0.635	**0.864**	**0.969**	**0.894**	0.834
		Rate of pressure build-up								
		Stage 1		Stage 2		Stage 3				
Dynamic yield stress	10 mins	**0.880**		0.517		0.779				
	30 mins	**0.829**		0.557		**0.858**				
Thixotropic index	10 mins	0.845		0.460		**0.958**				
	30 mins	**0.873**		0.538		0.801				

From Table 5.4 and as shown in the next section, the permeability coefficients influence the very early start of the plastic settlement (signifying the influence of the vibration) and this is reflected in the significant correlation coefficients they have up to 30 minutes. Afterwards, the dynamic yield stress starts to correlate well with the plastic settlement at 40 minutes with a significant correlation from 50 minutes. No significant correlation was obtained with the thixotropic index at 10 minutes concrete age probably because the concrete has not developed an adequate static yield stress (that is, after vibration) to reflect its true potential for structuration. The above patterns were, similarly, obtained for the plastic shrinkage and capillary pressure rate. The dynamic yield stress and thixotropy index were found to be collinearly related and were, hence, not combined for explaining the plastic cracking processes. Table 5.5 shows the typical forms of equations examined for the observed relationship between the permeability coefficient and plastic settlement, the exponential equation is the optimum fitting equation (see Section 5.4.6). Table 5.6 shows the residual sum of squares used in relation with the coefficients of determinations (R^2 and adjusted R^2) to observe how the relationship changes with time.

Table 5.5: Possible equation forms to describe the relationship between permeability coefficients and settlement

Settlement time	10 mins			20 mins			30 mins			40 mins		
Equation forms	R^2	AdJ R^2	RSS	R^2	AdJ R^2	RSS	R^2	Adj R^2	RSS	R^2	Adj R^2	RSS
Exponential	0.984	0.968	0.01	0.949	0.898	0.06	0.930	0.860	0.1	0.694	0.389	0.75
Quadratic	0.965	0.930	0.02	0.919	0.839	0.1	0.893	0.786	0.16	0.643	0.286	0.88
Linear	0.796	0.728	0.13	0.676	0.568	0.4	0.545	0.394	0.68	0.096	-0.204	2.24

AdJ R^2 – adjusted R^2, RSS – residual sum of squares

Table 5.6: Residual sum of squares (RSS) of the fitting equations

Time	30 mins	50 mins	75 mins	100 mins	125 mins	150 mins
Coefficient of permeability	*	0.968	-	-	-	-
Plastic settlement	0.479	0.108	0.242	0.281	1.489	1.119
Plastic shrinkage	0.0495	0.0058	0.0326	0.2625	0.9366	-
Rate of pressure build-up	Stage 1		Stage 2		Stage 3	
	1.189^{+}		25.016^{+}		27.571^{+}	

*As shown in Table 5.5 for the exponential form of equation, $^{+}$normalised RSS

5.5.4.1. Relationship between the early rheo-physical parameters and plastic cracking processes

Figure 5.17a reveals the influence of the permeability coefficient on the plastic settlement. Permeability influences bleeding (Equation 5.5) which emanates from the settlement (Lura *et al.*, 2007; Powers, 1968). Therefore, a kind of direct relationship is expected between the permeability

coefficient and plastic settlement and this is supported by the positive correlation coefficients obtained in Table 5.4. However, the form and extent of the direct relationship are unknown and scarce in the literature. An exponential function (with a quadratic exponent) was found to best represent the relationship between the two variables with good correlation. The permeability only had a direct influence up to 30 minutes after which the influence significantly reduced (that is, reducing R^2 in Figure 5.17a). Figure 5.17b shows the influence of the dynamic yield stress and thixotropy index on the plastic settlement of the concrete mixes as time progressed. Since the yield stress and thixotropy are the concrete's resistance to coarse particles' settling, an inverse relationship is expected with the plastic settlement. This is also suggested by the negative correlation coefficient in Table 5.4. The extent and nature of the inverse relationship are unknown. Consequently, a quadratic function was found to best describe the relationship.

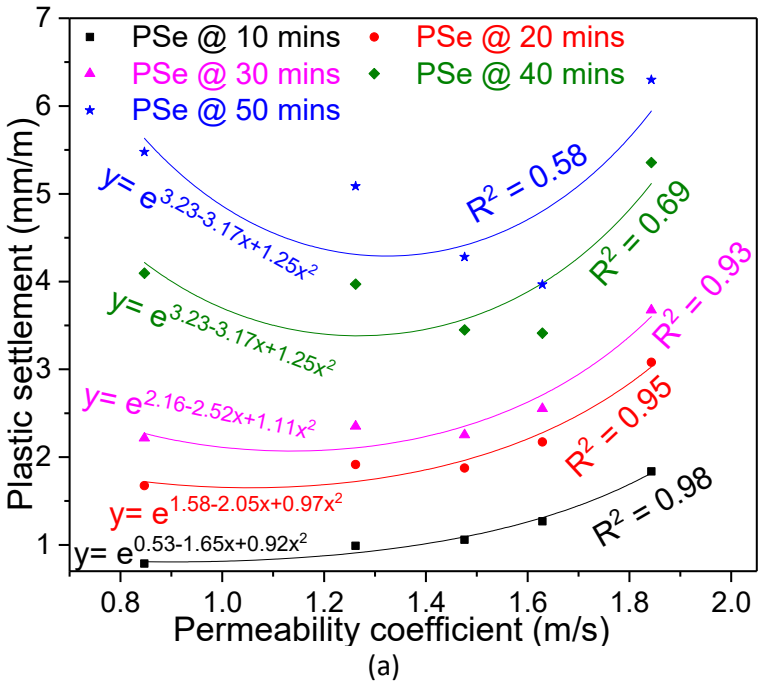

(a)

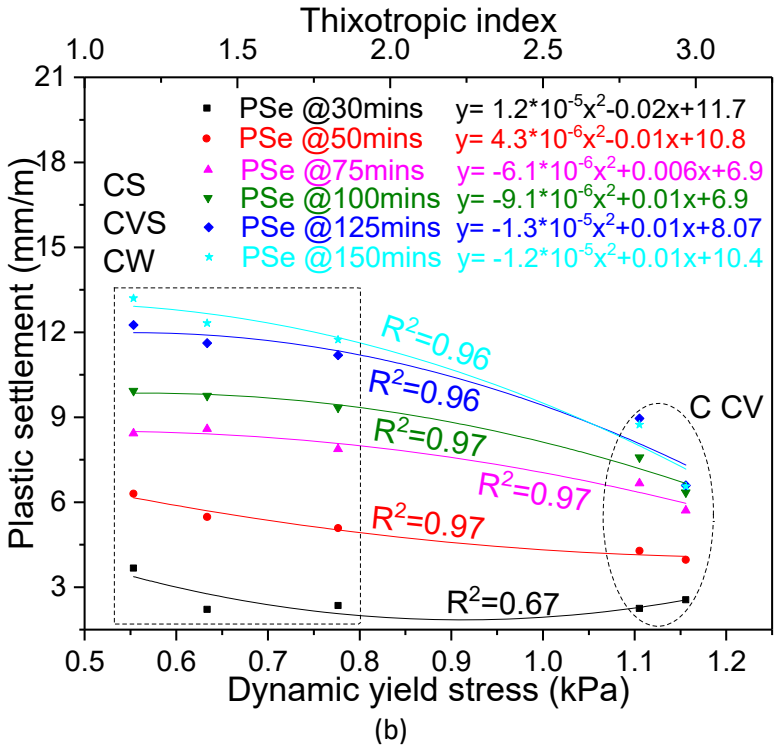

(b)

Figure 5.17: Relationship between the permeability coefficient, dynamic yield stress, thixotropic index and the plastic settlement (PSe) of the concrete mixes

From Figure 5.17, the dynamic yield stress and thixotropy index (Figure 5.6) is linked to the settlement after the influence of the permeability ends (this is confirmed by the reduced R^2 at 30 minutes). That is, the dynamic yield stress and immediate thixotropy (building up during the permeability predominance period) relates inversely to the observed plastic settlement afterwards. This is a useful tool to estimate the extent of plastic settlement of concrete from a simple rheological test. Also noticed in Figure 5.17b is the grouping of the mixes (C/CV and CS/CVS/CW – see Section 5.5.1) in relation to their rheo-physical parameters, reinforcing the fact that the plastic settlement and these rheo-physical properties are interdependent.

Plastic shrinkage is the result of contraction of concrete's pore menisci (Slowik *et al.*, 2008; Wittmann, 1976). The ease of the contraction can be hypothetically affected by the residual structures' stiffness (dynamic yield stress) and immediate structuration (thixotropy index) after vibration. Supposedly, the more fluid the concrete mixes (becomes), the less the potential for menisci contractions because the pores are more fluid-filled. How these translate to the experienced/measured plastic shrinkage afterwards and the interwoven influence of particles' settlement (highlighted in Section 5.5.3) is unknown, but the positive correlation coefficients obtained in Table 5.4 suggests a direct relationship. Figure 5.18a supports the direct relationship between the dynamic yield stress/thixotropic index and the cumulative plastic shrinkage at 30 and

60 minutes, respectively. Sixty minutes is the least time of the rapid rise in shrinkage due to evaporation and capillary pressure for the concrete mixes, hence, the reduced R^2 at 30 minutes. Figure 5.18b shows the relationship at later times.

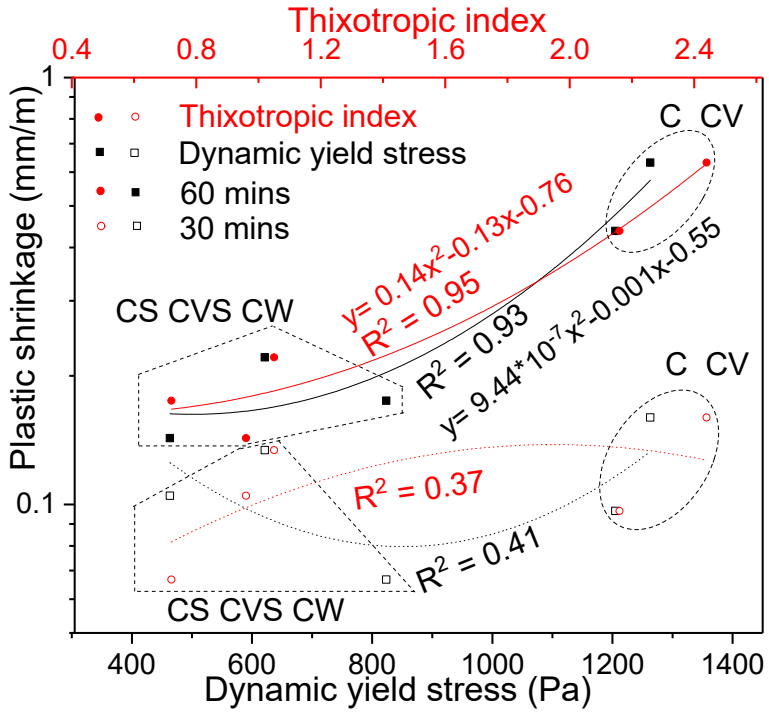

(a) Influence at 30 and 60 minutes plastic shrinkage

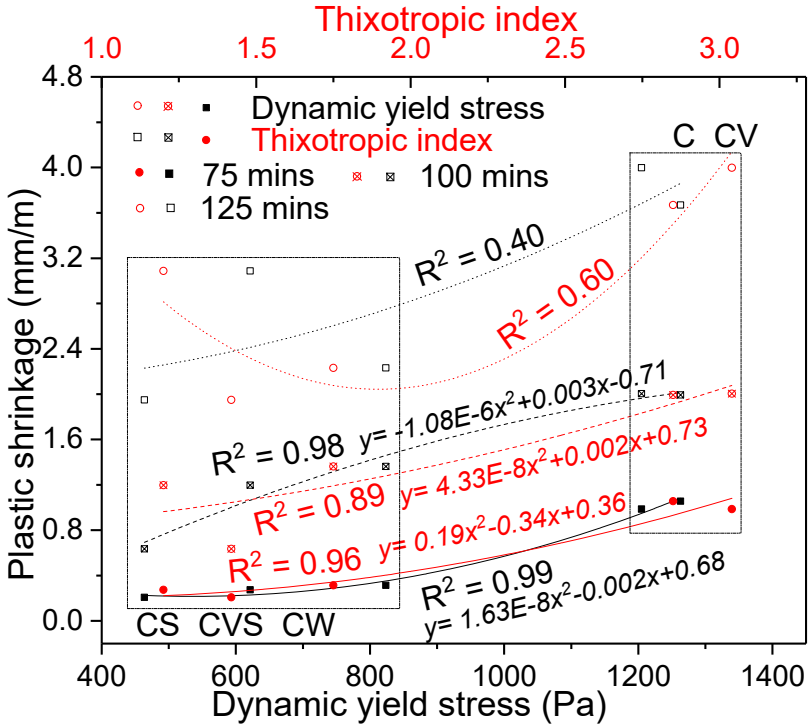

(b) Influence at 75, 100 and 125 minutes plastic shrinkage

Figure 5.18: Relationship between the dynamic yield stress, thixotropic index and the plastic shrinkage of the concrete mixes

It should be noted that the observed relationship was found to be only existent up to 110 minutes, depicted by the reduced R^2 of 0.98 at 100 minutes to 0.40 at 125 minutes for the dynamic yield stress and 0.89 to 0.6 respectively for thixotropy index in Figure 5.18b. This may be because only mixes C and CV had an indicative end of self-settlement around 95 minutes (see Section 5.5.3) showing the interwoven influence of the particles' settlement. This shows that the plastic phase is dominantly a gravitational shearing period and influences the shrinkage. The extent of plastic shrinkage can, therefore, be estimated up to the perceived time of end of self-settlement. Because concrete is not an isotropic material and from the settlement results in Figure 5.17, it can be reasoned that the more difficult the concrete shrinks vertically (plastic settlement), the easier it is to shrink horizontally (plastic shrinkage). This suggests a 3-dimensional anisotropic volume change (Fossen, 2010) as also observed by (Liu *et al.*, 2012).

Figure 5.19 shows a direct relationship between the rheo-physical parameters and capillary pressure rate (as also suggested by the correlation coefficients in Table 5.4) and quadratic functions best defines the relationship. The rate at the early stage (Stage 1) of the pressure build-up which is dominated by self-settlement has a good relationship with the early dynamic yield stress and thixotropic index while lesser relationship exists at later stages. This is evident in the R^2 on the figure, the insignificant correlation in Table 5.4 and the large residual sum of squares (RSS) shown inTable 5.6 for Stages 2 and 3. Similar to the shrinkage, the less the initial dynamic yield stress/thixotropic index, the less the capillary pressure build-up rate. Moreover, the rate of negative capillary pressure build-up in the concrete pores is responsible for the observed shrinkage (Combrinck and Boshoff, 2013; Slowik *et al.*, 2008).

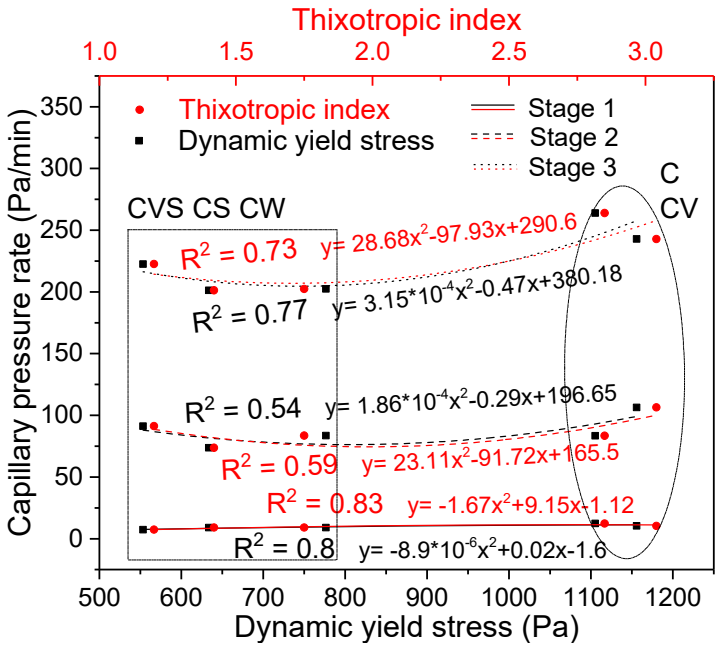

Figure 5.19: Relationship between the dynamic yield stress/thixotropy index and capillary pressure rate

Plastic settlement and shrinkage are known to continue until concrete's structuration/stiffening from thixotropy or hydration are adequate to resist them (Leemann *et al.*, 2014). Figure 5.20 represents the observed relationship between these indirect stiffening indicators of the concrete (plastic settlement/shrinkage end times) and its flow/fluid properties (static yield stress and slump values). The static yield stress indicates the required shear stress to break the structure and initiate the flow of the concrete while the slump simply indicates its workability, hence flowability. From Figure 5.19, the higher the ability for the concrete to flow easily, the more the time required for the settlement and shrinkage to end. This relationship reveals that, for the purpose of plastic cracking behaviour, the static yield stress/slump may be used as an indicator for the potential stiffening of the concrete. This is because the concrete mixes (C, CV, CS and CW) had similar initial and final setting times except for CVS with delayed setting time, and yet their plastic settlement and shrinkage end times varied based on their fluidity.

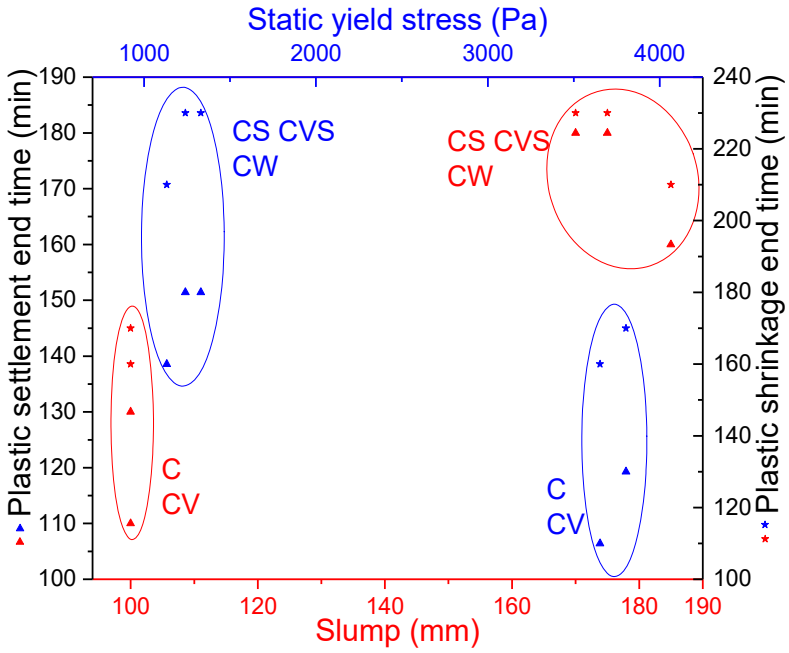

Figure 5.20: Relationship between the concrete's flow properties and settlement/shrinkage end time

From all these established links, simple rheological test such as torque decay (Figure 5.5) can be performed on a plastic concrete to predict the concrete's expected degree of plastic settlement, plastic shrinkage, and capillary pressure rate during the self-settlement period. Also, the duration of plastic settlement/shrinkage can be predicted from these simple rheological tests.

5.5.4.2. Relationship between the evolving rheo-physical parameters and plastic cracking processes

Based on the background discussed in Section 5.3, the relationship between the developing rheological parameters of the concrete (including that of the suspending fluid) with time and the plastic cracking process are examined in this section. Figure 5.21 shows that the increasing static yield stress due to thixotropy influences the measured plastic settlement. Similar to the relationship with dynamic yield stress in the previous section, the influence is insignificant below 30 minutes when the concrete recovers from the vibration. The inverse relationship and its increasing slope with time (rate of influence) reveal that the more or quicker the concrete builds up its yield stress, the less the affinity for plastic settlement. This implies that a higher rate of thixotropy will lead to a lesser plastic settlement, this combined with other properties such as viscoelasticity in restrained conditions may lead to a lesser propensity for plastic settlement cracking. Figure 5.22 shows a direct influence of the increasing yield stress on the plastic shrinkage above 50 minutes up to about 120 minutes. The increasing yield stress (from the direct relationship) and quicker thixotropy (from the

increasing slope with time) can increase the propensity for plastic shrinkage. However, the magnitude of the slopes suggests that the influence of the rheological parameters is more pronounced on the plastic settlement.

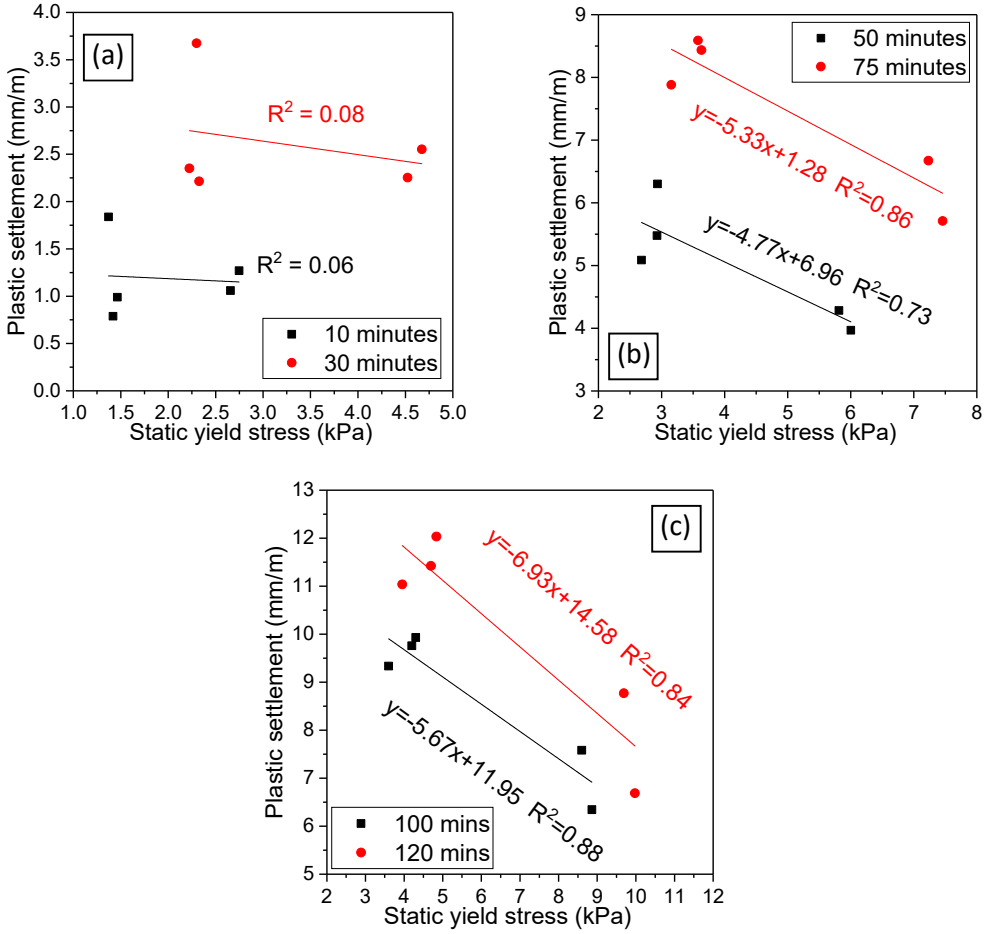

Figure 5.21: Relationship between the increasing static yield stress and plastic settlement

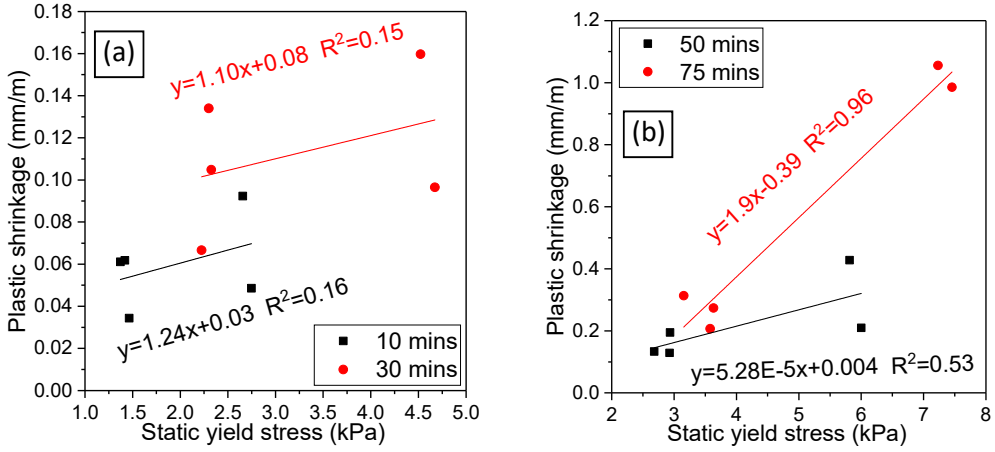

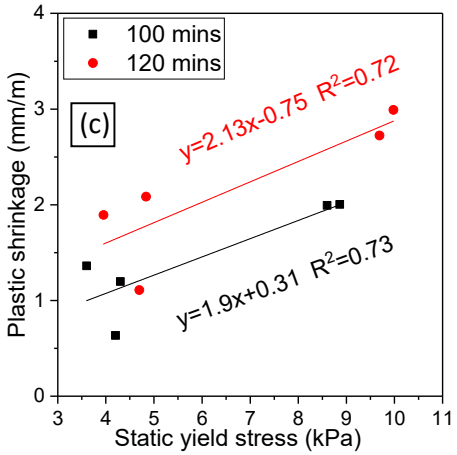

Figure 5.22: Relationship between the increasing static yield stress and plastic shrinkage

Figure 5.23 shows the relationship between the structuration rate (of the concrete and the suspending mortar) and the capillary pressure rate. Similar to the dynamic yield stress, the influence of the build-up rate of thixotropy (A_{thix}) is fairly significant on the capillary pressure before the rapid rise in capillary pressure (Stage 1) and the later Stage 3. It should be noted that the rate of rigidification (storage modulus – G_{rigid}) of the concrete and that of the suspending mortar is insignificant on the capillary build-up rate. Generally, the rigidification of both the concrete and suspending mortar showed little or no links with the plastic cracking process, as shown later in Figure 5.24 and Figure 5.25. Some relationship was only found between the plastic settlement and rigidification of the concrete at later times (close to initial setting time) as seen in Figure 5.24b. That is, the converging aggregate packing fraction with time due to plastic settlement can inadvertently lead to improved rigidification. Such converging aggregate fraction increases frictional contacts and interlock among coarse particles that can reflect in the rheo-physical properties (Mehdipour and Khayat, 2018) such as storage modulus.

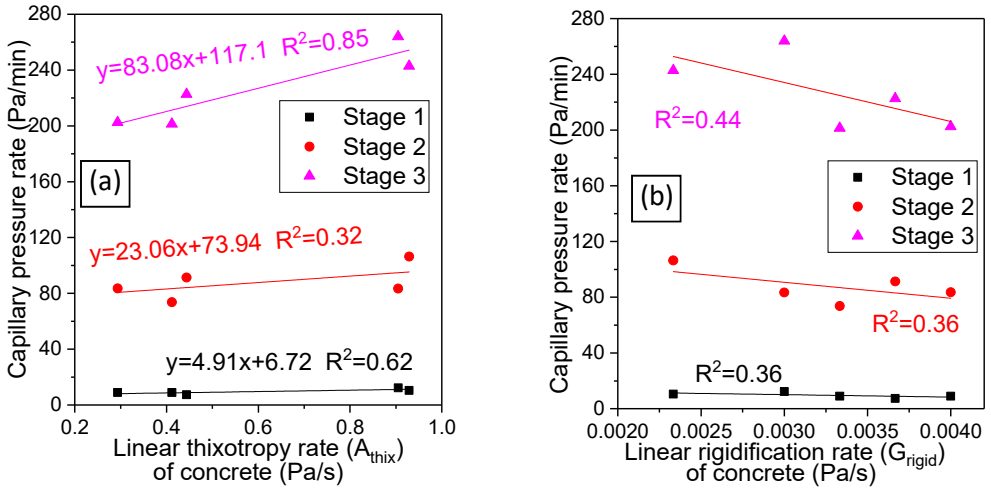

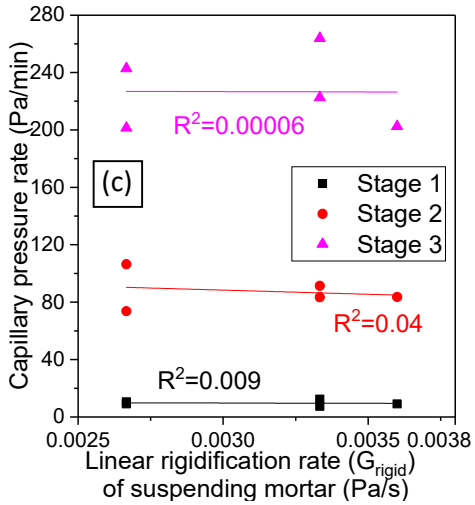

Figure 5.23: Relationship between the rate of structuration (concrete and mortar) and rate of capillary pressure

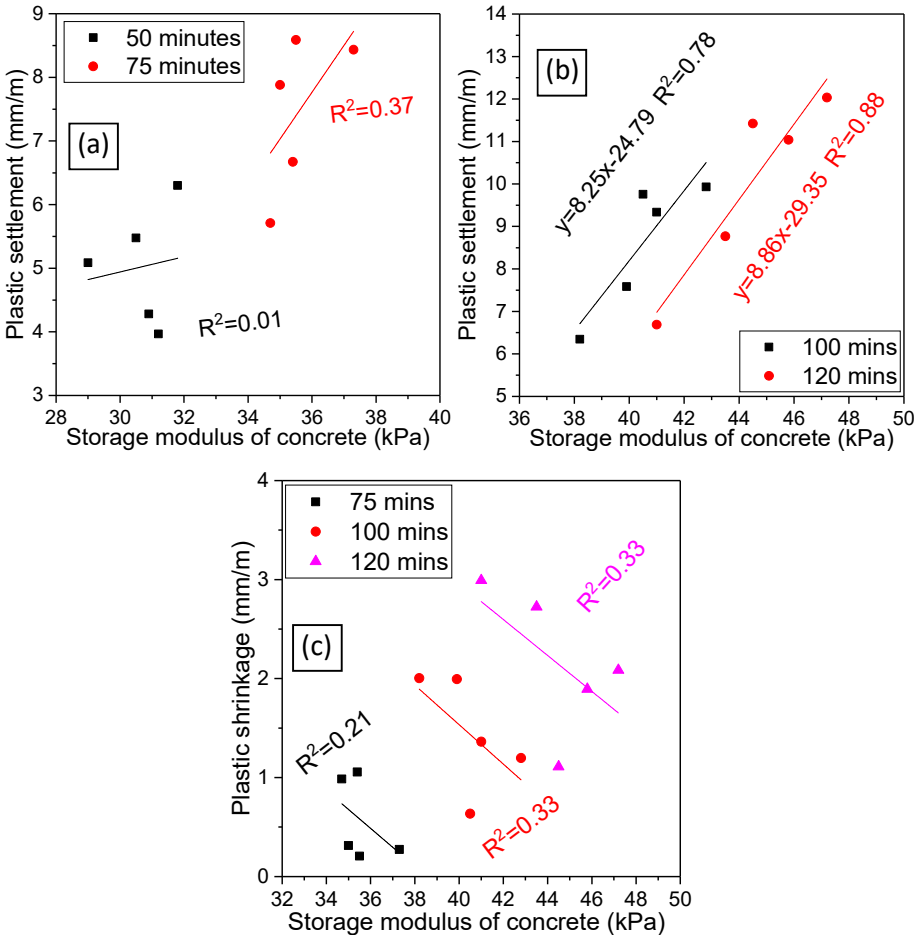

Figure 5.24: Relationship between the increasing storage modulus and plastic settlement and shrinkage

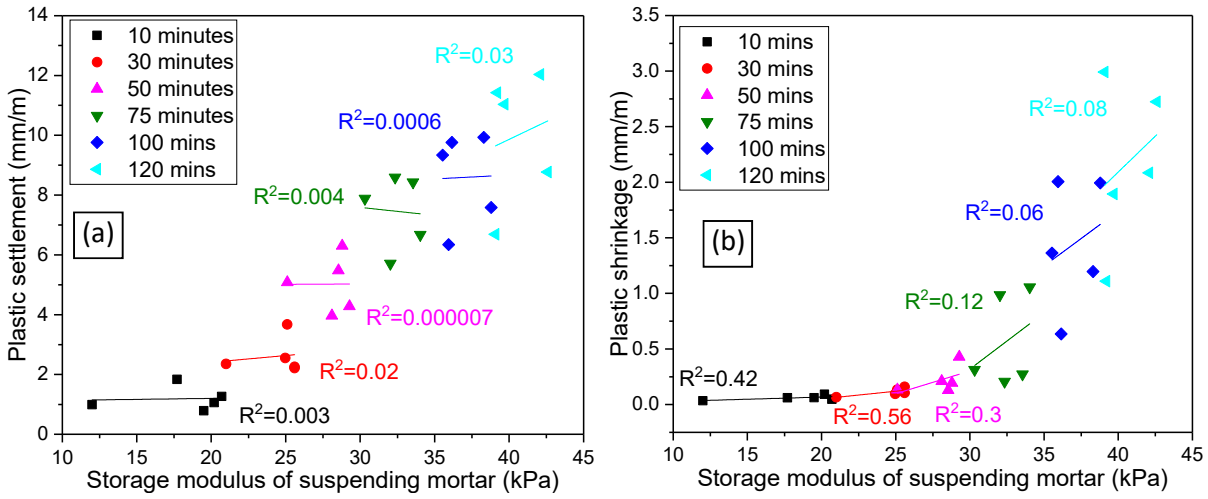

Figure 5.25: Relationship between the increasing storage modulus of the suspending mortar and plastic settlement and shrinkage respectively

5.6. Conclusions

The study sets out to investigate the possible links between plastic cracking behaviour of concrete and its rheo-physical properties as a step towards establishing the influence of rheology on plastic cracking behaviour of concrete. To achieve this, plastic cracking behaviour of rheologically modified concrete mixes were investigated and thereafter linked to the parameters of shear rheometry of the same concrete mixes. The observed links revealed that the plastic phase of plastic cracking behaviour subjected to self-settlement is majorly a shear phenomenon influenced by rheology and is characterisable by shear rheometry. The observed interdependence may only be valid up to the initial setting time. The following significant conclusions can be made:

- Self-settlement and evaporation are major contributors in plastic cracking behaviour. The vibration of concrete can potentially reduce the resistance of concrete to plastic settlement and jump-start self-settlement as a form of induced gravitational-shearing process. Three stages/indicators signify major changes in plastic cracking behaviour of concrete and can be earmarked from the plastic cracking behaviour plot. The first indicator is a concurrent rapid rise in capillary pressure and shrinkage with a plot kink in the settlement. The indicator for the second stage is a kink plot in shrinkage and change in the rate of the capillary pressure with a change in slope of the settlement plot while the third indicator marks the end of the settlement, shrinkage.
- The rheology modifiers increased the plastic settlement while delaying the start of the capillary pressure and shrinkage build-up by retaining the pore water. The modifiers also impacted the response of concrete to the indicators signifying changes in plastic cracking

behaviour. Inclusion of both viscosity modifying agent (VMA) and superplasticiser in concrete can reduce its potential for plastic cracking significantly while the inclusion of only VMA can increase the plastic cracking.

- Permeability properties of plastic concrete influences the extent of plastic settlement during the early period (about 30 minutes) characterised by constant bleeding rate while the plastic settlement afterwards is inversely influenced by the initial yield stress and thixotropic index.
- The early period of rapid plastic shrinkage (for about 40 minutes) is directly related to the initial yield stress and thixotropic index, revealing a 3-dimensional anisotropic volume change process. Like the plastic shrinkage, the negative capillary pressure rate was directly influenced for a similar period. The observed links for the plastic shrinkage and capillary pressure rate were mainly valid for the self-settlement (gravitational shearing) period, which indicated that the period is influenced by rheology.
- For the purpose of plastic cracking behaviour, the static yield stress and slump can be used as an indicator for the potential stiffening of concrete against settlement and shrinkage.
- By conducting a simple rotational shear rheology test such as torque decay during concrete's plastic state (such as within 30 minutes of concrete's end of mixing), the tendency for plastic settlement, plastic shrinkage, capillary pressure rate, and plastic settlement/shrinkage end times can be known.
- The higher the static yield stress of concrete and the more its evolution (thixotropy), the lesser the plastic settlement experienced, but the more the potential for plastic shrinkage and pressure build-up.
- The rigidification (storage modulus) of concrete and its suspending mortar has no significant influence on the plastic cracking processes. The plastic settlement can, however, improve the rigidification towards the initial setting time.

Chapter 6: Shear rheo-viscoelasticity approach to plastic cracking of concrete: experiments and model

This chapter has been submitted as a journal paper to the Cement and Concrete Research, Elsevier BV, with impact factor 5.618. Details of the paper are below:

Kolawole, J.T., Combrinck, R. & Boshoff, W.P. (2019). Shear rheo-viscoelasticity of plastic cracking of concrete: experiments and model. Submitted to Cement and Concrete Research.

Declaration by the candidate:

With regard to Chapter 6, the nature and scope of my contribution were as follows:

Nature of contribution	Extent of contribution (%)
This paper/chapter is part of the candidate's PhD research. All experimental work, the analysis, interpretation and presentation of data, as well as the writing of the manuscript were conducted by the candidate.	90%

The following co-authors have contributed to Chapter 6:

Nature of contribution	E-mail address	Nature of contribution	Extent of contribution (%)
Dr Riaan Combrinck	rcom@sun.ac.za	PhD research supervision, proofreading manuscript and insightful amendments	5%
Prof William Peter Boshoff	billy.boshoff@up.ac.za	PhD research supervision, proofreading manuscript and insightful amendments	5%

Signature of candidate: .....

Date: 8 October 2019

Declaration by co-authors:

The undersigned hereby confirm that

The declaration above accurately reflects the nature and extent of the contributions of:

1. The candidate and the co-authors to Chapter 6,
2. No other authors contributed to Chapter 6 besides those specified above, and
3. Potential conflicts of interest have been revealed to all interested parties and that the necessary arrangements have been made to use the material in Chapter 6 of this dissertation.

Signature of co-authors	Institutional affiliation	Date
	Department of Civil Engineering, Stellenbosch University	8 October 2019
	Department of Civil Engineering, University of Pretoria	8 October 2019

6.1. Abstract

The early or self-settlement phase of plastic cracking is majorly shear dominated and can be characterised by shear rheometry. This phase has pronounced viscoelastic behaviour that can potentially influence the observed plastic cracking of concrete. Furthermore, this phase is susceptible to microstructural damage/cracking that can be rapidly propagated by the later occurring plastic shrinkage. These are currently not identified in the available literature. Hence, this study experimentally determined the material properties and behaviour of rheologically modified concrete mixes and their plastic cracking. Von-Mises and Hencky, and Bresler-Pister theories were then used as failure criteria with hypothetically fully restrained plastic strain/stress analyses to model the occurrence of plastic cracking. Shear rheometry was used to determine the material properties. Incorporated rheology modifiers influenced the shear properties, viscoelastic abilities and plastic cracking of the concrete. The predictions of the model revealed that the plastic settlement is indeed mainly shear-related, the viscoelastic behaviour influences plastic cracking, and microcracking/damage can truly occur during the self-settlement period of plastic cracking behaviour. It was also concluded that plastic concrete damage tends to be strain-oriented with pressure-insensitive form of ductile failure.

6.2. Introduction

The term “plastic cracking” originates from the plastic state of concrete during its early hours, the early hours refers to the time between mixing and around the final set (Combrinck *et al.*, 2018a; Sant, Dehadrai, Bentz and Weiss, 2009). Concrete during this stage is referred to as plastic concrete because it can easily be shaped or moulded due to its fluid nature. Studying this phase of concrete is important because deficiencies at this early age can impair the finished product in terms of its serviceability and durability (Combrinck *et al.*, 2018a; Ghourchian *et al.*, 2018; Leemann *et al.*, 2014). Plastic cracking in concrete can come from two major sources of restrained strains, plastic settlement and shrinkage (Combrinck *et al.*, 2018a; Ghourchian *et al.*, 2018; Lura *et al.*, 2007). The plastic settlement has an initial period of gravitational induced “self-settlement” due to coarse particle settling (Kolawole *et al.*, 2019c).

Due to hydration, the rheological properties of freshly cast concrete transits gradually from a plastic phase with rheo-viscoelastic properties to a semi-plastic phase and later to a solid phase with dominant elastic properties (Kolawole *et al.*, 2019c). Concrete properties and responses to strains and stresses changes within this short period due to decreasing viscoelasticity and increasing hydration. Viscoelasticity is the property of materials that portray both viscous and elastic properties, when undergoing deformation, such material exhibits a rate-dependent strain by dissipating energy during loading and unloading (Sun *et al.*, 2006) as shown in Figure 6.1. Plastic settlement and shrinkage strains that lead to plastic cracking occur within this period of concrete until it gains enough strength to resist the plastic cracking. Hence, viscoelasticity has a role to play. Dynamic shear rheometry as a method of applying a controlled small amplitude oscillatory shear (SAOS) strain or stress (within the linear viscoelastic range - LVR) can be used to characterise the viscoelastic properties of plastic materials such as plastic concrete and differentiate between the elastic and viscous components (Choi *et al.*, 2016; Mezger, 2014; Roussel, 2012; Hyun *et al.*, 2011; Mernard, 1999; Banfill, 1991).

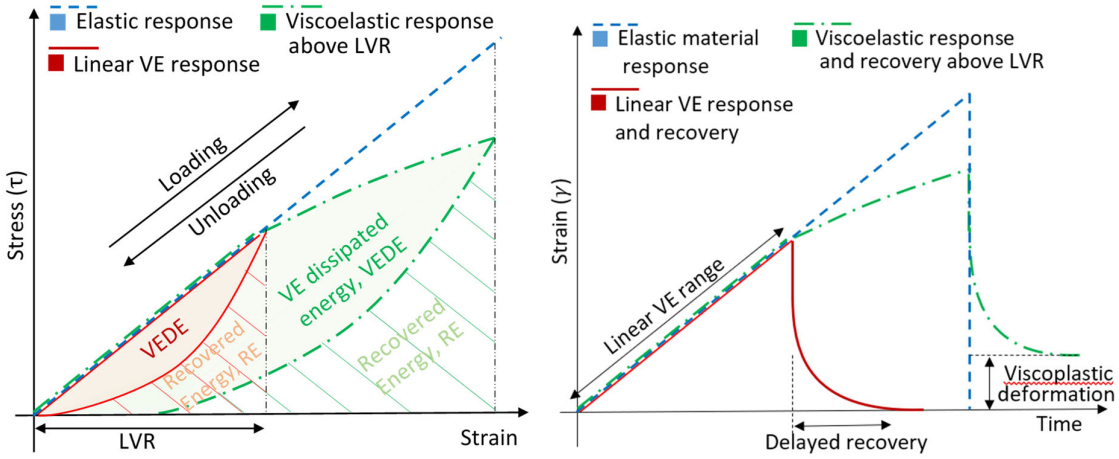

Figure 6.1: Typical response of viscoelastic material to loading and unloading

From some of the results of this study and previous studies of (Combrinck and Boshoff, 2019; Kolawole *et al.*, 2019c; Khan, 2018), Figure 6.2 shows the plastic-related properties of two concrete mixes. The phase transition of the concrete can be tied to these properties (tensile, shear and setting times). During the plastic phase (before initial setting time), there is no substantial development of the tensile strength/modulus but more of shear stregth/modulus, and plastic settlement strains dominate this phase. A companion study (Kolawole *et al.*, 2019c) established that this phase is majorly dominated by a slowly-occuring gravitational shearing process due to self-settlement of the particles. After the initial setting time, the concrete's solidification increases rapidly, turning into a semi-plastic material with some development of tensile properties that can potentially resist restrained tensile shrinkage dominating this period (Figure 6.2). Hence, it becomes characterisable by seemingly difficult tensile/extensional tensile testing. However, the application of a mechanical tensile test known for solid materials on a semi-plastic material is still questionable (Combrinck and Boshoff, 2019) and is highly susceptible to artefacts (Nguyen *et al.*, 2017) making some studies such as (Ghourchian *et al.*, 2019) circumvent such tests. Few published studies that have attempted to determine these tensile properties of semi-plastic concrete and acknowledged its link to plastic cracking includes Combrinck and Boshoff, (2019), Nguyen *et al.*, (2017), Roziere *et al.*, (2015), Dao *et al.*, (2009).

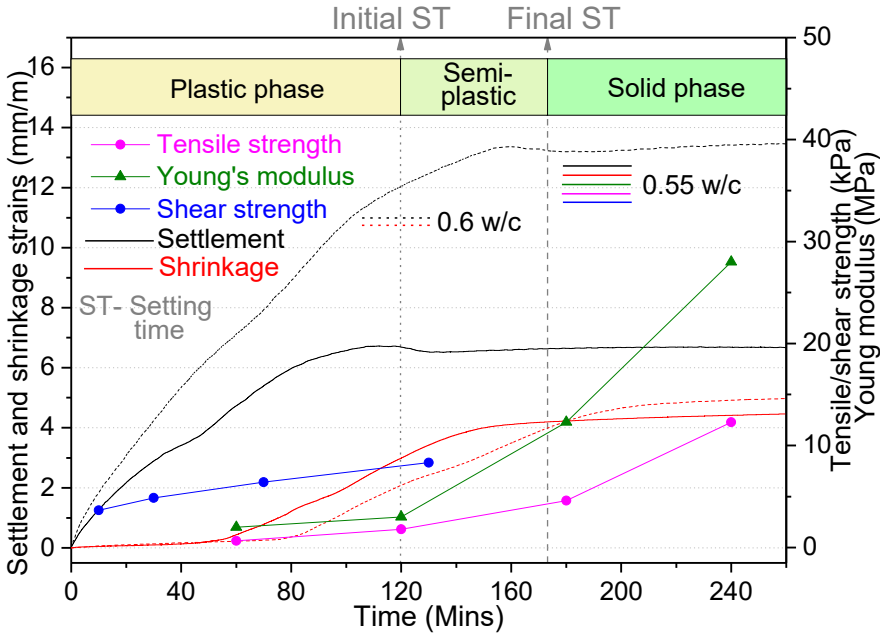

Figure 6.2: Plastic and semi-plastic phase of concrete dominated by settlement and shrinkage (compiled from this study and (Combrinck and Boshoff, 2019; Kolawole *et al.*, 2019c; Khan, 2018))

The earlier occuring restrained settlement can potentially induce shear microcracks that can be easily propagated by later occuring restrained tensile shrinkage (this is explained further in Section 6.4.1). Hence, understanding and avoiding these potential microcracks is significantly important to the serviceability design of concrete (Ghourchian *et al.*, 2019). Therefore, the plastic phase up to the initial setting time which is majorly settlement and shear-related is the focus of this study, the later phases are out of the scope of the study.

For the purpose of this study, shear rheometry was used as a tool to characterise the plastic phase of concrete in order to determine its resistant shear properties to plastic cracking which is scarce in the literature. Furthermore, there is scarcity of literature on the influence of plastic concrete's viscoelastic behaviour on its cracking, hence, dynamic shear rheometry was explored as a tool to characterise the viscoelasticity. The plastic settlement and shrinkage strains of the same concrete mixes are also investigated, and is reported in a companion paper of Kolawole *et al.* (2019c). With these, coupled with some of the rotational rheometry results of another companion study (Kolawole *et al.*, 2019a), the possible damage/microcracking during the rheo-dominant phase of the plastic concrete was modelled and compared to the plastic cracking results of the mixes. The concrete mixes contain rheology admixtures to modify their rheo-related properties. Currently available models on plastic cracking, as succinctly itemised in the state-of-the-art reviews by (Kayondo *et al.*, 2019; Safiuddin *et al.*, 2018), do not consider the roles of viscoelastic properties of plastic concrete on its cracking.

6.3. Background to the role of rheo-viscoelastic behaviour

The difficulty of measuring the viscoelastic (VE) properties of a concrete that is fluid and plastic, and also varies with time (due to hydration) is a major reason for the lack of literature identified in the previous paragraph. This fluid and plastic state of concrete makes shear rheometry a suitable technique to measure the VE properties. However, most of the currently available instruments and technologies on VE properties are limited to finer materials such as polymers and cement paste due to their classical geometry. Anton-Paar's special building material cell (BMC 90) was used with a Physica MCR501 rheometer for the dynamic rheometry test (Anton-Paar, 2009, 2012, 2016). Some shear properties of particular interest (such as yield strain, shear modulus, 1 and 2-hour yield stress, and concurrent normal stress) were also obtained with the MCR501 rheometer. Other shear resistance properties (such as peak and residual yield stress and thixotropy) of the fresh/plastic concrete mixes for this study were investigated using the ICAR rheometer (Germann Instruments A/S, 2015; Koehler and Fowler, 2004) and the detailed results reported in (Kolawole *et al.*, 2019a). More details about the test and BMC 90, including challenges and justification for its use, can be found in the companion paper (Kolawole *et al.*, 2019b).

To be able to use the BMC, a nominal coarse aggregate size of 6 mm was used, however, during trial tests (using the plastic cracking mix in Table 6.2) it was necessary to reduce the stone content of the mix due to coarse aggregate packing which made free descent of the modular vane into the cup difficult. The stone content in the mix was therefore reduced gradually, yielding a reduction of 60% in stone content. Reducing the stone content reduces the concrete's density and was found not to negatively influence the variability of the rheological behaviour between the mixes. This was confirmed with trial results such as yield stresses obtained using the ICAR rheometer on similar reduced stone content mixes and compared to that of the MCR501 as shown in Figure 6.3. This helps in evaluating equivalent shear and rheo-viscoelastic properties of the normal plastic cracking mixes (that is, 100% stone content). Attempts were made to examine the evolution of these properties with time up to a maximum of 2 hours which is the initial setting time of the concrete mixes.

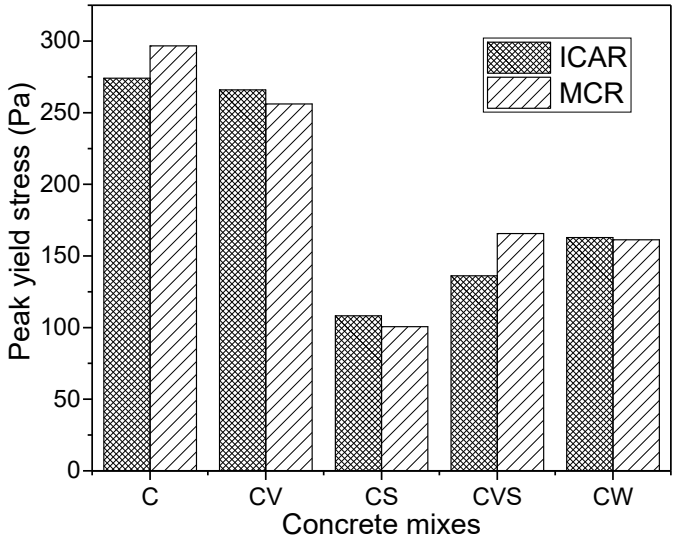

Figure 6.3: Relationship between results of ICAR and MCR501 rheometers

When a controlled strain is applied to a VE material (such as in an amplitude sweep test), there is a phase lag (δ) between the observed stress and applied strain, yielding rheo-viscoelastic properties such as complex shear modulus (G^*), shear storage modulus (G'), and shear loss modulus (G'') related as shown below (He *et al.*, 2018b; Qian and Kawashima, 2016; Mezger, 2014; Schultz and Struble, 1993).

$$G^* = \frac{\tau}{\gamma} = G' + iG'' = |G^*|\cos\delta + i|G^*|\sin\delta = \sqrt{|G'|^2 + |G''|^2}, \quad \tan\delta = \frac{G''}{G'} \qquad \text{Equation 6.1}$$

δ is the phase lag between the shear strain and stress, $i^2 = -1$.

The shear storage modulus (G') indicates the elastic portion or stored energy of the material which helps in shape recovery from the deformation while the shear loss modulus (G") indicates the viscous portion or lost energy which is responsible for permanent deformaton (He *et al.*, 2018a; Yuan, Lu, *et al.*, 2017; Mezger, 2014; Nehdi and Al Martini, 2009; Sun *et al.*, 2006; Nachbaur *et al.*, 2001; Isacsson and Zeng, 1998; Saasen *et al.*, 1991).

Another viscoelastic characterisation approach is the rheological creep and creep recovery test (Mezger, 2014; Banfill, 1991) that is similar to Figure 6.4, the recovered portion represents the elastic/stored portion of the deformation energy while the disspated portion indicates the viscous/lost portion of the deformation energy. It shows how much of the induced strain is dissipated. The values can be expressed as compliance (J) which is independent of the applied stress:

$$J(t) = \frac{\gamma(t)}{\tau_0} \qquad \text{Equation 6.2}$$

Rheological relaxation tests can also be used to characterise the viscoelastic ability of concrete to relax/dissipate stresses (Figure 6.5) (Mezger, 2014; Banfill, 1991). It can also be expressed as relaxation modulus to become a material intrinsic value independent of strain value:

$$G(t) = \frac{\tau(t)}{\gamma_0}$$ Equation 6.3

These theories and tests are mainly valid for small amplitude shear (Kim *et al.*, 2018; Yuan, Lu, *et al.*, 2017; Mezger, 2014; Roussel, 2012; Hyun *et al.*, 2011; Nehdi and Al Martini, 2009; Nachbaur *et al.*, 2001; Mernard, 1999), similar in value to the small deformations and strains associated with plastic cracking, especially in the shear-related self-settlement period which is the focus of this study. For example, the plastic settlement for this study occurred at a peak rate of 0.0146%/s with a maximum strain of 1.4% (Kolawole *et al.*, 2019c).

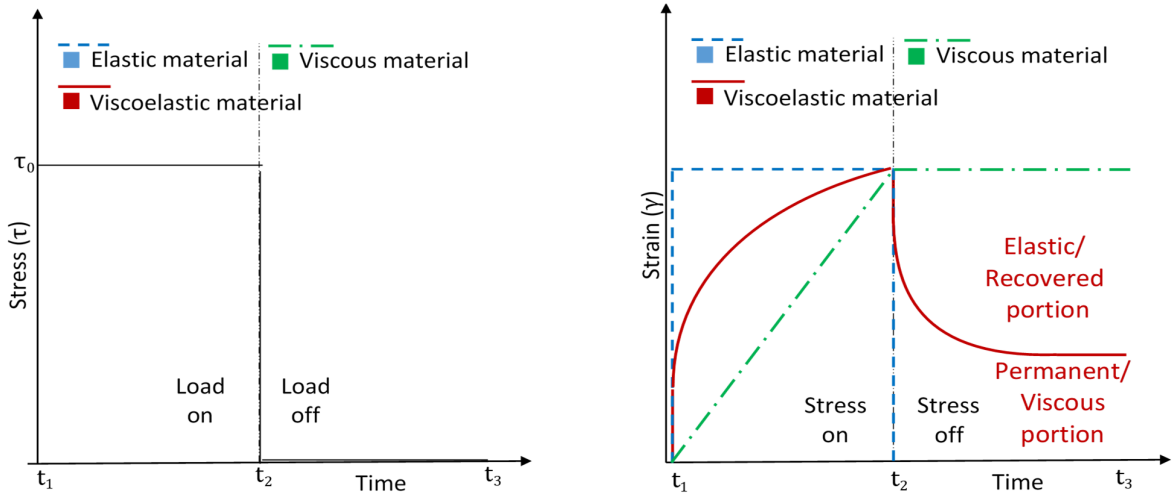

Figure 6.4: Creep and creep recovery test and viscoelastic response

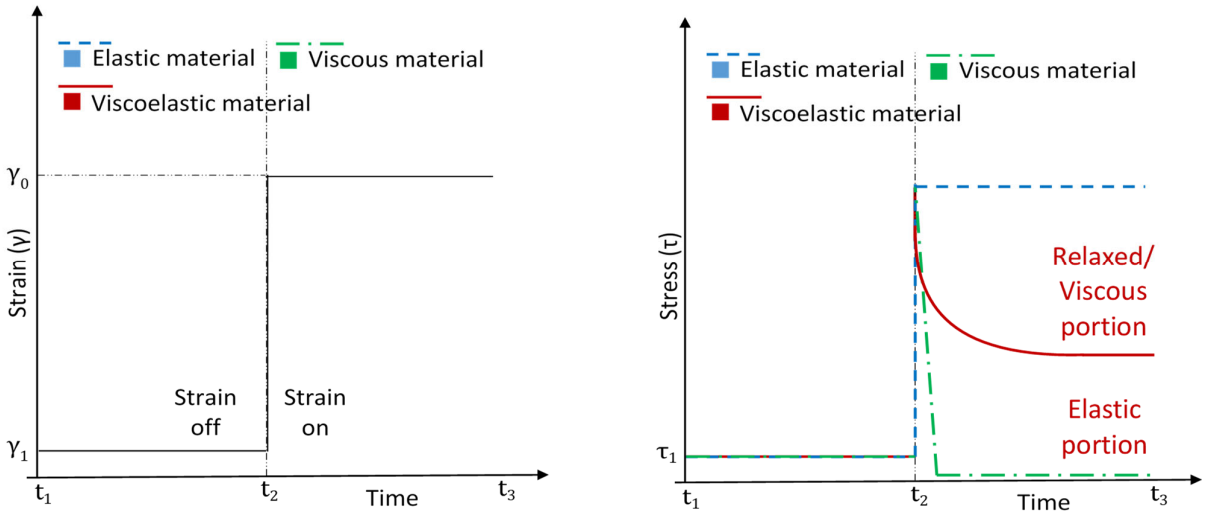

Figure 6.5: Stress relaxation test and viscoelastic response

The viscous dissipation (also known as damping) by the plastic concrete is due to the viscous drag of the suspending fluid (liquid phase) on the concrete particles (Roussel *et al.*, 2012), for example, a form of frictional resistance on the particles due to gravitational settlement.

The stiffness (shear modulus or modulus of rigidity) of plastic concrete to restrained small shear settlement deformations can be dampened due to the viscous portion of the viscoelasticity. This can be expressed as a damping factor as shown in Table 6.1. The strains from the plastic cracking behaviour of concrete may also be dampened/dissipated due to the viscoelastic response of the concrete in its plastic state. This dissipation can be obtained from the creep and creep recovery test and expressed as the damping factor in Table 6.1. Typically, such dissipation of strains can allow plastic materials to absorb considerable energy by plastic deformation (ductility) before damage (Kinloch and Young, 1995). In case of restrained plastic concrete, the undissipated strains may be referred to as the true cracking strains and expressed as damage factor, the sum of the damage factor and damping factor being one. Furthermore, the induced stresses from the plastic cracking behaviour may also be relieved due to the viscoelastic response of the plastic concrete (stress relaxation). The degree of relaxation (damping or relaxation factor) of the stress can be obtained from the stress relaxation test (Table 6.1). The above constitutes the roles of the rheo-viscoelastic behaviour of concrete in its plastic cracking behaviour and its proposed implementation for this study.

Table 6.1: Damping factors for modulus of rigidity, restrained strain and stress in plastic cracking behaviour

Test	Variable $f(x)$	Maximum value	Viscous portion	Elastic portion	Damping factor	Application
Amplitude sweep	Complex Shear modulus (G^*(strain))	G^*	G''	G'	$\left(\frac{G''}{G^*}\right)^2$	Modulus of rigidity
Creep and creep recovery	Creep Compliance (J(time))	$J_m(t_2)$	$J_v(t_3)$	$J_m - J_v$	$\frac{J_v}{J_m}$	Strain
Stress relaxation	Relaxation Modulus (G(time))	$G_0(t_2)$	$G_0 - G_e$	$G_e(t_3)$	$\frac{G_0 - G_e}{G_0}$	Stress

6.4. Analytical methods and model description

Available early age cracking-related models in literature are mostly focused on the later semi-plastic-to-solid phase of concrete with less attention to the potential damage/cracking due to the concrete's self-settlement (Kayondo *et al.*, 2019; Safiuddin *et al.*, 2018). As also noted earlier, these current models do not consider the roles of viscoelasticity of concrete in plastic cracking of concrete. For example, in the recent poromechanics model of plastic cracking by (Ghourchian *et al.*, 2019), the cummulative strain/stress during the plastic state of cement mortar were supposedly added as initial values at drying stage without considering the potential damage to the concrete due to shear yielding (that is, plastic settlement phase) before the start of the semi-plastic phase. Likewise, this poromechanics model does not examine the influence of viscoelasticity. This study intends to evaluate this potential damage/cracking that can be rapidly propagated by the plastic shrinkage by focusing on the shear dominated plastic settlement phase of plastic cracking. That is, the possible damage from the end of mixing up to the initial setting time of the concrete (about 120 minutes for this study). Furthermore, the roles of rheo-viscoelasticity during this period is considered in the model.

The rheo-viscoelastic behaviour is implemented in two ways (see Section 6.4.2), viz, on the free strain based on its viscous dissipation and on the free stress based on the stress relaxation to evaluate the cracking strain and stress respectively, assuming full restraint. Two failure criteria (Von-Mises and Hencky theory and Herschel-Pister theory) were used to predict the occurrence of shear-induced micro-cracking during the plastic phase. The model, therefore, intends to evaluate the susceptibility of concrete mixes to early shear-induced plastic cracking. All material properties were from shear rheometry, and this with the measured plastic settlement and shrinkage were the input for the analytical model.

6.4.1. Interaction between settlement and shrinkage in modelling plastic concrete

It should be noted that plastic settlement tends to lead to susceptible shear hairline and micro-cracks (Figure 6.6a) that are not readily visible because they occur within the concrete and the fluid nature of concrete during this plastic phase tends to fill and hide the cracks. Ideally, the former weak spots or micro-cracks due to differential settlement (Lin and Huang, 2010) are rapidly propagated and amplified by restrained shrinkage. However, the boundary between the two forms of cracking becomes fast-occuring, undistinguishable and overlapping (Combrinck *et al.*, 2018b,a). To emphasize these points, Figure 6.6 and Figure 6.7 show the forms of plastic settlement and shrinkage cracking obtained by (Combrinck *et al.*, 2018a) due to conscious effort to separate and understand

the two. Figure 6.6b-d are under pure settlement strains only, Figure 6.6e was due to pure plastic shrinkage strains only while Figure 6.6f was due to both plastic settlement and shrinkage. Figure 6.6b showed that the plastic settlement cracks were hidden and filled with fluid as at initial setting time while the shear cracks only became visible at final setting time (Figure 6.6c). On the other hand, cracks from pure shrinkage (Figure 6.6e) and combined settlement and shrinkage strains (Figure 6.6f) were already visible and large enough as at the initial setting time. Figure 6.7 shows the obtained crack widths due to restrained plastic shrinkage without and with differential settlement (induced by steel bar) buttressing the earlier statement that settlement cracks precedes and are rapidly amplified by plastic shrinkage. Some studies have suggested re-vibration to close up very early plastic (settlement) cracks (Combrinck *et al.*, 2018b; Aldalinsi *et al.*, 2014), but this may become impracticable in large bodies of concrete and due to practical implications such as surface finishing, dynamic stability, slip casting etc. Completely avoiding these cracks is a better solution.

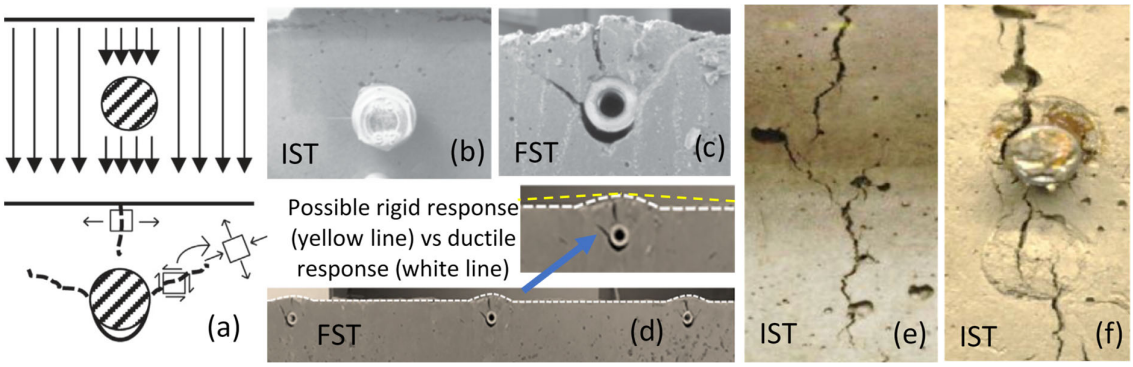

Figure 6.6: Forms and stages of plastic settlement and shrinkage cracks (Combrinck *et al.*, 2018a) (a) differential settlement and shear stress condition around the restraint (b) Pure settlement crack at initial setting time (IST) (c) Pure settlement crack at final setting time (FST) (d) flow response of the plastic concrete around the restraint (e) Pure shrinkage crack at initial setting time (IST) (f) Combined settlement and shrinkage crack at initial setting time (IST).

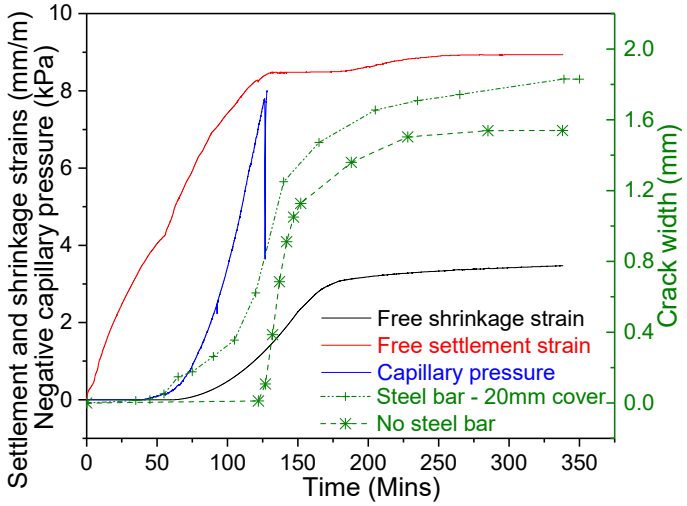

Figure 6.7: Influence of differential settlement on pure plastic shrinkage cracking (Combrinck *et al.*, 2018a)

6.4.2. Strain and stress analyses

Free or unrestrained plastic settlement and plastic shrinkage strains were measured for this study. More comprehensive details on the test methods, results and concrete mixes can be found in the companion paper (Kolawole *et al.*, 2019c). Ideally, certain percentages of these strains/stresses are responsible for cracking due to a degree of restraint (DOR) such as the (ASTM C1579, 2006) cracking mould used for this study (see Figure 6.14). The DOR have unique and complex variations in real life geometrical shapes and boundaries, even, along the body of the restrained concrete (Huang *et al.*, 2019; Knoppik-Wróbel and Klemczak, 2015). That is, parts of the concrete experiencing near 100% DOR has higher risks of cracking (Nilsson, 2003) which is crucial to serviceability limit state design of concrete structures (Ghourchian *et al.*, 2019; fib Model Code, 2010). Such potential local cracks or damage as shown in Figure 6.8 should therefore be completely avoided. Hence, full restraint was assumed for the study which allows for examining the susceptibility of any concrete mix to crack (depending on the environmental exposure) based on the mix's propensity for settlement and shrinkage.

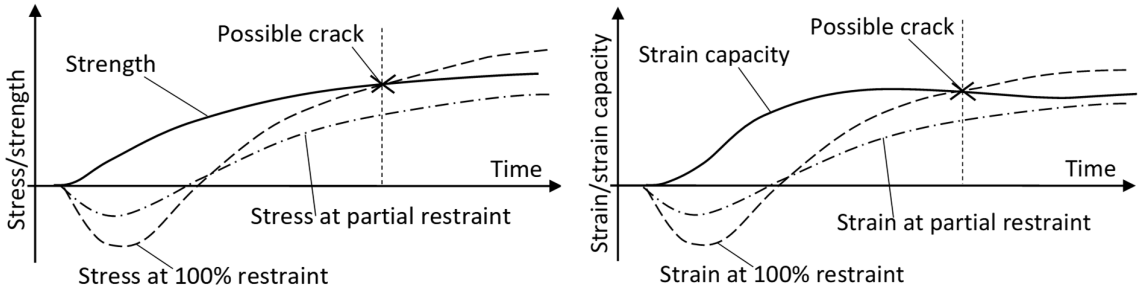

Figure 6.8: Cracking risk/potential in a concrete element at partial and full restraint (adapted from Nilsson, 2003)

Analytical analysis using plane strain/stress were in three cases based on the vital conclusion that the self-settlement phase is majorly shear-related (Kolawole *et al.*, 2019c). Comparisons were made between the three cases.

CASE I – A worst-case scenario or upper-limit, where the cracking strain/stress caused both shear and direct deformation of the concrete. The viscoelastic properties of the concrete mixes were incorporated in the analyses of the strain and stress of this case.

CASE II – A simple-case scenario or lower-limit, where the cracking strain/stress solely contributes to shear deformation of the concrete. The viscoelastic properties of the concrete mixes were also incorporated in this case.

CASE III – The first case with the viscoelastic properties of the concrete not included in the strain/stress analyses (as currently available in literature for existing models).

The stiffness (dynamic modulus) and the free strain/stress were evaluated from the rheometry test and cumulative unrestrained settlement and shrinkage strain/stress, respectively, based on

$$G = (1 - D_f^*)G^*; \quad \gamma_{xy} = \left(1 - D_f^s\right)\gamma_{xy}^t = D_f\gamma_{xy}^t; \quad \tau_{xy} = \left(1 - R_f\right)\tau_{xy}^t$$
$$E = (1 - D_f^*)E^*; \quad \varepsilon_x = \left(1 - D_f^s\right)\varepsilon_x^t = D_f\varepsilon_x^t; \quad \sigma_x = \left(1 - R_f\right)\sigma_x^t \qquad \text{Equation 6.4}$$
$$\varepsilon_y = \left(1 - D_f^s\right)\varepsilon_y^t = D_f\varepsilon_y^t; \quad \sigma_y = \left(1 - R_f\right)\sigma_y^t$$

γ_{xy}/τ_{xy} are the cracking shear strain/stress, $\gamma_{xy}^t/\tau_{xy}^t$ are the cumulative free shear strain/stress, ε_x/σ_x are the cracking shrinkage strain/stress, $\varepsilon_x^t/\sigma_x^t$ are the cumulative free shrinkage strain/stress, ε_y/σ_y are the cracking settlement strain/stress, $\varepsilon_y^t/\sigma_y^t$ are the cumulative free settlement strain/stress

D_f^* is the stiffness damping factor (Table 6.1), D_f^s is the strain damping factor, D_f is the damage factor, and R_f is the relaxation factor.

It should be noted that the damping factors for the stiffness of the concrete mixes were found to be very small and negligible (average of 0.0002 – Figure 6.16) and therefore, was neglected for the study.

The input fully restrained shear strains (e.g. arbitrary γ_{xy}) were, thereafter, evaluated based on the average concrete's cracking strains in the settlement/shrinkage moulds as shown in Figure 6.9 (assuming the full restraint shown in SECTION A-A). This is expressed in detail in the Appendix. The time-step shear stresses were estimated using the measured time-dependent shear modulus (G) and relation in Equation 6.5, the arbitrary time-step direct stresses and time-dependent elastic modulus (E) were estimated using Equation 6.6 and Equation 6.7 respectively (Hibbeler, 2014). The Poisson's ratio (v) was taken to be 1/3 (Ghourchian *et al.*, 2019) since it was a close approximation of the v obtained from the (1 and 2 hours age) G of this study and the (1 and 2 hours) E of similar concrete mixes obtained by the preceding study of (Khan, 2018).

$$\tau_{xy} = G\gamma_{xy} \qquad \text{Equation 6.5}$$

$$\varepsilon_x = \frac{1}{E}\left[\sigma_x - v(\sigma_y)\right] \qquad \text{Equation 6.6}$$
$$\varepsilon_y = \frac{1}{E}\left[\sigma_y - v(\sigma_x)\right]$$

$$E = 2G(1 + v) \qquad \text{Equation 6.7}$$

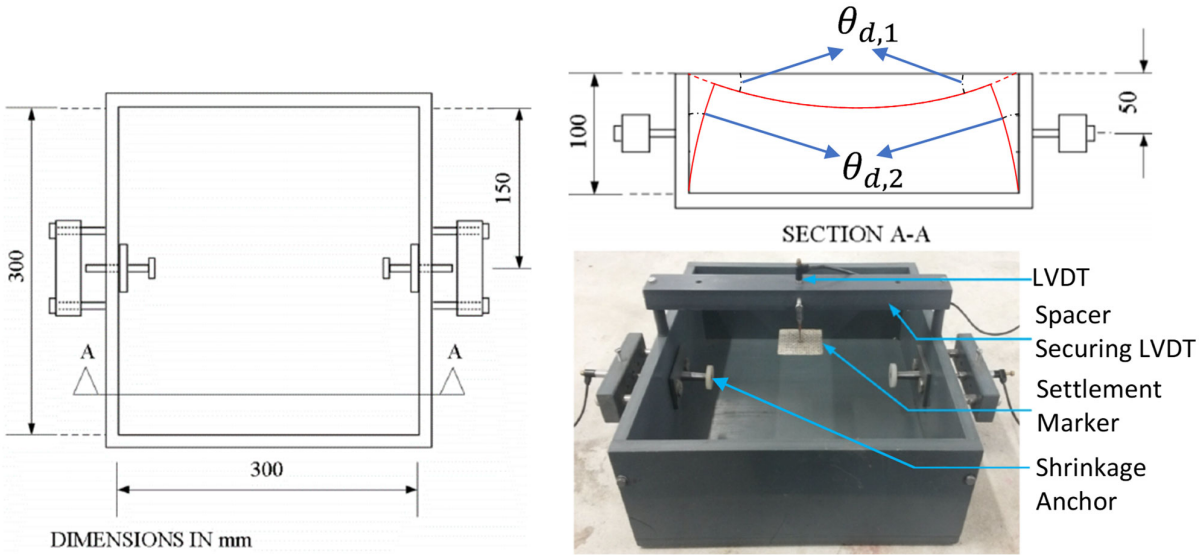

Figure 6.9: Settlement and shrinkage mould for estimating shear strains (θ_d), assuming full restraint

6.4.3. Failure criteria and yield parameters for the model

Concrete becomes increasingly brittle due to hydration as it surpasses its initial setting time. This brittleness is evident in the reducing strain capacity and creep potential reported in this study and those of (Combrinck and Boshoff, 2019; Nguyen *et al.*, 2017; Mehta and Burrows, 2001). In the earlier plastic phase, concrete is more ductile with restrained settlement tending to cause shear yielding as depicted in Figure 6.6d. The study by (Mettler *et al.*, 2016) also experimentally support the evidence that plastic concrete failure is characterised by ductile deformation with shear/slip plane that later transits to a brittle failure with age. As noted by (Hibbeler, 2014), the choice of failure criteria is not constant and should be based on the behaviour of the material at the time of consideration since a material can behave in a ductile or brittle manner depending on the conditions. These considerations resulted in the considered failure theories discussed in this section.

The total energy acting on a body due to certain stresses/strain has two components, the hydrostatic/dilatant component and deviatoric/distortional/shearing component. The former component leads to expansion or compression of the body while the latter leads to the yielding failure. Two failure criteria for crack initiation were examined for this study, Von-Mises and Hencky theory (vM-H) and Bresler-Pister theory (B-P). The vM-H theory is based on the principle that a material failure is solely dependent on the deviatoric energy component of the deformation (that is, yielding failure) while the B-P theory takes into account the influence of the hydrostatic energy component on the material's failure (that is, quasi-brittle failure).

6.4.3.1. Von Mises and Hencky theory

Both strain and stress were analysed for this theory and referred to as strain and stress paths, according to the vM-H theory (Hibbeler, 2014; Dede and Ayvaz, 2010; Jones, 2009),

$$U_d = \frac{1}{12G}\left[(\sigma_x - \sigma_y)^2 + (\sigma_y - \sigma_z)^2 + (\sigma_z - \sigma_x)^2 + 6\left(\tau_{xy}^2 + \tau_{xz}^2 + \tau_{yz}^2\right)\right] \quad \text{Equation 6.8}$$

U_d – deviatoric energy, G – shear modulus, $\sigma_{x/y/z}$ – arbitrary normal stress, $\tau_{xy/yz/xz}$ – arbitrary shear stress

Under simple yielding tests, the U_d can be expressed as,

$$U_d = \frac{1}{2}\frac{\tau_s^2}{G} \text{ for simple shear or } \frac{1}{6}\frac{\sigma_s^2}{G} \text{ for simple tension} \quad \text{Equation 6.9}$$

τ_s – shear strength, σ_s – tensile strength, γ_s – shear strain capacity

As noted earlier, simple tensile test during the fluid and plastic state of concrete is complicated and highly susceptible to significant artefact errors (Ghourchian *et al.*, 2019), hence, shear rheometry as a simple shear test serves as a suitable yield test and is used for this study. Moreover, the relation $\sigma_s = 2\tau_{max}$ (as often stipulated for solid elastic materials such as hardened concrete and used for failure criteria) was not obtained between those of this study and previous studies (see Figure 6.2).

Thefore, for failure to occur, the deviatoric energy of the stresses acting on the body must be equal or greater than that the body can accomodate. That is,

$$\frac{1}{12G}\left[(\sigma_x - \sigma_y)^2 + (\sigma_y - \sigma_z)^2 + (\sigma_z - \sigma_x)^2 + 6\left(\tau_{xy}^2 + \tau_{xz}^2 + \tau_{yz}^2\right)\right] \leq \frac{1}{2}\frac{\tau_s^2}{G} \quad \text{Equation 6.10}$$

$$\sqrt{\frac{1}{6}\left[\left(\sigma_x - \sigma_y\right)^2 + \left(\sigma_y - \sigma_z\right)^2 + (\sigma_z - \sigma_x)^2 + 6\left(\tau_{xy}^2 + \tau_{xz}^2 + \tau_{yz}^2\right)\right]} \leq \tau_s, \quad \text{Equation 6.11}$$

i.e., $\sqrt{J_2} \leq \tau_s$, J_2 – second stress invariant

In terms of the strains, the vM-H failure criteria is obtained as

$$\sqrt{2\left(\varepsilon_x^2 + \varepsilon_y^2 + \varepsilon_z^2\right) + \left(\gamma_{xy}^2 + \gamma_{xz}^2 + \gamma_{yz}^2\right) - 3\varepsilon_m^2} \leq \gamma_s;\ \varepsilon_m = \frac{\varepsilon_x + \varepsilon_y + \varepsilon_z}{3} \quad \text{Equation 6.12}$$

$\varepsilon_{x/y/z}$ – arbitrary normal strain, $\gamma_{xy/yz/xz}$ – arbitrary shear strain

In terms of the principal stress and strains ($\sigma_1, \sigma_2, \sigma_3$ *and* $\varepsilon_1, \varepsilon_2, \varepsilon_3$ respectively),

$$\sqrt{\frac{1}{6}\left[(\sigma_1 - \sigma_2)^2 + (\sigma_2 - \sigma_3)^2 + (\sigma_3 - \sigma_1)^2\right]} \leq \tau_s, \sqrt{2(\varepsilon_1^2 + \varepsilon_2^2 + \varepsilon_3^2) - 3\varepsilon_m^2} \leq \gamma_s \quad \text{Equation 6.13}$$

Vibration of the fresh concrete mixes in the cracking mould (as in this study) reduces the suspending mortar yield stress (Li and Cao, 2019; Banfill *et al.*, 2011) that resists aggregates' settlement (Peng and Jacobsen, 2013). This also reduces the concrete's static yield stress to a residual/dynamic yield stress, hence, the concrete's resistance to shear-induced cracking from differential settlement. Thereafter, the microstructure (strength) starts to build-up due to thixotropy and later due to extended hydration (Kolawole *et al.*, 2019c). The effects of the vibration can be simulated by shearing in a rheometer. Furthermore, results of such shear rheometry yield test (stress growth test) of the plastic concrete are similar to an "elastic-ductile-plastic" behaviour as shown in Figure 6.10, and shifts gradually to that of elastic-perfectly plastic as age increased. The study by (Mettler *et al.*, 2016) confirms this transition from a ductile plastic failure regime to a brittle cohesive frictional solid behaviour.

Therefore, the residual strength (τ_{rs}) in Figure 6.10, increased with time (up to the initial setting time) by the non-linear structural build-up model of (Ma *et al.*, 2018) (see (Kolawole *et al.*, 2019c) for details) were adopted as the yield parameters for the vM-H failure criteria. By this approach, it is assumed that the irreversible contribution of hydration to the concrete's yield stress before initial setting time is negligible. This assumption is based on the fact that substantial increase in the heat of hydration of cement is towards the initial setting time (Hu *et al.*, 2014). The influence of vibration (or pre-shearing) on the concrete's stiffness (G*) can be neglected since the companion study (Kolawole *et al.*, 2019c) shows that it does not influence the plastic cracking behaviour (especially settlement). G also recovers to the reference stiffness within a few minutes (Ma *et al.*, 2018) (about 15 minutes in the case of this study – (Kolawole *et al.*, 2019b)). The strain capacity (γ_s – see Figure 6.11) adopted was based on the reduction in storage modulus which also coincides with the peak normal stress (see the next section). This point known as critical strain (γ_s) is expressed as the breakage of the network of interactions between cement-based particles, signifying molecular stretching and micro-cracks (Roussel *et al.*, 2012) and it occurs before the higher magnitude of strain (γ_{s2}) where complete failure occurs (Roussel *et al.*, 2010, 2019). Details of the concrete's storage modulus properties and tests can be found in the companion study (Kolawole *et al.*, 2019b) and is summarised in Section 6.6.1. This form of γ_s is deemed more appropriate than the later occurring γ_{s2} signified in Figure 6.10 and Figure 6.11 since the presence of micro-cracks due to restrained plastic settlement inadvertently becomes weak spots for rapid propagation of cracks due to shrinkage. Note that Figure 6.11 is on a Log-scale and the broad ductile peak is therefore not visible. Initial vibration or pre-shearing has been shown not to really influence the γ_s (Yuan, Lu, *et al.*, 2017;

Qian and Kawashima, 2016). Equation 6.1 ($\gamma = \tau/G$) also proves this, since a similar reduction in both G and τ leaves γ fairly constant.

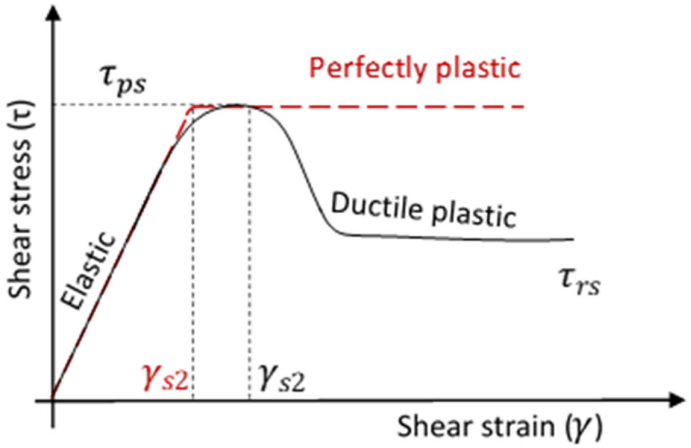

Figure 6.10: Adopted behaviour of plastic concrete (τ_{ps} & τ_{rs} – peak & residual shear strength)

6.4.3.2. Bresler-Pister theory

The Bresler-Pister (B-P) theory, also known as Drucker-Prager (D-P) Cap theory, is basically a D-P theory with provision for cap failure (Reiterer *et al.*, 2004; Boswell and Chen, 1987). That is, the deviatoric failure plane is bound by a hydrostatic failure model. The D-P theory can be expressed in terms of the shear properties (Singh *et al.*, 2019; Alejano and Bobet, 2012; Jiang and Wu, 2012),

$$\sqrt{J_2} = BI_1 + C, \quad B = \frac{2\,sin\varphi}{\sqrt{3}(3 + sin\varphi)}, \quad C = \frac{6c\,cos\varphi}{\sqrt{3}(3 + sin\varphi)} \qquad \text{Equation 6.14}$$

I_1 is the first stress invariant, c and φ are the material shear parameters defined by the Mohr-Coulomb model at failure

$\tau = \sigma(tan\varphi) + c$, c is the cohesion, φ is the angle of internal friction Equation 6.15

In this study, an indirect method to measure the cohesion (c) and coefficient of internal friction (φ) of plastic concrete via dynamic shear rheometry was attempted. The dynamic shear rheometer (see Section 6.5.2) was equipped with a normal stress sensor that allows the measurement of the normal stress (σ) concurrently with the shear stress (τ) (de Cagny *et al.*, 2019; Verrelli and Kilcullen, 2016). This normal stress has been shown to be influenced by the mass of the concrete above the vanes, even to the midpoint of the vane's height and was found by (Assaad *et al.*, 2014) to correlate well with direct shear tests. Furthermore, the rheometer's results have the advantage of being sensitive to the effective hydrostatic stress (Assaad *et al.*, 2014). The obtained σ and τ values during the yielding/peak phase (just before failure) of the concrete mixes were used in Equation 6.15 to evaluate the c and φ. Values of φ ranged from 75° to 80° which is known to mainly increase due to

an increase in aggregate content in cement-based materials (Rajgelj, 1985). The c-value increased as concrete age, that is hydration, increased (Ghourchian *et al.*, 2019; Alexandridis and Gardner, 1981).

The B-P theory is given as

$$\sqrt{J_2} = AI_1^2 + BI_1 + C \qquad \text{Equation 6.16}$$

B and C (same as that of D-P theory above) comes from simple boundary condition of pure distortion (that is, I_1 = 0) and equating to the D-P model (Ghourchian *et al.*, 2019). Coefficient A can be derived by considering a pure hydrostatic/dilatant failure (that is, J_2 = 0) as below.

From Equation 6.9 and Equation 6.10,

$$\sqrt{\frac{1}{2}\left[(\sigma_x - \sigma_y)^2 + (\sigma_y - \sigma_z)^2 + (\sigma_z - \sigma_x)^2 + 6\left(\tau_{xy}^2 + \tau_{xz}^2 + \tau_{yz}^2\right)\right]} = \sigma_s \qquad \text{Equation 6.17}$$

Therefore, the simple yield shear stress and associated normal stress (N_1) from the dynamic shear rheometry test can be used to evaluate the value of σ_s (de Cagny *et al.*, 2019; Verrelli and Kilcullen, 2016) corresponding to the equivalent isotropic stress at hydrostatic failure (σ_{s1}), that is,

$$\sqrt{{N_1}^2 + 6\tau_s^2} = \sigma_{s1} \qquad \text{Equation 6.18}$$

Therefore, from the J_2 = 0 boundary condition of pure hydrostatic failure,

$$0 = AI_1^2 + BI_1 + C \qquad \text{Equation 6.19}$$

$$A = -\frac{B\sigma_{s1} + C}{\sigma_{s1}^2} \qquad \text{Equation 6.20}$$

The B-P model can then be written as,

$$\sqrt{J_2} = \left(-\frac{B\sigma_{s1} + C}{\sigma_{s1}^2}\right) I_1^2 + BI_1 + C \qquad \text{Equation 6.21}$$

Though, from the companion study (Kolawole *et al.*, 2019b), pseudo-strain hardening was qualitatively observed for the concrete mixes, the potential influence of strain hardening on the failure criteria (Jones, 2009) were assumed to be negligible for the plastic concrete mixes.

6.5. Experimental materials and methods

Polysaccharide-based liquid viscosity modifying agent (VMA), polycarboxylate ester liquid superplasticizer (SP) and water were used to rheologically modify concrete into five mixes (Table 6.2) without drastically changing the setting time and compressive strength development (Table

6.2). The rheology modifiers were measured by weight as a percentage of the cement content and added to the mixing water before adding the water to the mixed dry constituents in the concrete mixer. Rheo-physical properties of the mixes shown in Table 6.2 were measured using the ICAR rheometer (Koehler and Fowler, 2004), full details of the rotational shear rheometry test can be found somewhere else (Kolawole *et al.*, 2019a). The dynamic shear rheometry and plastic cracking test procedures and methods for this study are shown in Section 6.5.1, the plastic cracking tests were carried out in a climate chamber with an electronically controlled closed loop system (Boshoff and Combrinck, 2013) with conditions of 40^{o}C ambient temperature, 10% relative humidity and 4 km/h wind speed. These conditions proved to be sufficient to cause plastic cracking in all the samples. The dynamic shear rheometry tests in the building material cell (BMC 90) were also done at 40^{o}C via a Peltier temperature device (Anton-Paar, 2012). The material constituents and properties of the concrete mixes are shown in Table 6.2. As noted earlier, the coarse aggregate content (6 mm Greywacke stone) was reduced by 60% for the dynamic shear rheometry tests. At least four samples were tested for the plastic cracking and two samples for the rheometry tests.

Table 6.2: Properties of the concrete mixes

Notations	Material constituent (kg/m^3)				
	C	CV	CS	CVS	CW
Water	217	217	217	217	223
Cement - CEM II 52.5N	395	395	395	395	374
Malsmebury sand	774	774	774	774	796
6mm Greywacke stone (Ideal)	1029	1029	1029	1029	1018
(Reduced – 40%)	412	412	412	412	407
VMA	-	0.6%	-	0.4%	-
Superplasticizer	-	-	0.6%	0.4%	-
Other properties					
w/c ratio	0.55	0.55	0.55	0.55	0.6
Slump (mm)	100	100	175	170	185
Initial setting time (mins)	120	120	120	150	130
Final setting time (mins)	165	165	165	195	165
Compressive strength (7 days, MPa)	36	39	35	42	32
(28 days, MPa)	47	51	47	50	42
Rheo-physical properties					
Static yield stress (Pa)	3652.4	3803.8	1240.7	1329.9	1131.9
Dynamic yield stress (Pa)	1155.9	1105.3	633.6	776.5	553.4
Plastic viscosity (Pa.s)	15.3	16.6	6.8	2.9	4.7
Thixotropy index	3.04	2.85	1.42	1.75	1.20
C – Control mix; CV – control mix + VMA; CS – control mix + SP; CVS – control mix + VMA + SP; CW – control mix + water					

6.5.1. Materials preparation and test procedure

All materials prior to mixing were stored in a climate room at 23°C ambient temperature and 65% relative humidity at least 24 hours before testing. This ensured constant and consistent temperature for all mix materials and the freshly mixed concrete. After adding stone, cement and sand respectively to the concrete mixer, the materials were dry mixed for one minute before adding the mixing water. Thereafter, the concrete was mixed for four minutes, that is, a total of five minutes mixing. The concrete age was taken as zero from the end of mixing. For the plastic cracking tests, concrete was then placed in the moulds halfway and vibrated for about 30 seconds, moulds were then filled with concrete and vibrated further for 2 minutes. For the dynamic shear rheometry tests, concrete was placed in the building material cell (BMC 90) cup (Kolawole *et al.*, 2019b) for testing without vibration as advised by the manufacturer. It took approximately ten minutes from the end of mixing to starting the tests.

6.5.2. Dynamic shear rheometry tests

Rheo-viscoelastic properties tests carried out include amplitude and frequency sweeps, creep and creep recovery, and stress relaxation. These tests were carried out at 10, 70 and 130 minutes of concrete age. More detailed description of these tests can be found in (Kolawole *et al.*, 2019b). It was ensured that selected values of the shear modulus were within the linear viscoelastic range (LVE). 50% of the shear strength and strain capacity of the concrete mixes were used as input stress and strain for the creep and creep recovery tests, and stress relaxation tests respectively (Khan, Castel, *et al.*, 2017; Khan, Kolawole, *et al.*, 2017; Khan *et al.*, 2016). These values of stress and strain did not cause a non-linear VE response. Creep and creep recovery test and stress relaxation test results were analysed to obtain the elastic and viscous components of the creep compliance and relaxation modulus respectively. Typical results for the amplitude sweeps, creep and creep recovery tests and stress relaxation tests are shown in Figure 6.11 to Figure 6.13 indicating values of the peak shear strength (τ_{ps}) at the concrete's yield point, strain capacities (γ_s), shear storage modulus (G'), shear loss modulus (G''), total and viscous components of the creep compliance (J_m & J_v), and total and elastic components of the relaxation modulus (G_0 & G_e) respectively. These values are used in calculating the damping factors in Table 6.1.

Table 6.3: Shear strain and stress values for the stress relaxation and creep and creep recovery tests

		C (%)	CV (%)	CS (%)	CVS (%)	CW (%)
Strain (%)	0-hour	0.8	0.8	0.8	0.8	0.5
	1-hour	5	5	2	5	5
	2-hour	7	7	10	9	9
Stress (Pa)	0-hour	148	148	194	80	80
	1-hour	1000	700	450	650	1000
	2-hour	1400	1400	1300	1200	1500

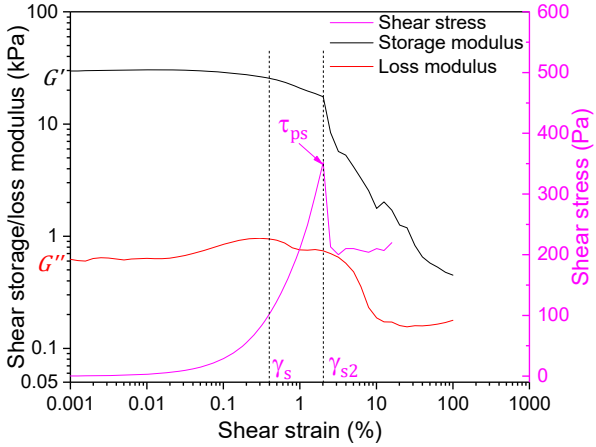

Figure 6.11: Amplitude sweep for Mix C showing the values of γ_s, τ_{ps}, G', and G''

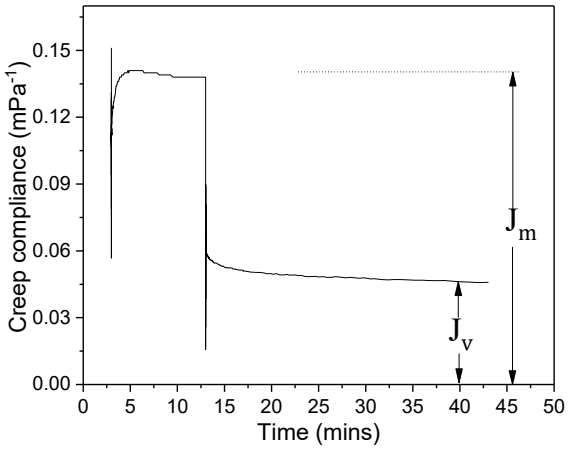

Figure 6.12: Creep and creep recovery test for Mix CV showing the values of J_m and J_v

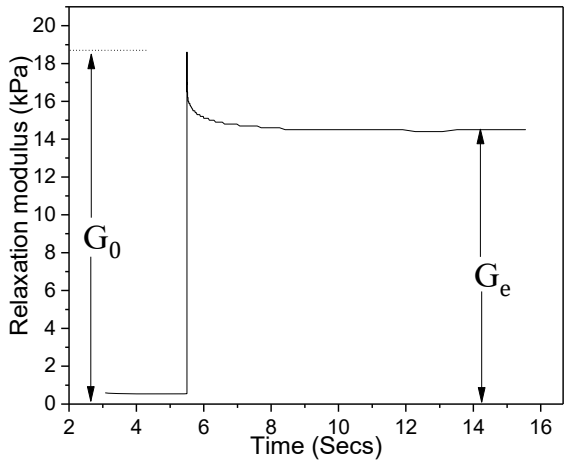

Figure 6.13: Stress relaxation test for Mix C showing the values of G_0 and G_e

6.5.3. Plastic cracking tests

The plastic cracking test was done using a mould similar to that of ASTM C1579 (2006) (Figure 6.14) and has been used by other authors to achieve similar results for plastic cracking (Combrinck *et al.*, 2019; Olivier *et al.*, 2018; Boshoff and Combrinck, 2013). The crack areas were measured at the

surface of the concrete mixes using high resolution photographs scaled using CAD software. The final stabilised cracks were obtained at about 2 hours after the final setting times. More details can be found in (Kolawole *et al.*, 2019c).

As shown earlier in Figure 6.6, the recent study by Combrinck *et al.* (2018a) showed that pure differential plastic settlement causes slowly occurring shear-induced cracks which can be hidden beneath the concrete surface and are independent of evaporation conditions. In the same study, pure restrained plastic shrinkage caused a rapid distinct single crack propagated across the depth of the concrete. Combrinck *et al.* (2018a) concluded that the ASTM C1579 (2006) mould results in earlier plastic settlement cracking amplified to the surface by restrained plastic shrinkage. Another study by (Ghourchian *et al.*, 2019), using X-ray radiography a on similar mould, supports the initiation of crack within the concrete that propagates to the surface. Moreover, the controlled climate conditions for this kind of test causes the boundary between the two forms of plastic cracking to overlap, making it indistinguishable and fast occurring.

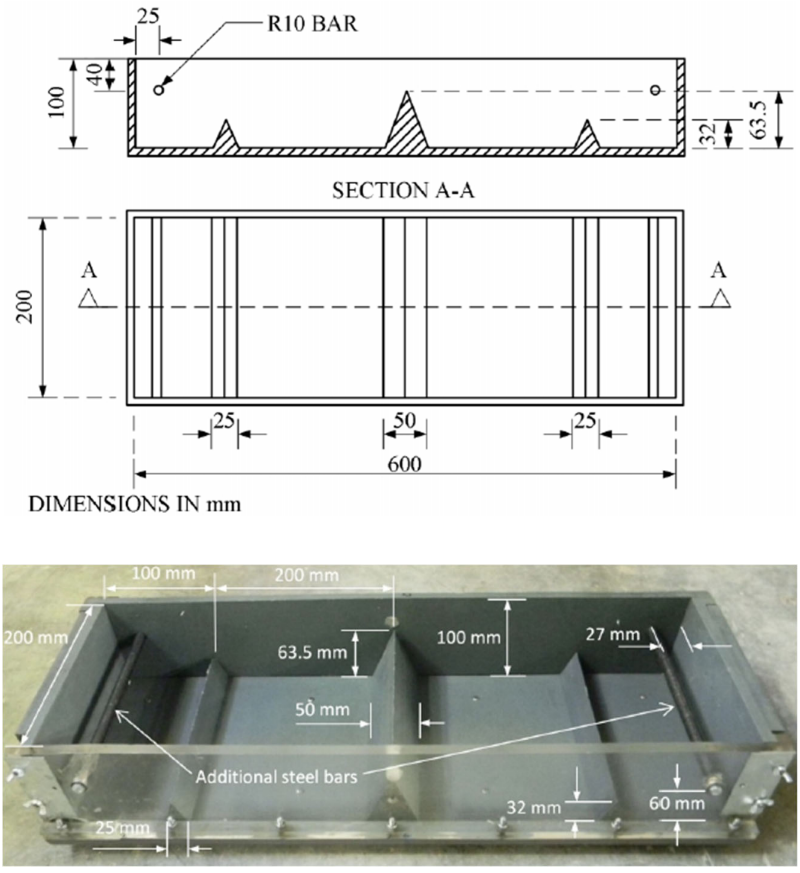

Figure 6.14: Plastic cracking mould based on ASTM C1579 (2006)

6.6. Experimental results and discussion

6.6.1. Shear and rheo-viscoelastic properties

As noted earlier, the properties were investigated at 10, 70 and 130 minutes, values between the times were linearly interpolated for input material properties in the model.

6.6.1.1. Shear strength and strain capacity

Figure 6.15 shows the estimated residual shear strength (τ_s) (increased by structuration model of (Ma *et al.*, 2018) – see (Kolawole *et al.*, 2019c)), strain capacity (γ_s) and shear modulus (G) of the concrete mixes. The shear properties generally increased with the concrete age for all the mixes except for the γ_s. The γ_s generally reduced with age except for Mixes C/CV/CW that showed an increase at 130 minutes. This trend of decreasing strain capacity and later increase has been reported for tensile properties of plastic concrete (Combrinck and Boshoff, 2019; Nguyen *et al.*, 2017; Roziere *et al.*, 2015; Dao *et al.*, 2009). The concrete's stiffness showed more development within the first hour. The rheology modifiers did not significantly influence the stiffness (G) of the concrete while generally reducing the τ_s and γ_s.

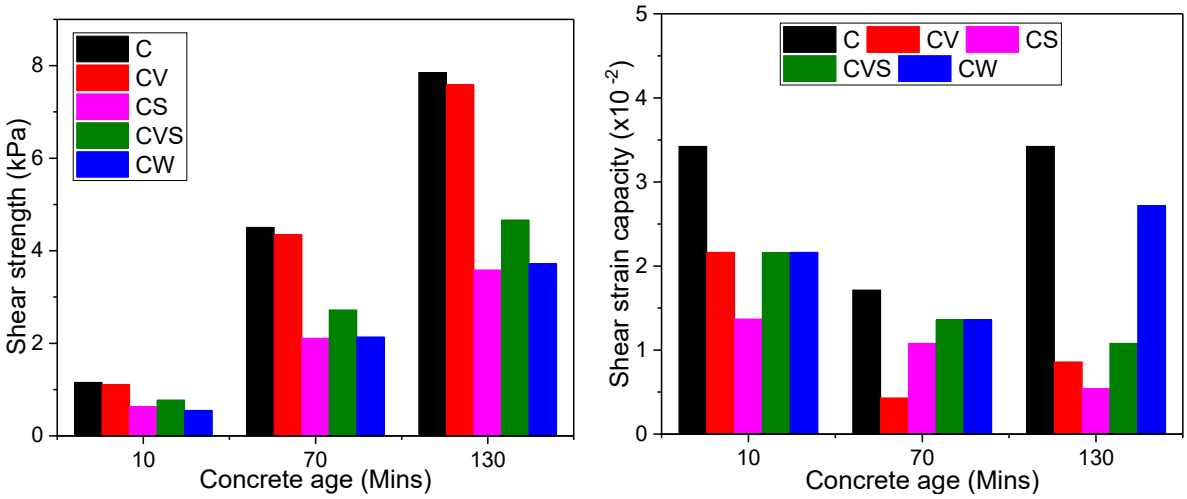

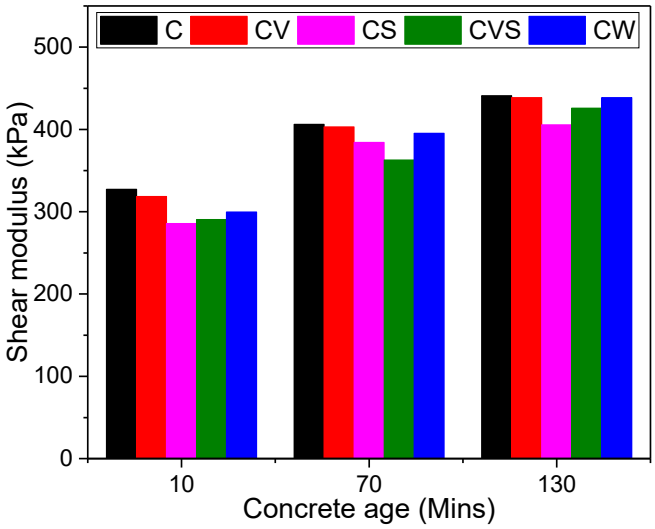

Figure 6.15: (a) Shear strength, (b) strain capacity and (c) shear modulus of the concrete mixes

6.6.2. Damping factors

The damping factors of the concrete mixes for modulus of rigidity, strain dissipation, and stress relaxation are shown in Figure 6.16 as calculated using the equations in Table 6.1. The modulus of rigidity showed little or no damping (maximum of 0.16%) for all the mixes at all ages and was therefore neglected. This implies that the stiffness of the plastic concrete mixes is completely effective in resisting the small cracking strains with negligible viscous component. Figure 6.16b reveals that the artificial rheology modifiers generally increases the strain dissipation ability of the concrete mixes and this ability reduces with concrete age. For the stress damping factors also referred to as relaxation factor, Figure 6.16c reveals that there is little or no difference in the ability of the mixes to relax stresses. That is, plastic concrete relaxes the early restrained stress of plastic cracking as an inherent behaviour which is not induced by rheology modifiers.

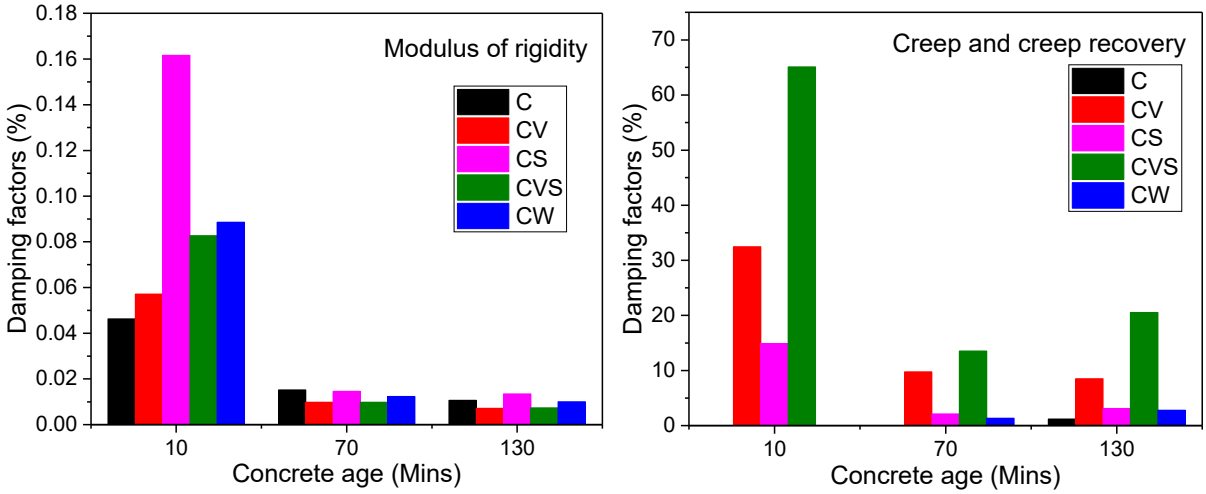

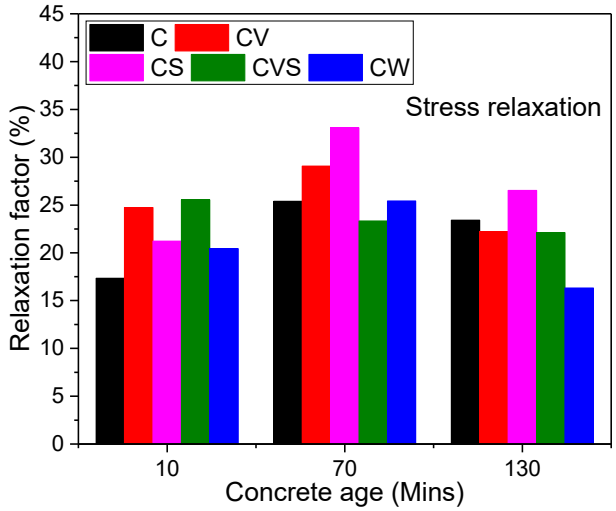

Figure 6.16: Damping factors of the concrete mixes for (a) modulus of rigidity (b) creep and creep recovery (c) stress relaxation

6.7. Plastic cracking

Background information on the influencing processes of the observed plastic cracking (including detailed plastic cracking behaviour of the concrete mixes) can be found in (Kolawole *et al.*, 2019c). The main processes are the bleeding, evaporation, negative capillary pressure build-up, plastic settlement and plastic shrinkage of the concrete mixes (Combrinck *et al.*, 2019; Sayahi, 2016; Leemann *et al.*, 2014; CCIP-048, 2010; Slowik *et al.*, 2008; Uno, 1998).

As noted in Section 6.5.3, the ASTM C1579 (2006) mould is believed to induce shear cracks within the concrete due to differential settlement that are rapidly propagated to the surface by restrained shrinkage. Figure 6.17 represents the development and summary of plastic cracking of the concrete mixes. The initial crack area is the measured surface crack area at crack initiation, the stabilised crack area is when the rate of cracking remains fairly constant, and the final crack area is measured at end of test. The cracking of Mixes C, CV and CS (as observed on the surface) started at 140 minutes after exposure, that is, about 20 minutes after their initial setting time. Mix CW started cracking at 160 minutes after exposure, that is, 30 minutes after its initial setting time while Mix CVS showed a delayed cracking that started at 200 minutes after exposure (50 minutes after its initial setting time). It should be noted that the appearance of the surface cracks indicated by the results may not necessarily translate to micro-crack initiation within the concrete induced by the mould's restraints. The cracks are propagated from the tip of the centre triangular constraint to the surface and magnified by the other two smaller side triangles and rods (Ghourchian *et al.*, 2019; Combrinck *et al.*, 2018a; Combrinck, 2016). According to (Safiuddin *et al.*, 2018; Dias, 2003; Samman *et al.*, 1996), increased water content in concrete can delay the initiation of the crack, and that too little or too

much water in concrete may cause no cracking. Therefore, the delay in the crack initiation at the surface by CW can be because of its increased liquid phase assisting in filling of microcracks induced by plastic settlement. Moreover, the initial crack area for Mix CW is relatively high, showing that the crack may not have readily shown on the surface but cracks may have occurred within the concrete before it appeared on the surface (Combrinck *et al.*, 2018a). Despite Mix CW having delayed crack initiation compared to Mixes C, CV, and CS, their cracking stabilised at around the same time (200 minutes) indicating the crack propagation.

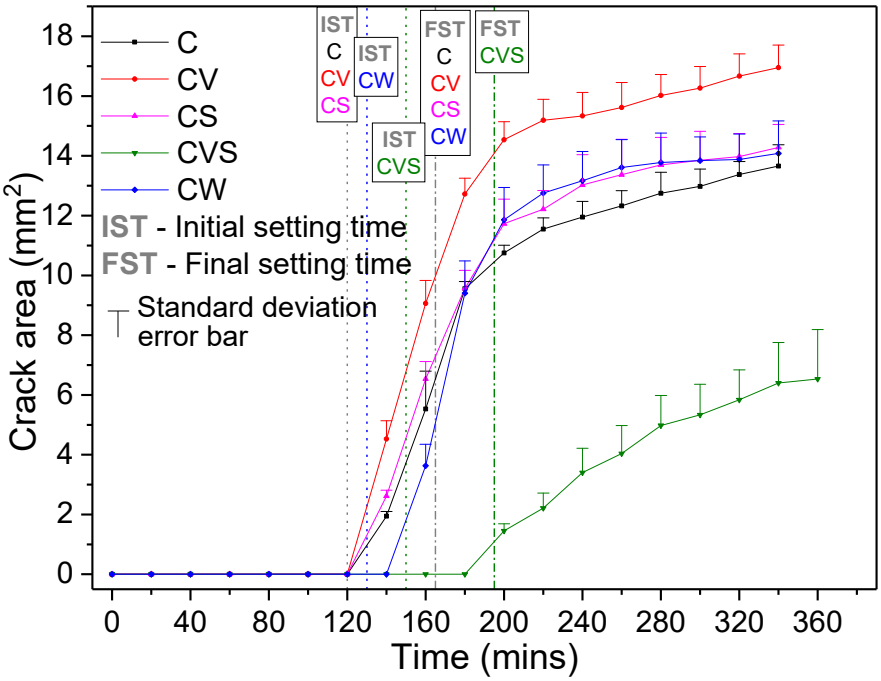

(a) Plastic cracking area

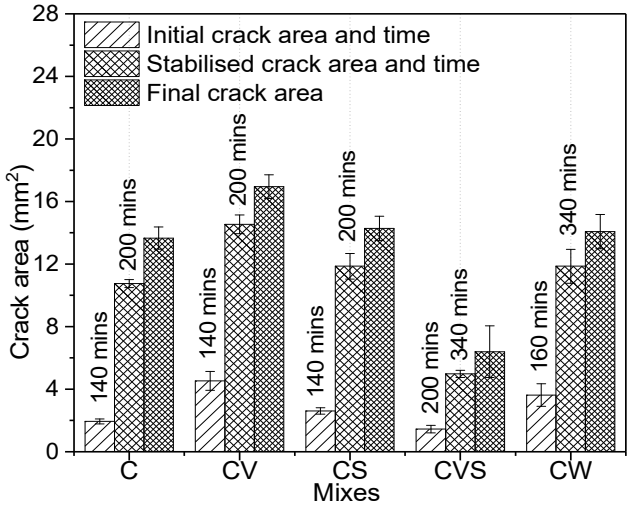

(b) Cracking details

Figure 6.17: Plastic cracking results of the concrete mixes

6.8. Verification of model and discussion

The cracking reported in the previous section was observed and measured from the surface, hence, initial cracking time depicted in Figure 6.17b may not give the true presentation of the crack initiation. It is, therefore, suggested that the initial surface crack area depicted in Figure 6.17b can be said to appear at a magnitude directly proportional to each concrete mix's crack initiation and resistance while the stabilised and final crack areas can be linked to the crack propagation of the mixes. These were examined to verify the model.

6.9. Von-Mises and Hencky theory

Using the Von-Mises and Hencky theory (vM-H) theory, results and verification of the proposed model for the three case scenarios (see Section 6.4.2) are shown in the following sections. Material properties and failure criteria in terms of strain and stress paths are examined.

6.9.1. Strain path results

- **CASE I/II**

Results of the failure criteria are shown in Figure 6.18, CASE I/II represents results that incorporated the viscoelasticity of the concrete mixes (Section 6.4.2). It was found that CASE II has similar criteria as CASE I in which the γ_{max} has the same path with the vM-H, hence, only Mix C (the control) of CASE II's strain path is presented for reference purpose. This similarity confirms earlier statements that the plastic phase is shear dominated. The results revealed that the internal damage/microcrack of the concrete mixes before the end of the plastic phase is probable. Mixes C, CV, CS, CVS and CW are likely to crack at 90, 52, 77, 113, and 60 minutes respectively which correlate very well with the respective initial crack areas of 1.94, 4.53, 2.61, 1.45 and 3.63 mm^2 as shown in Figure 6.18a. That is, the quicker the crack initiation as predicted by the model, the more the magnitude of the surface crack initiation observed in the ASTM C1579 (2006) mould. The good correlation implies that the magnitude of the initial crack at the surface truly indicates the initiation of shear-induced damage/microcracking in the concrete. Furthermore, these predicted crack times fall within the self-settlement periods of the plastic settlement for each concrete mix (see (Kolawole *et al.*, 2019c)), confirming that microstructural damage/cracking occurred during the early plastic phase. To examine the model's prediction of crack propagation, the experimental crack propagation was derived from subtracting the initial crack area from the stabilised and final crack areas and correlated with the area between the vM-H strain path and the material's strain capacity after crack initiation (such as the typical shaded portion of Mixes C and CV in Figure 6.18). From the result of the correlation shown in Figure 6.19b, the model does not sufficiently explain the crack propagation

of the concrete. This could due to the stabilised and final cracks that are more into the semi-plastic-to-solid phase of the plastic cracking, this period is more of induced tensile (less ductile) cracking with pronounced resistant tensile properties which the model does not cover. This also explains why the earlier stabilised crack at 200 minutes has slightly higher correlation than the final crack at 340 minutes (Figure 6.19b).

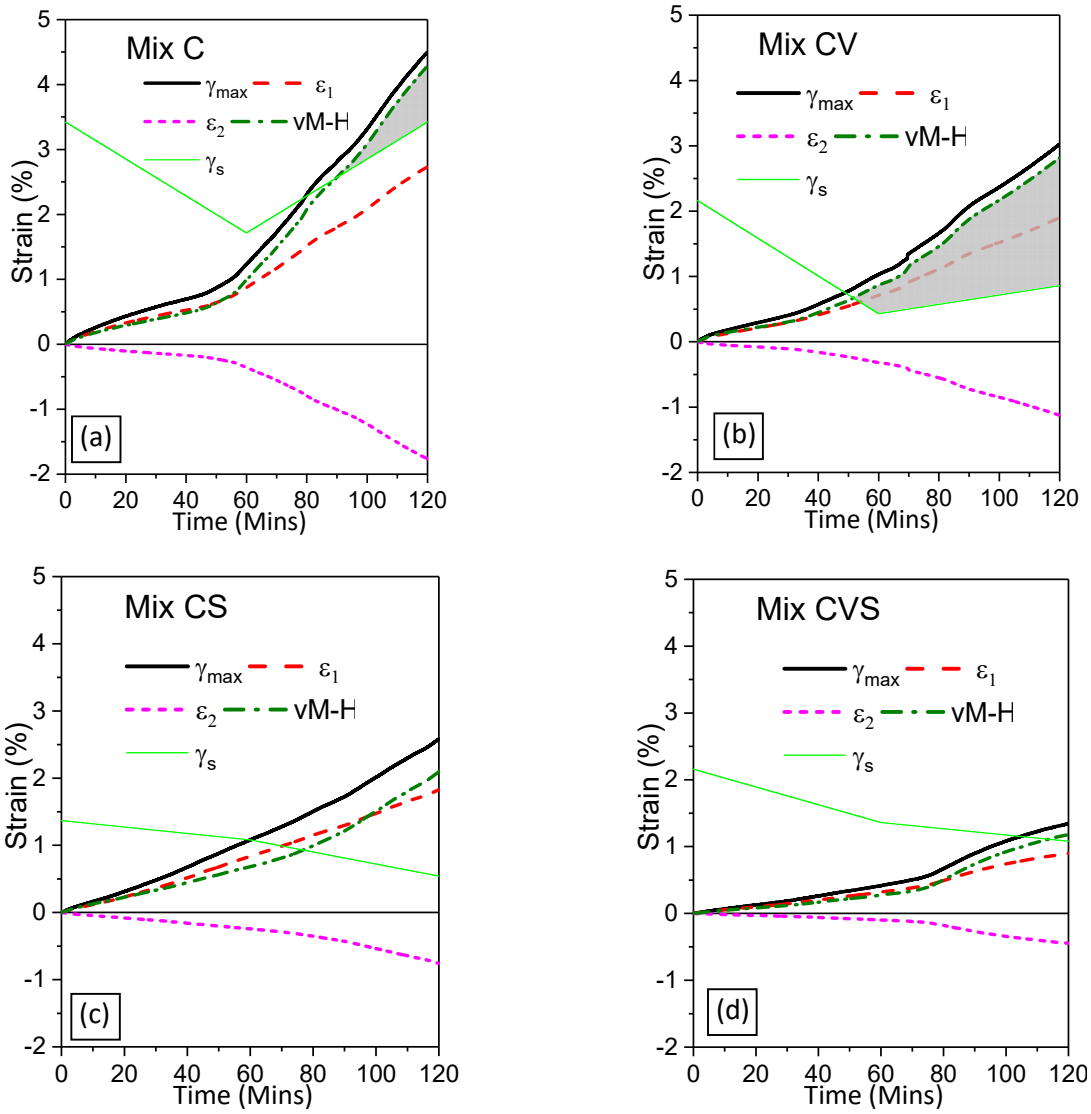

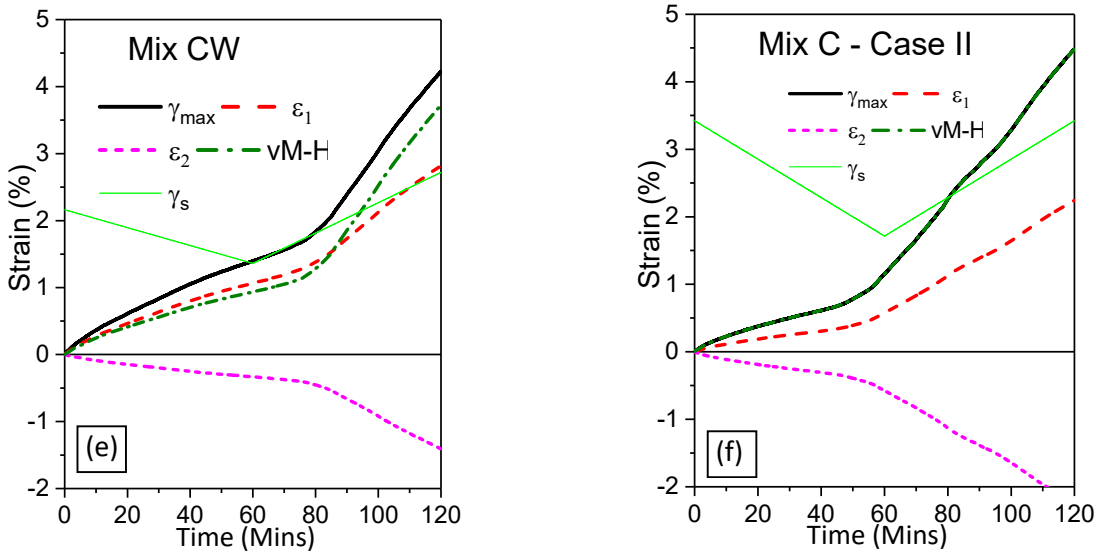

Figure 6.18: Strain path and material properties according to the Von Mises-Hencky theory (a-e: CASE I, f: CASE II)

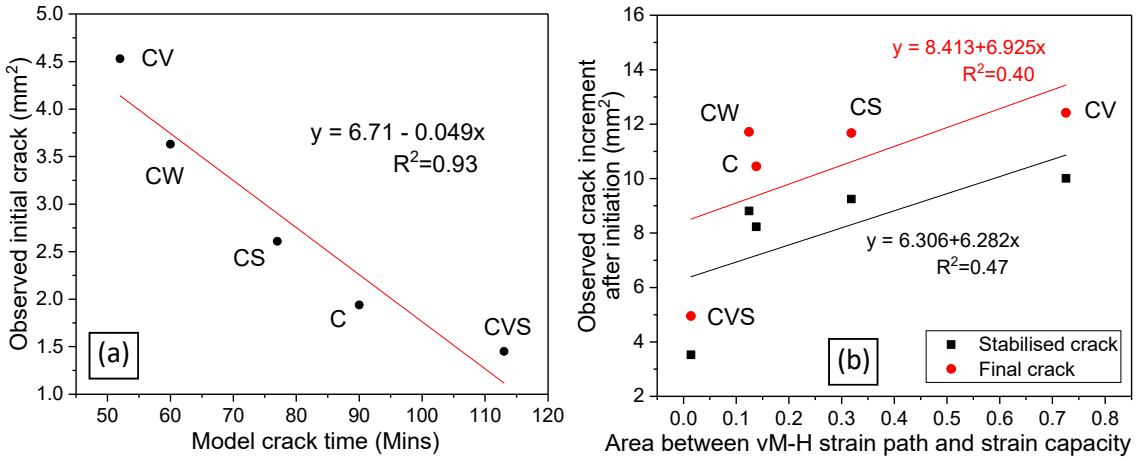

Figure 6.19: Relationship between model outputs and observed cracking

In practical terms, the correlation in Figure 6.19a can help to estimate the expected initial surface crack area of a concrete mix after modelling the crack time. To prevent plastic cracking, that is zero initial surface crack area, a minimum model crack time of about 136 minutes (obtained by solving the equation $y = 6.71 - 0.049x$) is required. To achieve this model crack time, adjustable input parameters include free plastic settlement/shrinkage and material properties such as shear and rheo-viscoelastic properties (creep, stress relaxation, shear strength, strain capacity and modulus). The plastic settlement/shrinkage was shown in a companion paper (Kolawole *et al.*, 2019c) to be correlated to the rheo-physical material properties (yield stress and thixotropy). Therefore, with further research and verifying the model for more mixes, it can be possible to control the rheo-related material properties to avoid earlier occurring hidden settlement cracks propagatable by shrinkage. A recommended approach is to improve the ductility of the concrete for better strain

capacity and dissipation, as well as the yield stress and thixotropy for lesser plastic settlement. This is envisaged as a pre-emptive passive method than the on-site active methods such as capillary pressure control/mitigation generally suggested by previous authors (Ghourchian *et al.*, 2019; Slowik *et al.*, 2014; Combrinck and Boshoff, 2009).

- **CASE III**

This is the case where the viscoelastic properties of the concrete mixes were not incorporated in the model which is the trend of currently available models in the literature. By observing the results in Figure 6.20 (a-d), Mixes C and CW have similar results as CASE I/II implying that the influence of their viscoelastic strain dissipation is negligible. Furthermore, strain paths of the other mixes (especially CV and CVS) have higher values leading to quicker predicted crack initiation. By comparing the CASE III model results with the observed initial cracking (Figure 6.20e), the model fails to correlate well, emphasizing the significance of the role of viscoelastic behaviour in the plastic cracking of concrete, especially for Mix CVS. It should be noted that the resulting relationship equation is similar to that of the CASE I/II, indicating the accuracy of the model.

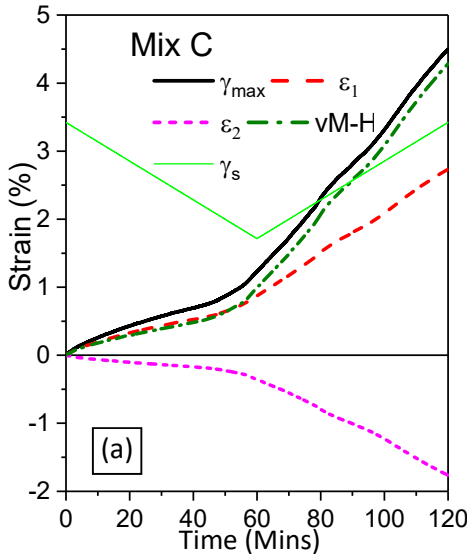

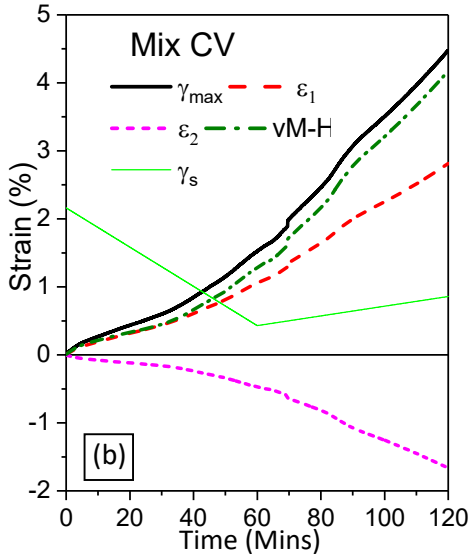

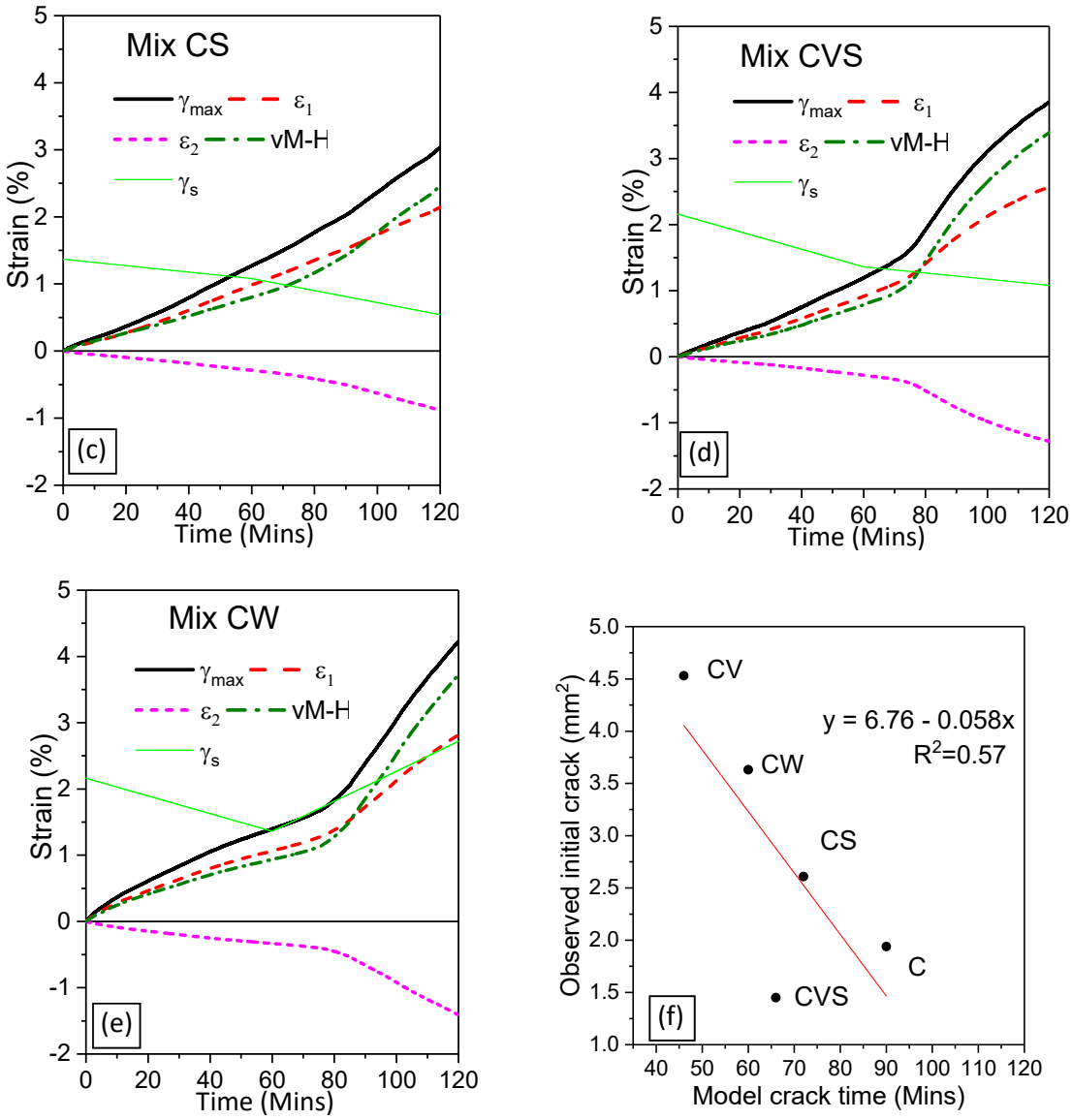

Figure 6.20: Strain path and material properties according to the Von Mises-Hencky theory (CASE III)

6.9.2. Stress path results

Figure 6.21 shows the model results in terms of stress path. Similar to the strain case, CASE II has similar result to CASE I with the vM-H stress path the same as the maximum shear stress (τ_{max}). CASE III for each of the concrete stress paths are faintly embossed on the graphs. Figure 6.21f shows how the model results correlate with the observed initial cracking and unlike the strain path results, the model does not fit. This is mainly due to Mix CV having relatively high shear strength but low strain capacity. It should be noted that the utilised strain capacities were the ones that correspond with micro-crack initiation and not the higher strains corresponding to the shear strength (i.e. γ_s vs γ_{s2} – see Section 6.4.3.1 and Figure 6.11). It was observed in the study of (Kolawole *et al.*, 2019a), that the Mix CV due to the incorporated viscosity modifying agent (VMA) has influencing entangling

polymers engineered to augment the microstructure cohesiveness (for example, viscosity) in withstanding more shear stress during the plastic phase. However, this polymer entanglement's bridging does not necessarily inhibit micro-cracks due to the molecular stretching caused by the plastic strains. A similar study by (Khan, 2018), indeed, showed that the Mix CV has lower tensile strength after its plastic phase. Removing Mix CV data point makes the model results in Figure 6.21e have a R^2 of 0.87 which is still lower than that of the strain path. Furthermore, the stress path generally led to a quicker (by about 40 minutes) crack initiation when compared to the strain path except for Mix CVS with similar crack times. These show that strain is a better path/criteria for modelling cracking at the plastic phase of concrete which has been noted by some other authors (Combrinck and Boshoff, 2019; Nguyen *et al.*, 2017; Roziere *et al.*, 2015). CASE III model results (Figure 6.21f) have no fit with the cracking results revealing the significance of viscoelastic relaxation of stress.

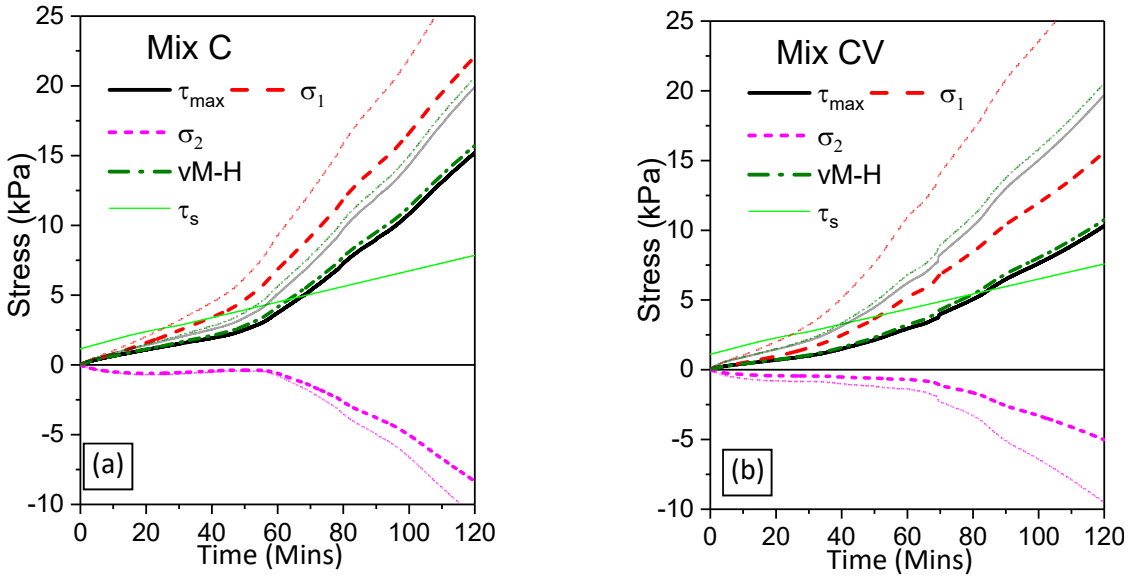

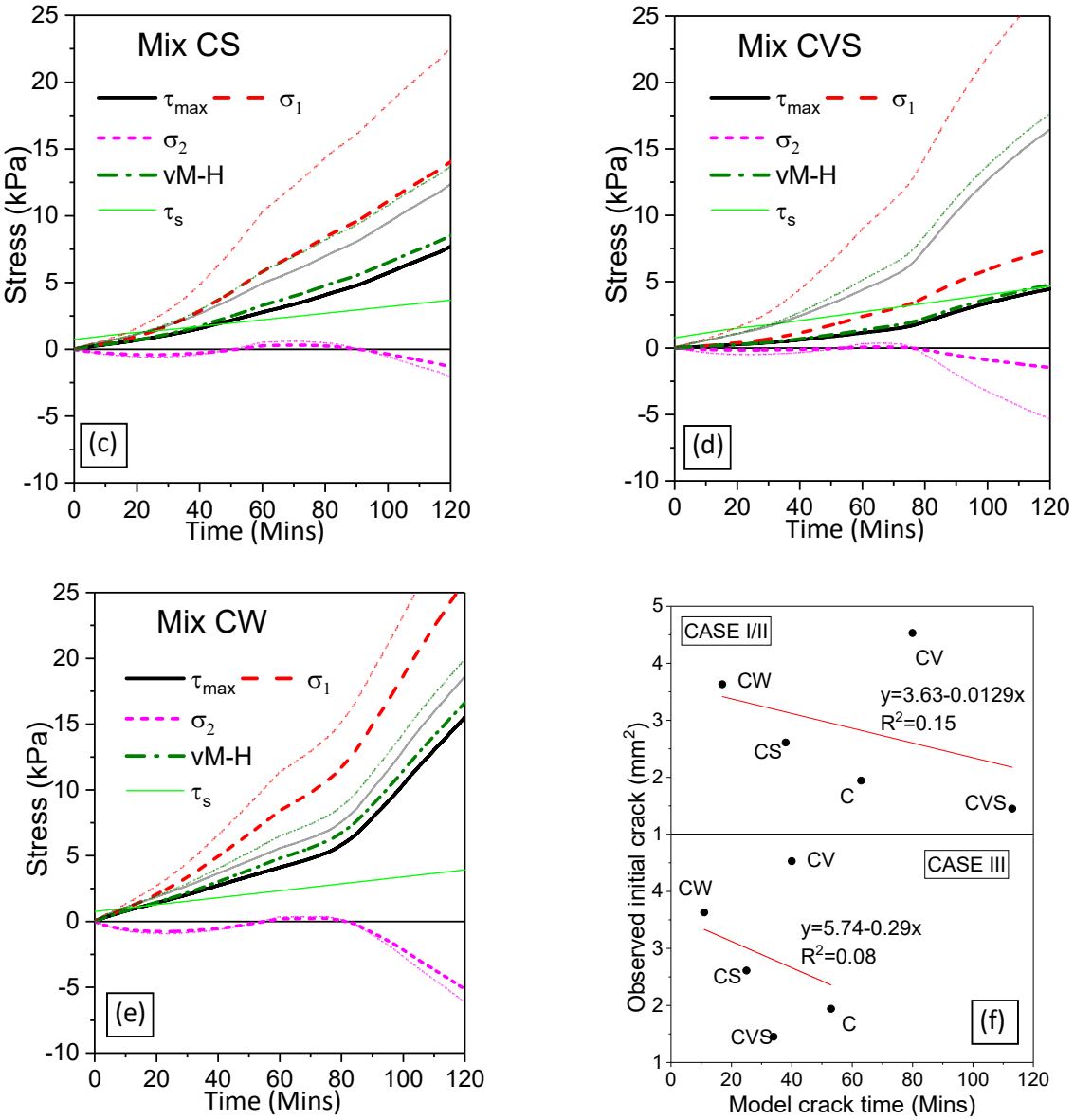

Figure 6.21: Stress path and material properties according to the Von Mises-Hencky theory (the thin lines in a-e represent CASE III)

6.10. Bresler-Pister theory

This theory takes into consideration the influence of the hydrostatic/dilatant pressure on the ductile failure of the concrete specimens and the possible microstructure failure/cracking due to the hydrostatic pressure. Figure 6.22 shows the results of the model (CASE I and III), where 1 and 2 hours strength envelopes are superimposed. Markers on the plots represent the stress points at 1 hour concrete age. CASE II resulted in vM-H theory as shown in Section 6.9.2. The model shows that cracks would have occurred in all the mixes at 1 hour concrete age except for Mix CVS while Mix CS may have the quickest crack initiation. The model does not have a good fit to the observed cracking. Even at the shrinkage dominated phase, the study by (Ghourchian *et al.*, 2019) also showed that the

B-P theory does not have a good fit. Furthermore, the recent experimental study by (Mettler *et al.*, 2016) showed that plastic concrete exhibits a pressure-insensitive form of ductile failure that gradually transits into a crack prevailing brittle form of failure (that has a dependence on hydrostatic stress components) as age progressed, and that the failure modes during this plastic phase are well represented by the von Mises criterion. These support the results obtained in this study.

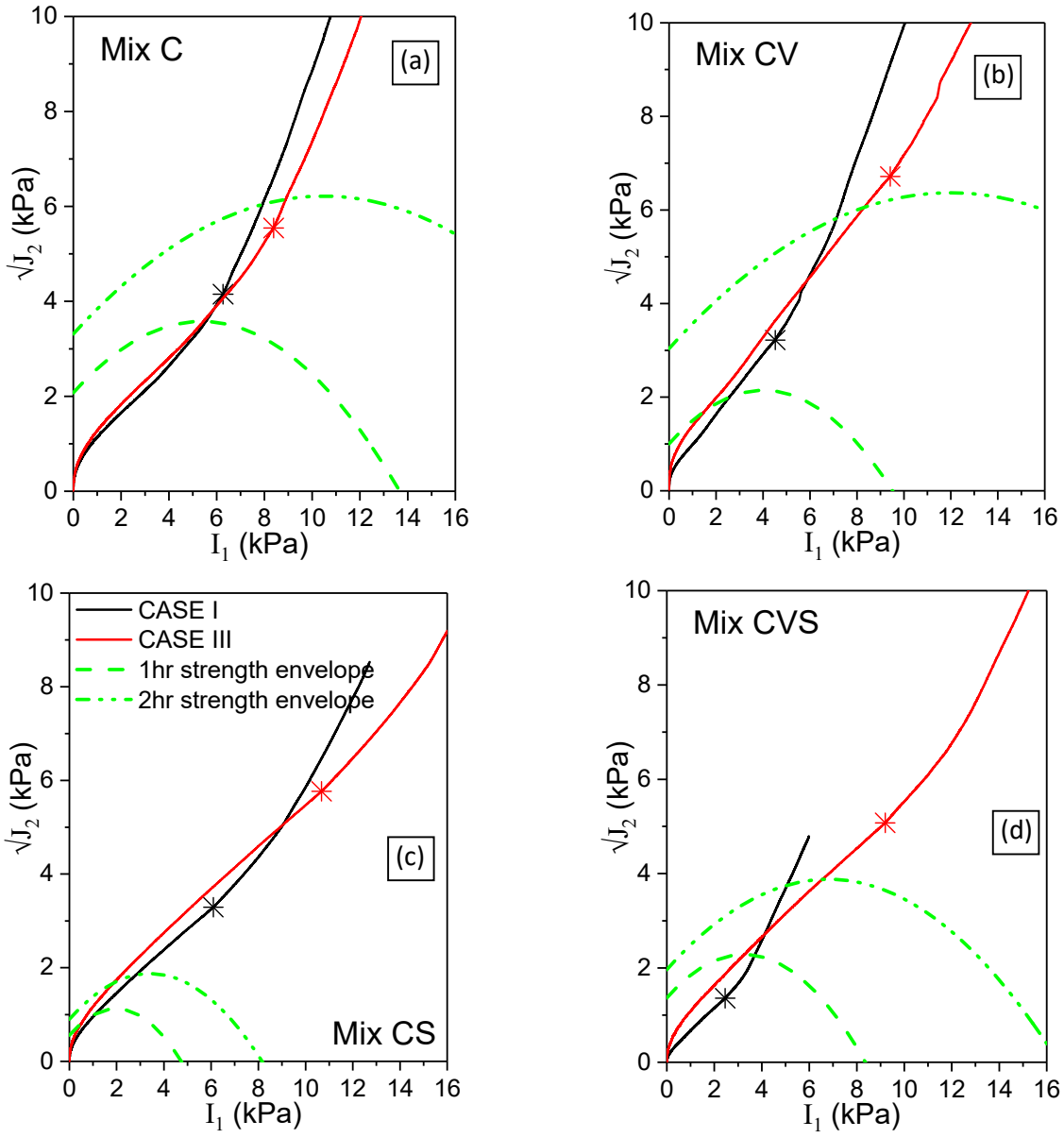

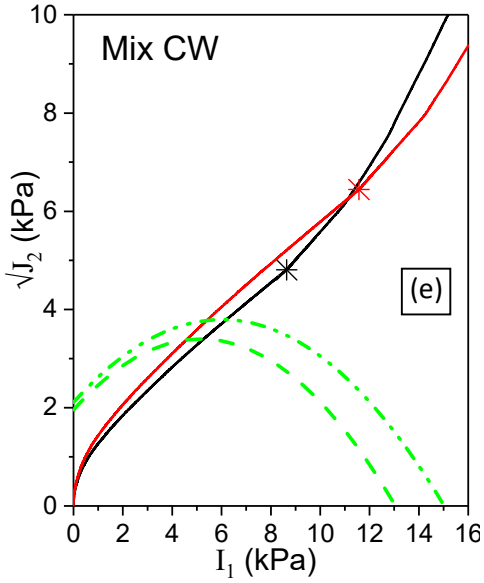

Figure 6.22: Stress path and strength envelopes for the concrete mixes according to Bresler-Pister theory

6.11. Conclusions

This study investigated the plastic phase of plastic cracking which is majorly shear settlement dominated in an attempt to predict and examine possible damage/cracking associated. A shear rheo-viscoelastic approach was used to experimentally establish the material properties and behaviour of rheologically modified plastic concrete mixes. Viscosity modifying agent (VMA), superplasticiser (SP) and water were used as rheology modifiers. Von-Mises and Hencky (vM-H) and Bresler-Pister (B-P) theories were used as failure criteria to model the plastic crack initiation.

The results show that the rheology modifiers, including their viscoelastic effects, influenced the yield properties and cracking of plastic concrete without significantly influencing its stiffness (shear modulus). Plastic concrete has an inherent ability to relax early restrained cracking stress, this relaxation scarcely depends on the material constituents. The strain dissipation of plastic concrete mainly depends on the material constituents, especially artificial rheology modifiers. These viscoelastic properties of plastic concrete have significant effects in modelling the cracking occurrence. The modelling results revealed that damage/microcracking can truly occur during the early settlement dominated period of plastic cracking behaviour. It is possible to judge the internal initiation of plastic cracking from the magnitude of the surface initial crack since it may be difficult to detect such shear-induced microcracking. Plastic concrete can be concluded to be majorly a strain-oriented failure, stress related failure criteria seems to predict its cracking/failure less accurately. Furthermore, plastic cracking tends to be a pressure-insensitive form of failure in which ductile failure takes prominence. It is therefore possible to accurately predict plastic cracking

occurrence with simple failure criteria such as Von-Mises and Hencky theory. Based on the similarity between CASE I and II of the vM-H theory, it can be concluded that restrained settlement and shrinkage occurring during the plastic phase mainly contribute to shear deformation. It was also concluded that it is possible to passively control concrete design materials that could avoid damage/cracking during the plastic phase which can be easily and rapidly propagated by the plastic shrinkage.

Chapter 7: Conclusions and recommendations

The results of this study were presented in four phases from Chapter 3 to Chapter 6. These were based on the objectives of the study earlier presented in Section 1.2. Significant conclusions drawn based on these objectives and results are presented in this chapter, and finally some recommendations for future studies are given.

7.1. Rheological and thixotropic behaviour of concrete

This phase examined the rheo-physical properties (with emphasis on thixotropy) of rheologically modified conventional concrete using various methods. Readily available rheology modifiers such as viscosity modifying agent (VMA), superplasticiser (SP) and water were utilised to vary the rheology of conventional concrete. From the results obtained, the following conclusions can be made.

- Inclusion of the VMA in concrete did not significantly change its rheological and thixotropic properties except for the plastic viscosity. VMA significantly increased the plastic viscosity of concrete as resting time increased. The inclusion of SP, both VMA and SP, and more water in concrete significantly influenced its thixotropic and rheology properties, mainly reducing these properties in a similar pattern.
- Thixotropic properties of concrete containing both VMA and SP (CVS) can become unstable due to pre-shearing. While the SP in CVS initially dominated its thixotropic behaviour, VMA's influence later surpassed the influence of SP.
- The inclusion of VMA or SP in concrete can cause shear thickening. However, the shear thickening behaviour of VMA concrete can be changed by the shear history while that of SP concrete was found to be independent of resting time and shear history.
- Pre-shearing concrete before resting can make it rheopectic, though its rheopexy may diminish into thixotropy as resting time increases. However, concrete containing SP may retain its rheopexy for longer rest periods. Furthermore, concrete containing SP and more water may turn rheopectic when being sheared continuously at high speeds (e.g. ≥ 0.275 rev/s).
- Thixotropy evaluation results showed fairly similar relation between the mixes, independent of concrete's condition pre-history except for thixotropic loop area. This implies that the hysteresis loop is limited as a qualitative evaluation method while other methods such as thixotropy index, structuration rate/state/time are better for quantitative evaluation.

This phase of the study contributes to the body of knowledge on thixotropy of conventional concrete, revealing how rheology modifiers influence the shear thinning/thickening, structuration and thixotropic structure breakdown of concrete. These results can help concrete batchers to make informed decisions on related thixotropic applications such as potential pumping difficulty due to shear thickening, and mix instability due to continuous shearing in a ready-mix truck. As a recommendation, the thixotropy of the concrete can be further evaluated using dynamic rheometry and comparatively gauged with the results of this paper.

7.2. Rheo-viscoelastic behaviour of cement-based materials

This phase of the study evaluated the rheo-viscoelastic behaviour of rheologically modified fresh cement-based materials. The cement-based materials are paste, mortar, and concrete which progressively allow for examining the trend in the viscoelastic (VE) behaviour and how the rheology modifiers influenced the trend. The following inferences and conclusions can be made:

- Increase in the aggregate volume fraction and size dampens the effects of the rheology modifiers on the VE behaviour of the cement-based materials.
- Satisfactory conclusions on the VE behaviour of concrete may not be approximate-able from that of cement paste as generally suggested in literature, especially, those containing admixtures such as rheology modifiers.
- The inclusion of sand in the cement paste tends to yield a more ductile cement-based material (mortar) in the fresh state while including both the sand and stone tend to make the ensuing concrete more brittle.
- The inclusion of the viscosity modifying agent (VMA) mostly did not change the linear elastic response of the cement-based material. However, the progressive inclusion of the aggregates reduced this ability. The other rheology modifiers (superplasticiser (SP), VMA+SP, and water) generally reduced the linear elastic response of the cement-based materials.
- Without the substantial influence of hydration, fresh cement-based materials' microstructure tends to thicken (pseudo-strain hardening) due to low and extended linear deformation. Increase in aggregate volume fraction tends to reduce the flocculation, and hence, the thickening property.
- Similarly, sudden application of step stress/force can cause the microstructure of fresh cement-based material to thicken. Quick stress relaxation from a step strain application can also be followed by microstructure thickening. Increased aggregate volume fraction reduced these effects.

- Increasing aggregate solid volume fraction and size reduce the flocculation-driven time-dependent VE behaviour (structuration) of the fresh cement-based material, making hydration the main driving source of structuration/thixotropy for fresh cement concrete.

7.3. Plastic cracking behaviour of concrete and its interdependence on rheo-physical properties

This phase of the study investigated the possible links between plastic cracking behaviour of concrete and its rheo-physical properties as a step towards establishing the influence of rheology on plastic cracking behaviour of concrete. To achieve this, plastic cracking processes of rheologically modified concrete mixes were investigated and thereafter linked to the results of shear rheometry of the same concrete mixes. The observed links revealed that the plastic phase of plastic cracking behaviour subjected to plastic settlement is majorly a shear phenomenon influenced by rheology and is characterisable by shear rheometry. The following significant conclusions can be made:

- The vibration of concrete can potentially reduce the resistance of concrete to plastic settlement and jump-start self-settlement as a form of induced gravitational-shearing process. Three stages/indicators signify major changes in plastic cracking behaviour of concrete and can be earmarked from the plastic cracking behaviour plot. The first indicator is a concurrent rapid rise in capillary pressure and shrinkage with a kink plot in the settlement. The indicator for the second stage is a kink plot in shrinkage and change in the rate of the capillary pressure with a change in slope of the settlement plot while the third indicator marks the end of the settlement, shrinkage.
- The rheology modifiers increased the plastic settlement while delaying the start of the capillary pressure and shrinkage build-up by retaining the pore water. The modifiers also impacted the response of concrete to the indicators signifying changes in plastic cracking behaviour. Inclusion of both viscosity modifying agent (VMA) and superplasticiser in concrete can reduce plastic cracking significantly while the inclusion of only VMA can increase the plastic cracking.
- Permeability properties of plastic concrete influences the extent of plastic settlement during the early period (about 30 minutes) characterised by constant bleeding rate while the plastic settlement afterwards is inversely influenced by the initial yield stress and thixotropic index.
- The early period of rapid plastic shrinkage (for about 40 minutes) is directly related to the initial yield stress and thixotropic index, revealing a 3-dimensional anisotropic volume change process. Like the plastic shrinkage, the negative capillary pressure rate was directly

influenced for a similar period. The observed links for the plastic shrinkage and capillary pressure rate were mainly valid for the self-settlement (gravitational shearing) period, which indicated that the period is influenced by rheology.

- For the purpose of plastic cracking behaviour, the static yield stress and slump can be used as an indicator for the potential stiffening of concrete against settlement and shrinkage.
- By conducting a simple rotational shear rheology test such as torque decay during concrete's plastic state (such as within 30 minutes of concrete's end of mixing), the tendency for plastic settlement, plastic shrinkage, capillary pressure rate, and plastic settlement/shrinkage end times can be known.
- The higher the static yield stress of concrete and the more its evolution (thixotropy), the lesser the plastic settlement experienced, but the more the potential for plastic shrinkage and pressure build-up. The rigidification (storage modulus) of concrete and its suspending mortar has no significant influence on the plastic cracking processes.

7.4. Shear rheo-viscoelasticity approach to plastic cracking of concrete

This phase of the study investigated the plastic phase of plastic cracking which is majorly shear settlement dominated in an attempt to predict and examine possible damage/cracking associated. A shear rheo-viscoelastic approach was used to experimentally establish the material properties and behaviour of rheologically modified plastic concrete mixes. Viscosity modifying agent (VMA), superplasticiser (SP) and water were used as rheology modifiers. Von-Mises and Hencky (vM-H) and Bresler-Pister (B-P) theories were used as failure criteria to model the plastic crack initiation. The results show that:

- The rheology modifiers, including their viscoelastic effects, influenced the yield properties and cracking of plastic concrete without significantly influencing its stiffness (shear modulus).
- Plastic concrete has an inherent ability to relax early restrained cracking stress, this relaxation scarcely depends on the material constituents. The strain dissipation of plastic concrete mainly depends on the material constituents, especially artificial rheology modifiers. These viscoelastic properties of plastic concrete have significant effects in modelling the cracking occurrence.
- The modelling results revealed that damage/microcracking can truly occur during the early settlement dominated period of plastic cracking behaviour. It is possible to judge the internal

initiation of plastic cracking from the magnitude of the surface initial crack since it may be difficult to detect such shear-induced microcracking.

- Plastic concrete can be concluded to be majorly a strain-oriented failure, stress related failure criteria seems to predict its cracking/failure less accurately. Furthermore, plastic cracking tends to be a pressure-insensitive form of failure in which ductile failure takes prominence. It is therefore possible to accurately predict plastic cracking occurrence with simple failure criteria such as Von-Mises and Hencky theory.
- Based on the similarity between CASE I and II of vM-H theory, it can be concluded that restrained settlement and shrinkage occurring during the plastic phase mainly contributes to shear deformation.
- It is possible to passively control concrete design materials that could avoid damage/cracking during the plastic phase which can be easily and rapidly propagated by the plastic shrinkage.

7.5. Recommendations

From the postulations/theories, experiments, observations, results and conclusions that make up this study, the following aspects with potential for future studies can be identified.

- Standardising rheological methods in obtaining the failure values corresponding to standard biaxial failure stress for fresh and plastic concrete.
- An improved method of detecting and evaluating internal cracks in plastic concrete.
- A method to adequately quantify the degree of restraint in typical moulds such as the (ASTM C1579, 2006).
- Methods of making concurrent measurements of free and restrained plastic cracking strain/stress to examine the influence of viscoelasticity and compare with results of independent application of viscoelastic properties on free plastic strain/stress.
- Measuring the tensile properties of plastic concrete during the semi-plastic phase and implementing this with the earlier shear properties in the plastic phase to form a holistic approach to plastic cracking.
- Implementing both shear and tensile phases of plastic cracking in a finite element method of modelling for predicting the occurrence and propagation of cracking in restrained plastic concrete.

References

Abebe, Y.A. & Lohaus, L. 2017. Rheological characterization of the structural breakdown process to analyze the stability of flowable mortars under vibration. *Construction and Building Materials*. 131:517–525.

ACI 116R. 2000. *Cement and concrete terminology*. American Concrete Institute Committee 116: New York, US.

ACI 305.1. 2006. *Specification for hot weather concreting*. American Concrete Institute Committee 305: Farmington Hills.

ACI 308R. 2001. *Guide to curing concrete*. America Concrete Institute: Kansas City, US.

ACI 309.1R. 2008. *Report on behavior of fresh concrete during vibration*. American Concrete Institute. [Online], Available: https://www.concrete.org/store/productdetail.aspx?ItemID=309108&Format=DOWNLOAD&Language=English&Units=US_AND_METRIC [2019, May 27].

Ahari, R.S., Erdem, T.K. & Ramyar, K. 2015. Thixotropy and structural breakdown properties of self consolidating concrete containing various supplementary cementitious materials. *Cement and Concrete Composites*. 59:26–37.

Al-Qassag, O., Darwin, D. & O'Reilly, M. 2016. *Effect of a Rheology Modifier on Settlement Cracking of Concrete*. University of Kansas Center for Research, Inc.: Kansas. [Online], Available: https://kuscholarworks.ku.edu/handle/1808/20712 [2018, November 06].

Aldalinsi, M., Ferregut, C., Carrasco, C., Tandon, V. & Alderette, M. 2014. A Method to Reduce Plastic Shrinkage Cracking of Concrete Using the Re-Vibration Technique. In American Society of Civil Engineers: Reston, VA *Structures Congress 2014*. 1942–1954.

Alejano, L.R. & Bobet, A. 2012. Drucker–Prager Criterion. *Rock Mechanics and Rock Engineering*. 45(6):995–999.

Alexandridis, A. & Gardner, N.J. 1981. Mechanical behaviour of fresh concrete. *Cement and Concrete Research*. 11(3):323–339.

Alhozaimy, A.M. & Al-Negheimish, A.I. 2009. Plastic shrinkage in hot and arid environments. *Concrete international*. 31:26–32.

Ali, I. & Kesler, C.E. 1965. *Rheology of Concrete: A Review of Research*. (Bulletin (University of Illinois at Urbana Champaign. Engineering Experiment Station)). University of Illinois: Illinois. [Online],

Available: https://books.google.co.za/books?id=j3tfvgAACAAJ.

Altoubat, S.A. & Lange, D.A. 2001. Creep, Shrinkage, and Cracking of Restrained Concrete at Early Age. *ACI Materials Journal*. 98(4):323–331.

Anton-Paar. 2009. *Physica MCR Series - Instruction Manual*. Anton Paar Germany GmbH: Ostfildern.

Anton-Paar. 2012. *Electrorheological Device - Petlier Temperature Device*. Anton Paar Germany GmbH: Ostfildern.

Anton-Paar. 2016. *BMC 90 - Building material cell*. Anton Paar Germany GmbH: Ostfildern.

Artelt, C. & Garcia, E. 2008. Impact of superplasticizer concentration and of ultra-fine particles on the rheological behaviour of dense mortar suspensions. *Cement and Concrete Research*. 38(5):633–642.

Assaad, J., Khayat, K.H. & Mesbah, H. 2003a. Assessment of Thixotropy of Flowable and Self-Consolidating Concrete. *ACI Materials Journal*. 100(2):99–107.

Assaad, J., Khayat, K.H. & Mesbah, H. 2003b. Variation of formwork pressure with thixotropy of self-consolidating concrete. *ACI Materials Journal*. 100(1):29–37.

Assaad, J., Khayat, K.H. & Daczko, J. 2004. Evaluation of Static Stability of Self-Consolidating Concrete. *ACI Materials Journal*. 101(3):207–215.

Assaad, J.J., Harb, J. & Maalouf, Y. 2014. Measurement of yield stress of cement pastes using the direct shear test. *Journal of Non-Newtonian Fluid Mechanics*. 214:18–27.

ASTM C1579. 2006. *Standard Test Method for Evaluating Plastic Shrinkage Cracking of Restrained Fiber Reinforced Concrete (Using a Steel Form Insert)*. West Conshohocken. [Online], Available: https://www.astm.org/Standards/C1579.htm [2018, October 28].

ASTM C232. 2004. *Standard Test Methods for Bleeding of Concrete*. New York.

Banfill, P.F.G. 1991. Rheology of fresh cement and concrete - a review. In E. & F.N. Spon: Liverpool *Rheology of fresh cement and concrete*. 373. [Online], Available: https://www.crcpress.com/Rheology-of-Fresh-Cement-and-Concrete-Proceedings-of-an-International-Conference/Banfill/p/book/9780419153603 [2019, May 16].

Banfill, P.F.G. 2003. The rheology of fresh cement and concrete - a review. In Durban, South Africa *Proceedings of the 11th International Congress on the Chemistry of Cement (ICCC), Cement's Contribution to Development in the 21st Century*. 50–62.

Banfill, P.F.G., Teixeira, M.A.O.M. & Craik, R.J.M. 2011. Rheology and vibration of fresh concrete: Predicting the radius of action of poker vibrators from wave propagation. *Cement and Concrete Research*. 41(9):932–941.

Barnes, H.A. 1989. Shear-Thickening ("Dilatancy") in Suspensions of Nonaggregating Solid Particles Dispersed in Newtonian Liquids. *Journal of Rheology*. 33(2):329–366.

Barnes, H.A. 1997. Thixotropy—a review. *Journal of Non-Newtonian Fluid Mechanics*. 70(1–2):1–33.

Barnes, H.A., Hutton, J.F. & Walters, K. 2001. *An introduction to rheology*. Elsevier.

Bazant, Z.P. 1975. Theory of creep and shrinkage in concrete structures: a precis of recent developments. In 2nd ed. S. Nemat-Nasser (ed.). Pergamon Press: New York *Mechanics Today*. 1–93.

Bazant, Z.P. & Gettu, R. 1992. Rate Effects and Load Relaxation in Static Fracture of Concrete. *ACI Materials Journal*. 89(5).

Bellotto, M. 2013. Cement paste prior to setting: A rheological approach. *Cement and Concrete Research*. 52:161–168.

Bentz, D.P., Ferraris, C.F., Galler, M.A., Hansen, A.S. & Guynn, J.M. 2012. Influence of particle size distributions on yield stress and viscosity of cement–fly ash pastes. *Cement and Concrete Research*. 42(2):404–409.

Bhatty, J.I. & Banfill, P.F.G. 1982. Sedimentation behaviour in cement pastes subjected to continuous shear in rotational viscometers. *Cement and Concrete Research*. 12(1):69–78.

Bissonnette, B. & Pigeon, M. 1995. Tensile creep at early ages of ordinary, silica fume and fiber reinforced concretes. *Cement and Concrete Research*. 25(5):1075–1085.

Boshoff, W.P. & Combrinck, R. 2013. Modelling the severity of plastic shrinkage cracking in concrete. *Cement and Concrete Research*. 48:34–39.

Boswell, L.F. & Chen, Z. 1987. A general failure criterion for plain concrete. *International Journal of Solids and Structures*. 23(5):621–630.

Bouras, R., Chaouche, M. & Kaci, S. 2008. Influence of Viscosity-Modifying Admixtures on the Thixotropic Behaviour of Cement Pastes. *Applied Rheology*. 18(4):1–8. [Online], Available: http://www.complexfluids.ethz.ch/cgi-bin/AR/ar_contents?getpdf=18_45604&RA=146.232.18.245&text=%3Cfont color=000000%3ERachid Bouras, Mohend Chaouche, Salah Kaci%3Cbr%3E%3Cb%3EInfluence

of Viscosity-Modifying Admixtures on the Thixo.

Bouras, R., Kaci, A. & Chaouche, M. 2012. Influence of viscosity modifying admixtures on the rheological behavior of cement and mortar pastes. *Korea-Australia Rheology Journal*. 24(1):35–44.

Briffaut, M., Benboudjema, F., Torrenti, J.-M. & Nahas, G. 2012. Concrete early age basic creep: Experiments and test of rheological modelling approaches. *Construction and Building Materials*. 36:373–380.

Brooks, J.J. 2005. 30-year creep and shrinkage of concrete. *Magazine of Concrete Research*. 57(9):545–556.

Brower, L.E. & Ferraris, C.F. 2006. Comparison of Concrete Rheometers. *Special Publication*. 233:117–136.

BS EN 1097-6. 2013. *Tests for mechanical and physical properties of aggregates - Determination of particle density and water absorption*. BSI Standards Limited.

BS EN 196-3. 2005. *Methods of testing cement. Determination of setting times and soundness*. London.

BS EN 933-1. 2012. *Tests for geometrical properties of aggregates. Determination of particle size distribution. Sieving method*. [Online], Available: https://shop.bsigroup.com/ProductDetail/?pid=000000000030241873 [2019, November 06].

de Cagny, H., Fazilati, M., Habibi, M., Denn, M.M. & Bonn, D. 2019. The yield normal stress. *Journal of Rheology*. 63(2):285–290.

CCIP-048. 2010. *Technical Report No. 22: Non-structural cracks in concrete*. The Concrete Society: A Cement and Concrete Industry Publication: Surrey, UK.

Chhabra, R.P. 2010. Non-Newtonian Fluids: An Introduction. In Springer New York: New York, NY *Rheology of Complex Fluids*. 3–34.

Chia, K.-S., Kho, C.-C. & Zhang, M.-H. 2005. Stability of Fresh Lightweight Aggregate Concrete under Vibration. *ACI Materials Journal*. 102(5):347–354.

Choi, M., Park, K. & Oh, T. 2016. Viscoelastic Properties of Fresh Cement Paste to Study the Flow Behavior. *International Journal of Concrete Structures and Materials*. 10(S3):65–74.

Choplin, L. & Marchal, P. 2010. Mixer-type rheometry. In First ed. C. Gallegos (ed.). Encyclopedia of

life support systems (EOLSS) Publishers: United Kingdom *RHEOLOGY - Volume II*. 32–51.

Chougnet, A., Audibert, A. & Moan, M. 2007. Linear and non-linear rheological behaviour of cement and silica suspensions. Effect of polymer addition. *Rheologica Acta*. 46(6):793–802.

Chryso. 2012. *Quad 20 - rheology robustness enhancer*. Chryso-Group: Paris.

Chryso. 2014. *Optima 206 - high range water reducing super plasticizing admixture*. Paris.

Combrinck, R. 2011. Plastic shrinkage cracking in concrete in conventional and low volume fibre reinforced concrete. MSc Thesis, Department of Civil Engineering, Stellenbosch University.

Combrinck, R. 2016. Cracking of Plastic Concrete in Slab-Like Elements. PhD Thesis, Department of Civil Engineering, Stellenbosch University.

Combrinck, R. & Boshoff, W.P. 2009. *Report number ISI2009-31: Plastic shrinkage cracking of fresh concrete*. Institute of Structural Engineering, Department of Civil Engineering, Stellenbosch University.

Combrinck, R. & Boshoff, W.P. 2013. Typical plastic shrinkage cracking behaviour of concrete. *Magazine of Concrete Research*. 65(8):486–493.

Combrinck, R. & Boshoff, W.P. 2019. Tensile properties of plastic concrete and the influence of temperature and cyclic loading. *Cement and Concrete Composites*. 97:300–311.

Combrinck, R., Steyl, L. & Boshoff, W.P. 2017. Influence of depth on the cracking of plastic concrete. In Brussels *Early age cracking and serviceability in cement-based materials and structures - EAC2*.

Combrinck, R., Steyl, L. & Boshoff, W.P. 2018a. Interaction between settlement and shrinkage cracking in plastic concrete. *Construction and Building Materials*. 185:1–11.

Combrinck, R., Steyl, L. & Boshoff, W.P. 2018b. Influence of concrete depth and surface finishing on the cracking of plastic concrete. *Construction and Building Materials*. 175:621–628.

Combrinck, R., Kayondo, M., le Roux, B.D., de Villiers, W.I. & Boshoff, W.P. 2019. Effect of various liquid admixtures on cracking of plastic concrete. *Construction and Building Materials*. 202:139–153.

Conte, T. & Chaouche, M. 2016. Rheological behavior of cement pastes under Large Amplitude Oscillatory Shear. *Cement and Concrete Research*. 89:332–344.

Coussot, P., Nguyen, Q.D., Huynh, H.T. & Bonn, D. 2002. Viscosity bifurcation in thixotropic, yielding

fluids. *Journal of Rheology*. 46(3):573–589.

Cyr, M., Legrand, C. & Mouret, M. 2000. Study of the shear thickening effect of superplasticizers on the rheological behaviour of cement pastes containing or not mineral additives. *Cement and Concrete Research*. 30(9):1477–1483.

Dao, V.T.N., Dux, P.F. & Morris, P.H. 2009. Tensile Properties of Early-Age Concrete. *ACI Materials Journal*. 106(6):483–492.

Dao, V.T.N., Dux, P.F., Morris, P.H. & O'Moore, L. 2010. Plastic Shrinkage Cracking of Concrete. *Australian Journal of Structural Engineering*. 10(3):207–214.

Dede, T. & Ayvaz, Y. 2010. Plasticity models for concrete material based on different criteria including Bresler–Pister. *Materials & Design*. 31(1):278–286.

Dias, W.P.S. 2003. Influence of mix and environment on plastic shrinkage cracking. *Magazine of Concrete Research*. 55(4):385–394.

Dzuy, N.Q. & Boger, D. V. 1985. Direct Yield Stress Measurement with the Vane Method. *Journal of Rheology*. 29(3):335–347.

Elsharief, A., Cohen, M.D. & Olek, J. 2003. Influence of aggregate size, water cement ratio and age on the microstructure of the interfacial transition zone. *Cement and Concrete Research*. 33(11):1837–1849.

Esmaeilkhanian, B., Khayat, K.H., Yahia, A. & Feys, D. 2014. Effects of mix design parameters and rheological properties on dynamic stability of self-consolidating concrete. *Cement and Concrete Composites*. 54:21–28.

Ferraris, C.F. & Gaidis, J.M. 1992. Connection between the rheology of concrete and rheology of cement paste. *ACI Materials Journal*. 89(4):388–393.

Ferraris, C.F. & Martys, N.S. 2012. Concrete rheometers. In First ed. N. Roussel (ed.). Woodhead Publishing *Understanding the Rheology of Concrete*. 63–82.

Ferron, R.P., Gregori, A., Sun, Z. & Shah, S.P. 2007. Rheological Method to Evaluate Structural Buildup in Self-Consolidating Concrete Cement Pastes. *ACI Materials Journal*. 104(3):242–250.

Feys, D., Verhoeven, R. & De Schutter, G. 2008. Fresh self compacting concrete, a shear thickening material. *Cement and Concrete Research*. 38(7):920–929.

fib Model Code. 2010. *fib Bulletin 55. Model Code 2010 First complete draft Volume 1*. (fib Bulletins).

fib. The International Federation for Structural Concrete: Switzerland.

Flatt, R.J. 2004. Dispersion forces in cement suspensions. *Cement and Concrete Research*. 34(3):399–408.

Flatt, R. & Schober, I. 2012. Superplasticizers and the rheology of concrete. In 1st ed. Nicolas Roussel (ed.). Woodhead Publishing *Understanding the Rheology of Concrete*. 144–208.

Fossen, H. 2010. *Structural geology*. Cambridge University Press.

Franck, A. 2004. *Understanding rheology of structured fluids*. TA Instruments - AAN016: New Castle, US.

Franck, A.J. 2005. *Understanding instrument inertia corrections in oscillation*. TA Instruments - APN006.

Geiker, M.R., Brandl, M., Thrane, L.N., Bager, D.H. & Wallevik, O. 2002. The effect of measuring procedure on the apparent rheological properties of self-compacting concrete. *Cement and Concrete Research*. 32(11):1791–1795.

Gerhart, P.M., Gerhart, A.L. & Hochstein, J.I. 2018. *Fundamentals of Fluid Mechanics*. Eigth ed. Wiley & Sons: Kendallville. [Online], Available: https://www.wiley.com/en-us/Fundamentals+of+Fluid+Mechanics%2C+8th+Edition-p-9781119547990 [2019, September 19].

Germann Instruments A/S. 2015. *ICAR rheometer manual*. German Instruments A/S: Copenhagen.

Ghourchian, S., Wyrzykowski, M. & Lura, P. 2016. The bleeding test: A simple method for obtaining the permeability and bulk modulus of fresh concrete. *Cement and Concrete Research*. 89:249–256.

Ghourchian, S., Wyrzykowski, M., Baquerizo, L. & Lura, P. 2018. Susceptibility of Portland cement and blended cement concretes to plastic shrinkage cracking. *Cement and Concrete Composites*. 85:44–55.

Ghourchian, S., Wyrzykowski, M., Plamondon, M. & Lura, P. 2019. On the mechanism of plastic shrinkage cracking in fresh cementitious materials. *Cement and Concrete Research*. 115:251–263.

Gibbs, G.B. 1966. Creep and stress relaxation studies with polycrystalline magnesium. *Philosophical Magazine*. 13(122):317–329.

Gill, S.M. & Banfill, P.F.G. 1988. The viscometric examination of cement pastes with interrupted helical impellers. *Advances in Cement Research*. 1(2):92–98.

Gołaszewski, J. & Szwabowski, J. 2004. Influence of superplasticizers on rheological behaviour of fresh cement mortars. *Cement and Concrete Research*. 34(2):235–248.

Gregory, T. & O'Keefe, S.J. 1990. Rheological measurements on fresh polymer-modified cement paste. In P.F.G. Banfill (ed.). Taylor and Francis: Liverpool *Rheology of Fresh Cement and Concrete: Proceedings of an International ... - Google Books*. 353. [Online], Available: https://books.google.co.za/books?id=MUtZDwAAQBAJ&pg=PA69&lpg=PA69&dq=Gregory,+T+and+O'Keefe,+S+J,+"Rheological+measurements+on+fresh+polymer-modified+cement+pastes",&source=bl&ots=7CjtZdFPxg&sig=ACfU3U0Ruv57b9EwhK0fvDT5UrpoCwOl4A&h [2019, June 21].

He, Z., Jiang, R. & Li, Y. 2018a. Dynamic Rheological Behavior of Low Water-to-binder Ratio Mortars under Large Amplitude Oscillatory Shear (LAOS). *Journal of Wuhan University of Technology-Mater. Sci. Ed.* 33(3):608–618.

He, Z., Jiang, R. & Li, Y. 2018b. Viscoelasticity characteristics of mortars in static and dynamic rheological test. *Shuili Xuebao/Journal of Hydraulic Engineering*. 49(5):561–569.

Hibbeler, R.C. 2014. *Mechanics of materials*. Ninth ed. Prentice Hall: New Jersey.

Hocevar, A., Kavcic, F. & Bokan-Bosiljkov, V. 2013. Rheological parameters of fresh concrete - comparison of rheometers. *Gradevinar*. 65(2):99–109.

Hocking, R.R. 2003. *Methods and Applications of Linear Models*. Second ed. John Wiley & Sons, Inc.: New Jersey.

Hoffman, R.L. 1998. Explanations for the cause of shear thickening in concentrated colloidal suspensions. *Journal of Rheology*. 42(1):111.

Holt, E. & Leivo, M. 2004. Cracking risks associated with early age shrinkage. *Cement and Concrete Composites*. 26(5):521–530.

Hossain, A.B. & Weiss, J. 2004. Assessing residual stress development and stress relaxation in restrained concrete ring specimens. *Cement and Concrete Composites*. 26(5):531–540.

Hu, J. & Wang, K. 2011. Effect of coarse aggregate characteristics on concrete rheology. *Construction and Building Materials*. 25(3):1196–1204.

Hu, J., Ge, Z. & Wang, K. 2014. Influence of cement fineness and water-to-cement ratio on mortar

early-age heat of hydration and set times. *Construction and Building Materials*. 50:657–663.

Hu, Z., Hilaire, A., Ston, J., Wyrzykowski, M., Lura, P. & Scrivener, K. 2019. Intrinsic viscoelasticity of C-S-H assessed from basic creep of cement pastes. *Cement and Concrete Research*. 121:11–20.

Huang, L., Hua, J., Kang, M., Luo, Q. & Zhou, F. 2019. Influence of Steel Plates and Studs on Shrinkage Behavior and Cracking Potential of High-Performance Concrete. *Materials*. 12(3).

Hyun, K., Wilhelm, M., Klein, C.O., Cho, K.S., Nam, J.G., Ahn, K.H., Lee, S.J., Ewoldt, R.H., et al. 2011. A review of nonlinear oscillatory shear tests: Analysis and application of large amplitude oscillatory shear (LAOS). *Progress in Polymer Science*. 36(12):1697–1753.

Isacsson, U. & Zeng, H. 1998. Cracking of asphalt at low temperature as related to bitumen rheology. *Journal of Materials Science*. 33(1):2165–2170.

Isik, I.E. & Ozkul, M.H. 2014. Utilization of polysaccharides as viscosity modifying agent in self-compacting concrete. *Construction and Building Materials*. 72:239–247.

Jarny, S., Roussel, N., Rodts, S., Bertrand, F., Le Roy, R. & Coussot, P. 2005. Rheological behavior of cement pastes from MRI velocimetry. *Cement and Concrete Research*. 35(10):1873–1881.

Jayasree, C., Murali Krishnan, J. & Gettu, R. 2011. Influence of superplasticizer on the non-Newtonian characteristics of cement paste. *Materials and Structures*. 44(5):929–942.

Jiang, J.-F. & Wu, Y.-F. 2012. Identification of material parameters for Drucker–Prager plasticity model for FRP confined circular concrete columns. *International Journal of Solids and Structures*. 49(3–4):445–456.

Jiang, W. & Roy, D.M. 1992. Microstructure and Flow Behavior of Fresh Cement Paste. *MRS Proceedings*. 289:161.

Jiang, S.P., Mutin, J.C. & Nonat, A. 1995. Studies on mechanism and physico-chemical parameters at the origin of the cement setting. I. The fundamental processes involved during the cement setting. *Cement and Concrete Research*. 25(4):779–789.

Jiang, S.P., Mutin, J.C. & Nonat, A. 1996. Studies on mechanism and physico-chemical parameters at the origin of the cement setting II. Physico-chemical parameters determining the coagulation process. *Cement and Concrete Research*. 26(3):491–500.

Jiao, D., Shi, C., Yuan, Q., An, X., Liu, Y. & Li, H. 2017. Effect of constituents on rheological properties of fresh concrete-A review. *Cement and Concrete Composites*. 83:146–159.

Jones, R.M. 2009. *Deformation theory of plasticity*. First ed. Bull Ridge Publishing: Virgina.

Juradin, S. 2011. Determination of rheological properties of fresh concrete and similar materials in a vibration rheometer. *Materials Research*. 15(1):103–113.

Kayondo, M., Combrinck, R. & Boshoff, W.P. 2019. State-of-the-art review on plastic cracking of concrete. *Construction and Building Materials*. 225:886–899.

Khan, M.Y. 2018. The tensile material properties of plastic concrete and the influence on plastic cracking. SUNScholar Research Repository.

Khan, I., Castel, A. & Gilbert, R.I. 2016. Prediction of early-age creep and cracking age of concrete: a proposed modification for AS3600 provisions. *Australian Journal of Structural Engineering*. 17(2):151–166.

Khan, I., Castel, A. & Gilbert, R.I. 2017. Tensile creep and early-age concrete cracking due to restrained shrinkage. *Construction and Building Materials*. 149:705–715.

Khan, M.Y., Kolawole, J.T., Boshoff, W.P. & Combrinck, R. 2017. Influence of relaxation and cyclic loading on the tensile material properties of plastic concrete. In S. Staquet & D. Aggelis (eds.). RILEM Publications S.A.R.L.: Brussels *2nd International RILEM/COST Conference on Early Age Cracking and Serviceability in Cement-based Materials and Structures (EAC2)*. 379–384. [Online], Available: https://www.rilem.net/publications/proceedings-500218.

Khayat, K.H. 1998. Viscosity-enhancing admixtures for cement-based materials — An overview. *Cement and Concrete Composites*. 20(2):171–188.

Khayat, K.H. & Mikanovic, N. 2012. Viscosity-enhancing admixtures and the rheology of concrete. In First ed. N. Roussel (ed.). Woodhead Publishing: Cambridge *Understanding the Rheology of Concrete*.

Khayat, K., Saric-Coric, M. & Liotta, F. 2002. Influence of thixotropy on stability characteristics of cement grout and concrete. *ACI Materials Journal*. 99(3):234–241.

Khayat, K.H., Yahia, A. & Sayed, M. 2008. Effect of supplementary cementitious materials on rheological properties, bleeding, and strength of structural grout. *ACI Materials Journal*. 105(6):585–593.

Khayat, K.H., Omran, A. & Magdi, W.A. 2012. Evaluation of thixotropy of self-consolidating concrete and influence on concrete performance. In IBRACON: Maceio *ANAIS DO 54º CONGRESSO BRASILEIRO DO CONCRETO - CBC2012 – 54CBC*.

Kim, J.H., Yim, H.J. & Kwon, S.H. 2014. Quantitative measurement of the external and internal bleeding of conventional concrete and SCC. *Cement and Concrete Composites*. 54:34–39.

Kim, J.H., Kwon, S.H., Kawashima, S. & Yim, H.J. 2017. Rheology of cement paste under high pressure. *Cement and Concrete Composites*. 77:60–67.

Kim, Y.J., Cho, B.-Y., Lee, S.-J., Hu, J. & Wilde, J.W. 2018. Investigation of Rheological Properties of Blended Cement Pastes Using Rotational Viscometer and Dynamic Shear Rheometer. *Advances in Materials Science and Engineering*. 2018:1–6.

Kinloch, A.J. & Young, R.J. 1995. *Fracture behaviour of polymers*. First ed. Springer-Science+Business Media Dordrecht: Dordrecht.

Knoppik-Wróbel, A. & Klemczak, B. 2015. Degree of restraint concept in analysis of early-age stresses in concrete walls. *Engineering Structures*. 102:369–386.

Koehler, E.P. 2013. Thixotropy of SCC and its effects on formwork pressure. In America Concrete Institute: Minneapolis *ACI Spring 2013 Convention*.

Koehler, E.P. & Fowler, D.W. 2004. *Development of a portable rheometer for fresh Portland cement concrete*. ICAR Report 105-3F.

Kolawole, J.T., Combrinck, R. & Boshoff, W.P. 2019a. Measuring the thixotropy of conventional concrete: The influence of viscosity modifying agent, superplasticiser and water. *Construction and Building Materials*. 225:853–867.

Kolawole, J.T., Combrinck, R. & Boshoff, W.P. 2019b. Rheo-viscoelastic behaviour of cement-based materials: cement paste, mortar and concrete. *Submitted to Construction and Building Materials*.

Kolawole, J.T., Combrinck, R. & Boshoff, W.P. 2019c. Plastic cracking behaviour of concrete and its interdependence on rheo-physical properties. *Submitted to Construction and Building Materials*.

Kolver, K., Igarashi, S. & Bentur, A. 1999. Tensile creep behavior of high strength concretes at early ages. *Materials and Structures*. 32(5):383–387.

Kruger, J., Zeranka, S. & van Zijl, G. 2019. An ab initio approach for thixotropy characterisation of (nanoparticle-infused) 3D printable concrete. *Construction and Building Materials*. 224:372–386.

Kwak, H.-G. & Ha, S.-J. 2006. Plastic shrinkage cracking in concrete slabs. Part I: a numerical model.

Magazine of Concrete Research. 58(8):505–516.

Lapasin, R., Papo, A. & Rajgelj, S. 1983. Flow behavior of fresh cement pastes. A comparison of different rheological instruments and techniques. *Cement and Concrete Research*. 13(3):349–356.

Larson, R.G. & Wei, Y. 2019. A review of thixotropy and its rheological modeling. *Journal of Rheology*. 63(3):477–501.

Leemann, A., Nygaard, P. & Lura, P. 2014. Impact of admixtures on the plastic shrinkage cracking of self-compacting concrete. *Cement and Concrete Composites*. 46:1–7.

Li, Z. & Cao, G. 2019. Rheological behaviors and model of fresh concrete in vibrated state. *Cement and Concrete Research*. 120:217–226.

Li, H., Huang, F., Xie, Y., Yi, Z. & Wang, Z. 2017. Effect of water–powder ratio on shear thickening response of SCC. *Construction and Building Materials*. 131:585–591.

Lin, S.-T. & Huang, R. 2010. Effect of viscosity modifying agent on plastic shrinkage cracking of cementitious composites. *Materials and Structures*. 43(5):651–664.

Liu, J., Tian, Q. & Miao, C. 2012. Investigation on the plastic shrinkage of cementitious materials under drying conditions: mechanism and theoretical model. *Magazine of Concrete Research*. 64(6):551–561.

Lootens, D., Jousset, P., Martinie, L., Roussel, N. & Flatt, R.J. 2009. Yield stress during setting of cement pastes from penetration tests. *Cement and Concrete Research*. 39(5):401–408.

Lura, P., Pease, B., Mazzotta, G.B., Rajabipour, F. & Weiss, J. 2007. Influence of Shrinkage-Reducing Admixtures on Development of Plastic Shrinkage Cracks. *ACI Materials Journal*. 104(2):187–194.

Lura, P., Couch, J., Jensen, O.M. & Weiss, J. 2009. Early-age acoustic emission measurements in hydrating cement paste: Evidence for cavitation during solidification due to self-desiccation. *Cement and Concrete Research*. 39(10):861–867.

Ma, S., Qian, Y. & Kawashima, S. 2018. Experimental and modeling study on the non-linear structural build-up of fresh cement pastes incorporating viscosity modifying admixtures. *Cement and Concrete Research*. 108:1–9.

Mahaut, F., Mokéddem, S., Chateau, X., Roussel, N. & Ovarlez, G. 2008. Effect of coarse particle volume fraction on the yield stress and thixotropy of cementitious materials. *Cement and*

Concrete Research. 38(11):1276–1285.

Mahaut, F., Chateau, X., Coussot, P. & Ovarlez, G. 2008. Yield stress and elastic modulus of suspensions of noncolloidal particles in yield stress fluids. *Journal of Rheology*. 52(1):287–313.

Mallick, S., Anoop, M.B. & Balaji Rao, K. 2019. Early age creep of cement paste - Governing mechanisms and role of water-A microindentation study. *Cement and Concrete Research*. 116:284–298.

Mangesana, N., Chikuku, R.S., Mainza, A.N., Govender, I., van der Westhuizen, A.P. & Narashima, M. 2008. Journal of the South African Institute of Mining and Metallurgy. *Journal of the Southern African Institute of Mining and Metallurgy*. 108(4):237–243. [Online], Available: http://www.scielo.org.za/scielo.php?script=sci_arttext&pid=S2225-62532008000400005 [2019, July 10].

Mardani-Aghabaglou, A., Tuyan, M., Yılmaz, G., Arıöz, Ö. & Ramyar, K. 2013. Effect of different types of superplasticizer on fresh, rheological and strength properties of self-consolidating concrete. *Construction and Building Materials*. 47:1020–1025.

Maritz, J. 2012. An investigation into the use of low volume - fibre reinforced concrete for controlling plastic shrinkage cracking. MSc Thesis, Department of Civil Engineering, Stellenbosch University.

Marques, S.P.C. & Creus, G.J. 2012. *Computational Viscoelasticity*. (SpringerBriefs in Applied Sciences and Technology). Springer Berlin Heidelberg: Berlin, Heidelberg.

Maybury, J. & Ho, J.C.M. 2017. Shear thickening of cement powder paste – why and how to mitigate? *HKIE Transactions*. 24(4):193–203.

Mazzeo, F.A. 2008. *Importance of oscillatory time sweeps in rheology*. TA Instruments: New Castle.

Mehdipour, I. & Khayat, K.H. 2018. Understanding the role of particle packing characteristics in rheo-physical properties of cementitious suspensions: A literature review. *Construction and Building Materials*. 161:340–353.

Mehta, K. & Burrows, R.W. 2001. Building durable structures in the 21st century. *Concrete international*. 57–63.

Mehta, P.K. & Monteiro, P.J.M. 2006. *Concrete: microstructure, properties, and materials.* McGraw-Hill. [Online], Available: https://books.google.co.za/books/about/Concrete.html?id=3j5EAQAAIAAJ&redir_esc=y

[2019, May 21].

Mernard, K.P. 1999. *Dynamic Mechanical Analysis: A Practical Introduction*. 1st ed. CRC Press: New York.

Mettler, L.K., Wittel, F.K., Flatt, R.J. & Herrmann, H.J. 2016. Evolution of strength and failure of SCC during early hydration. *Cement and Concrete Research*. 89:288–296.

Mewis, J. & Wagner, N.J. 2009. Thixotropy. *Advances in Colloid and Interface Science*. 147–148:214–227.

Mezger, G.T. 2006. *The rheology handbook*. Second ed. Hannover: Vincentz Network: Hannover.

Mezger, T.G. 2014. *Rheology handbook : for users of rotational and oscillatory rheometers.* 4th ed. Vincentz Network: Hanover.

Morris, P.H. & Dux, P.F. 2005. A Review of ACI Recommendations for Prevention of Plastic Cracking. *ACI Materials Journal*. 102(5):307–314.

Mostafa, A.M. & Yahia, A. 2016. New approach to assess build-up of cement-based suspensions. *Cement and Concrete Research*. 85:174–182.

Mostafa, A.M. & Yahia, A. 2017. Physico-chemical kinetics of structural build-up of neat cement-based suspensions. *Cement and Concrete Research*. 97:11–27.

Nachbaur, L., Mutin, J.C., Nonat, A. & Choplin, L. 2001. Dynamic mode rheology of cement and tricalcium silicate pastes from mixing to setting. *Cement and Concrete Research*. 31(2):183–192.

Nehdi, M. & Al Martini, S. 2007. Effect of Temperature on Oscillatory Shear Behavior of Portland Cement Paste Incorporating Chemical Admixtures. *Journal of Materials in Civil Engineering*. 19(12):1090–1100.

Nehdi, M. & Al Martini, S. 2009. Estimating time and temperature dependent yield stress of cement paste using oscillatory rheology and genetic algorithms. *Cement and Concrete Research*. 39(11):1007–1016.

Newman, J.B. & Choo, B.S. 2003. *Advanced concrete technology : constituent materials*. Butterworth-Heinemann.

Nguyen, D.H., Dao, V.T.N. & Lura, P. 2017. Tensile properties of concrete at very early ages. *Construction and Building Materials*. 134:563–573.

Nilsson, M. 2003. Restraint factors and partial coefficients for crack risk analyses of early age concrete structures. Lulea University of Technology.

Nonat, A., Mutin, J.C., Lecoq, X. & Jiang, S.P. 1997. Physico-chemical parameters determining hydration and particle interactions during the setting of silicate cements. *Solid State Ionics*. 101–103:923–930.

Ogee, A., Ellis, M., Scibilia, B., Pammer, C. & Steele, C. 2013. *Multiple Regression Analysis: Use Adjusted R-Squared and Predicted R-Squared to Include the Correct Number of Variables*. Pennsylvania. [Online], Available: https://blog.minitab.com/blog/adventures-in-statistics-2/multiple-regession-analysis-use-adjusted-r-squared-and-predicted-r-squared-to-include-the-correct-number-of-variables [2019, June 30].

Olhero, S.. & Ferreira, J.M.. 2004. Influence of particle size distribution on rheology and particle packing of silica-based suspensions. *Powder Technology*. 139(1):69–75.

Olivier, G., Combrinck, R., Kayondo, M. & Boshoff, W.P. 2018. Combined effect of nano-silica, super absorbent polymers, and synthetic fibres on plastic shrinkage cracking in concrete. *Construction and Building Materials*. 192:85–98.

Østergaard, L., Lange, D.A., Altoubat, S.A. & Stang, H. 2001. Tensile basic creep of early-age concrete under constant load. *Cement and Concrete Research*. 31(12):1895–1899.

Pane, I. & Hansen, W. 2002. Early age creep and stress relaxation of concrete containing blended cements. *Materials and Structures*. 35(2):92–96.

Papo, A. & Caufin, B. 1991. A study of the hydration process of cement pastes by means of oscillatory rheological techniques. *Cement and Concrete Research*. 21(6):1111–1117.

Papo, A. & Piani, L. 2004. Effect of various superplasticizers on the rheological properties of Portland cement pastes. *Cement and Concrete Research*. 34(11):2097–2101.

Pasternack, B. & Lruzzi, A. 1965. Patterns in Residuals: A Test for Regression Model Adequacy in Radionuclide Assay. *Technometrics*. 7(4):603–621.

Peng, Y. & Jacobsen, S. 2013. Influence of water/cement ratio, admixtures and filler on sedimentation and bleeding of cement paste. *Cement and Concrete Research*. 54:133–142.

Perrot, A., Lecompte, T., Khelifi, H., Brumaud, C., Hot, J. & Roussel, N. 2012. Yield stress and bleeding of fresh cement pastes. *Cement and Concrete Research*. 42(7):937–944.

Petrou, M.F., Harries, K.A., Gadala-Maria, F. & Kolli, V.G. 2000. A unique experimental method for

monitoring aggregate settlement in concrete. *Cement and Concrete Research*. 30(5):809–816.

Phan, T.H., Chaouche, M. & Moranville, M. 2006. Influence of organic admixtures on the rheological behaviour of cement pastes. *Cement and Concrete Research*. 36(10):1807–1813.

Powers, T.C. 1968. *The properties of fresh concrete*. Wiley: New York.

Powers, V. 1993. *The Bakelizer*. Washington, D.C., US. [Online], Available: https://www.acs.org/content/acs/en/education/whatischemistry/landmarks/bakelite.html#citation.

Prakash, N. & Santhanam, M. 2006. A study on the interaction between viscosity modifying agent and high range water reducer in self compacting concrete. In Springer Netherlands: Dordrecht *Measuring, Monitoring and Modeling Concrete Properties*. 449–454.

Qian, Y. & Kawashima, S. 2016. Use of creep recovery protocol to measure static yield stress and structural rebuilding of fresh cement pastes. *Cement and Concrete Research*. 90:73–79.

Qian, Y. & Kawashima, S. 2018. Distinguishing dynamic and static yield stress of fresh cement mortars through thixotropy. *Cement and Concrete Composites*. 86:288–296.

Quanji, Z. 2010. Thixotropic behavior of cement-based materials: effect of clay and cement types. Iowa State University.

Rahman, M.K., Baluch, M.H. & Malik, M.A. 2014. Thixotropic behavior of self compacting concrete with different mineral admixtures. *Construction and Building Materials*. 50:710–717.

Rajgelj, S. 1985. Cohesion aspects in rheological behaviour of fresh cement mortars. *Materials and Structures*. 18(2):109–114.

Reiterer, M., Kraft, T., Janosovits, U. & Riedel, H. 2004. Finite element simulation of cold isostatic pressing and sintering of SiC components. *Ceramics International*. 30(2):177–183.

Rossi, P. & Acker, P. 1988. A new approach to the basic creep and relaxation of concrete. *Cement and Concrete Research*. 18(5):799–803.

Roussel, N. 2006. A thixotropy model for fresh fluid concretes: Theory, validation and applications. *Cement and Concrete Research*. 36(10):1797–1806.

Roussel, N. 2007. A Theoretical Frame to Study Stability of Fresh Concrete. *Materials and Structures*. 39(1):81–91.

Roussel, N. 2012. *Understanding the rheology of concrete*. PA : Woodhead Publishing: Philadelphia.

Roussel, N., Lemaître, A., Flatt, R.J. & Coussot, P. 2010. Steady state flow of cement suspensions: A micromechanical state of the art. *Cement and Concrete Research*. 40(1):77–84.

Roussel, N., Ovarlez, G., Garrault, S. & Brumaud, C. 2012. The origins of thixotropy of fresh cement pastes. *Cement and Concrete Research*. 42(1):148–157.

Roussel, N., Bessaies-Bey, H., Kawashima, S., Marchon, D., Vasilic, K. & Wolfs, R. 2019. Recent advances on yield stress and elasticity of fresh cement-based materials. *Cement and Concrete Research*. 124:105798.

Roziere, E., Cortas, R. & Loukili, A. 2015. Tensile behaviour of early age concrete: New methods of investigation. *Cement and Concrete Composites*. 55:153–161.

Saak, A.W., Jennings, H.M. & Shah, S.P. 2001. New Methodology for Designing Self-Compacting Concrete. *ACI Materials Journal*. 98(6):429–439.

Saasen, A., Marken, C., Dawson, J. & Rogers, M. 1991. Oscillating rheometer measurements on oilfield cement slurries. *Cement and Concrete Research*. 21(1):109–119.

Safiuddin, M., Kaish, A., Woon, C.-O., Raman, S., Safiuddin, M., Kaish, A.B.M.A., Woon, C.-O. & Raman, S.N. 2018. Early-Age Cracking in Concrete: Causes, Consequences, Remedial Measures, and Recommendations. *Applied Sciences*. 8(10):1730.

Samman, T.A., Mirza, W.H. & Wafa, F.F. 1996. Plastic Shrinkage Cracking of Normal and High-Strength Concrete: A Comparative Study. *ACI Materials Journal*. 93(1):36–40.

Sant, G., Ferraris, C.F. & Weiss, J. 2008. Rheological properties of cement pastes: A discussion of structure formation and mechanical property development. *Cement and Concrete Research*. 38(11):1286–1296.

Sant, G., Dehadrai, M., Bentz, D. & Weiss, W.J. 2009. Detecting the fluid-to-solid transition in cement pastes: assessment techniques. *Concrete international*. 31(6).

Sant, G., Dehadrai, M., Bentz, D., Lura, P., Ferraris, C.F., Bullard, J.W. & Weiss, J. 2009. Detecting the Fluid-to-Solid Transition in Cement Pastes: Comparing experimental and numerical techniques. *Concrete International*. 31(6):53–58.

Saric-Coric, M., Khayat, K.. & Tagnit-Hamou, A. 2003. Performance characteristics of cement grouts made with various combinations of high-range water reducer and cellulose-based viscosity modifier. *Cement and Concrete Research*. 33(12):1999–2008.

Sayahi, F. 2016. Plastic shrinkage cracking in concrete. PhD Thesis, Department of Civil,

Environmental and Natural Resources Engineering, Lulea University of Technology.

Schmidt, W., Brouwers, H.J.H., Kuhne, H.-C. & Meng, B. 2010. Effects of superplasticizer and viscosity-modifying agent on fresh concrete performance of SCC at varied ambient temperatures. In K.H. Khayat & D. Feys (eds.). RILEM Bookseries 1 *Design, production and placement os self-consolidating concrete*. 65–77.

Schultz, M.A. & Struble, L.J. 1993. Use of oscillatory shear to study flow behavior of fresh cement paste. *Cement and Concrete Research*. 23(2):273–282.

Shen, D., Jiang, J., Wang, W., Shen, J. & Jiang, G. 2017. Tensile creep and cracking resistance of concrete with different water-to-cement ratios at early age. *Construction and Building Materials*. 146:410–418.

Shen, D., Jiang, J., Jiao, Y., Shen, J. & Jiang, G. 2017. Early-age tensile creep and cracking potential of concrete internally cured with pre-wetted lightweight aggregate. *Construction and Building Materials*. 135:420–429.

Singh, A., Seshagiri Rao, K. & Ayothiraman, R. 2019. A Closed-Form Analytical Solution for Circular Opening in Rocks Using Drucker–Prager Criterion. *Indian Geotechnical Journal*. 49(4):437–454.

Slowik, V., Schmidt, M. & Fritzsch, R. 2008. Capillary pressure in fresh cement-based materials and identification of the air entry value. *Cement and Concrete Composites*. 30(7):557–565.

Slowik, V., Hübner, T., Schmidt, M. & Villmann, B. 2009. Simulation of capillary shrinkage cracking in cement-like materials. *Cement and Concrete Composites*. 31(7):461–469.

Slowik, V., Schmidt, M., Kässler, D. & Eiserbeck, M. 2014. Capillary Pressure Monitoring in Plastic Concrete for Controlling Early-Age Shrinkage Cracking. *Transportation Research Record: Journal of the Transportation Research Board*. 2441(1):1–5.

Sonebi, M. & Bartos, P.J.M. 2002. Filling ability and plastic settlement of self-compacting concrete. *Materials and Structures*. 35(8):462–469.

Spangenberg, J., Roussel, N., Hattel, J.H., Stang, H., Skocek, J. & Geiker, M.R. 2012. Flow induced particle migration in fresh concrete: Theoretical frame, numerical simulations and experimental results on model fluids. *Cement and Concrete Research*. 42(4):633–641.

Struble, L.J. & Schultz, M.A. 1993. Using creep and recovery to study flow behavior of fresh cement paste. *Cement and Concrete Research*. 23(6):1369–1379.

Subramaniam, K. V. & Wang, X. 2010. An investigation of microstructure evolution in cement paste

through setting using ultrasonic and rheological measurements. *Cement and Concrete Research*. 40(1):33–44.

Sun, Z., Voigt, T. & Shah, S.P. 2006. Rheometric and ultrasonic investigations of viscoelastic properties of fresh Portland cement pastes. *Cement and Concrete Research*. 36(2):278–287.

Szecsy, R.S. 1997. Concrete Rheology. PhD Thesis, Department of Civil Engineering, University of Illinois at Urbana-Champaign.

Tao, Z. & Weizu, Q. 2006. Tensile creep due to restraining stresses in high-strength concrete at early ages. *Cement and Concrete Research*. 36(3):584–591.

Tattersall, G.H. & Baker, P.H. 1988. The effect of vibration on the rheological properties of fresh concrete. *Magazine of Concrete Research*. 40(143):79–89.

Tattersall, G.H. & Banfill, P.F.G. 1983. *The rheology of fresh concrete*. First ed. Pitman Advanced Pub. Program: London. [Online], Available: https://trid.trb.org/view/199391 [2018, October 10].

Taylor, M.A. & Maurer, G.K. 1973. Short-term stress relaxation of concrete. *Magazine of Concrete Research*. 25(84):123–135.

Uno, P.J. 1998. Plastic Shrinkage Cracking and Evaporation Formulae. *ACI Materials Journal*. 95(4):365–375.

Ur'ev, N.B., Baru, R.L., Izhik, A.P., Choi, S. V & Saskovets, V. V. 1997. Rheology and thixotropy of cement - water suspensions in the presence of superplasticizers. *Colloid Journal*. 59(6):833–839.

Verrelli, D.I. & Kilcullen, A.R. 2016. Normal Stress Differences and Yield Stresses in Attractive Particle Networks. *Advances in Condensed Matter Physics*. 2016:1–21.

Wallevik, J.E. 2005. Thixotropic investigation on cement paste: Experimental and numerical approach. *Journal of Non-Newtonian Fluid Mechanics*. 132(1–3):86–99.

Wallevik, J.E. 2009. Rheological properties of cement paste: Thixotropic behavior and structural breakdown. *Cement and Concrete Research*. 39(1):14–29.

Walpole, R.E., Myers, R.H., Myers, S.L. & Ye, K. 2012. *Probability and Statistics for Engineers and Scientists*. 9th ed. Prentice Hall: Boston.

Wang, Z., Shu, X., Rutherford, T., Huang, B. & Clarke, D. 2015. Effects of asphalt emulsion on properties of fresh cement emulsified asphalt mortar. *Construction and Building Materials*.

75:25–30.

Ward, M.A. & Cook, D.J. 1969. The mechanism of tensile creep in concrete. *Magazine of Concrete Research*. 21(68):151–158.

Wittmann, F.H. 1973. Interaction of Hardened Cement Paste and Water. *Journal of the American Ceramic Society*. 56(8):409–415.

Wittmann, F.H. 1976. On the action of capillary pressure in fresh concrete. *Cement and Concrete Research*. 6(1):49–56.

Yahia, A. 2011. Shear-thickening behavior of high-performance cement grouts — Influencing mix-design parameters. *Cement and Concrete Research*. 41(3):230–235.

Yim, H.J., Kim, J.H., Kwak, H.-G. & Kim, J.K. 2013. Evaluation of internal bleeding in concrete using a self-weight bleeding test. *Cement and Concrete Research*. 53:18–24.

Yoo, D., Shin, H. & Yoon, Y. 2016. Ultrasonic Monitoring of Setting and Strength Development of Ultra-High-Performance Concrete. *Materials*. 9(294):1–13.

Yuan, Q., Lu, X., Khayat, K.H., Feys, D. & Shi, C. 2017. Small amplitude oscillatory shear technique to evaluate structural build-up of cement paste. *Materials and Structures*. 50(2):1–12.

Yuan, Q., Zhou, D., Khayat, K.H., Feys, D. & Shi, C. 2017. On the measurement of evolution of structural build-up of cement paste with time by static yield stress test vs. small amplitude oscillatory shear test. *Cement and Concrete Research*. 99:183–189.

Zhang, H. Ed. 2011. 6 - Building Mortar. In (Woodhead Publishing Series in Civil and Structural Engineering). Woodhead Publishing *Building Materials in Civil Engineering*. 150–423.

Zhang, J., Gao, X. & Su, Y. 2019. Influence of Poker Vibration on Aggregate Settlement in Fresh Concrete with Variable Rheological Properties. *Journal of Materials in Civil Engineering*. 31(7):04019128.

Appendix

ANALYSIS OF STRESS AND STRAIN

1. CASE I/III

Input fully restrained shear strains (e.g. arbitrary γ_{xy})

- Maximum shear strain due to cracking settlement strain ($\gamma_{xy,1}$)

$$\gamma_{xy,1}\,(\theta_{d,1}) = 2 \times \frac{Cracking\ settlement\ strain\ (\varepsilon_y)}{Mould\ width/2} \times 100 \qquad \text{Equation A1}$$

  Mould width is 300 mm

- Maximum shear strain due to cracking shrinkage strain ($\gamma_{xy,2}$)

$$\gamma_{xy,2}\,(\theta_{d,2}) = 2 \times \frac{Cracking\ shrinkage\ strain\ (\varepsilon_x)}{2 \times Mould\ depth} \times 300 \qquad \text{Equation A2}$$

  Mould depth is 100 mm

- Fully restrained cracking shear strain (γ_{xy})

$$\gamma_{xy} = \gamma_{xy,1} + \gamma_{xy,2} \qquad \text{Equation A3}$$

γ_{xy} can also be obtained from the cumulative the shear strains by estimating $\gamma_{xy}^{t} = \gamma_{xy,1}^{t} + \gamma_{xy,2}^{t}$, and multiplying by D_f as shown in Equation 6.5.

Principal shear strains (e.g. γ_{max})

$$\gamma_{max} = 2 \times \sqrt{\left(\frac{\varepsilon_x - \varepsilon_y}{2}\right)^2 + \left(\frac{\gamma_{xy}}{2}\right)^2} \qquad \text{Equation A4}$$

Principal normal strains (e.g. $\varepsilon_1, \varepsilon_2$)

$$\varepsilon_1, \varepsilon_2 = \frac{\varepsilon_x + \varepsilon_y}{2} \pm \sqrt{\left(\frac{\varepsilon_x - \varepsilon_y}{2}\right)^2 + \left(\frac{\gamma_{xy}}{2}\right)^2} \qquad \text{Equation A5}$$

Principal shear stress (e.g. τ_{max})

$$\tau_{max} = \sqrt{\left(\frac{\sigma_x - \sigma_y}{2}\right)^2 + (\tau_{xy})^2} \qquad \text{Equation A6}$$

Principal normal stress (e.g. σ_1, σ_2)

$$\sigma_1, \sigma_2 = \frac{\sigma_x + \sigma_y}{2} \pm \sqrt{\left(\frac{\sigma_x - \sigma_y}{2}\right)^2 + (\tau_{xy})^2} \qquad \text{Equation A7}$$

2. CASE II

Input fully restrained shear strains (e.g. arbitrary γ_{xy}) is similar to CASE I/III

Principal shear strains (e.g. γ_{max})

$$\gamma_{max} = 2 \times \sqrt{\left(\frac{0-0}{2}\right)^2 + \left(\frac{\gamma_{xy}}{2}\right)^2} = \gamma_{xy} \qquad \text{Equation A8}$$

Principal normal strains (e.g. $\varepsilon_1, \varepsilon_2$)

$$\varepsilon_1, \varepsilon_2 = \frac{0+0}{2} \pm \sqrt{\left(\frac{0-0}{2}\right)^2 + \left(\frac{\gamma_{xy}}{2}\right)^2} = \pm\frac{\gamma_{xy}}{2} \qquad \text{Equation A9}$$

Principal shear stress (e.g. τ_{max})

$$\tau_{max} = \sqrt{\left(\frac{0-0}{2}\right)^2 + \left(\tau_{xy}\right)^2} = \tau_{xy} \qquad \text{Equation A10}$$

Principal normal stress (e.g. σ_1, σ_2)

$$\sigma_1, \sigma_2 = \frac{0+0}{2} \pm \sqrt{\left(\frac{0-0}{2}\right)^2 + \left(\tau_{xy}\right)^2} = \pm\tau_{xy} \qquad \text{Equation A11}$$

DERIVATION OF BRESLER-PISTER (B-P) PARAMETERS

B-P theory can be written as

$$\sqrt{J_2} = A_1 I_1^2 + B_1 I_1 + C_1 \qquad \text{Equation A12}$$

From Drucker-Prager (D-P) theory

$$\sqrt{J_2} = BI_1 + C, \quad B = \frac{2\,sin\varphi}{\sqrt{3}(3+sin\varphi)}, \quad C = \frac{6c\,cos\varphi}{\sqrt{3}(3+sin\varphi)} \qquad \text{Equation A13}$$

From Mohr-Coulomb's shear parameters at failure

$\tau = \sigma(tan\varphi) + c$, c is the cohesion, φ is the angle of internal friction Equation A14

For the first boundary condition of pure shear failure, i.e. $I_1 = 0$ and equating B-P and D-P theories,

$\sqrt{J_2} = C_1$ and $\sqrt{J_2} = C$, therefore, $C_1 = C$ Equation A15

Differentiating $\sqrt{J_2}$ with respect to I_1 under pure shear failure and equating the derivatives,

$$\frac{\partial\sqrt{J_2}}{\partial I_1} = B_1 \quad \text{and} \quad \frac{\partial\sqrt{J_2}}{\partial I_1} = B, \text{therefore } B_1 = B \qquad \text{Equation A16}$$

For the second boundary condition of pure hydrostatic failure, i.e. $\sqrt{J_2} = 0$

$$0 = AI_1^2 + BI_1 + C \qquad \text{Equation A17}$$

From von-Mises and Hencky (Vm-H) theory under pure tension/dilatancy

$$\frac{1}{12G}\left[(\sigma_x-\sigma_y)^2+\ (\sigma_y-\sigma_z)^2+(\sigma_z-\sigma_x)^2+6\left(\tau_{xy}^2+\tau_{xz}^2+\tau_{yz}^2\right)\right]\leq\frac{1}{6}\frac{\sigma_s^2}{G} \quad \text{Equation A18}$$

$$\sqrt{\frac{1}{2}\left[(\sigma_x-\sigma_y)^2+\ (\sigma_y-\sigma_z)^2+(\sigma_z-\sigma_x)^2+6\left(\tau_{xy}^2+\tau_{xz}^2+\tau_{yz}^2\right)\right]}=\sigma_s \quad \text{Equation A19}$$

From the dynamic shear rheometry test where $\sigma_x=\sigma_r=0$, $\sigma_y=\sigma_\theta=0$, $\sigma_z=\sigma_z=N_1$, and $\tau_{xy}=\tau_{r\theta}=0$, $\tau_{xz}=\tau_{rz}=0$, $\tau_{yz}=\tau_{\theta z}=\tau_s$

$$\sqrt{\frac{1}{2}[(N_1)^2+(N_1)^2+6(\tau_s^2)]}=\sigma_s \quad \text{Equation A20}$$

$\sqrt{N_1^2+3\tau_s^2}=\sigma_{s1}$ where σ_{s1} is the equivalent isotropic stress under pure hydrostatic failure — Equation A21

From Equation A17,

$A\ =-\frac{B\sigma_{s1}+C}{\sigma_{s1}^2}$, therefore — Equation A22

$$\sqrt{J_2}\ =\left(-\frac{B\sigma_{s1}+C}{\sigma_{s1}^2}\right)I_1^2+BI_1+C \quad \text{Equation A23}$$

First stress invariant (I_1) and second stress invariant (J_2)

$$I_1=\sigma_1+\sigma_2,\qquad J_2=\frac{1}{6}\left[(\sigma_1-\sigma_2)^2+\ (\sigma_2)^2+(\sigma_1)^2\right] \quad \text{Equation A24}$$